ISOLATION AND CHARACTERIZATION OF VITILEVUAMIDE FROM THE ASCIDIANS *DIDEMNUM CUCULLIFERUM* AND *POLYSYNCRATON LITHOSTROTUM*

by

Annette M. Fernandez

A dissertation submitted to the faculty of
The University of Utah
in partial fulfillment of the requirements for the degree of

Doctor of Philosophy

Department of Medicinal Chemistry

The University of Utah

December 1996

THE UNIVERSITY OF UTAH GRADUATE SCHOOL

SUPERVISORY COMMITTEE APPROVAL

of a dissertation submitted by

Annette Melanie Fernandez

This dissertation has been read by each member of the following supervisory committee and by majority vote has been found to be satisfactory.

Chair: **Chris M. Ireland**

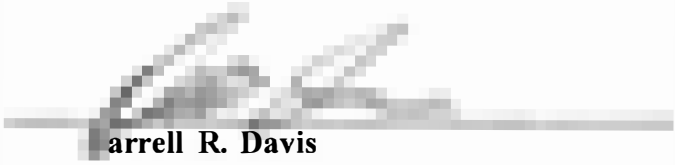

arrell R. Davis

Charles L.

THE UNIVERSITY OF UTAH GRADUATE SCHOOL

FINAL READING APPROVAL

To the Graduate Council of the University of Utah:

I have read the dissertation of [redacted] in its final form and have found that (1) its format, citations and bibliographic style are consistent and acceptable; (2) its illustrative materials including figures, tables, and charts are in place; and (3) the final manuscript is satisfactory to the supervisory committee and is

Date

Chris M. Ireland
Chair, Supervisory Committee

Approved for the Major Department

Approved for the Graduate Council

ABSTRACT

This dissertation was oriented towards the isolation and structure elucidation of novel biologically active metabolites from marine organisms collected in the South Pacific. In this investigation I focused on the characterization and biological evaluation of vitilevuamide, a novel bicyclic depsipeptide isolated from two Fijian ascidians, *Polysyncraton lithostrotum* and *Didemnun cuculliferum.*

The first chapter reviews cyclic peptides of marine origin along with their biological activity. This provides an overview of the types of peptides isolated from marine sources along with their structural uniqueness and similarities. The subsequent chapters deal with different aspects of the chemical and biological characterization of vitilevuamide.

The alcohol extract of the ascidians was fractionated to yield vitilevuamide which displayed potent cytotoxic activity toward the human colon tumor cell line HCT 116. The structure of this peptide was elucidated primarily using nuclear magnetic resonance (NMR) spectroscopic techniques and tandem mass spectrometry (MS/MS). The peptide was partially linearized using alcoholic ammonia in order to facilitate analysis by tandem mass spectrometry.

Chapter 3 deals with the synthesis of two not commercially available amino acids. The first is homoisoleucine (Hil) and the second N-methyl methoxinine (Nmm), a novel amino acid. The synthesis of Hil was successfully completed according to reported procedure. In the case of Nmm, several synthetic routes were attempted prior to successful synthesis of the molecule.

Chapter 4 deals with stereospecific assignments of the amino acids. Their absolute configurations were determined by HPLC analysis of derivatized constituent amino acids

obtained from acid hydrolysis of the peptide. New conditions were determined for the unambiguous assignment of isoleucine (Ile), Nmm and Hil. Liquid chromatography mass spectrometry (LCMS) was utilized in order to verify the stability of lanthionine (Lan) prior to assignment of stereochemistry.

The biological profile of vitilevuamide is discussed in Chapter 5. The cytotoxicity of the peptide was evaluated in a panel of six human tumor cell lines. Vitilevuamide also scored positive in an in-house mechanism based antitumor screen geared towards the detection of tubulin interactive compounds.

To my family for all their
love, support, and understanding

TABLE OF CONTENTS

LIST OF ABBREVIATIONS

Ala	alanine
ATCC	American Type Tissue Culture
CI	chemical Ionization
CID	collision induced dissociation
COLOC	correlation by long range coupling
COSY	correlated spectroscopy
DB-cAMP	dibuteryl cyclic adenosine mono phosphate
DC	differential cytotoxicity
DCI	Desorbtive Chemical Ionization
DEPT	distortionless enhancement by polarization transfer
DMSO	dimethyl sulfoxide
DLM	dextro meso levo
ED_{50}	effective dose 50%
EI	electron impact
ESMS	electrospray mass spectrometry
FAB	fast atom bombardment
FDAA	1-fluoro-2,4-dinitrophenyl-5-L-alanineamide
FID	free induction decay
GC	gas chromatography
HCT	human colon tumor
Hil	homoisoleucine
HIP	hydroxyisovalerylpropionate

HMBC	heteronuclear multiple bond correlation
HMQC	heteronuclear multiple quantum coherence
HPLC	high performance liquid chromatography
HR	high resolution
IC_{50}	inhibitory concentration 50%
ID_{50}	inhibitory dose 50%
I.D.	internal diameter
Ile	isoleucine
%ILS	percent increased life span
IR	infrared
Lan	lanthionine
LC	liquid chromatography
Leu	leucine
LR	low resolution
MS	mass spectrometry
MS/MS	tandem mass spectrometry
MTT	3-[4,5-dimethylthiazol-2-yl]-2,5-phenyltetrazolium bromide; thiazolyl blue
NCDDG	National Cooperative Drug Discovery Group
NCI	National Cancer Institute
Nmm	N-methyl methoxinine
NMO	N morpholino oxide
NMR	nuclear magnetic resonance
nOe	nuclear Overhauser enhancement
NOESY	nuclear Overhauser enhancement spectroscopy
PBS	phosphate buffered saline
Phe	phenyl alanine
Pro	proline

PS-DQF	phase sensitive double quantum filtered
RP	reverse phase
ROESY	rotating frame Overhauser enhancement spectroscopy
RT	retention time
SCUBA	self-contained underwater breathing apparatus
T/C	treated/control
TEA	triethylamine
TFA	trifluoroacetic acid/trifluoroacetate
TFA-ME	trifluoroacetic acid - methyl ester
Thr	threonine
TLC	thin-layer chromatography
TPAP	tetra propyl ammonium perruthenate
TOCSY	total correlation spectroscopy
Tyr	tyrosine
UV	ultraviolet
Val	valine

ACKNOWLEDGMENTS

I would like to thank my advisor, Professor Chris M. Ireland, for his guidance, both scientific and paternal. His support has enabled me to grow as a scientist and a person as well as pursue new avenues. For that I will always be grateful. To the rest of the Ireland group (past and present) my sincere thanks. The Department of Medicinal Chemistry has always been very generous in its support both emotionally as well as scientifically. Thank you for giving me the oppurtunity to be in God's country.

To the Loosers and the Priets, my warmest gratitude. My Ph. D. would never have been so much fun without your love, encouragement and prayers. For my friends Nelson, Deepa, Lalita, Sukrut, Supreetha, Meena and Sujata; thank you for being there when I needed you. To everyone else who has been instrumental in my success, it has been a priviledge indeed.

Lastly, and most importantly, I thank my parents for their undemanding love. Thank you for helping me achieve my heart's desire. Noel and Mishu, thank you for being my emotional anchors. It is only with your help that I am able to say 'I did it!'.

CHAPTER 1

INTRODUCTION

Rationale for Studying Marine Organisms

The greater depth of the sea compared to land elevation places over 95% of the biosphere under marine waters.[1] "Often, standing on the shore at low tide, has one longed to walk on and under the waves, and see it all but for a moment." These wistful words of Charles Kingsley in his book 'Glaucus' published in 1855, reflected the feeling amongst both professional and amateur marine biologists of that period.[2] Since then modern technology has contributed greatly towards making this a reality. A depth of 50m can now be easily accessed because of the advent of SCUBA whereas further depths can be reached using submersibles such as the Johnson-Sea-Link II.[3]

More than 95% of the animal species on earth are invertebrates, and marine organisms make up the majority of invertebrate phyla.[2] History has proven that marine organisms, especially invertebrates such as ascidians, sponges, soft corals and mollusks, produce many secondary metabolites that are unprecedented within the terrestrial environment.[4] Early investigations were largely of a cataloging nature where one simply searched for new metabolites. As the field matured and more compounds were reported, the likelihood of encountering a known compound increased dramatically.

However, recent studies in the field of marine natural products are becoming more sophisticated. Instead of randomly searching for new metabolites, research has become more applied. Scientists target compounds that exhibit pharmacologically useful activity. Assay systems have been developed to detect a diverse array of biomedically important compounds. This has resulted in the discovery of compounds that have anticancer,

antiviral and antiinflammatory action. CNS membrane-active toxins, ion channel effectors and metabolites that interact with DNA and micro-filament processes have also been identified.

Each phylum affords a characteristic distribution of compound structural types. For example, during the years from 1977 to 1985, 85% of the metabolites isolated from coelenterates were terpenoids, sponges yielded 37% terpenoid and 41% nitrogenous metabolites, and ascidians demonstrated a specialized ability to biosynthesize amino acid derivatives, producing up to 89% nitrogenous compounds.[5] This ability has focused significant attention on ascidians.

History of Marine Natural Products

The birth of the field of marine natural products is generally credited to Bergman,[6] who in 1950 isolated several modified arabino nucleosides from a *Cryptotethya crypta* sponge. These compounds, which served as models for the synthesis of the clinically important drugs Ara-A and Ara-C, generated a great deal of interest in marine organisms as a potential source of pharmaceutical agents.[7] This is based on the premise that sessile, soft bodied, shell-less marine organisms have no physical means of protection,and hence might use chemicals (secondary metabolites) in defense against predation. It is these metabolites that are being pursued by investigators .[8,9]

Research efforts have not concentrated on all marine invertebrates equally. The most intensely studied organisms from 1977 to 1987 were algae, which supplied investigators with 883 new compounds. Next were sponges with 736 new molecules. These were followed by coelenterates, which yielded 560 new compounds. In utter contrast, ascidians were the source of only 65 metabolites during that time period.[5]

It was not until 1974 that Fenical isolated the first ascidian metabolite, geranyl hydroquinone (**1**) from *Aplidium* sp.[10] Compound **1** exhibited chemopreventive activity against some forms of leukemia, Rous sarcoma, and mammary carcinoma in test animals.

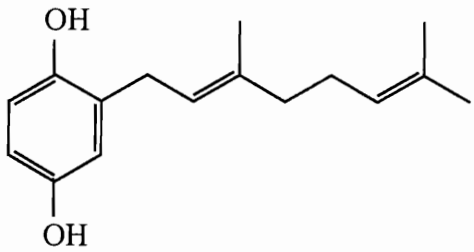

1

Since then, ascidians have been targeted for the specific purpose of isolating compounds of biomedical importance.

In fact between 1988 and mid 1992 an incredible surge of interest in ascidian chemistry yielded approximately 165 new ascidian metabolites. This is roughly a threefold increase over the previous 10-year period.[11] These results, which include structurally unprecedented families of biologically active secondary metabolites, have attracted the attention of both synthetic chemists and pharmacologists.

Ascidian Morphology

Ascidians belong to the phylum chordata, which encompasses all vertebrates including mammals. Therefore, they represent the most highly evolved group of animals commonly investigated by marine natural product chemists.[12] They are commonly referred to as tunicates because their body is covered by a sac-like case or a tunic, or as sea squirts because many species expel streams of water through a siphon when disturbed. Ascidians are hermaphrodites, they have independent male and female gonads within the same body. Sperm are released into the sea, mature eggs maybe released into the sea or they may be harbored within the animal until fertilization is complete.

While adult ascidians are exclusively marine invertebrates and bear little resemblance to other chordates, their larvae resemble amphibian tadpoles. The larval body is divided into a trunk and a tail. The tadpole has a well-developed nervous system predominantly located in the trunk region. Its digestive tract is an enlarged and perforated pharynx leading

to a tubular gut. Organs like the notochord and pharyngeal slits which are present in this stage are lost during development.[13]

Solitary or colonial, all ascidians possess a general body plan. The oral siphon marks the anterior end of the animal. The posterior end is arbitrarily designated and lies somewhere beyond the gut loop. The tunic encases the mantle which houses the brachial sac within which is present the digestive tract, the 'kidney', the nervous system, the circulatory system and the reproductive organs. Solitary individuals can reach a maximum length of 30 cm from base to apex.

Ascidians, like many other marine invertebrates, are known to exist in obligate and nonobligate symbiosis with microorganisms. There is literature evidence of associations of some ascidians with unicellular prokaryotic alga *Prochloron*[14,15] and some cyanophytes.[16,17] The exact nature of the symbiosis is unclear, but the increased incidence of algal-tunicate symbiosis in low nutrient tropical waters seems to suggest that the algae may play a nutritional role in the host's survival.[18] Such an example involves *Lissoclinum bistratum*, the source of the cyclic peptide bistratamides and the polyether metabolites, bistramides. The findings of Hawkins and co-workers, which suggested that bistratamides were localized in algal cells while bistramides were concentrated in tunicate tissue, are consistent with different origins for these metabolites.[19]

Cyclic Peptides From Ascidians

Peptides have continued to be one of the major structural classes isolated from ascidians. Ulicylamide (**2**) and ulithiacyclamide (**3**) were the first of a series of cyclic peptides isolated from *Lissoclinum patella*.[20] The genus *Lissoclinum* is a prolific producer of two classes of cyclic peptides, the heptapeptide lissoclinamides and the octapeptide patellamides/ulithiacyclamides. Each of these classes is characterized by the presence of thiazole and oxazoline amino acids. These peptides exhibit *in vitro* toxicity with the presence of the oxazoline ring proving important to their potency.[21] The majority of these

peptides have been isolated from one species of tunicate, *L. patella*, with some metabolite variation being observed with differences in the collection site.

The structures of **2** and **3** were elucidated by interpretation of spectral data and a detailed analysis of FABMS data.[22] Structure elucidation for these peptides has been fraught with difficulty and major or minor revisions have been made for a number of the originally proposed peptides. Both compounds were tested for antitumor activity against L1210 murine leukemia cells cultured *in vitro*. Compound **3** exhibited an IC_{50} of 0.35 μg/mL, whereas compound **2** had an IC_{50} of 7.2 μg/mL. Ulithiacyclamide also exhibited *in vivo* activity against the murine leukemia P1534J with an ILS of 178 at 10 mg/kg.[20]

Recently another ulithiacyclamide, ulithiacyclamide B (**4**), which incorporates a phenylalanine (Phe) amino acid in the place of alanine (Ala) was isolated.[23] Although highly toxic, both compounds **3** and **4** showed no selectivity against solid tumor cell lines. Compounds **3** and **4** exhibited IC_{50}'s of 35 ng/mL and 17 ng/mL respectively, against the KB cell line.

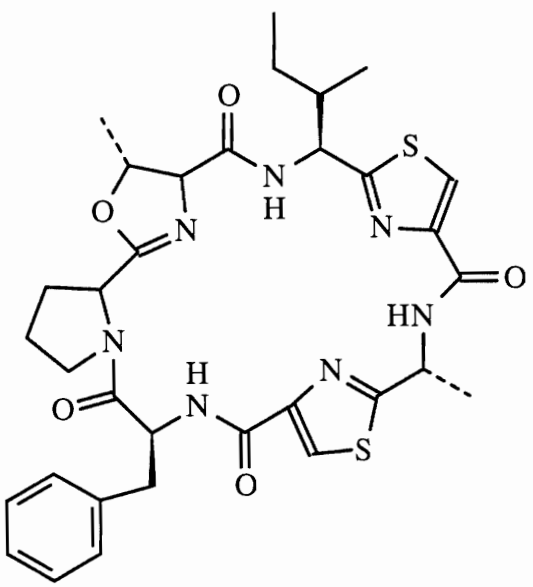

2

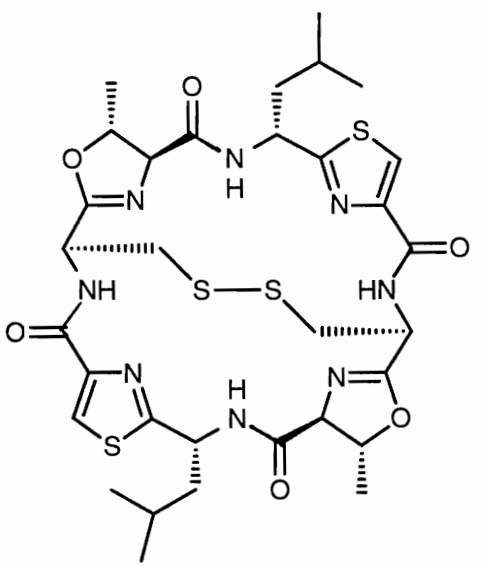

3

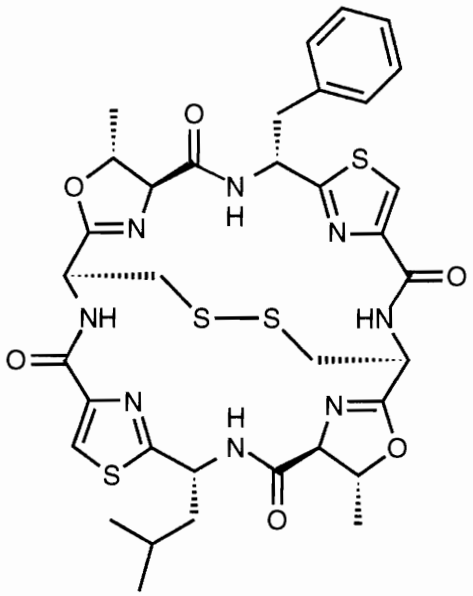

4

The three cyclic peptides to be initially isolated in the patellamide category include patellamide A, B and C. These compounds exhibited cytotoxic activity against L1210 murine leukemia cells cultured *in vitro*.[24] The absolute configuration for all the amino acids except the thiazole was established by gas chromatography (GC) retention correlation of the TFA-ME derivatives on a column coated with an optically active liquid phase. During the course of this research a new method for establishing the absolute configuration of thiazole amino acids was developed.[25] The work on these compounds also resulted in a new method for sequencing small peptides based on the observation of homoallylic coupling between α-protons of α-amino acids using a COSY-45 experiment.[26] This, in part, helped to revise the structures of patellamide A (**5**), B (**6**) and C (**7**).
Since then two new patellamides have been isolated, patellamide D (**8**)[27] and E (**9**).[28] The crystallization of compound **8** resulted in X-ray diffraction analysis confirming the structure that was initially proposed. This helped determine the absolute configuration of each amino acid as well as the solid state conformation of the peptide. The peptide assumes a severely folded conformation in which the 24-membered modified peptide backbone is

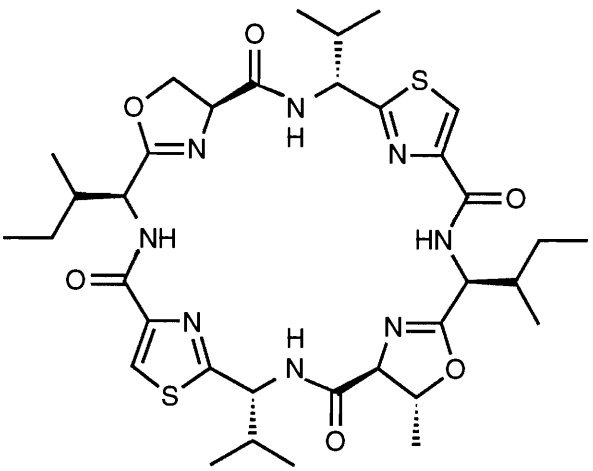

5

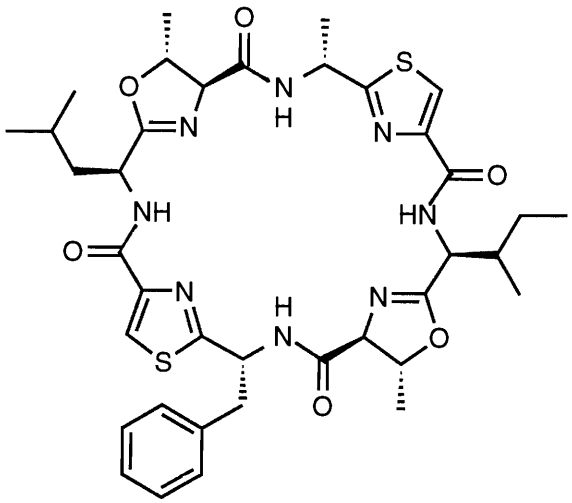

6

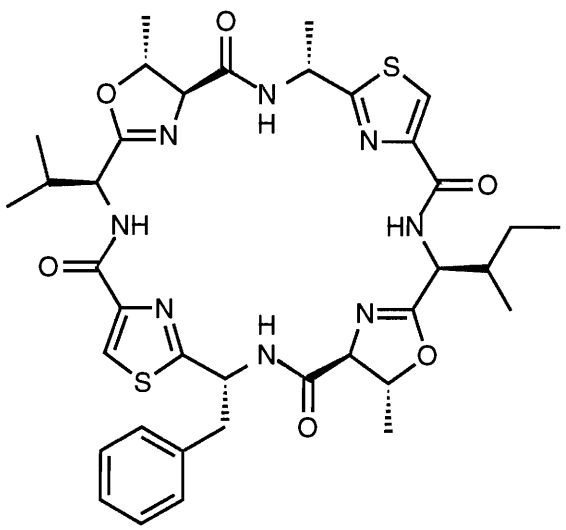

7

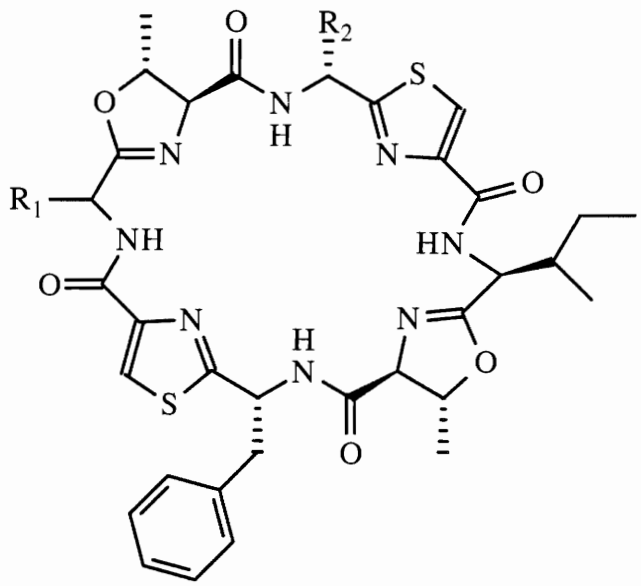

8 R_1 = L-Ile; R_2 = D-Ala

9 R_1 = L-Val; R_2 = D-Val

shaped like a twisted "figure eight" and deviates significantly from its twofold symmetry.

The structure of compound **9** was determined by chemical and spectral methods and analyzed further by molecular modeling calculations. The spectral data showed characteristic similarities to other patellamides and a 14 mass unit difference suggested that it was a homolog of compound **6**. The absolute stereochemistry was established by comparing the amino acids from the acid hydrolysis with standard amino acids, both suitably derived for HPLC analysis. Patellamide E was weakly cytotoxic against human colon tumor (HCT) cells *in vitro* at an IC_{50} of 125 μg/mL.

A lone member of the family, ascidacyclamide (**10**), was isolated from an unidentified ascidian collected from Rodda Reef, Queensland, Australia.[29] The compound had a strong lethal effect on PV_4 cultured cells transformed with poloma virus. T/C 100% was observed at 15 μg/mL.

Two new proline containing octapeptides, Tawicyclamides A (**11**) and B (**12**) were isolated from *L. patella* collected at Tawitawi, Philippines. The tawicyclamides possess

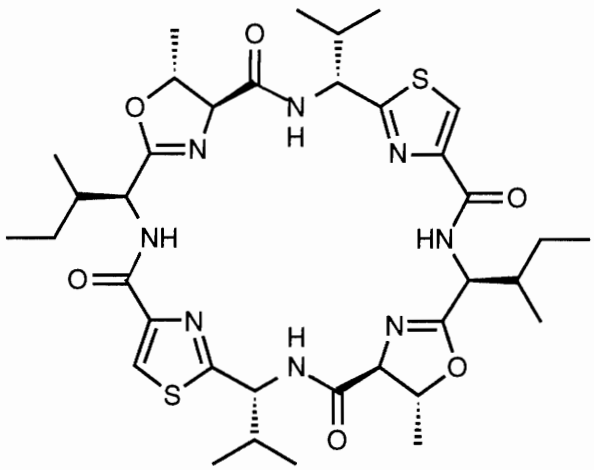

10

one thiazoline and two thiazole amino acids but lack the oxazoline ring that is characteristic of all previously discovered *Lissoclinum* peptides. The presence of the thiazoline ring was confirmed by nickel peroxide oxidation to yield the corresponding dehydrotawicyclamides A (**13**) and B (**14**).[30] The unambiguous structure of compound **11** was established by interpretation of the CID spectra of its protonated molecular ion and several fragment ions resulting from unimolecular dissociations.

The structure elucidation of compound **12** was performed by spectral analysis. The structure was also confirmed by single crystal X-ray analysis. This identified the three-dimensional structure of the peptide. Since only the relative stereochemistry could be determined in the X-ray experiment, the absolute configuration was set by the chirality of the amino acids determined by HPLC analysis.

The tawicyclamides and their dehydro analogs exhibited weak cytotoxicity against HCT 116 cells, IC_{50}'s ~ 30 μg/mL. This is again consistent with structure-activity studies that suggest that the oxazoline ring is important for cytotoxicity in this class of peptides. These peptides possess a thiazoline ring and a proline, existing in a *cis* conformation, that facilitates an unusual conformation. A conformational reorganization occurred upon

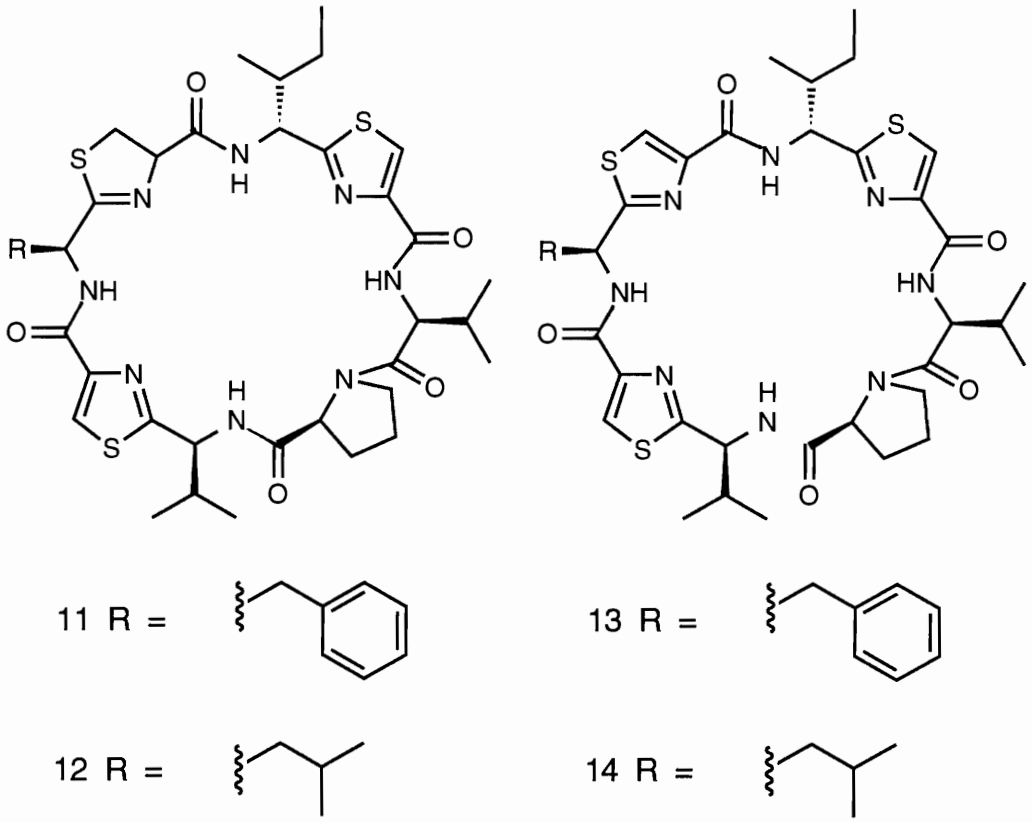

oxidation to a thiazole. This prompted an investigation of the conformation of compound **11** and its dehydro analog.

The tawicyclamides assume a conformation in which the valine-proline bond is *cis* while the dehydrotawicyclamides assume an all-*trans* amide bond conformation. Absolute configurations of individual amino acids were determined by HPLC analysis of derivatized amino acids obtained from hydrolysis. X-ray crystallographic and molecular modeling studies indicated that compound **12** existed in a three-dimensional conformation very similar to that of compound **8**. This shape, described as having the contour of a tennis ball seam, underwent extensive modification upon oxidation. These changes result in a saddle shape similar to that described for compound **10**.

The heptapeptide class of the Lissoclinum peptides includes the lissoclinamides. Eight peptides, lissoclinamide 1 - 8 (**15-22**)[27,31,32] have been isolated and characterized. Their differences rest in the oxidation states of the two sulfur containing rings and in the

absolute stereochemistry of the amino acids. Compound **20**, which contains two thiazole rings, can be easily distinguished from compounds **18** and **22**, which incorporate two thiazoline rings.

The remainder of these compounds contain the same thiazole and thiazoline rings. Of the lissoclinamides, compound **22** was cytotoxic against MRC5CV1 and T24 cell lines with IC_{50} values of 0.04 μg/mL, whereas compound **19** was reported active against the same cell lines with an IC_{50} value of 0.8 μg/mL.[32] The other lissoclinamides did not exhibit any significant cytotoxicity.

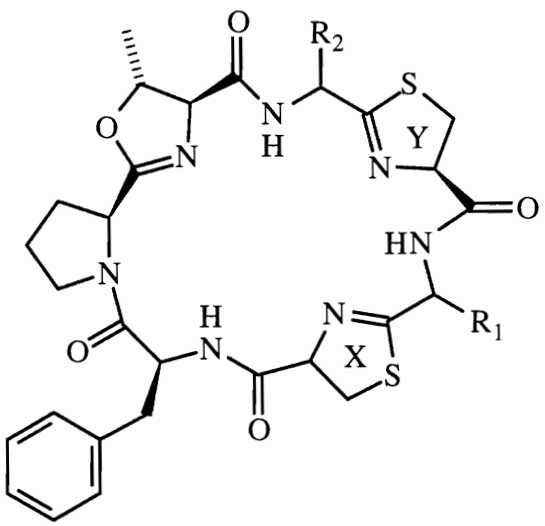

15 X = thiazole; Y = thiazoline; R_1 = L-Ala; R_2 = L-Ile

16 X = thiazole; Y = thiazoline; R_1 = D-Ala; R_2 = L-Ile

17 X = thiazole; Y = thiazole; R_1 = L-Ile; R_2 = D-Val

18 X = thiazole; Y = thiazoline; R_1 = L-Phe; R_2 = D-Val

19 X = thiazole; Y = thiazole; R_1 = L-Phe; R_2 = D-Val

20 X = thiazole; Y = thiazoline; R_1 = D-Phe; R_2 = D-Val

21 X = thiazoline; Y = thiazoline; R_1 = D-Phe; R_2 = Val

22 X = thiazole; Y = thiazoline; R_1 = D-Phe; R_2 = D-Val

Lissoclinum patella collected in the Fiji islands has been the source of a new family of cyclic peptides, the patellins. They include both hexapeptides, patellins 1 (**23**) and 2 (**24**), as well as octapeptides, patellins 3 (**25**), 4 (**26**) and 5 (**27**).[33,34] These peptides are unique in that they lack the trademark thiazole and oxazoline rings, but contain a thiazoline ring and two novel threonine amino acids which are modified as their dimethylallyl ethers.

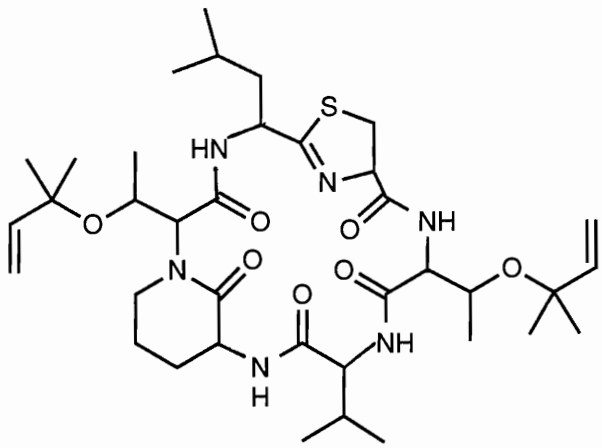

23

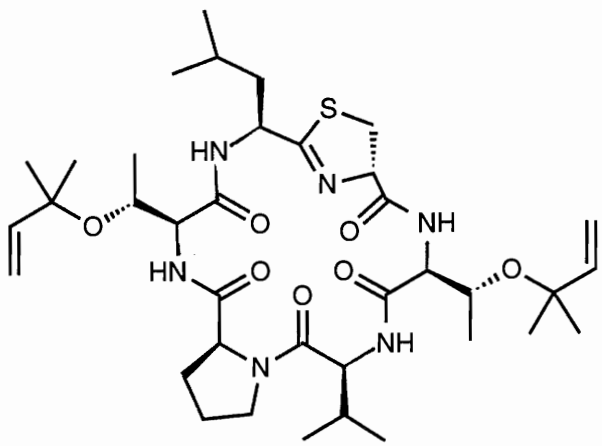

24

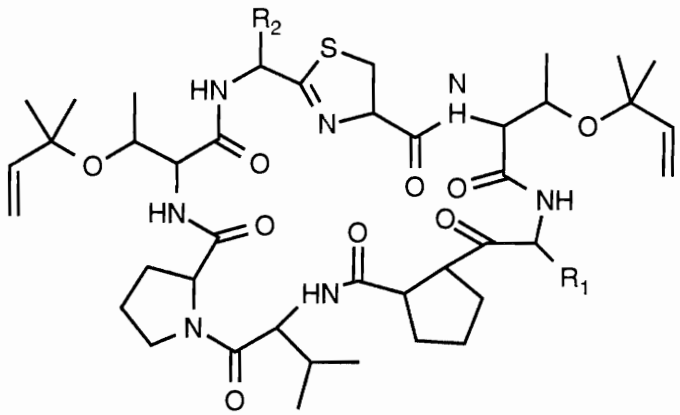

25 R_1 = R_2 = Leu

26 R_1 = Leu; R_2 = Val

27 R_1 = Val; R_2 = Phe

Preliminary NMR studies suggested that compound **24** was a mixture of either two closely related compounds or multiple conformers of a single compound. The ratio of the doubled signals varied as a function of temperature and solvent, confirming the possibility of multiple conformers. Spectra obtained in solvents with high dielectric constants showed a greater difference in conformer distribution, while using solvents with low dielectric constants resulted in spectra displaying nearly equal conformer populations.

The structure was further investigated using a combination of X-ray crystallography and molecular mechanics calculations. One of the striking features of the crystal structure is that the peptide has all of the nonpolar residues on one side while the thiazoline and the carbonyls are on the other side. The solution-phase conformers of patellin 2 arise from *cis-trans* isomerization of the Val-Pro amide bond, based on NMR and molecular modeling studies. However, like other small proline containing peptides, compound **24** exhibits only trans amide bonds in the crystal structure.[35]

A different species of Lissoclinum, *Lisssoclinum bistratum*, collected from the Great Barrier Reef in Australia, yielded three cyclic peptides. Bistratamide A (**28**) has two thiazoline rings whereas bistratamide B (**29**) has one each of a thiazole and thiazoline ring.

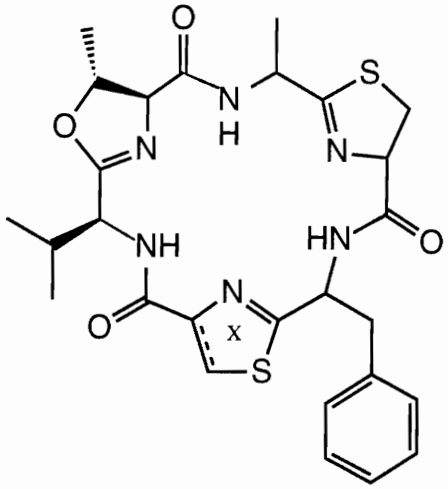

28 X = Thiazole

29 X = Thiazoline

Compounds **28** and **29** showed marginal toxicity against human MRC5CV1 fibroblasts and T24 bladder carcinoma cells with IC_{50}'s in the range of 50 and 100 μg/mL respectively.[27]

The third hexapeptide **30** was isolated simultaneously from *L. bistratum* (cycloxazoline),[36] as well as the terrestrial cyanobacteria, *Westiellopsis prolifica* (westiellamide).[37] This provided circumstantial evidence that the peptides found in ascidians may be, at least in part, synthesized by the harbored *Prochloron.* The three-dimensional structure of the peptide was established by X-ray crystallography.

Compound **30** assumes a planar conformation with no folding due to the small size of the macrocyclic ring.[38] This peptide is a symmetrical trimer containing three oxazoline rings formed by the condensation of valine and threonine amino acids. It is cytotoxic against the same cell lines as the bistratamides with IC_{50}'s of 0.5 μg/mL.

A Philippine specimen of *L. bistratum* contained bistratamides C (**31**) and D (**32**).[39] The structure of both these peptides was identified by spectral analysis. The three dimensional conformation of compound **31** was investigated by computational techniques. Both these peptides exhibited an IC_{50}'s of 125 μg/mL in the *in vitro* HCT 116 tumor cell

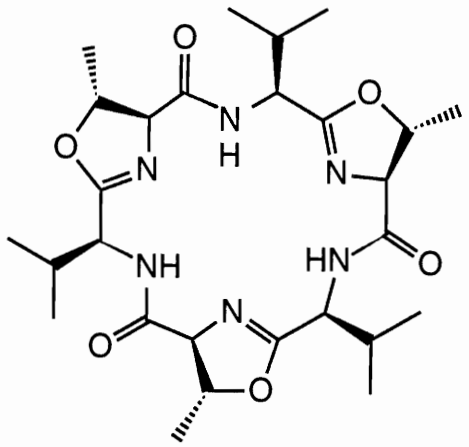

30

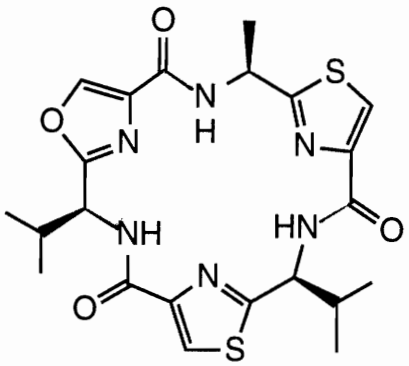

31

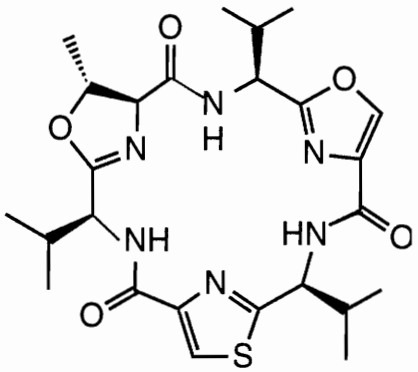

32

model. Compound **32** however showed depressant effects when introduced directly into the central nervous system of mice by intracerebral injection. At a 65 μg dose, mice exhibited decreased motor activity, sluggishness and sedation relative to control.

The extract of *L. bistratum* collected at Nairai, Fiji islands yielded the cyclic hexapeptides nairaiamides A (**33**) and B (**34**).[40] These compounds were found to be similar to a cyclic hexapeptide, axinastatin,[41] isolated from an *Axinella* sp. sponge as well

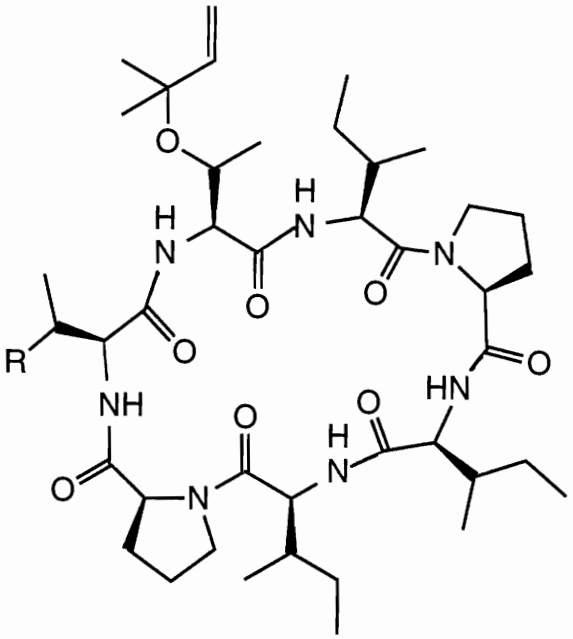

33 R = Methyl

34 R = Ethyl

as pseudoaxinellin from the Papua New Guinea sponge *Pseudoaxinella massa*.[42] A ^{13}C edited 2D HMQC-TOCSY NMR experiment was performed in order to assign the different resonances and thereby identify the amino acids. The peptides possess two proline (Pro) residues, a dimethylallylthreonine and several isoleucine (Ile). The Ile-Pro amide bonds were found to be *cis* in solution based on ^{13}C chemical shift data and ^{1}H - ^{1}H nOe's.

The first metabolite from an ascidian to enter phase III clinical trials was Didemnin B (**35**), a cyclic depsipeptide isolated from the Caribbean ascidian *Tridemnum solidum*.[43,44] Didemnin B along with didemnins A (**36**) and C (**37**) were first isolated in 1981 and were proposed to contain the unique structural unit hydroxyisovalerylpropionate (HIP) and a new allo stereoisomer of statine.[45] Compounds **37** and **38** inhibit Herpes simplex viruses I and II at 0.1 μM and 0.05 μM concentrations, Rift valley fever virus at 1.37 and 0.004 μg/mL, Venezuelan Equine encephalomyelitis at 0.43 and 0.08 μg/mL and

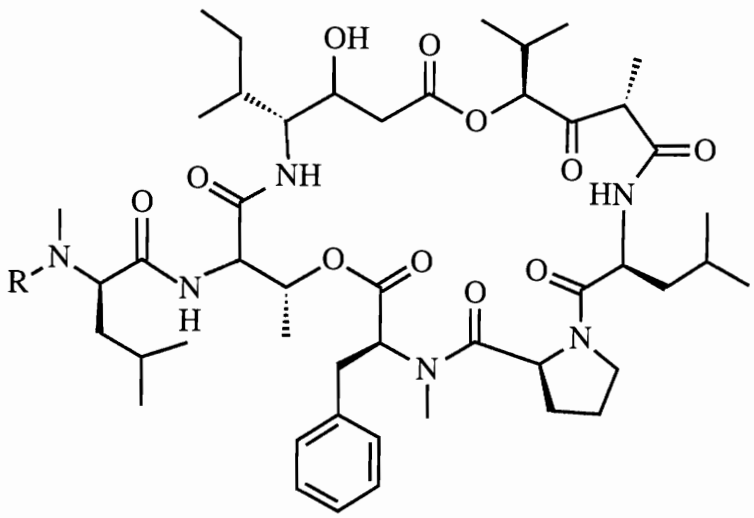

OMe

35 R =

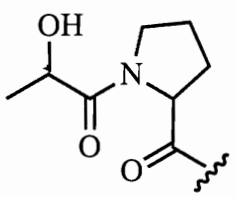

36 R = H

37 R =

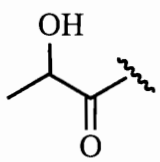

yellow fever virus at 0.4 and 0.08 μg/mL, respectively. Didemnin B also demonstrated *in vivo* anticancer activity against P388 murine leukemia (%ILS 99) at 1.0 mg/kg.[46]

Didemnins D (**38**) and E (**39**) incorporate the same cyclic depsipeptide skeleton as didemnins A-C, but their side chains contain three and two contiguous L-glutamines, respectively, and are terminated in a L-pyroglutamate residue.[47] The structure of nordidemnin B (**40**), also isolated from the same ascidian, was initially assigned by gas chromatography mass spectrometry (GC/MS) of the hydrolysate products. The structure elucidation was instigated by the fact that there existed a difference of 14 mass units

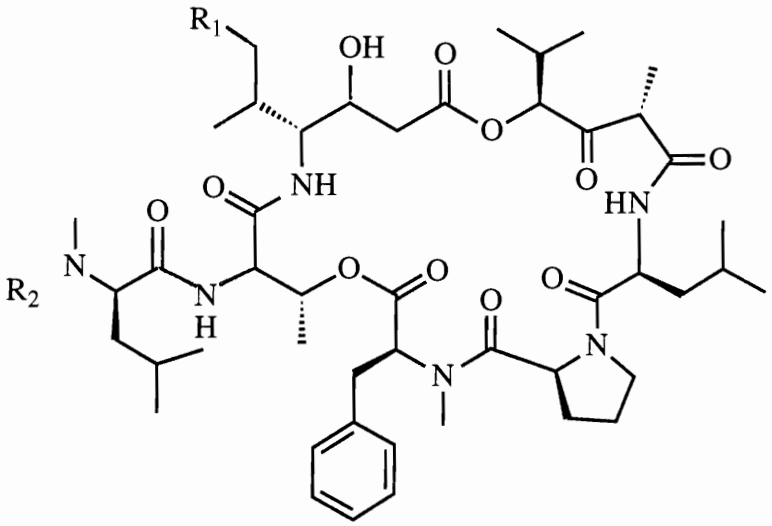

X =

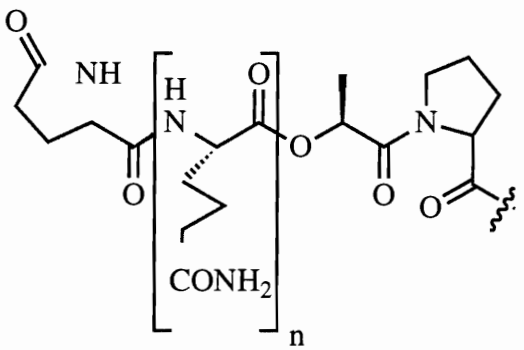

Y =

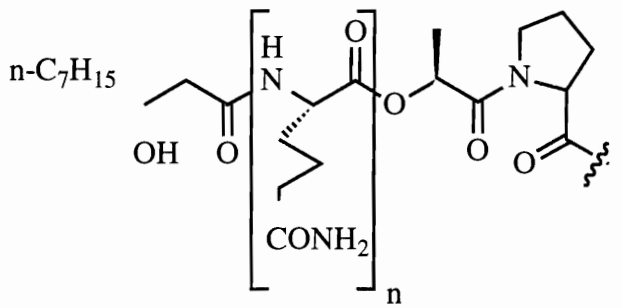

38 R_1 = Methyl; R2 = X (N=2)

39 R_1 = Methyl; R2 = X (N=2)

41 R_1 = Methyl; R2 = Y (N=3)

42 R_1 = Methyl; R2 = Y (N=4)

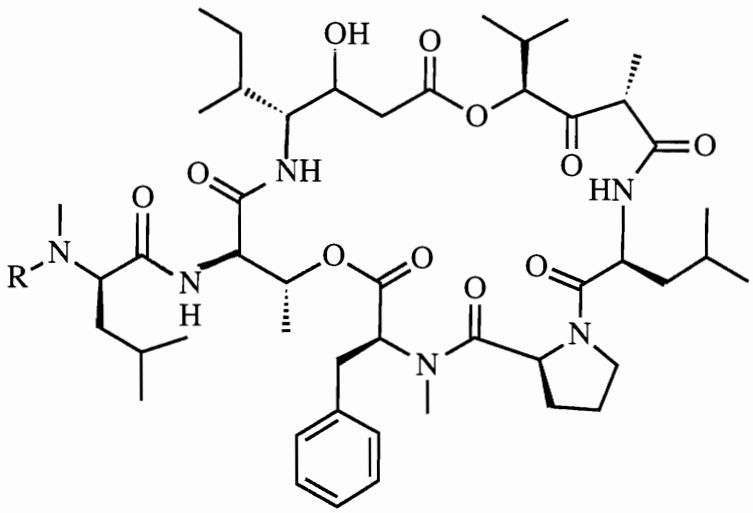

OMe

40 R =

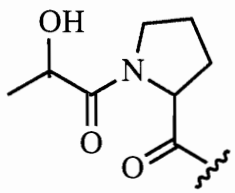

between compound **35** and **40**; however there were no detailed ^{1}H and ^{13}C experiments reported in the literature. The structure has since then been verified by total synthesis and NMR spectroscopy.[48,49]

Didemnins X (**41**), Y (**42**)[50-51] and H (**43**)[52] are three more additions to the didemnin family of depsipeptides. They contain three and four L-glutamine residues respectively, capped with a new N-terminal blocking group, a 3-hydroxydecanoyl group. All three compounds were isolated from the ether extract of *D. cyanophorum.* The structure of compound **43** was elucidated by means of a combination of mass spectroscopy and two-dimensional NMR experiments. Compound **43**, at a concentration of 0.74 μM, elicits a positive response with the HPLC procedure described by Pezzuto to detect

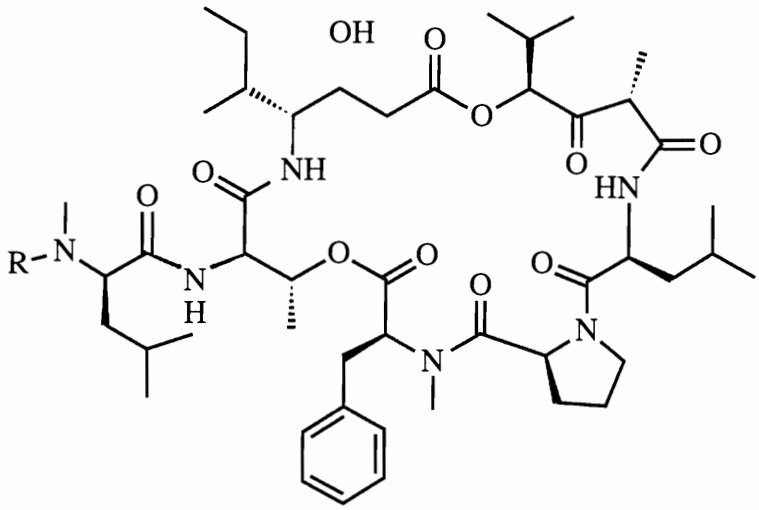

R =

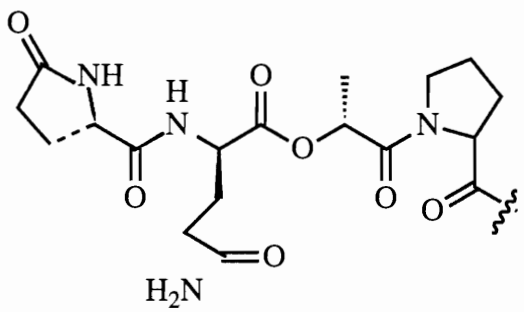

43

compounds capable of interacting with DNA.[53] Didemnin H is found to reduce (60% - 70%) the DNA peak while compounds **35** and **36** show negative responses.

The ascidian *Cystodytes dellechiajei* was the source of three cyclic tetrapeptides, each of which was a symmetrical dimer of either L-Leu-L-Pro **44**, L-Leu-L-Val **45** or L-Pro-L-Phe (**46**).[54] These peptides were found to be cytotoxic to L1210 leukemia cells at an IC_{50} of 0.5 μg/mL.

The most unusual cyclic peptides, diazonamides A (**47**) and B (**48**) have been isolated from the Philippine ascidian *Diazona chinensis*.[55] This ascidian was collected off the ceilings of small caves along the northwest coast of Siquijor Island, Philippines. A

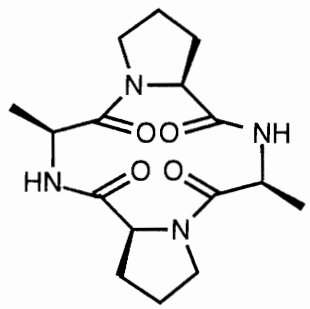

44 R = $CH_2CH(Me)_2$

45 R = iPr

46 R = CH_2Ph

combination of ^1H NMR, ^{13}C NMR and HRFABMS experiments led to assignments of several structural fragments. However, the missing connectivities were established by single crystal X-ray diffraction analysis of the p-bromobenzamide derivative of compound **48** made by reacting it with p-bromobenzoylchloride in pyridine.

These peptides are highly unsaturated, chlorinated and made up of derivatives of at least three amino acids; a tryptophan substituted at the 2- and 4- positions of the indole, a 3,4,5 trisubstituted tyrosine and an L-Valine. UV spectra of the diazonamides show little evidence of their degree of unsaturation. The likely biosynthetic origin of parts of the molecule is unclear. These structural units have cyclized in an unprecedented manner to form an extremely rigid framework which does not allow conformational freedom for the polycyclic core.

Compound **47** was cytotoxic *in vitro* against HCT 116 and B16 murine melanoma cell lines with IC_{50} values less than 15 ng/mL. Compound **48** was found to be less active than **47**.

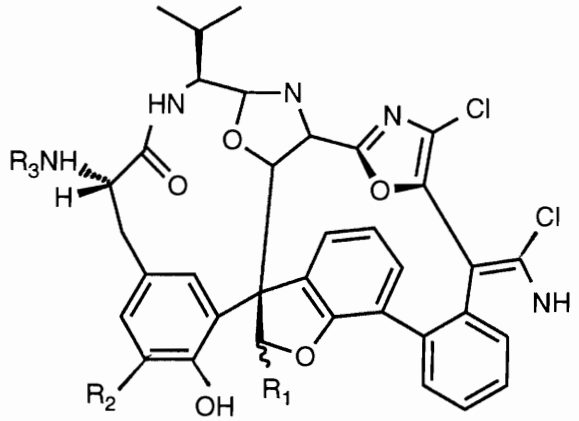

47 R1 = OH; R2 = H; R3 = 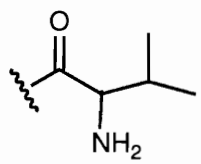

48 R1 = OH; R2 = Br; R3 = H

Summary

Although natural products of marine origin have been studied by chemists for some years, their biomedical potential was not fully recognized until recently. Simultaneously, emphasis on ascidian chemistry has been initiated very recently compared to other marine invertebrates. Hence it is highly significant that the first marine metabolite to enter clinical trials, Didemnin B, is an ascidian metabolite.

A survey of the compounds discussed reveals a trend in biological activities. Cytotoxicity against various tumor cell lines is the most frequently listed activity for most of the metabolites. This highlights the changed rationale in the investigation of the chemistry of marine organisms. Whereas early investigations were largely of a cataloging nature, recent studies are focused on potential applications of these metabolites either to the treatment of human disease or to the understanding of different mechanistic pathways in human disease etiology.

The isolation of biosynthetically unrelated secondary metabolites from a single organism suggests different origins for each class of compounds. Further understanding of the symbiotic association between ascidians and algae thus poses a challenge for marine scientists.

CHAPTER 2

THE STRUCTURE ELUCIDATION OF VITILEVUAMIDE

Collection and Isolation of Vitilevuamide

This chapter describes the isolation and characterization of a novel bicyclic depsipeptide, vitilevuamide (**49**). Compound **49** was isolated from the MeOH extract of two ascidians, *Didemnum cuculliferum* (Order: Aplousobranchia, Family: Didemnidae) and *Polysyncraton lithostrotum* (Order: Aplousobranchia, Family: Didemnidae) from Namenalala Island, Fiji Islands.

Isolation of Vitilevuamide

The crude MeOH extract of *Didemnum cuculliferum* showed potent cytotoxicity against HCT 116 cell lines with an IC_{50} in the ng range. This instigated the isolation of the molecule responsible for the pharmacological activity. The MeOH extract was concentrated and successively partitioned with a series of solvents of increasing polarity.[56] Repeated silica gel flash chromatography of the chloroform soluble fraction yielded a semi-pure molecule. C18 HPLC was performed to yield the pure peptide vitilevuamide.

Vitilevuamide was also detected during the workup of *Polysyncraton lithostrotum.* A scheme was adopted to facilitate the isolation of vitilevuamide along with another molecule of pharmacological interest from the same ascidian. This involved silica gel flash chromatography of the chloroform soluble fraction followed by reverse phase and amino flash chromatography. A step gradient was used in all the flash chromatography procedures. The peptide isolated was pure and no HPLC was required for further purification. Figures 2.1 and 2.2 illustrate the isolation processes adopted.

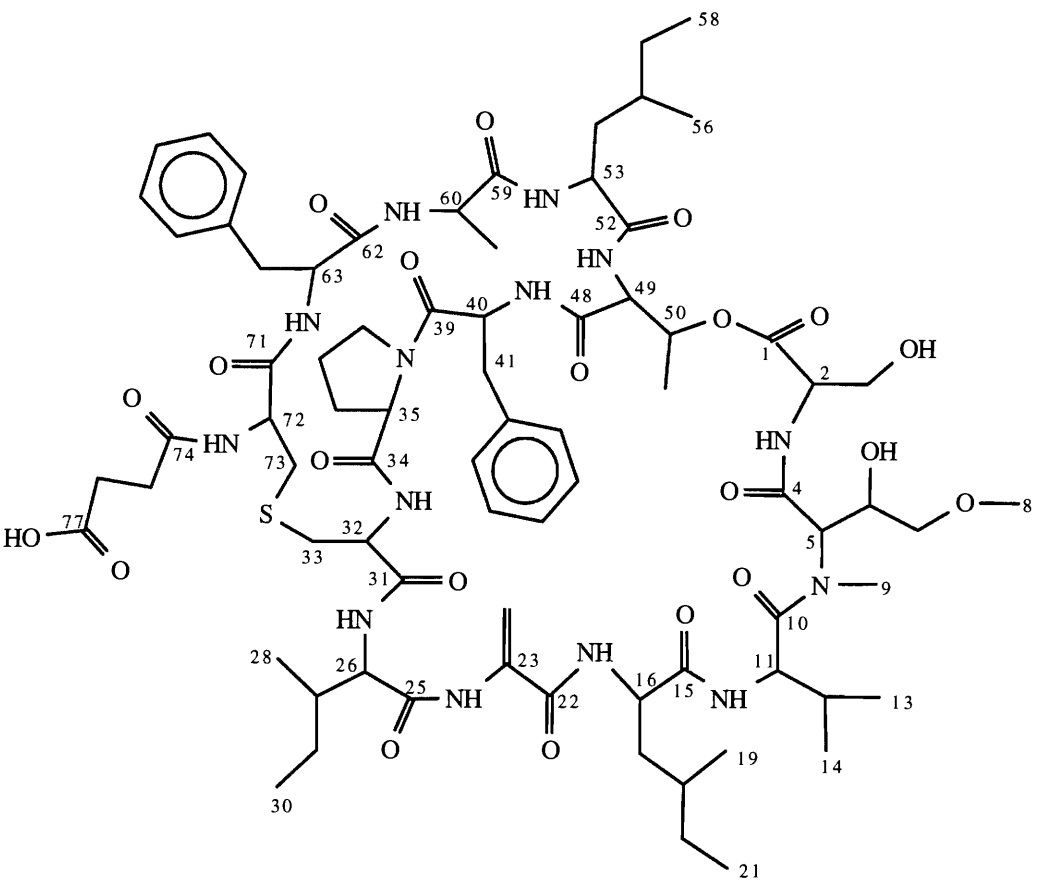

49

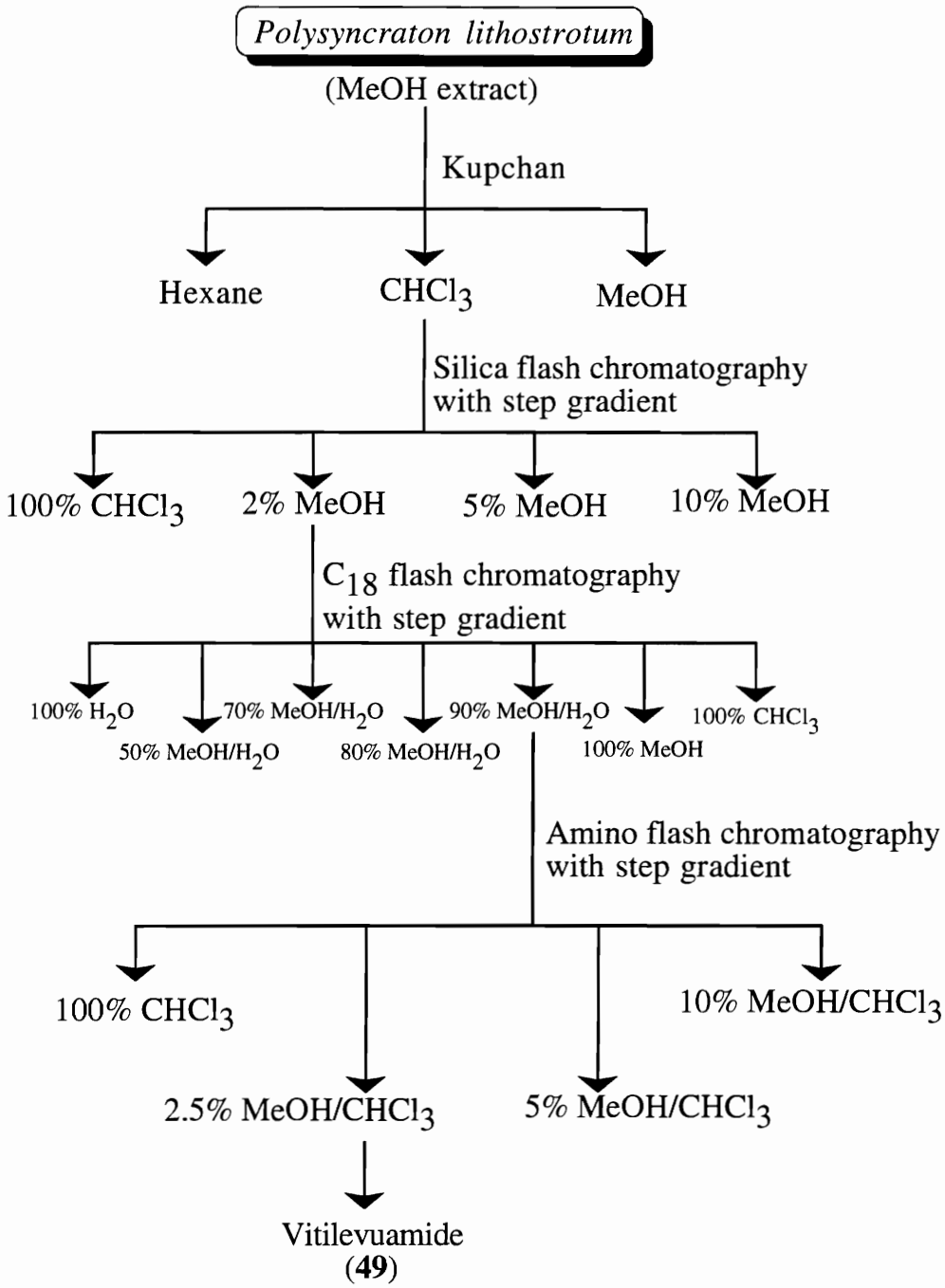

Figure 2.1. Isolation flow diagram for vitilevuamide from the ascidian *Polysyncraton lithostrotum*

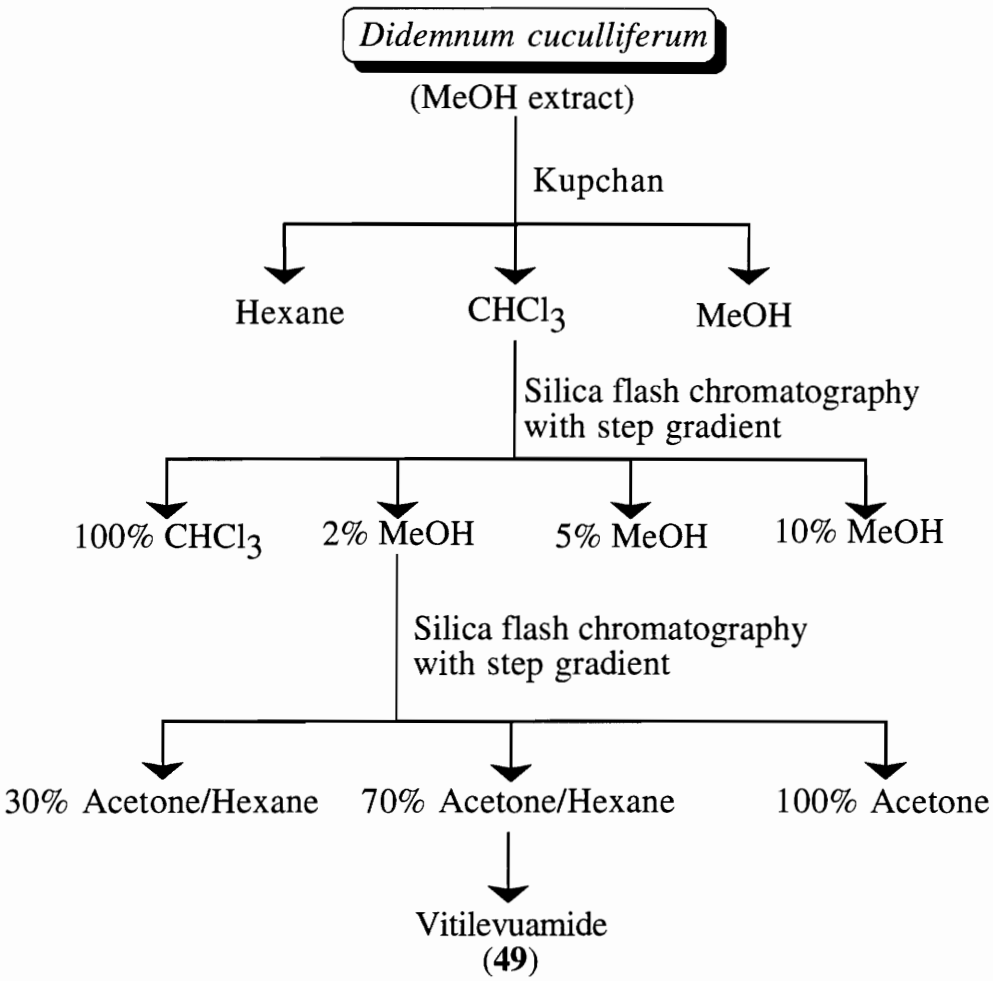

Figure 2.2. Isolation flow diagram for vitilevuamide from the ascidian *Didemnum cuculliferum*

Structure Determination of Vitilevuamide

A positive ion HRFABMS showed a protonated molecular ion at *m/z* 1603.811768, in agreement with the molecular formula $C_{77}H_{114}N_{14}O_{21}S$. Infrared (IR) bands at 3280, 1652, 1558 and 1538 cm^{-1} were indicative of amide NH and carbonyl stretches for peptides. The absence of IR bands corresponding to an ammonium ion and the presence of an ester carbonyl band at 1734 cm^{-1} suggested that vitilevuamide was cyclic or had terminal end modifications.

Ultraviolet (UV) spectroscopy of the compound showed an absorption at 230 nm with an extinction coefficient of 2032. Weaker absorptions were observed at 210 (ε = 1719) and 250 (ε = 1985) nm respectively.

NMR Experimentation

A variable solvent study was performed in order to determine the deuterated solvent of choice for the NMR study. The solvents that were considered included $CDCl_3$, CD_2Cl_2, C_6D_6 and a mixture of C_6D_6 and CD_2Cl_2. Benzene was selected as the deuterated solvent for all NMR experiments based on resolution in both proton and carbon domains. In order to determine the appropriate temperature for maximum resolution of protons, a variable temperature study was also performed. An optimum temperature of 22°C was thus established. Table 2.1 provides a list of the rate of change in chemical shift of selected protons over a temperature range of 55°C.

Resonances in the ^1H NMR spectrum (Figure 2.3) included 11 doublets between 10.49 and 6.40 ppm and a singlet at 10.11 ppm attributable to amide NH protons. The presence of a singlet amide proton at 10.11 ppm suggested a 90° angle between the α and amide protons or the absence of an α-proton in one amino acid. The multiplets between 5.67 and 4.81 ppm corresponded to peptide α-protons.

The ^{13}C NMR spectrum (Figure 2.4) of vitilevuamide contains 70 resonances, 7 of which represent two overlapped carbons each. The degenerate carbons include carbonyls

Table 2.1. Variable temperature study

CHEMICAL - SHIFT (ppm)	$\Delta\delta/\Delta T$ (ppb/K)
9.994	1.39520
9.518	-14.0020
8.975	1.07140
8.886	-0.81667
8.373	-3.05950
8.232	-4.53810
7.912	-0.63810
7.866	-1.38810
7.772	-0.64524
7.752	-1.00480
6.496	-1.18100
6.094	1.40950
4.597	1.27860
3.381	0.36667
3.280	0.73095

Temperature range used: -20°C to 35°C in increments of 5°C

at 173.28 ppm, aromatic carbons at 130.24, 130.05, 128.89 and 128.72 ppm as well as α-carbons at 57.03 and 55.51ppm.

A Distortionless Enhancement by Polarization Transfer (DEPT) experiment [57-59] (appendix A) established the number of protons attached to each carbon. The DEPT experiment uses polarization transfer through scalar coupling from ^{1}H to ^{13}C to enhance the intensity of the ^{13}C signals. 45, 90 and 135 degree pulses distinguish the three

different types of carbons. In the case of vitilevuamide, a 135 degree pulse was used which results in the methyls and methines being positively phased while the methylenes are negatively phased. The DEPT experiment does not detect quaternary carbons since they have no protons for magnetization transfer.

The multiplicity of the carbons was also confirmed by a Heteronuclear Multiple Quantum Coherence (HMQC) [60-61] (Appendix A) experiment which permitted assignment of protons to their directly attached carbons. The advantage of an HMQC experiment lies in its ability to distinguish two overlapped protons bound to different carbons and two diastereotopic protons bound to the same carbon.

A Double Quantum Filter Correlated Spectroscopy (DQF-COSY) [62-63] (Appendix A) experiment and a Total Correlation Spectroscopy (TOCSY) [64-65] (Appendix A) experiment aided in the identification of spin systems based on scalar coupling between protons. Since the spin systems of many amino acids are unique, they can be distinguished easily in a DQF-COSY spectrum. DQF-COSY cross peaks can be expected for each resolved scalar coupling in a spin system. The presence of a cross peak is an indication that the coupled nuclei are two or three bonds apart. However, one does observe problems associated with cross peaks near the diagonal being distorted and crosspeaks for long chains not resolved due to signal degeneracy.

In such a situation the TOCSY experiment supports the assignment of COSY spectra in a useful manner. This experiment correlates and identifies protons in a specific spin system by the transfer of magnetization from each ^{1}H to every other ^{1}H in the spin system via isotopic mixing using a pulse sequence that employs a spin lock. In the case of an amino acid, this allows one to trace from an amide proton through α, β, and if mixing times are sufficiently long, the entire proton spin system. Thus additional correlations are found for protons that are not directly coupled to each other but have common coupling partners. The cross peaks appear inphase and are easily resolved.

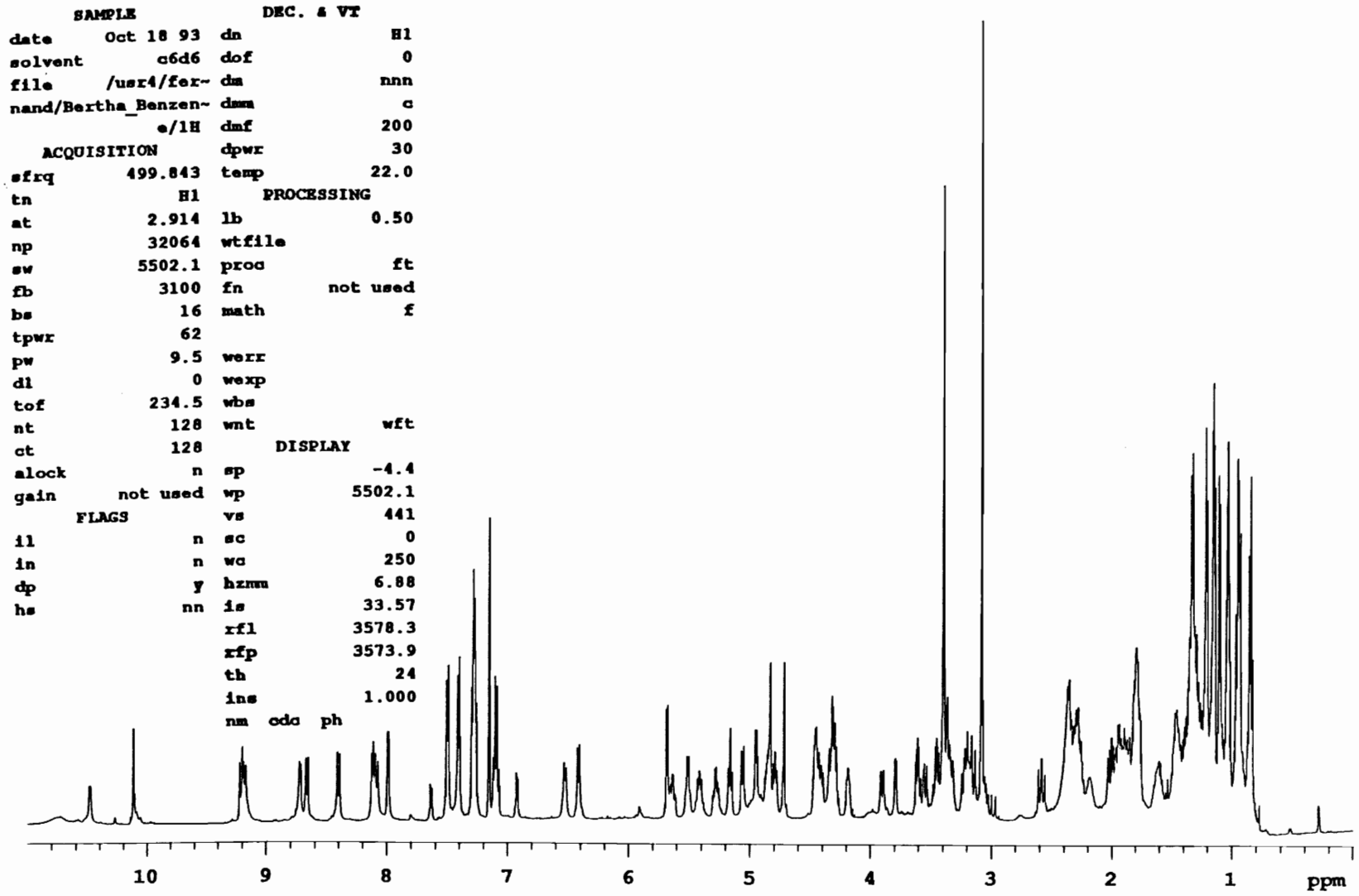

Figure 2.3. 500 MHz proton NMR spectrum of vitilevuamide

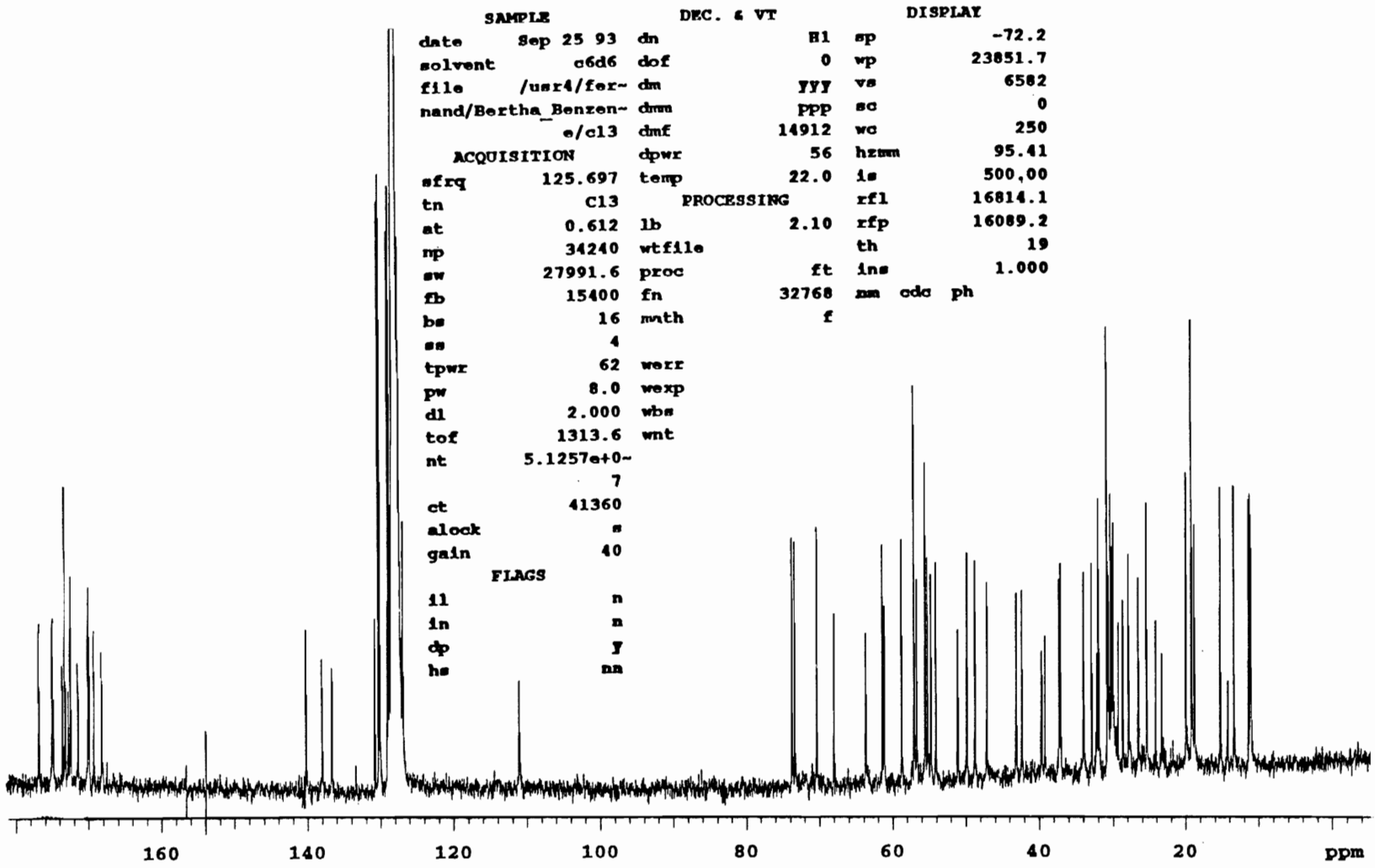

Figure 2.4. 125 MHz carbon NMR spectrum of vitilevuamide

Another experiment that validates data obtained from carbon and proton experiments and provides additional resolving power is the HMQC-TOCSY [66-68] (Appendix A). By first transferring ^{1}H magnetization via the large scalar one-bond coupling to (and back from) the attached carbons then proceeding with the isotopic mixing step, a spectrum is obtained that identifies the ^{1}H-^{1}H spin systems by the chemical shifts of the ^{1}H-bearing ^{13}C's in the spin system.

Thus for an amino acid the magnetization is first transferred from the α-proton to the α-carbon and back, labeling the ^{1}H magnetization with the chemical shift of that carbon. This magnetization is then propagated throughout the entire ^{1}H spin system via spin lock, labeling each proton in the spin system with the chemical shift of the carbon on which the magnetization originated. In a 2D spectrum, we see cross peaks to the NH, α and β-protons at the chemical shift of the α-carbon (Figure 2.5).

The above mentioned experiments gave information on the various amino acids present in the peptide; however sequential information was not obtained. Sequential assignment requires correlation across the amide bond, which separates the proton spin systems of adjacent amino acids. This can be done in two ways, using through space homonuclear correlation experiments or long range multiple bond correlation experiments.

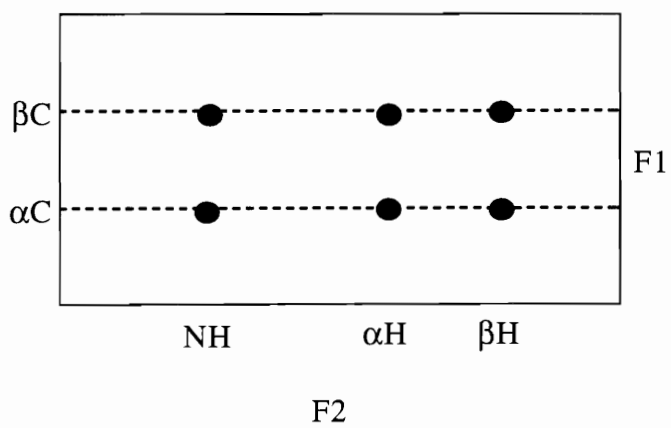

Figure 2.5. Schematic of a 2D $^{1}H\{^{13}C\}$-HMQC-TOCSY spectrum for Ala

When only homonuclear experiments can be used NOESY [69-72] or ROESY [73-76] provide necessary information.

The HMBC experiment [77] (Appendix A) that utilizes heteronuclear coupling, allows for the detection of cross peaks between adjacent spin systems thus permitting sequential assignment of amino acids in a peptide. The experiment can be optimized to detect correlations between protons and carbons having a certain coupling constant. This allows two three or four bond connectivities to be assigned. In the case of vitilevuamide, different experiments were optimized to observe coupling constants of 6, 8 and 10 Hz. Linear prediction [78] of the free induction decay (FID) was performed on the HMBC (J = 8 Hz). The FID was extended in the positive direction in order to improve the resolution of the 2D spectrum acquired.

A 200 and 500 millisecond (ms) Rotating Frame Overhauser Enhancement Spectroscopy (ROESY), (Appendix A) was also performed to detect Nuclear Overhauser Effect (nOe) signals between amide and aliphatic protons. These nOe signals correspond to short distances and are usually observed for sequentially adjacent residues.

Analysis of NMR Data

From the ^{1}H NMR data it was evident that the peptide had a minimum of twelve amino acids, one of which lacked an α-proton. The ^{13}C, DEPT and HMQC experiments helped define the multiplicities of the carbons and assign their respective protons. Based on the above experiments the degenerate aromatic carbons were assigned to the ortho and meta-carbons of Phe 9 and 13. Threonine (Thr) and N-methyl methoxinine (Nmm) contain overlapped α-carbons (C49 and C5) at 57.03 ppm and the α-carbons of Phe 9 (C40) and Lanthionine (Lan) 14 coalesce at 55.40 ppm (C72).

In the case of two overlapped protons at 2.29 ppm in the ^{1}H NMR spectrum, the HMQC experiment allowed for distinction between the two different carbons they were bonded to. One of the protons was directly bonded to C17 at 43.06 ppm in

Table 2.2 NMR[a] assignments for vitilevuamide in C_6D_6

Atom no	$\delta\ ^{13}C$	(mult.)	$\delta\ ^{1}H$	(mult.,J (Hz))	HMBC correlations
N 1			8.66	(d, 8.79)	C14
1	170.09	(s)			
2	54.77	(d)	5.06	(ddd, 2.47,2.58,5.05)	C13, C14
3	63.60	(t)	3.91	(dd, 2.47,11.48)	C13
			4.33	(m)	
4	169.32	(s)			
5	57.03	(d)	5.68	(d,5.86)	C5,C14,C51
6	68.05	(t)	4.31	(m)	
7	70.17	(t)	3.61	(m)	
			3.45	(m)	
8	58.65	(q)	3.09	(s)	
9	32.49	(q)	3.40	(s)	C5
OH			3.77	(d, 4.44)	
N 3			8.12	(d, 6.90)	C4, C35, C55
10	173.63	(s)			
11	56.63	(d)	4.42	(m)	
12	30.58	(d)	2.26	(bm)	
13	19.12	(q)	1.03	(bm)	
14	18.95	(q)	0.93	(bm)	C35, C55, C66
N 4			8.09	(d, 10.66)	C1, C45
15	175.07	(s)			
16	54.09	(d)	5.27	(ddd, 4.46,10.45)	
17	42.77	(t)	2.29	(bm)	C1, C54, C67
			1.80	(bm)	
18	30.29	(d)	2.17	(m)	
19	18.72	(q)	1.10	(d, 6.78)	
20	30.74	(t)	1.48	(bm)	
			1.28	(bm)	
21	11.55	(q)	0.93	(bm)	
N 5			10.11	(s)	C8, C15
22	168.26	(s)			
23	140.21	(s)			
24	111.11	(t)	4.71	(s)	C8, C15, C16
			4.83	(s)	
N 6			8.00	(d, 5.23)	C7, C31, C48
25	172.49	(s)			
26	60.92	(d)	4.19	(bm)	C10, C48
27	36.94	(d)	1.89	(bm)	
27	11.55	(q)	0.93	(bm)	
28	15.01	(q)	1.21	(d, 6.76)	
29	25.10	(t)	1.78	(bm)	
			1.31	(bm)	
30	10.90	(q)	0.84	(bm)	

Table 2.2 contd.

Atom no	δ ^{13}C	(mult.)	δ ^{1}H	(mult.,J (Hz))	HMBC correlations
31	172.84	(s)			
32	50.94	(d)	4.79	(dd, 7.17,9.59)	C7, C47
33	31.95	(t)	3.16	(bs)	
			2.01	(dd, 15.34,17.38)	C7
34	174.99	(s)			
35	61.42	(d)	5.16	(dd, 7.6,15.1)	C2, C61
36	29.95	(t)	1.94	(bm)	C2, C44
			1.79	(bm)	
37	25.11	(t)	1.61	(bm)	
			1.44	(bm)	C30
38	47.01	(t)	3.20	(bm)	
			2.35	(bm)	
N9			10.49	(d, 4.95)	C11
39	169.96	(s)			
40	55.40	(d)	4.31	(m)	C11, C49
41	37.13	(t)	3.21	(bm)	C13, C17, C19, C37
			3.05	(bs)	C13, C17, C19, C37
42	136.28	(s)			
43	130.12	(d)	7.41	(d, 7.38)	C23
44	128.89	(d)	7.28	(m)	C17, C18
45	127.57	(d)	7.08	(d, 7.37)	C19
46	128.89	(d)	7.28	(m)	C17, C18
47	130.12	(d)	7.41	(d, 7.38)	C23
N10			8.72	(d, 6.26)	C3, C11
48	170.14	(s)			
49	57.03	(d)	4.95	(dd, 1.12,6.32)	C3, C11, C27
50	73.25	(d)	5.51	(ddd, 1.23,5.86,6.49)	C13
51	19.94	(q)	1.14	(d, 6.69)	
N11			9.22	(d, 9.87)	C3, C10
52	174.94	(s)			
53	49.81	(d)	5.62	(ddd, 3.35,10.05,10.89)	
54	42.29	(t)	1.97	(m)	C3
			1.87	(bm)	
55	31.83	(d)	1.78	(m)	
56	13.39	(q)	1.15	(d, 6.56)	
57	27.78	(t)	1.93	(bm)	
			1.40	(bm)	
58	11.22	(q)	1.03	(bm)	
N12			8.40	(d,10.43)	C6
59	171.49	(s)			
60	48.60	(d)	5.40	(q, 6.7,10.47)	
61	30.15	(d)	1.35	(bm)	C10, C43

Table 2.2 contd.

Atom no	$\delta\ ^{13}C$	(mult.)	$\delta\ ^{1}H$	(mult.,J (Hz))	HMBC correlations
N13			6.43	(d, 7.78)	C6, C9, C38, C50
62	173.28	(s)			
67	128.39	(d)	7.28	(m)	
68	127.00	(d)	7.10	(d, 7.58)	
69	128.39	(d)	7.28	(m)	
70	129.82	(d)	7.50	(d, 7.38)	
N14			6.54	(d, 8.22)	C6
71	172.54	(s)			
72	55.40	(d)	4.44	(bm)	
73	39.48	(t)	3.33	(m)	
			2.59	(dd, 11.66,14.12)	C2, C36, C52
74	173.28	(s)			
75	30.41	(t)	3.38	(bm)	
			1.86		
76	28.61	(t)	2.29	(bm)	
			1.78	(bm)	
77	176.82	(s)			

[a] Proton and carbon data were acquired at 500 and 125 MHz, respectively.

[b] From a DEPT experiment.

[c] The HMBC experiment was optimized to observe $^{n}J_{CH}$ couplings of 8 Hz.

homoisoleucine (Hil) 4 whereas the other belonged to the succinate side chain and was attached to C76 at 28.61 ppm. Table 2.2 contains the NMR assignments for **49**.

In the case of Hil 11, DQF-COSY correlations were observed from the amide-proton at 9.22 ppm to the α-proton at 5.62 ppm and from the α-proton to the two β-protons at 1.97 and 1.87 ppm. Correlations were observed further down the spin system from the β-protons to the γ-proton at 1.78 ppm which in turn shows a vicinal connectivity to the γ methyl (C56) at 1.15 ppm and the ε protons at 1.40 and 1.93 ppm respectively. The spin system terminates with a correlation from the ε protons to the ε methyl (C58) at 1.03 ppm.

This established the presence of a Valine (Val), Thr, Lan, Ser, Isoleucine (Ile), Alanine (Ala), Proline (Pro), Dehydroalanine (Dha), two Phe, two Hil and an Nmm residue. Figure 2.6 depicts the amino acid spin networks derived from ^{1}H, ^{13}C, DEPT, DQF COSY and HMQC NMR experiments.

The α-proton of Nmm at 5.68 ppm shows a vicinal connectivity to the β-proton at 4.31 ppm. Correlations are seen from the 4.31 ppm proton to the two γ-protons at 3.61 and 3.45 ppm and the hydroxyl proton at 3.77 ppm. The COSY experiment does not provide any additional information. There was no indication of the relationship of the O-methyl protons and the N-methyl protons with the rest of the spin system. The presence of the N- and O-methyl group was confirmed by HMBC connectivity between the methyl singlets at 3.38 and 3.06 ppm to the α- and γ-carbons (C5 and C7) respectively.

Evidence for the presence of Lan was derived from an HMBC (J = 8 Hz) experiment. The 2.01 ppm β-proton of Lan 7 showed a two-bond connectivity to its α-carbon at 51.02 ppm (C32) and a three-bond connectivity to 39.48 ppm the β-carbon (C73) of Lan 14.

Similarly, the 2.59 ppm β-proton of Lan 14 showed a three-bond connectivity to the β-carbon (C33) of Lan 7. Figure 2.7 depicts the HMBC correlations. Figure 2.8 shows the HMBC trace through 2.01 ppm of Lan 7 and Figure 2.9 depicts the HMBC trace through 2.59 ppm of Lan 14.

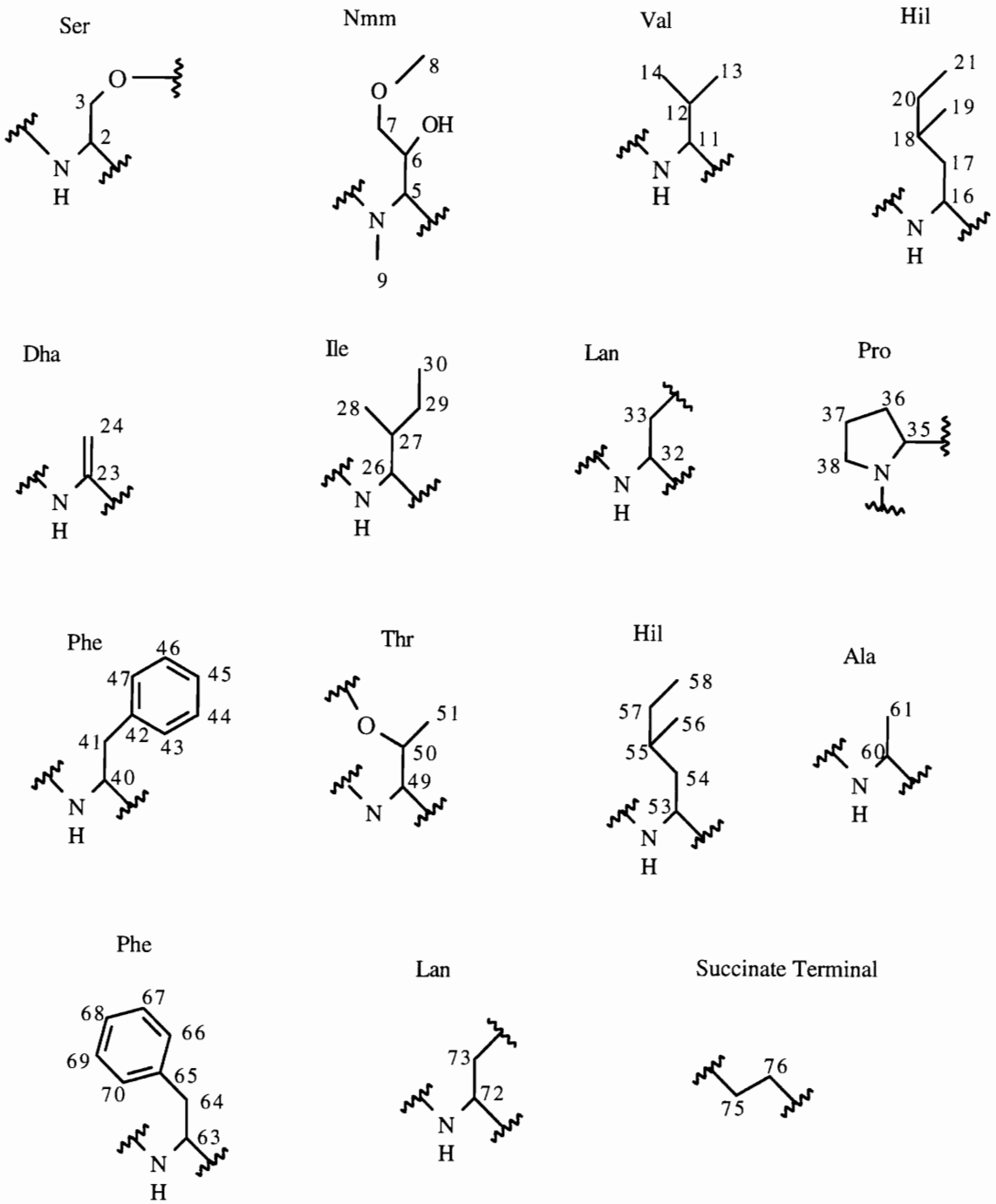

Figure 2.6 Proton, Carbon, COSY, TOCSY and HMQC derived amino acid spin networks for vitilevuamide

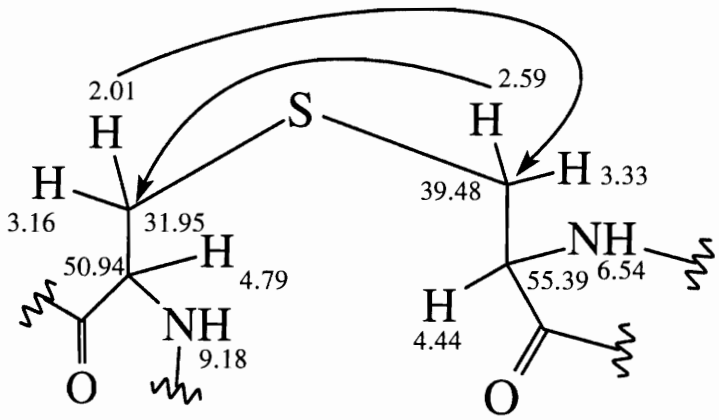

Figure 2.7. HMBC correlations for Lan

The presence of a terminal succinate residue was established by using a combination of DQF COSY, TOCSY, HMQC and HMBC experiments. COSY and TOCSY experiments established the connectivity between protons at 1.86, 3.38 ppm (C75) and 1.78, 2.29 ppm (C76). HMBC experiments showed a two-bond correlation between the proton at 2.29 ppm and the carbonyl at 176.87 ppm (C77), whereas the proton at 1.78 ppm showed correlations to both carbonyls at 176.87 (C77) and 173.28 ppm (C74).

Because of the degeneracy of the 1.78 proton, an HMBC trace through the 1.78 ppm proton showed correlations to Ile 6 (C27 at 36.94 ppm, C28 at 15.01 ppm, C29 at 25.10 ppm and C30 at 10.90 ppm) and Pro 8 (C34 at 175.00 and C35 at 61.38 ppm). Figure 2.10 shows the HMBC correlations of the terminal succinate and Figures 2.11 and 2.12 depict the HMBC traces through protons 2.29 and 1.78 ppm respectively. The ambiguity in the chemical shift of the carbons in HMBC experiment and ^{13}C NMR experiment is due to lack of digital resolution in the HMBC experiment.

A characteristic feature of this peptide is an ester link between the oxygen of Thr 10 and the carbonyl of Ser 1. This was evident from a three-bond correlation between the β-proton of Thr (5.50 ppm) and the carbonyl of Ser at 169.85 ppm (C4) in an HMBC

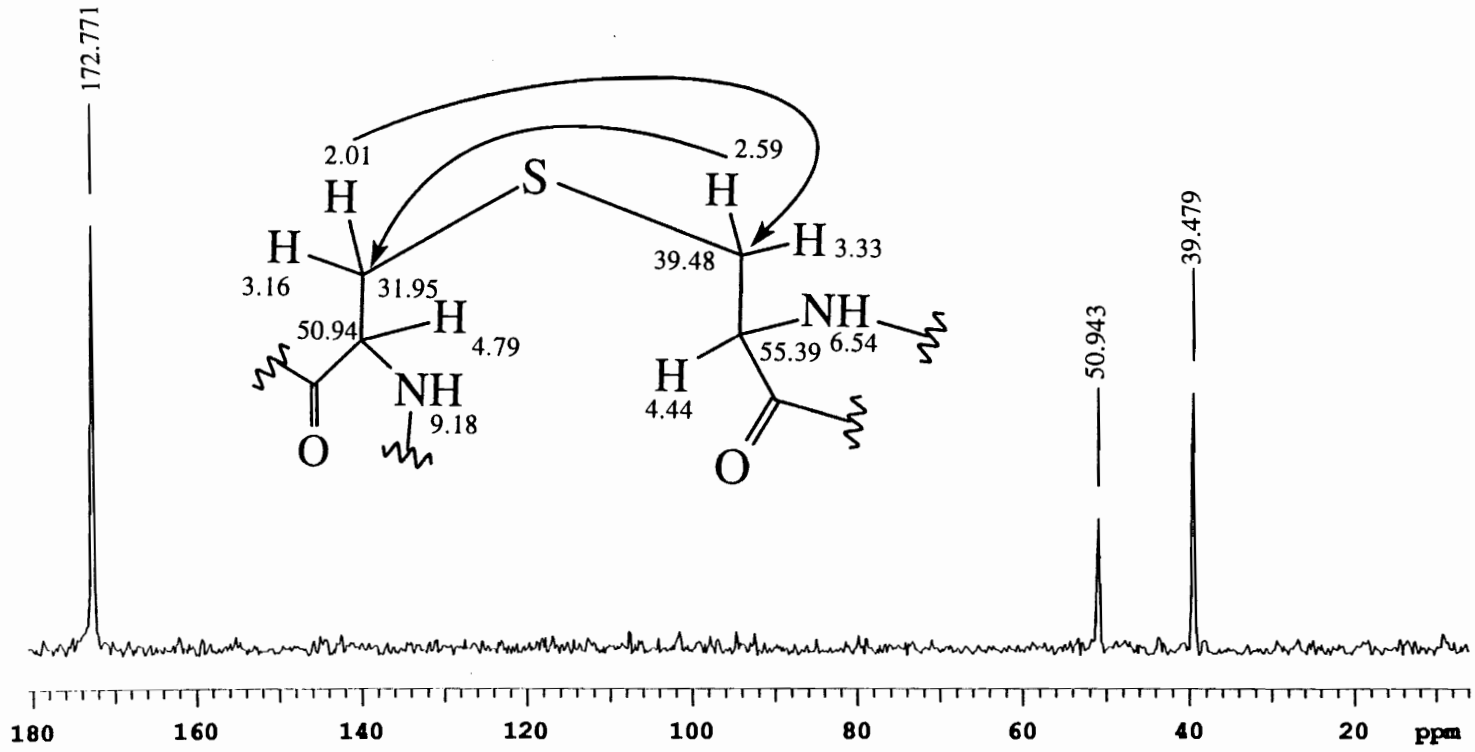

Figure 2.8 HMBC trace through 2.01ppm of Lan 7

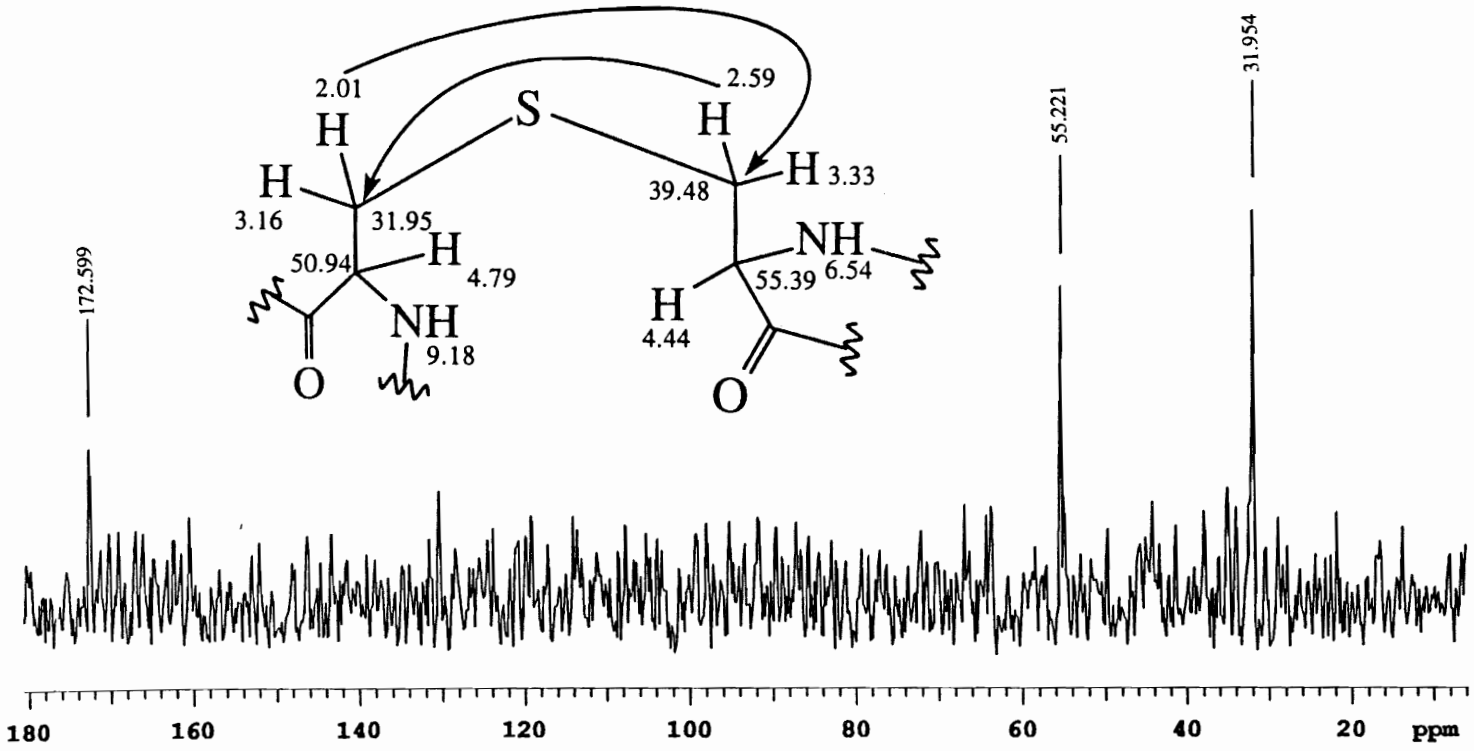

Figure 2.9 HMBC trace through 2.59 ppm of Lan 14

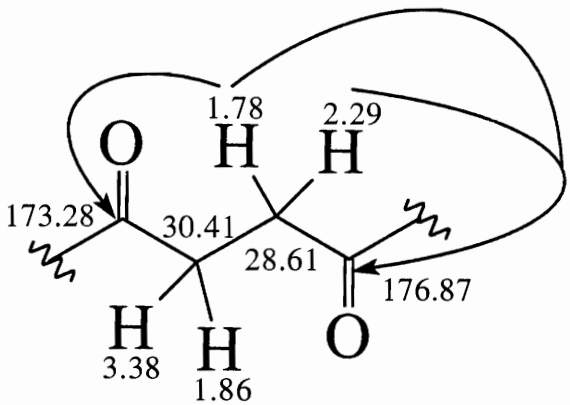

Figure 2.10 HMBC correlations for terminal succinate

experiment (J = 8 Hz). This accounted for the two missing degrees of unsaturation required by the molecular formula. A pictorial representation is shown in Figure 2.13 whereas the HMBC connectivity is depicted in Figure 2.14.

An HMBC trace through the α-proton of Val at 4.42 ppm shows a three-bond and a four-bond connectivity to carbonyls at 173.63 (C10) and 175.00 (C15) ppm respectively as depicted in figure 2.15. This trace also shows correlations to carbons at 30.58 ppm (C12) and 18.95 ppm (C14) belonging to the same spin system.

A similar trace through the amide proton of Nmm at 5.68 ppm showed a two- and three-bond connectivity to carbonyls at 173.62 (C10) and 169.17 ppm (C4) respectively, along with correlations to 32.49 ppm (C9) and 70.17 ppm (C7) of the same spin system. This helped establish the sequence from Val to Nmm. The trace is depicted in Figure 2.16.

An HMBC trace through the amide proton at 8.66 ppm and the α-proton at 5.06 ppm of Ser showed two- and three-bond connectivities to carbonyls at 169.85 ppm (C1) and 169.32 ppm (C4) respectively. This is depicted in Figures 2.17 and 2.18. This allowed for the sequential assignment of Ser along with the other two amino acids. Earlier discussed HMBC correlations were suggestive of an ester linkage between Ser carbonyl (C1) and the hydroxy group of Thr.

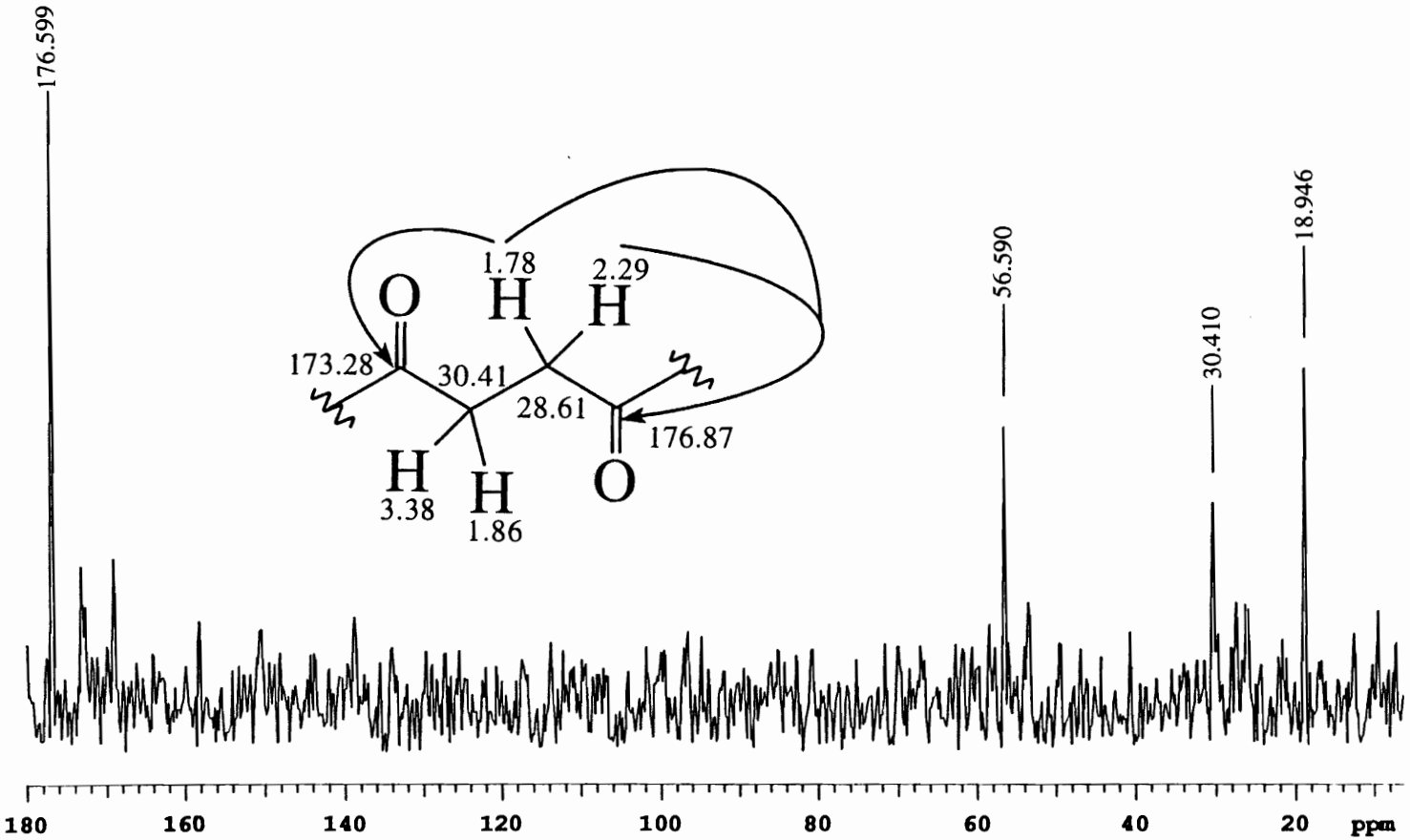

Figure 2.11 HMBC trace through 2.29 ppm of the terminal succinate

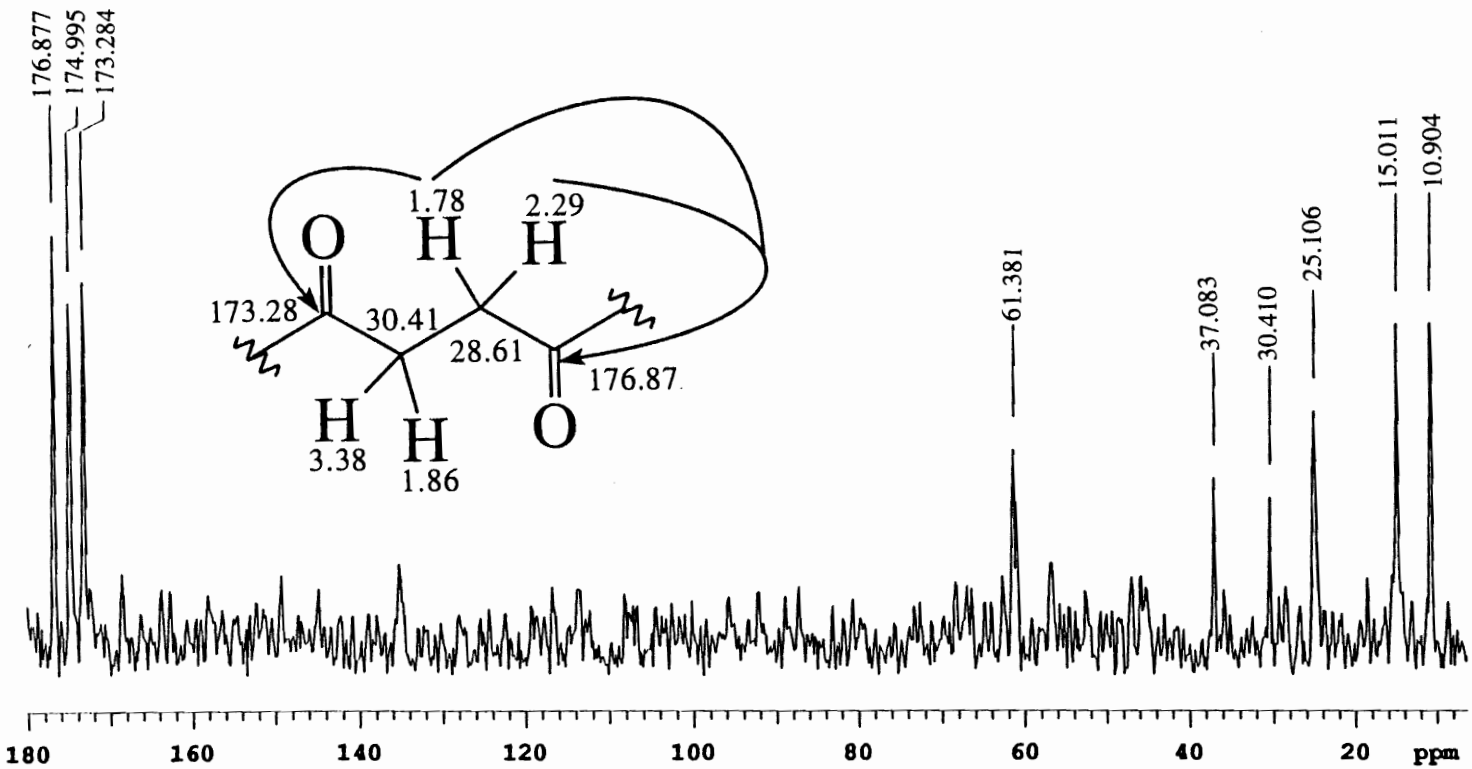

Figure 2.12 HMBC trace through 1.78 ppm of the terminal succinate

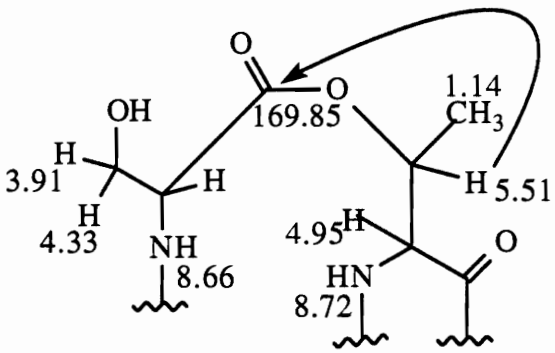

Figure 2.13. HMBC correlations of the depsipeptide link

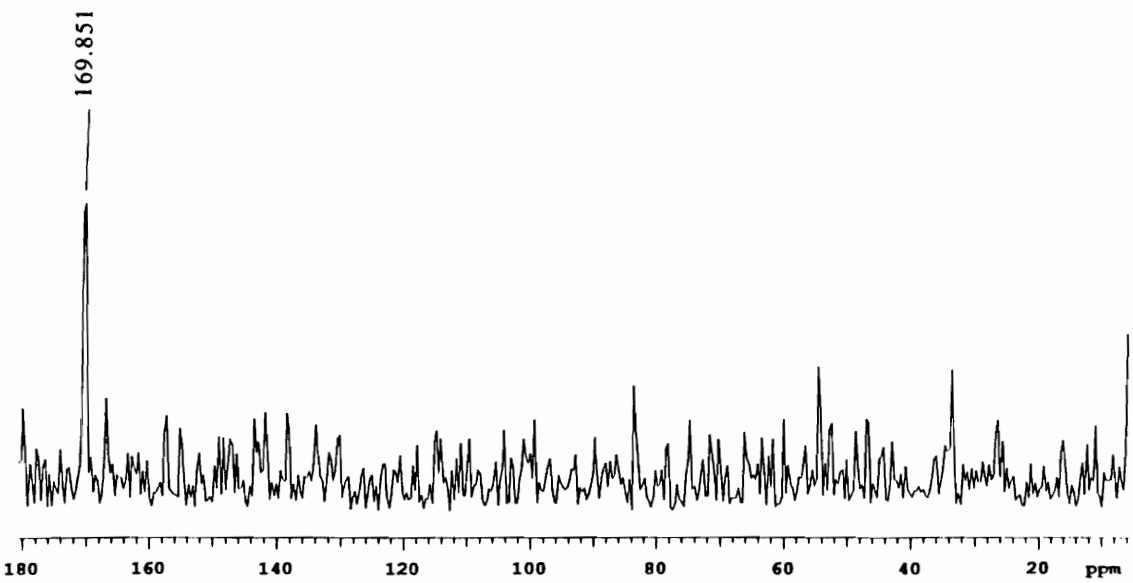

Figure 2.14. HMBC trace through 5.52 ppm of the depsipeptide link

An HMBC trace through the amide proton of Thr at 8.72 ppm showed two- and three-bond connectivities to carbonyls at 170.19 (C48) and 174.99 ppm (C52) respectively. This is depicted in Figure 2.19. A trace through the amide-proton at 10.49 ppm and the β-proton at 3.21 ppm of Phe 9 established a two- and three-bond connectivity to carbonyls at 170.19 (C48) and 169.85 (C39) ppm respectively. Correlations to carbons at 136.28 ppm (C42), 130.12 (C43, C47), and 55.40 ppm (C40) of the same spin system were also observed. This is depicted in Figures 2.20 and 2.21.

The sequential assignment continued with an HMBC trace through the β-proton of Pro at 1.94 ppm which showed a four-bond correlation to a carbonyl at 175.00 ppm depicted in Figure 2.22. The β-proton of Pro also showed correlations to carbons at 47.01 ppm (C38) and 25.11 ppm (C37). A trace through the δ-proton at 2.35 showing a correlation to the carbonyl at 169.85 ppm depicted in Figure 2.23. The sequential assignment could not be further continued without ambiguity.

An HMBC trace through the amide proton of Hil 11 at 9.22 ppm showed two- and three-bond correlations to carbonyls at 171.56 and 174.99 ppm respectively as depicted in Figure 2.24. A trace through the amide proton of Ala at 8.40 ppm showed a two-bond correlation to 173.28 ppm whereas a trace through the methyl protons at 1.35 ppm showed a three-bond correlation to 171.56 ppm (C59) and a two-bond correlation to 48.60 ppm (C60). This is depicted in Figures 2.25 and 2.26 respectively.

An HMBC trace through the amide proton of Phe 13 at 6.43 ppm showed a two-bond correlation to the carbonyl at 172.60 ppm (C71). The β-proton at 3.57 ppm showed a three-bond correlation to the carbonyl at 173.28 ppm (C62) which provided additional sequential information. It also showed two-bond correlations to carbons at 55.22 ppm (C63) and 137.87 ppm (C65) and three-bond correlations to 130.06 ppm (C66, C70). Four-bond correlations were observed to carbons at 129.82 ppm (C67, C69). This is depicted in Figures 2.27 and 2.28. This allowed for the partial sequential assignment of the amino acids as shown in Figure 2.29.

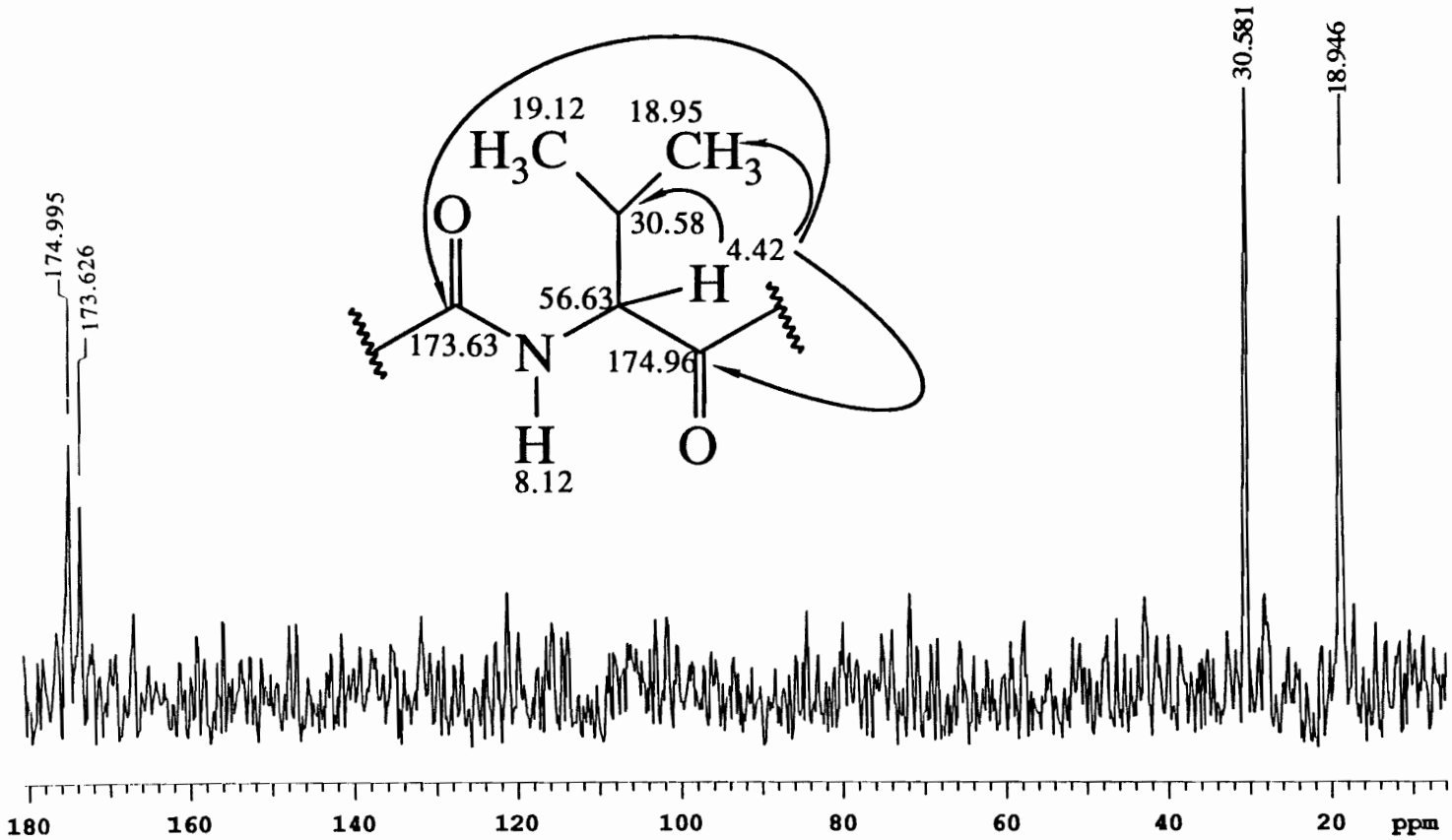

Figure 2.15. HMBC trace through 4.42 ppm of Val

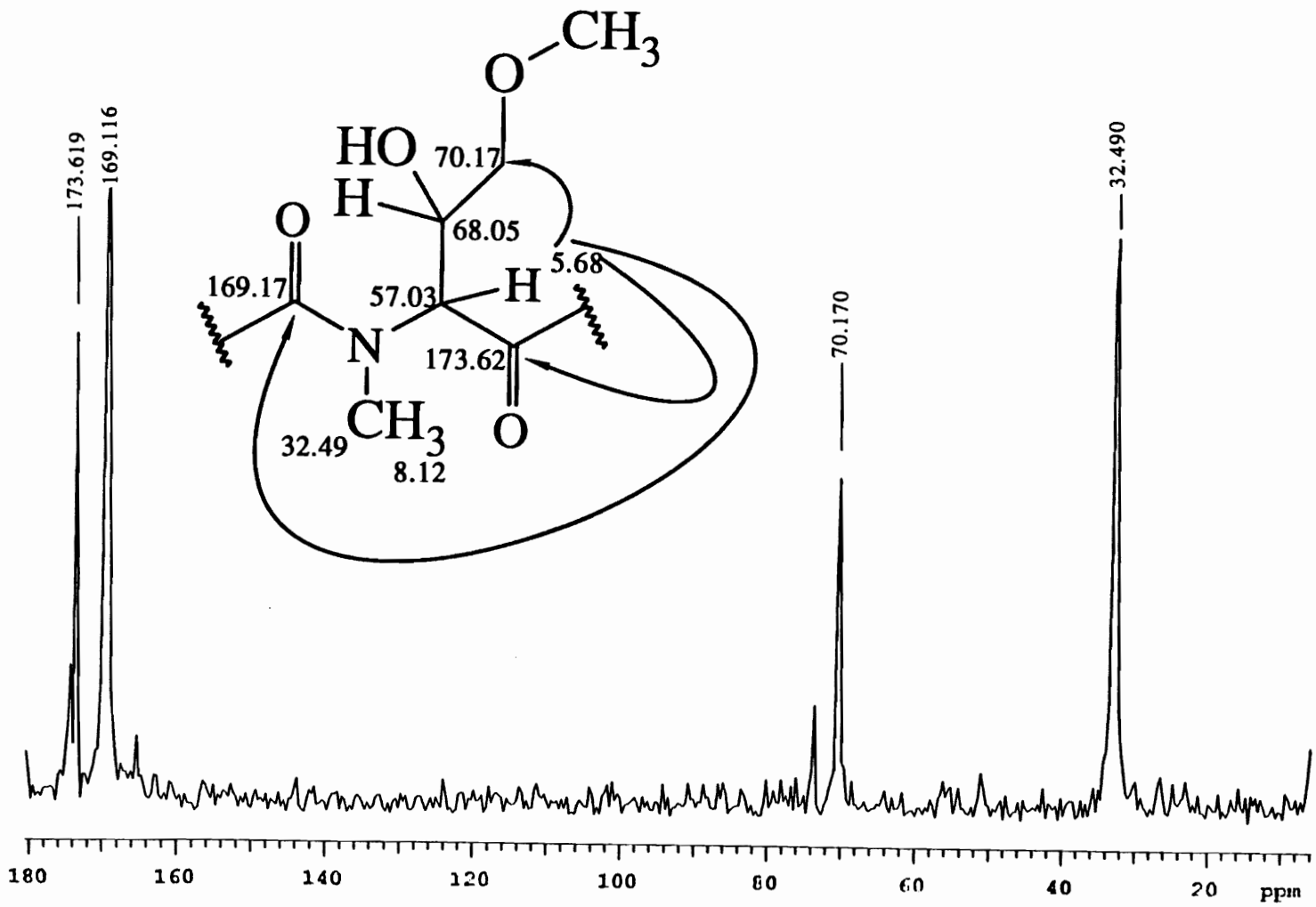

Figure 2.16. HMBC trace through 5.68 ppm of Nmm

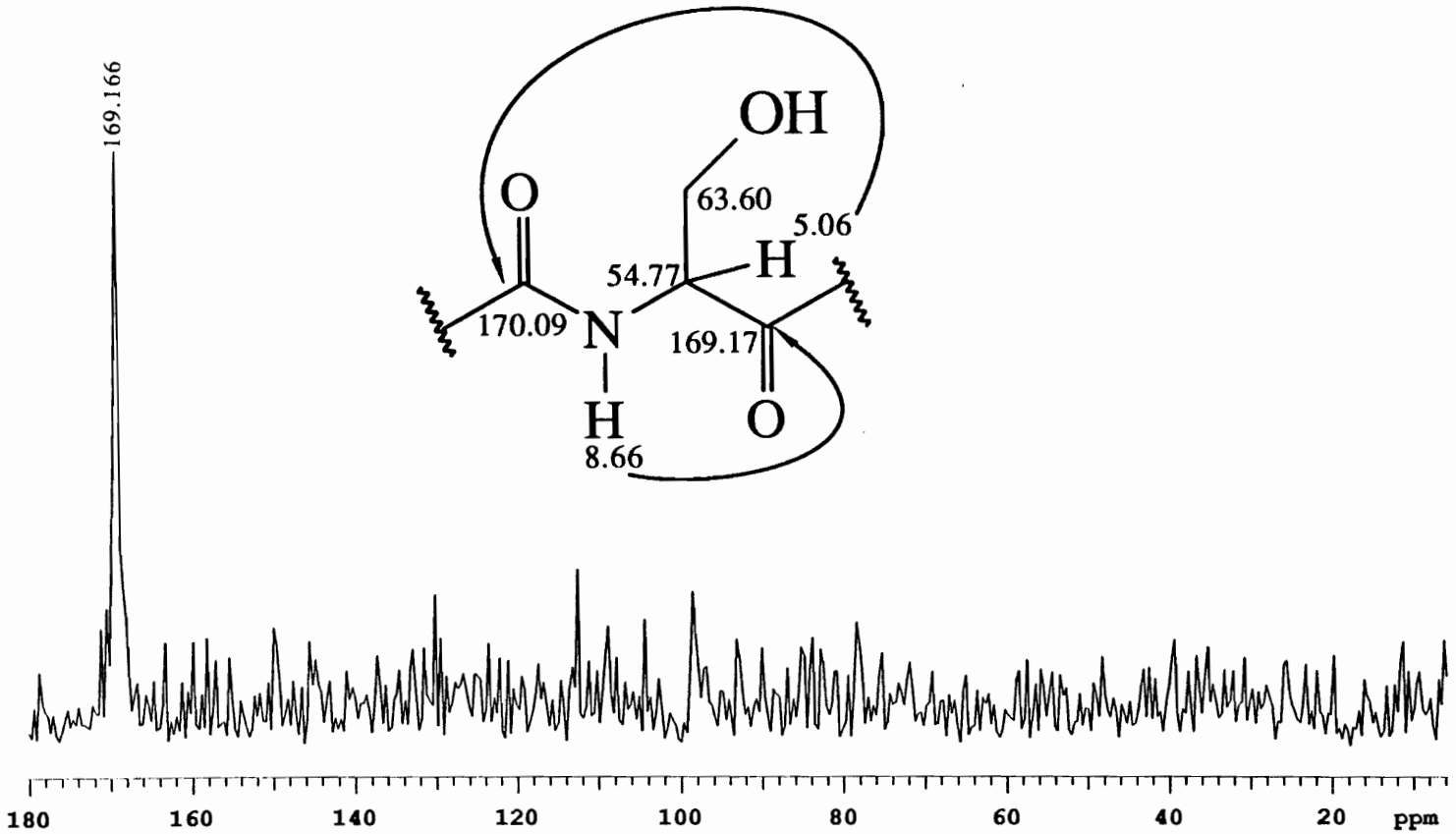

Figure 2.17. HMBC trace through 8.66 ppm of Ser

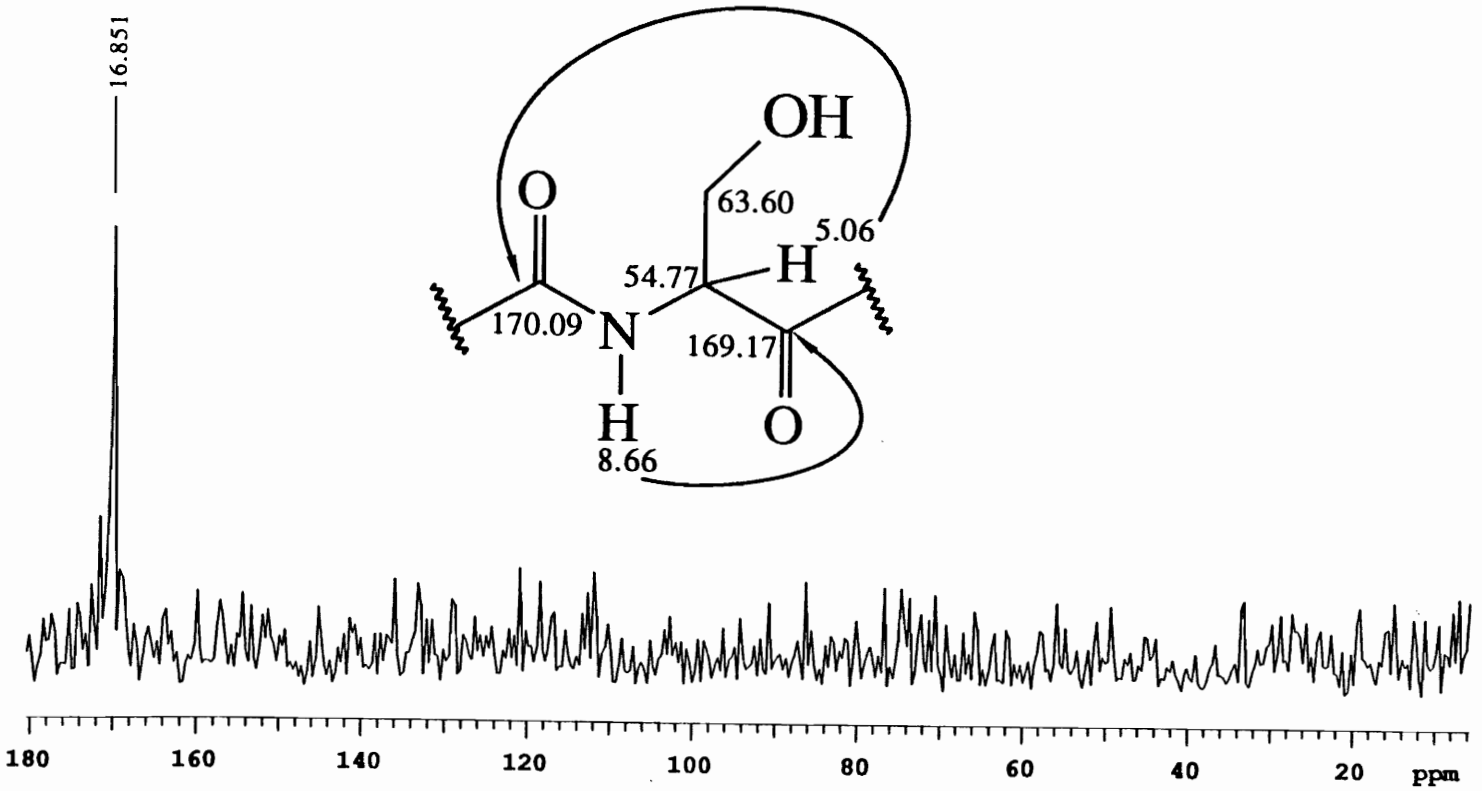

Figure 2.18. HMBC trace through 5.06 ppm of Ser

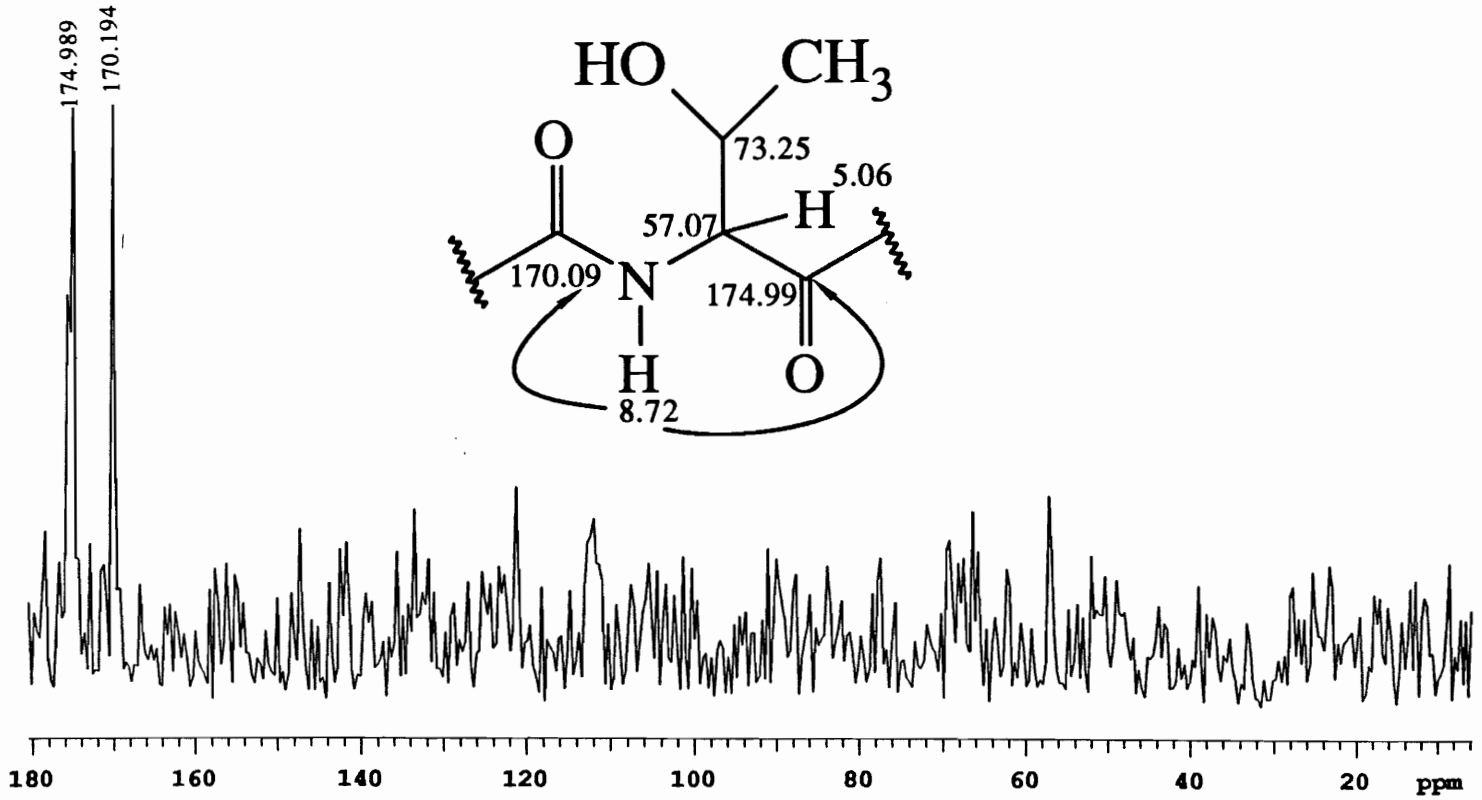

Figure 2.19. HMBC trace through 8.72 ppm of Thr

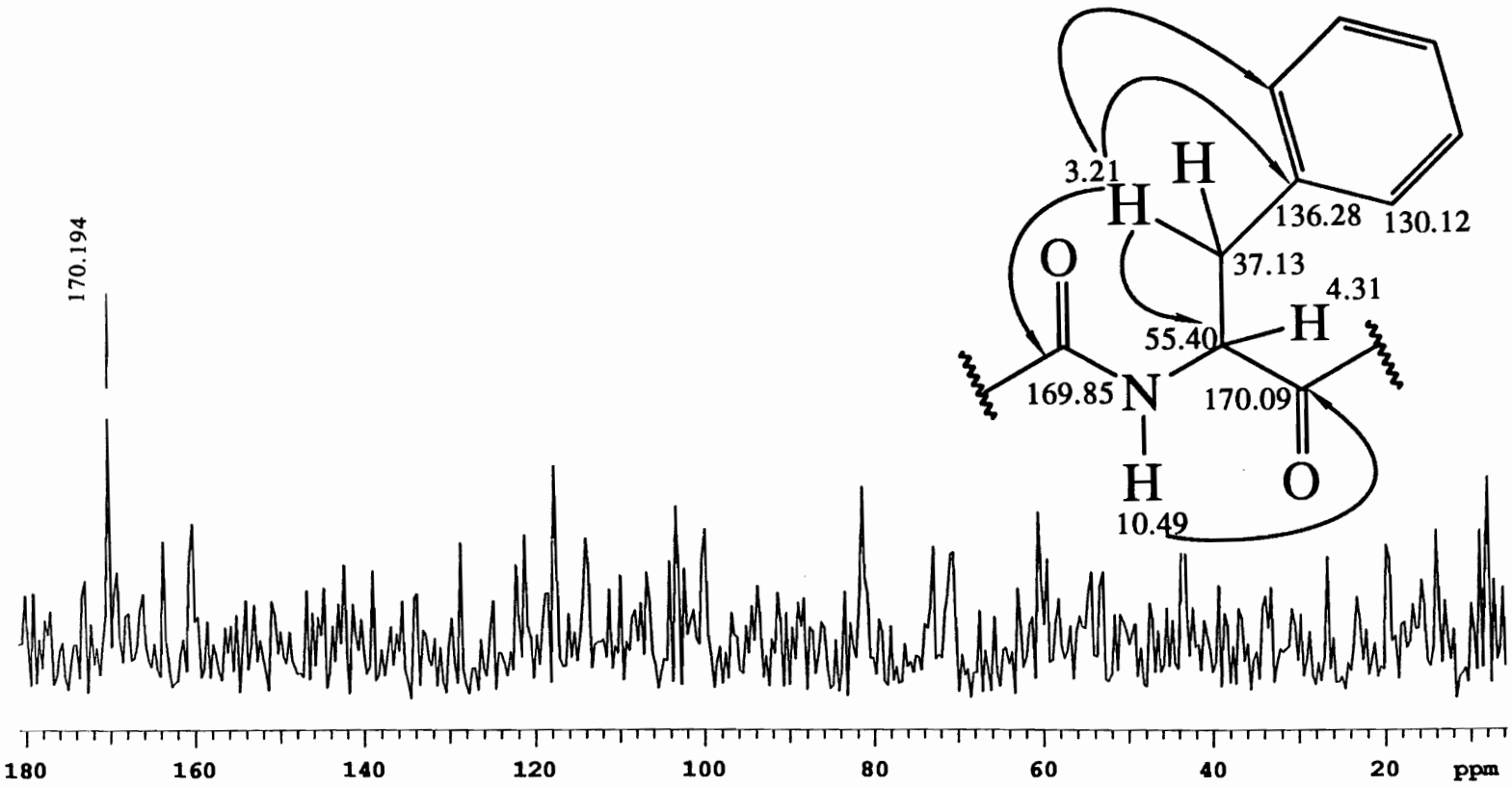

Figure 2.20. HMBC trace through 10.49 ppm of Phe

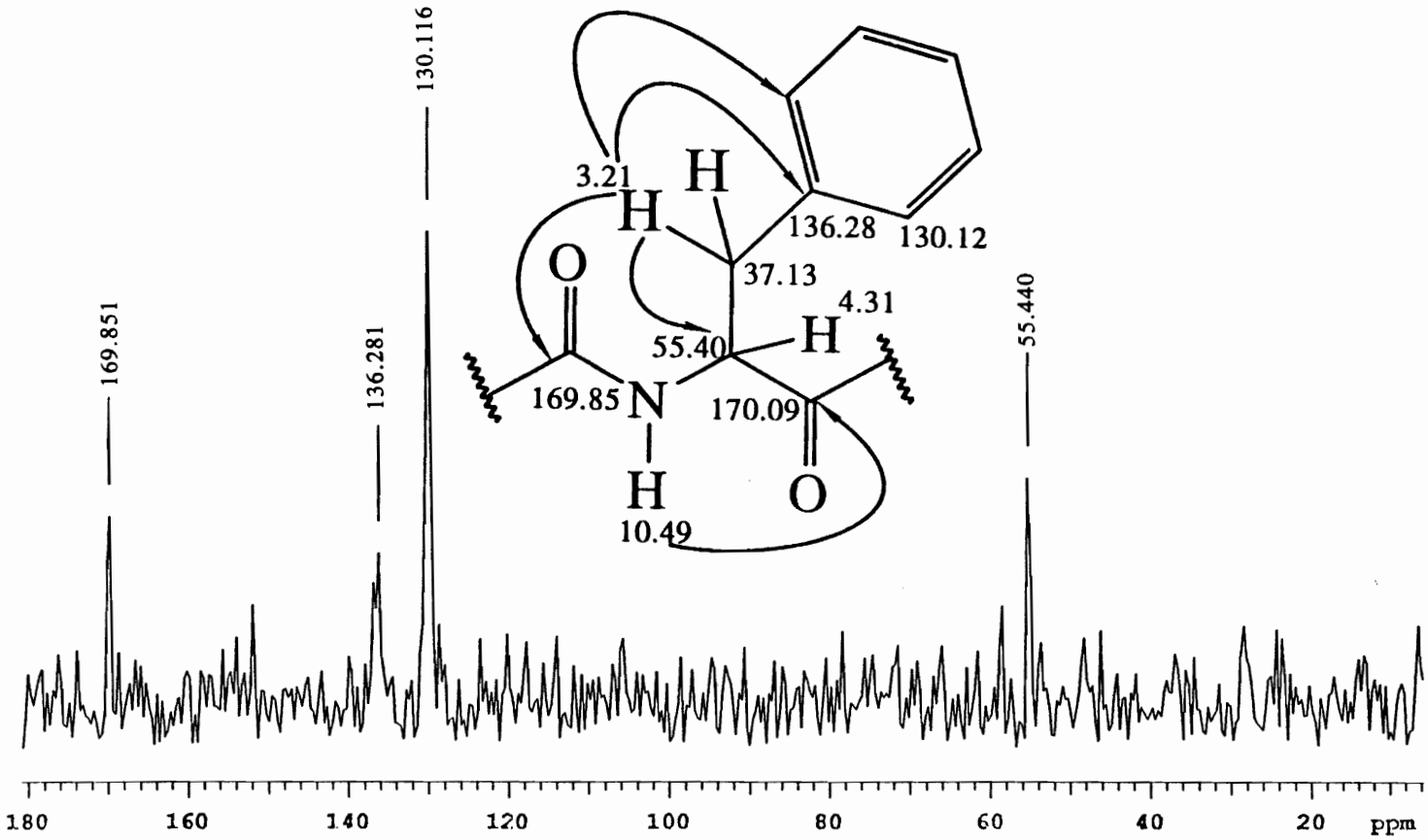

Figure 2.21. HMBC trace through 3.21 ppm of Phe

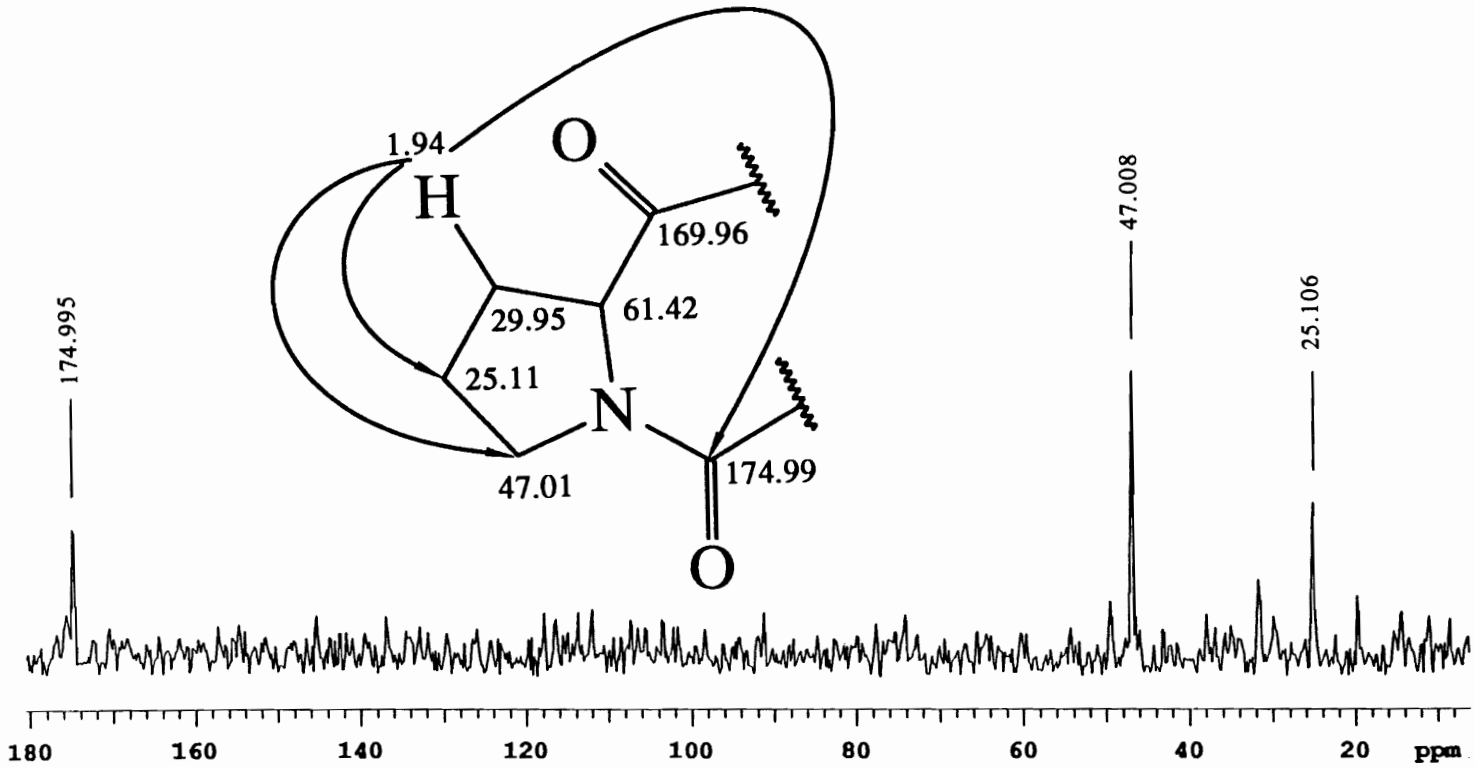

Figure 2.22. HMBC trace through 1.94 ppm of Pro

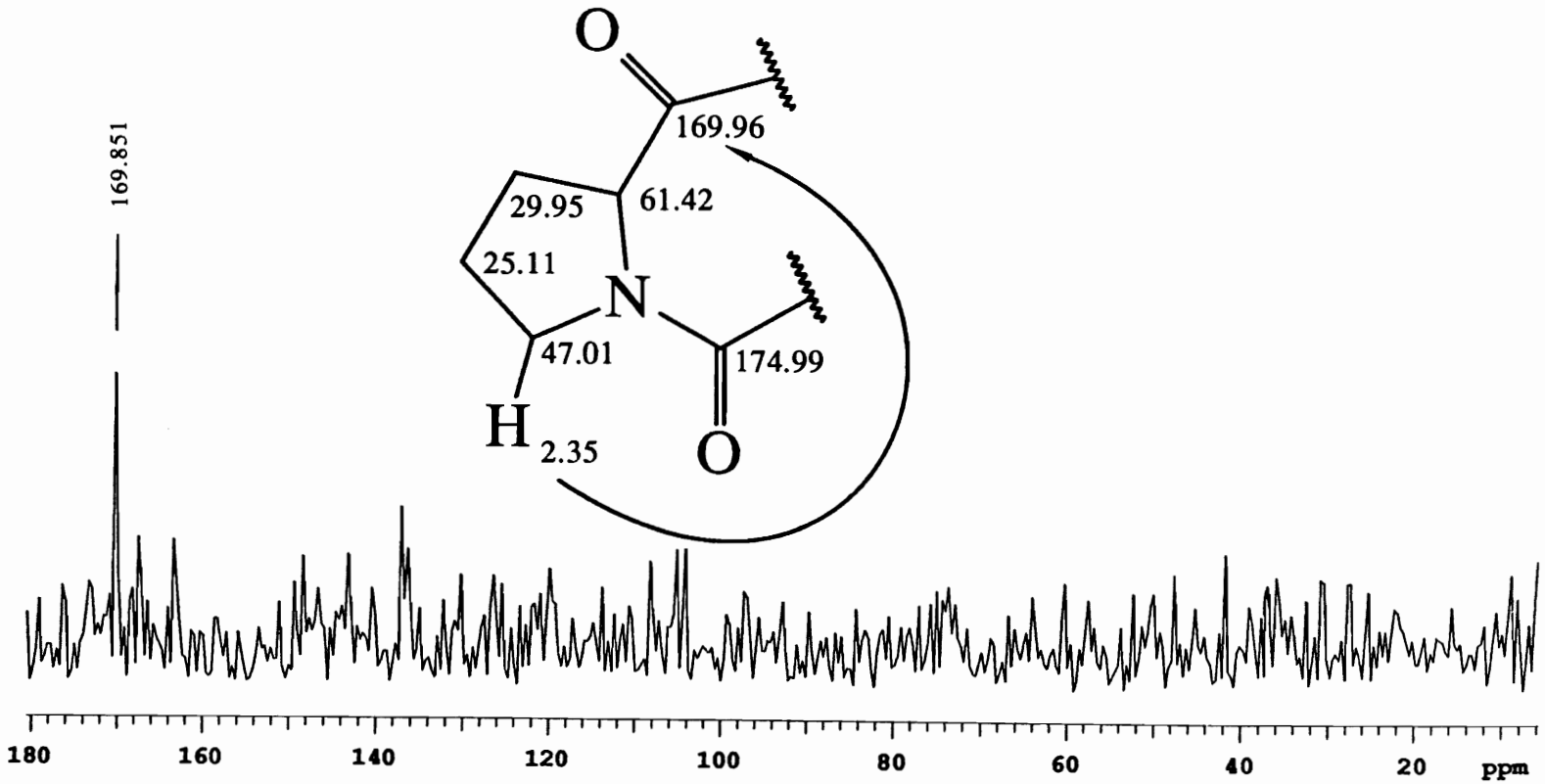

Figure 2.23. HMBC trace through 2.35 proton of Pro

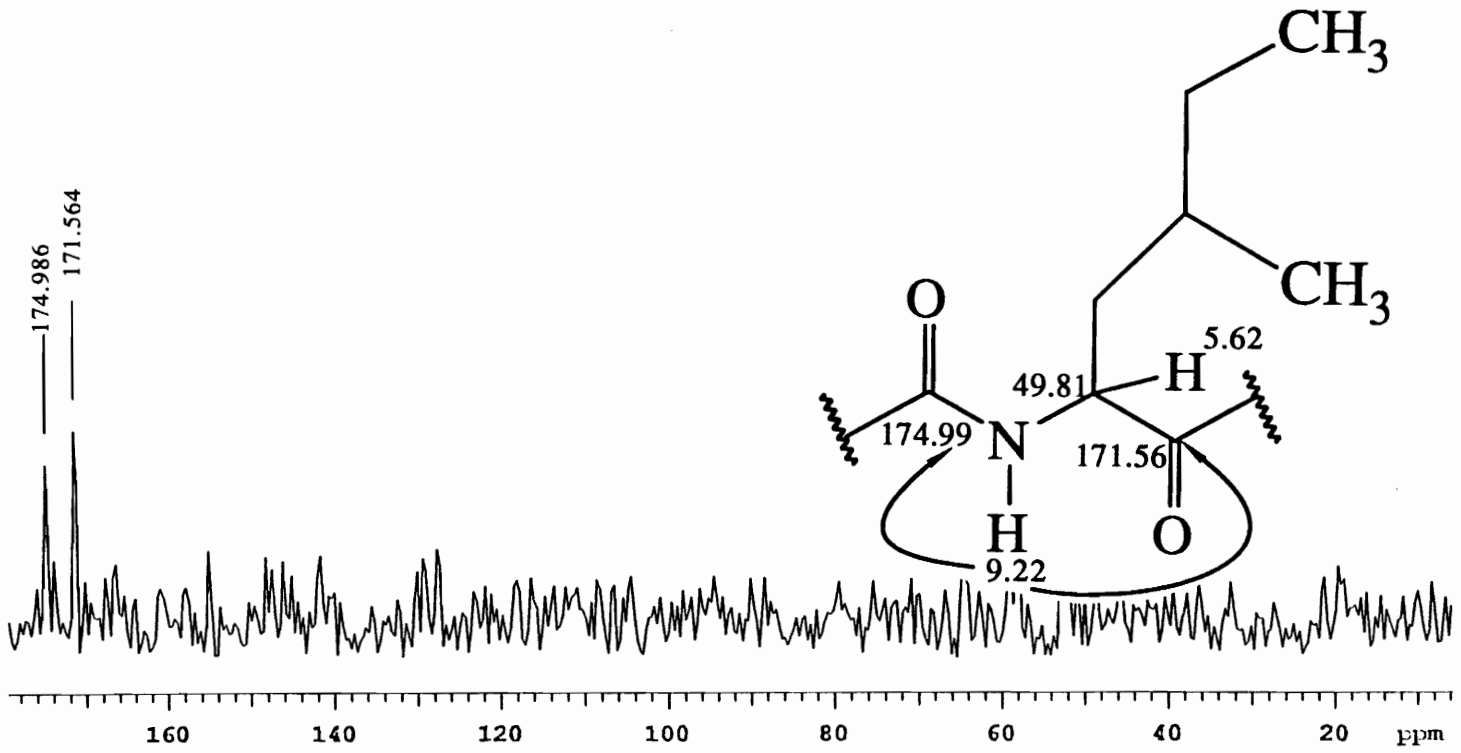

Figure 2.24. HMBC trace through 9.22 proton of Hıl 11

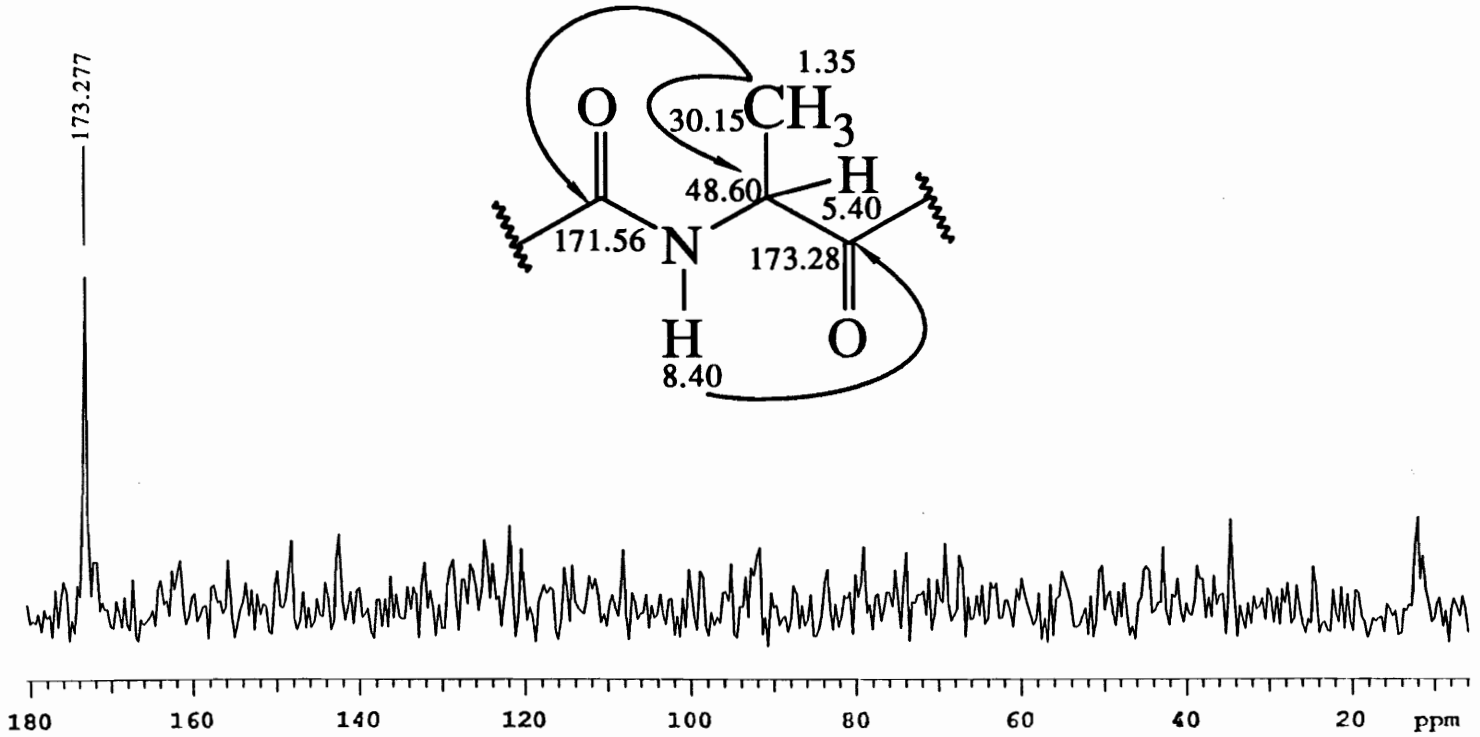

Figure 2.25. HMBC trace through 8.40 ppm of Ala

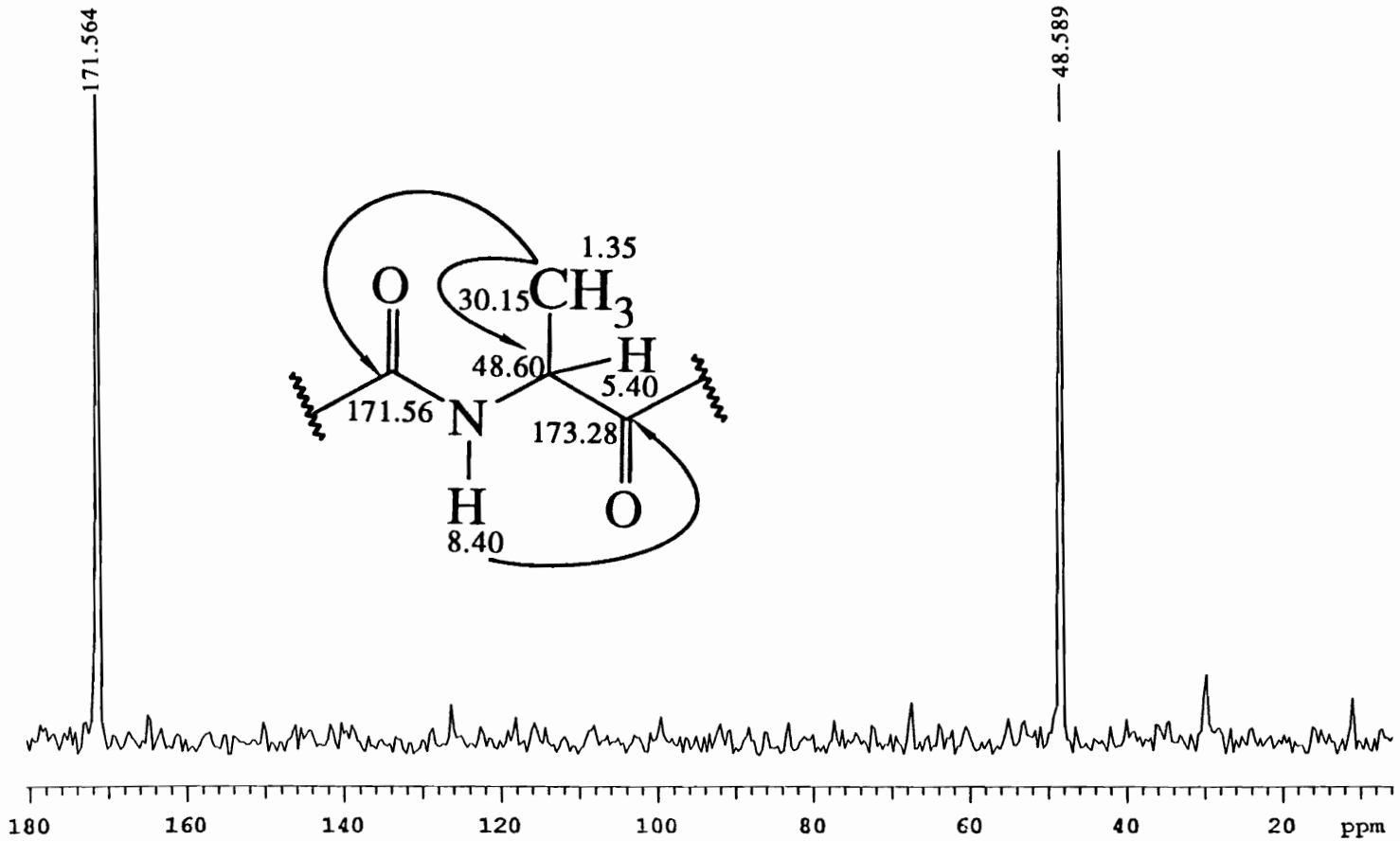

Figure 2.26. HMBC trace through 1.35 ppm of Ala

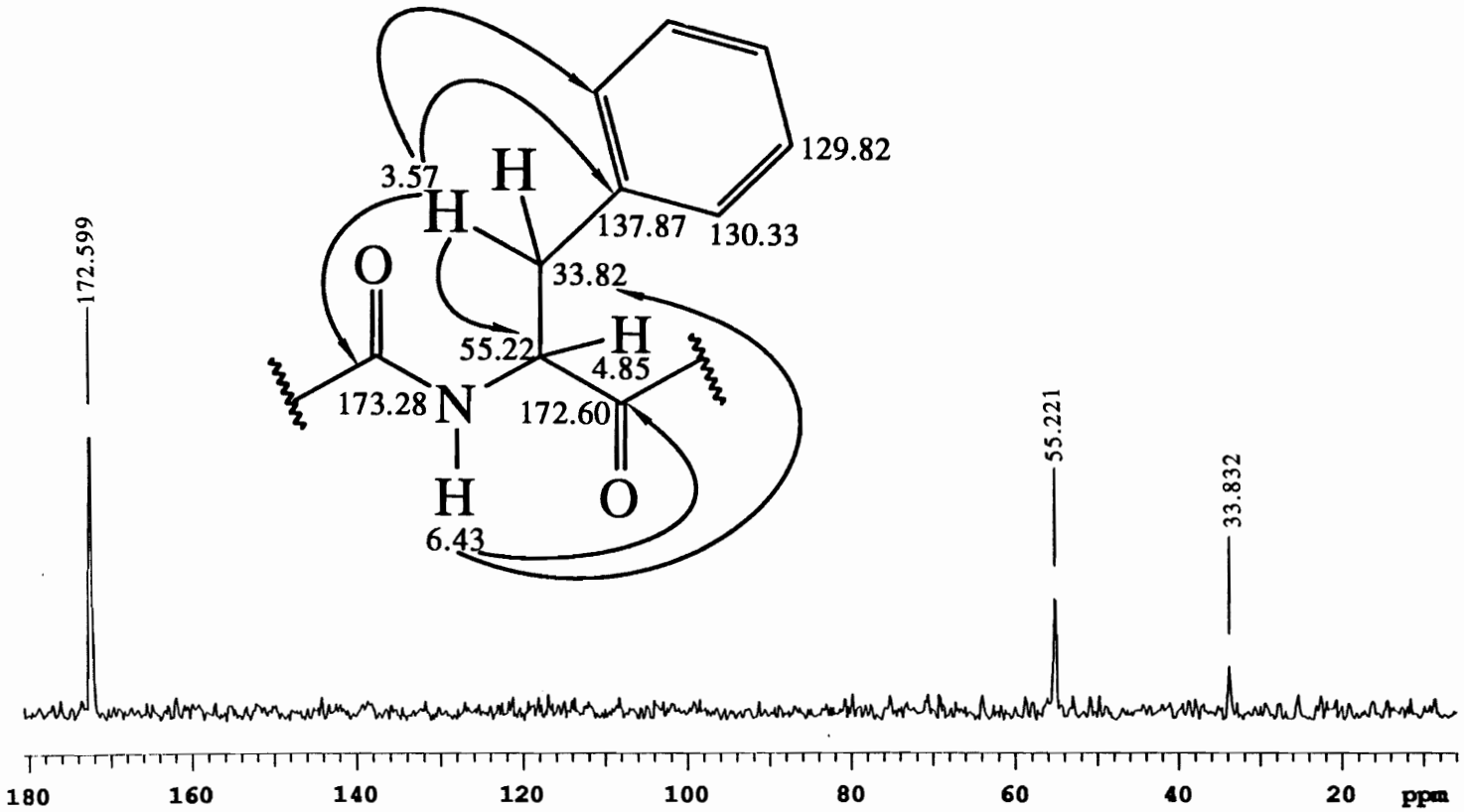

Figure 2.27. HMBC trace through 6.43 ppm of Phe 13

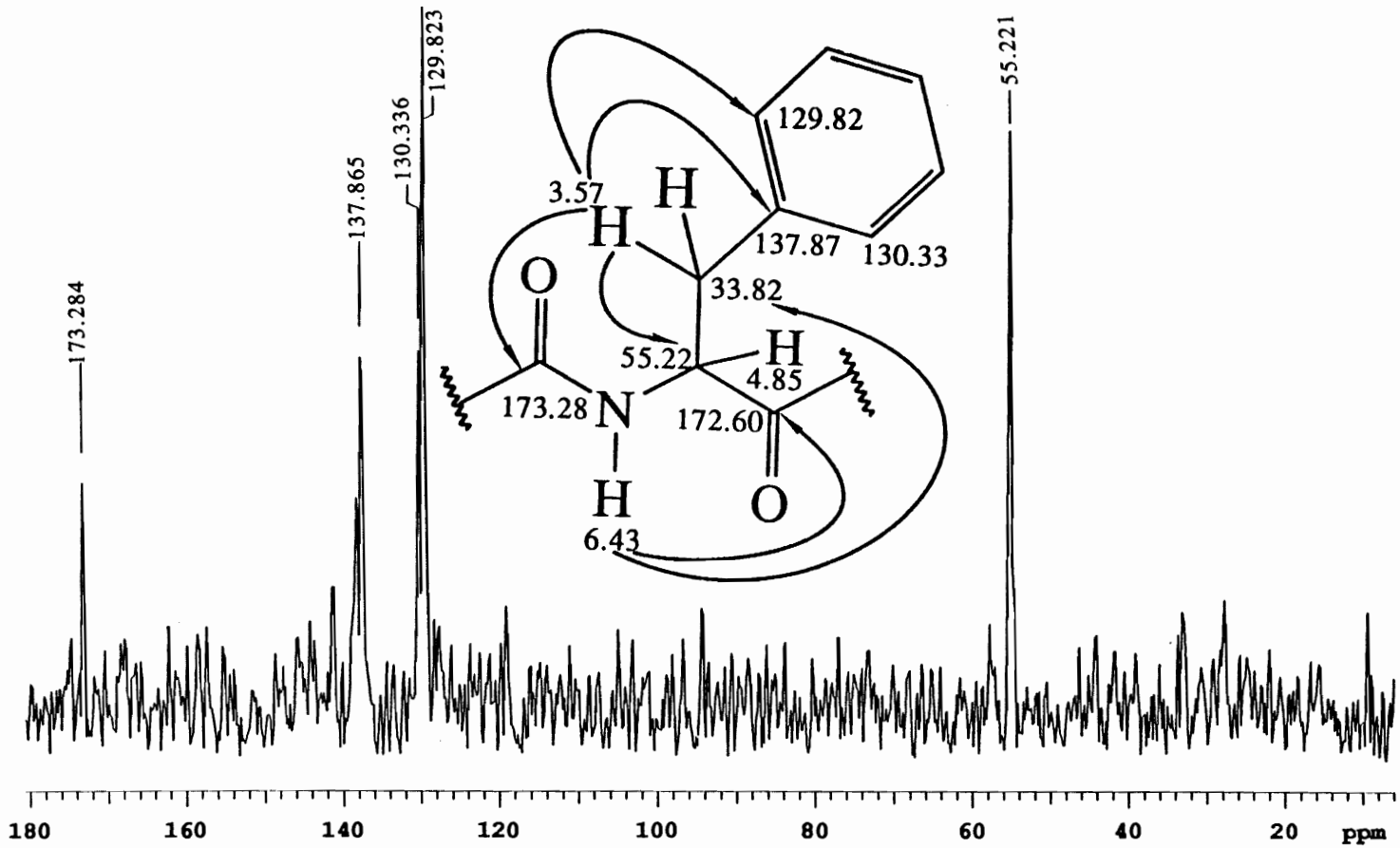

Figure 2.28. HMBC trace through 3.57 ppm of Phe 13

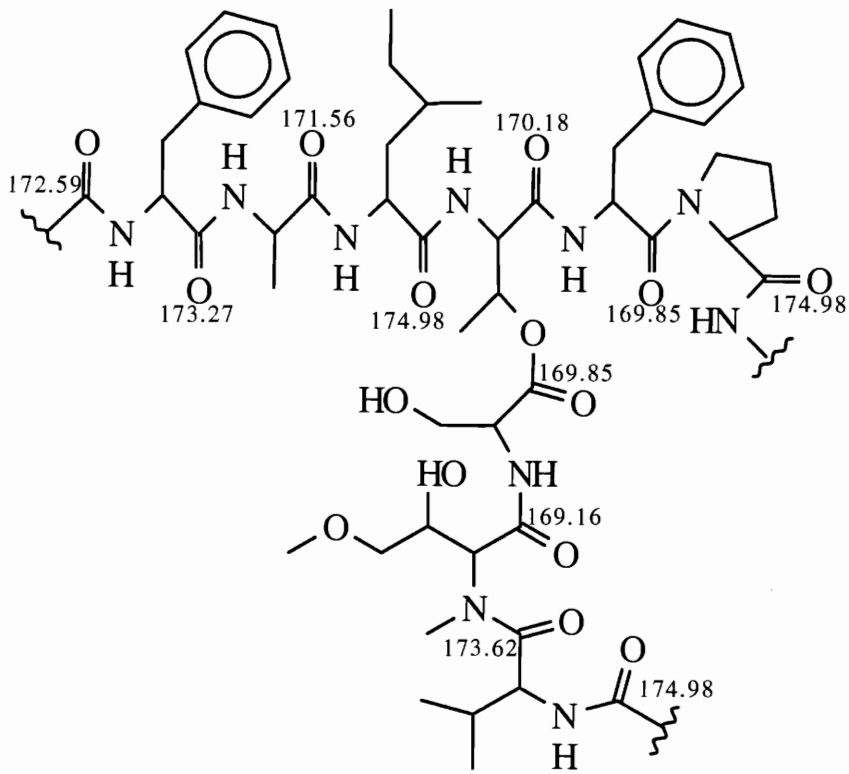

Figure 2.29. Partial sequential assignments of vitilevuamide

An HMBC trace through the β proton of Dha at 4.71 ppm showed three- and four-bond correlations to carbonyls at 168.14 and 172.59 ppm along with a two bond correlation to the α-carbon at 140.05 ppm (C23) as depicted in Figure 2.30. A trace through the Hil 4 amide proton at 8.09 ppm showed a two-bond correlation to the carbonyl at 168.14 ppm (C22) and a three-bond to the β-carbon at 42.77 ppm (C17).

A trace through the α-proton of Hil 4 at 5.27 ppm showed a three-bond correlation to the carbonyl at 175.00 (C15) ppm as shown in Figure 2.31 and 2.32. An HMBC trace through the amide proton of Ile at 8.00 ppm showed a two-bond correlation to the carbonyl at 172.93 ppm (C31). Three- and four-bond correlations were observed to the α- and β-carbons within the same spin system at 60.92 ppm (C26) and 36.94 ppm (C27) respectively. A trace through the α-proton at 4.19 ppm showed a three-bond correlation to the carbonyl at 172.59 ppm (C25) and a two-bond correlation to a carbon at 36.94 ppm (C27). This is illustrated in Figures 2.33 and 2.34 respectively.

An HMBC trace through the Lan 7 amide proton at 9.18 ppm showed a two-bond correlation to the carbonyl at 175.00 ppm (C34) and its β-carbon at 31.95 ppm (C33). The α-proton at 4.79 ppm showed a three-bond correlation to the carbonyl at 172.93 ppm (C31) and a two-bond correlation to the β-carbon at 31.81 ppm (C33) as shown in Figures 2.35 and 2.36 respectively. An HMBC trace through the amide proton of Lan 14 at 6.54 ppm showed two- and three-bond correlations to carbonyls at 173.28 (C74) and 172.60 ppm (C71) respectively as shown in Figure 2.37.

The information derived from the above mentioned experiments allowed the sequential assignment of some of the amino acids. Figure 2.38 shows a pictorial representation of these sequences. The terminal carbonyls of these sequences showed multiple overlap with each other. Hence it was difficult to make unambiguous assignments in order to completely assign all amino acids in the structure. The HMBC experiment is an inverse detected experiment with greater resolution in the proton than in the carbon dimension. As a result a long range HETCOR[79] (Appendix A) experiment was performed

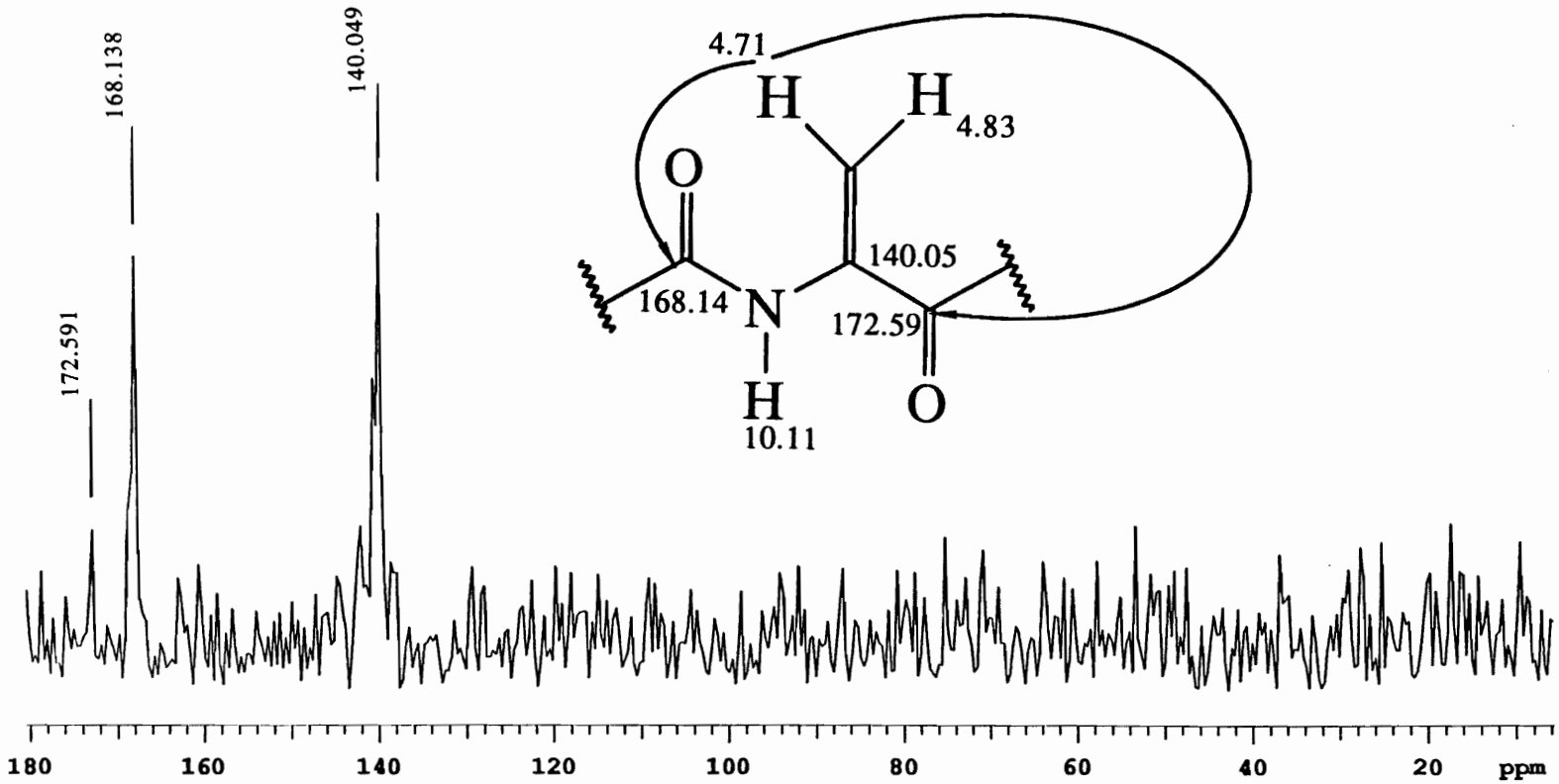

Figure 2.30. HMBC trace through 4.71 ppm of Dha

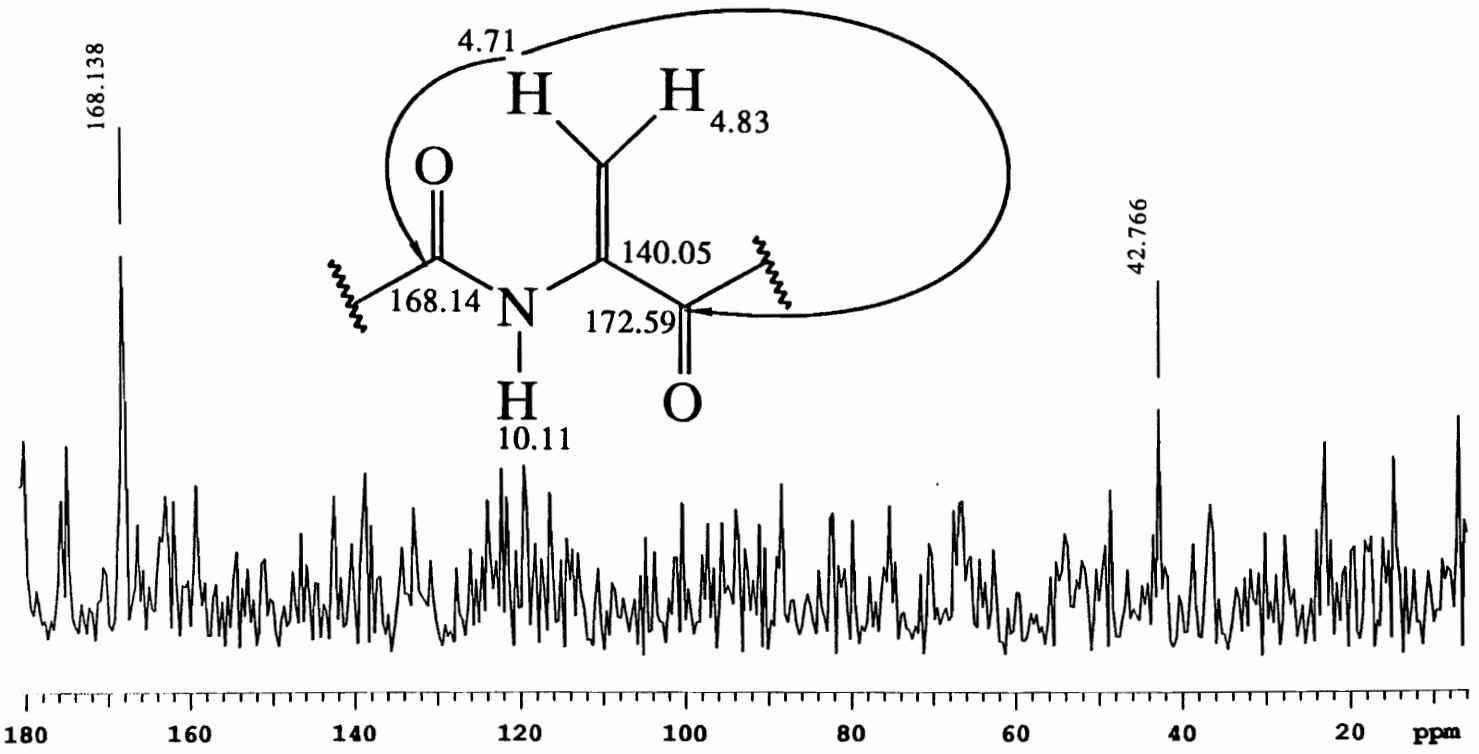

Figure 2.31 HMBC trace through 8.09 proton of Hil 4

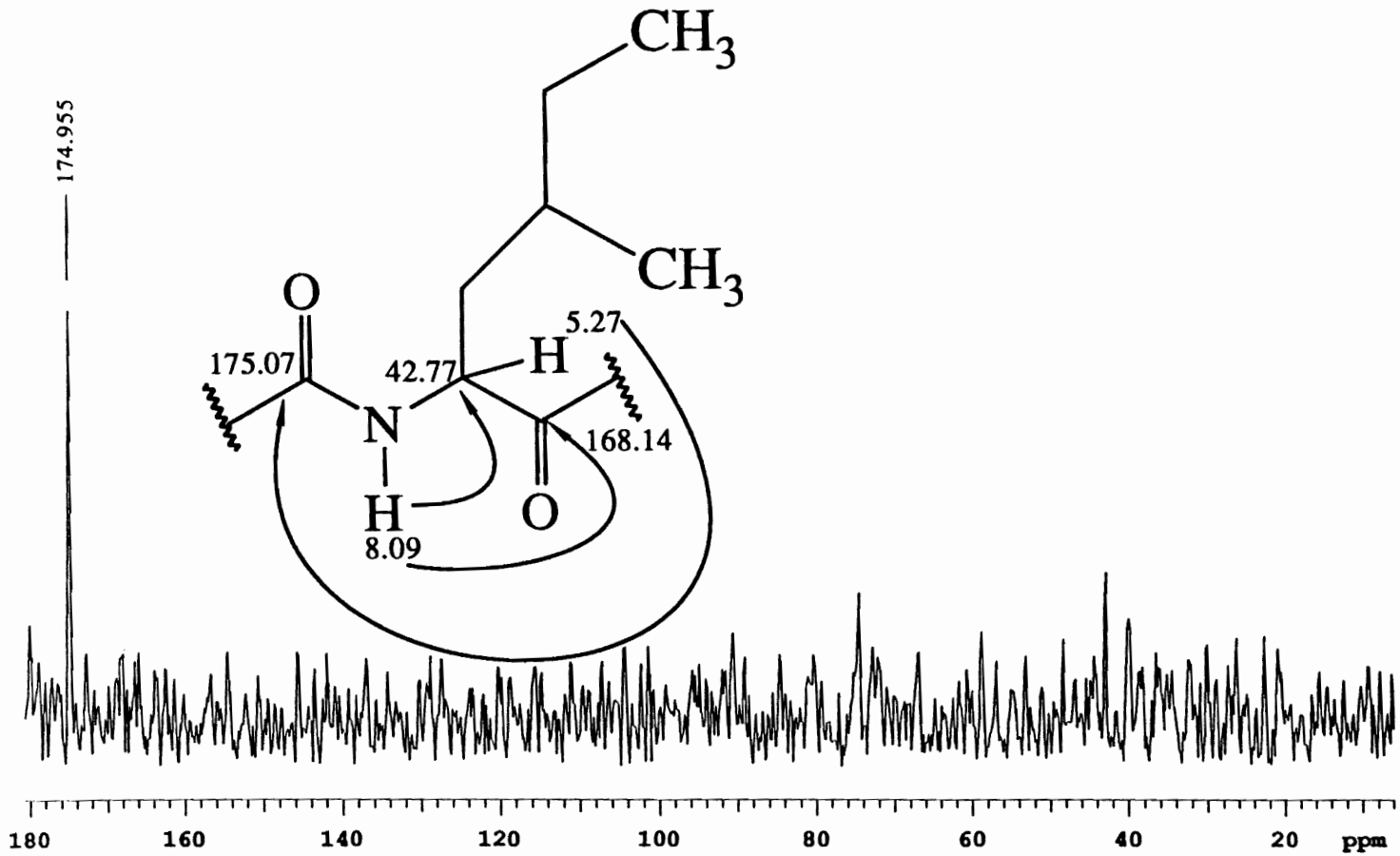

Figure 2.32. HMBC trace through 5.27 ppm of Hil 4

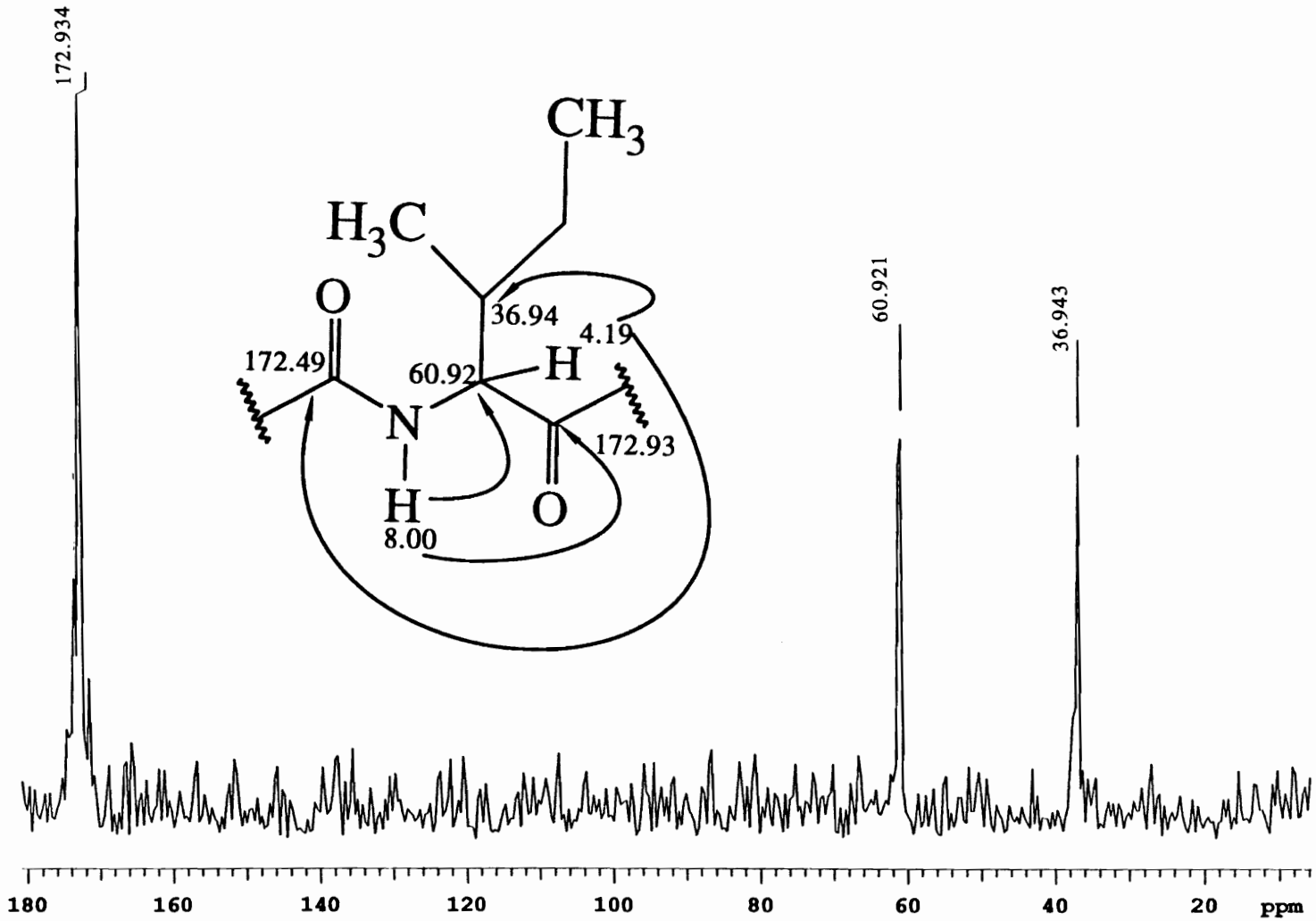

Figure 2.33. HMBC trace through 8.00 ppm of Ile

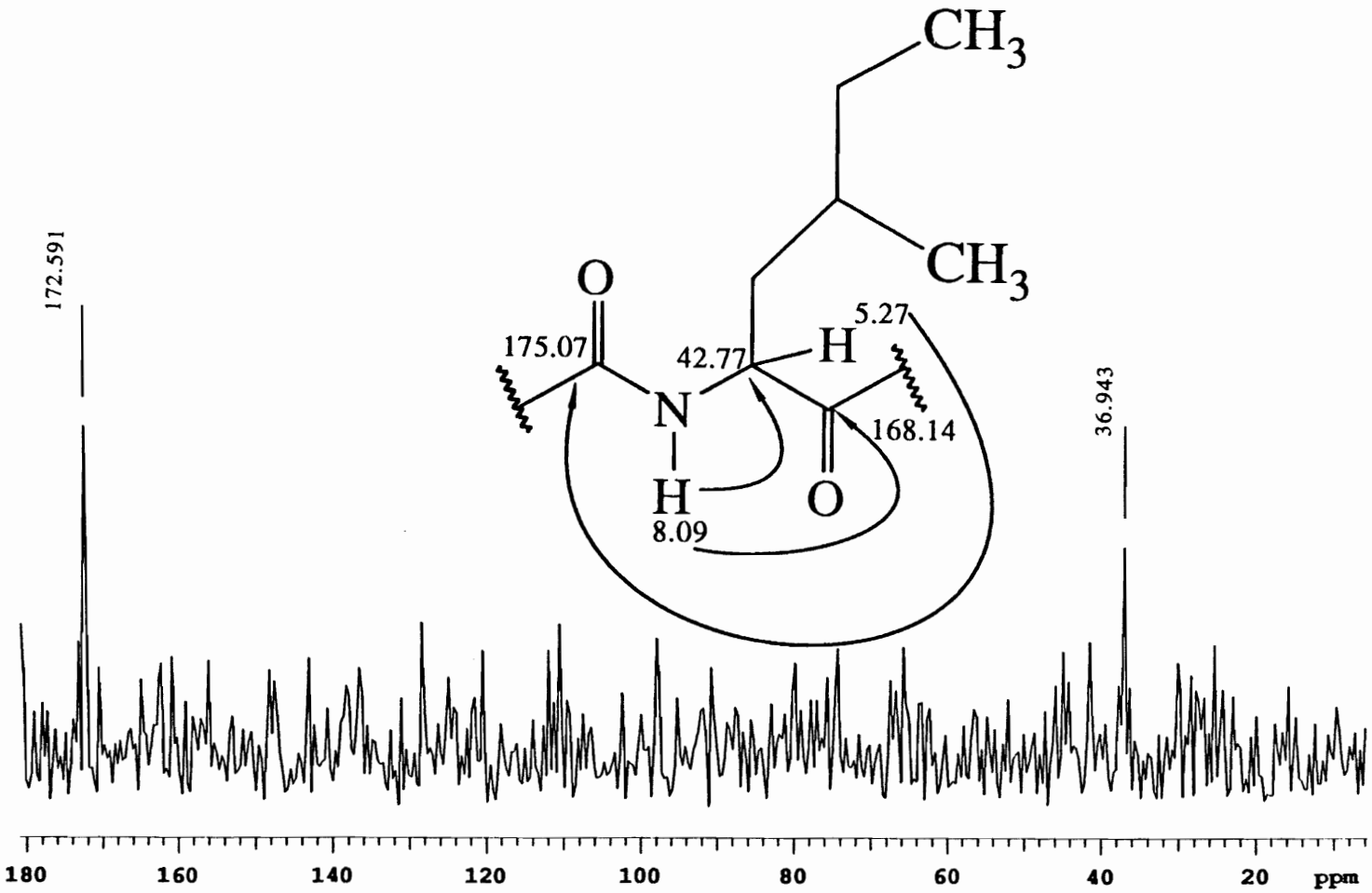

Figure 2.34. HMBC trace through 4.19 ppm of Ile

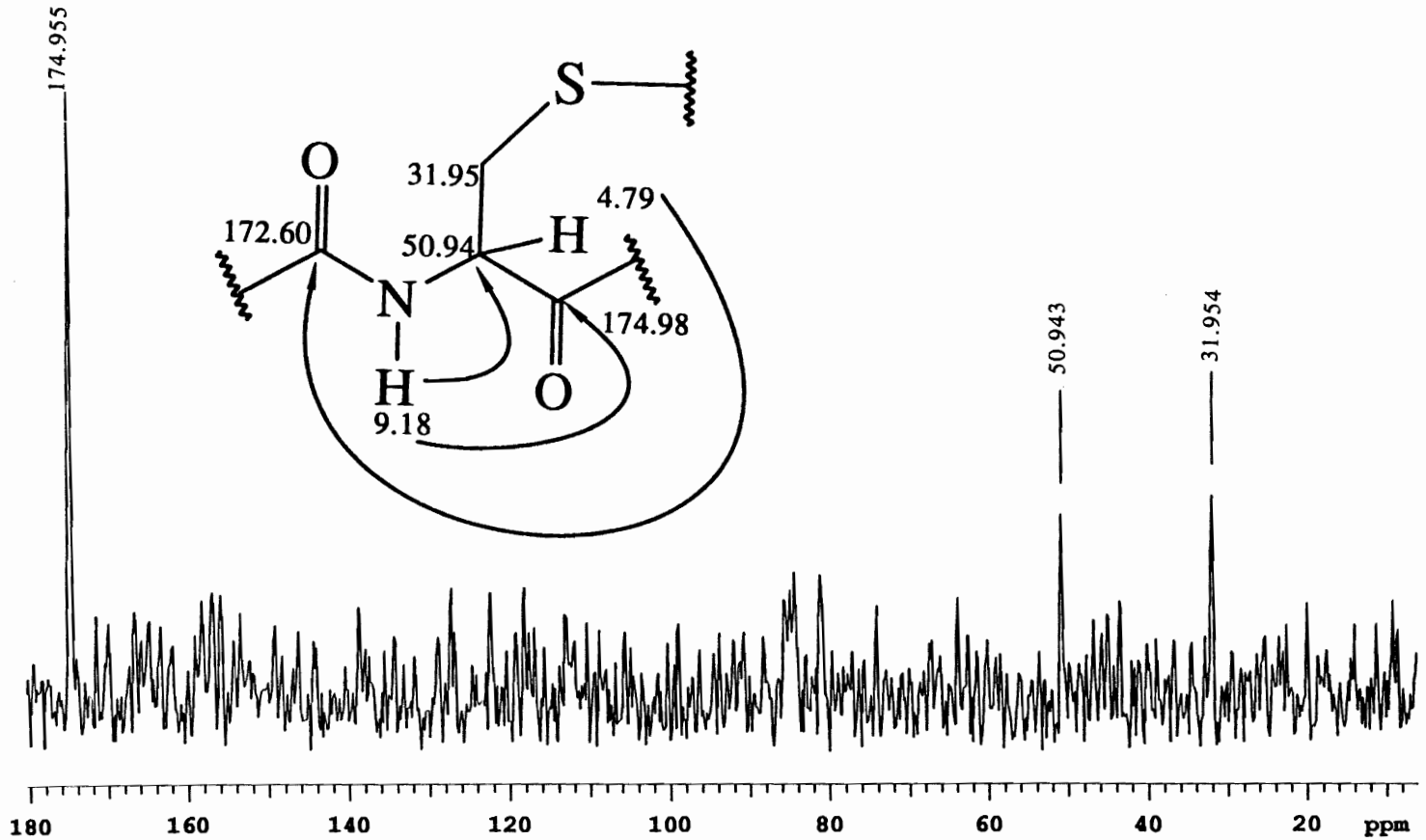

Figure 2.35. HMBC trace through 9.18 ppm of Lan 7

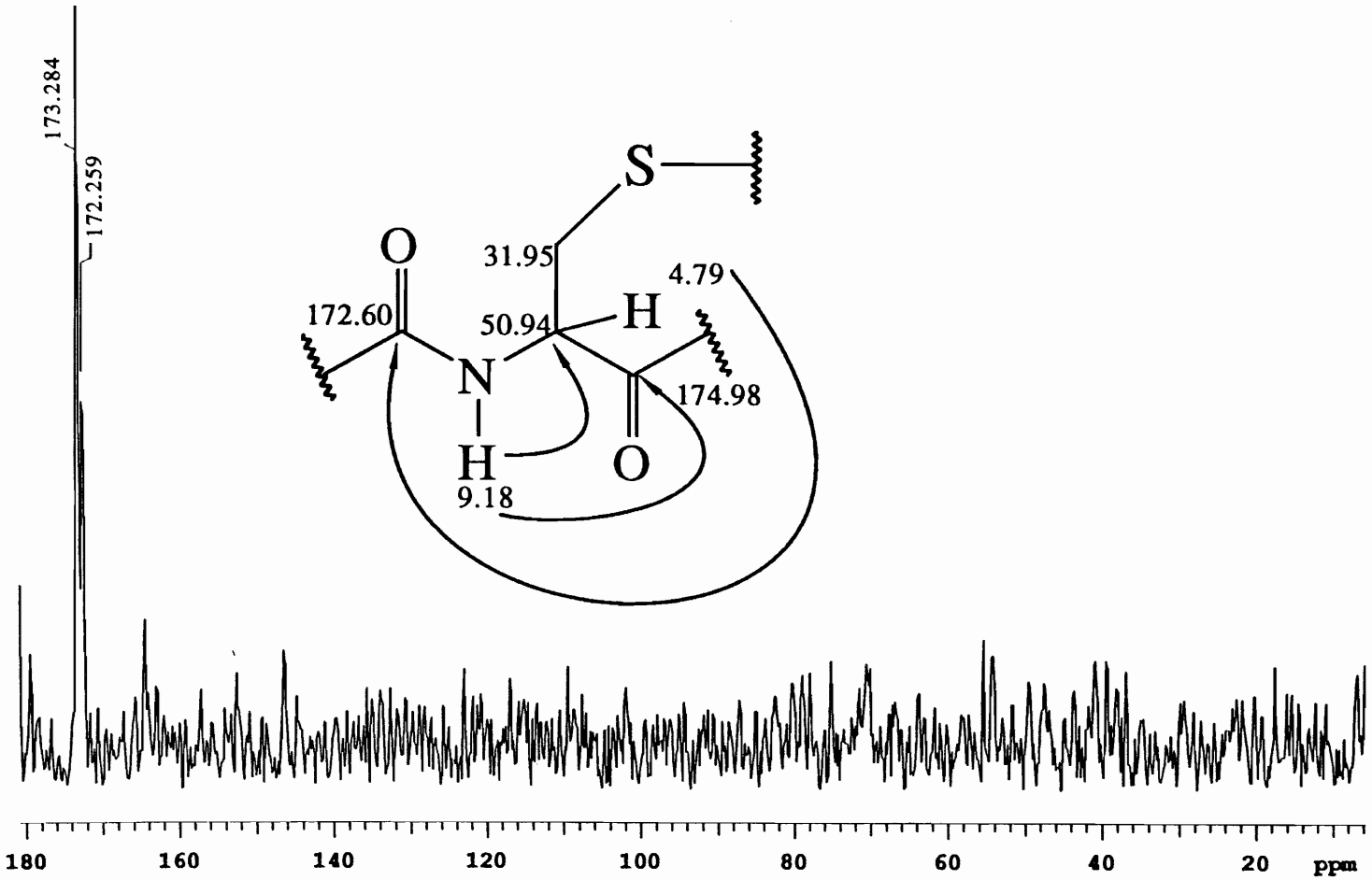

Figure 2.36. HMBC trace through 4.79 ppm of Lan 7

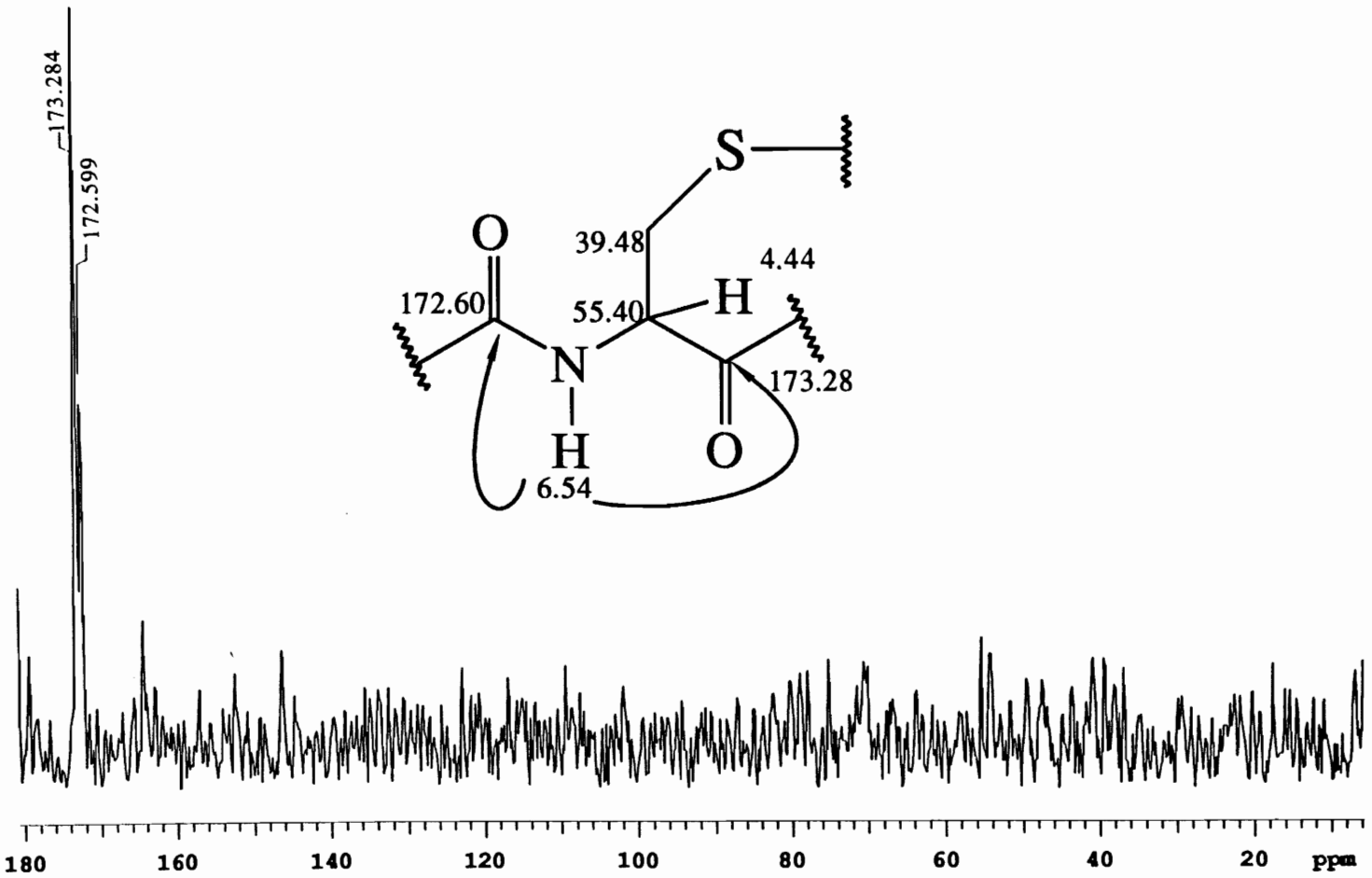

Figure 2.37. HMBC trace through 6.54 ppm of Lan 14

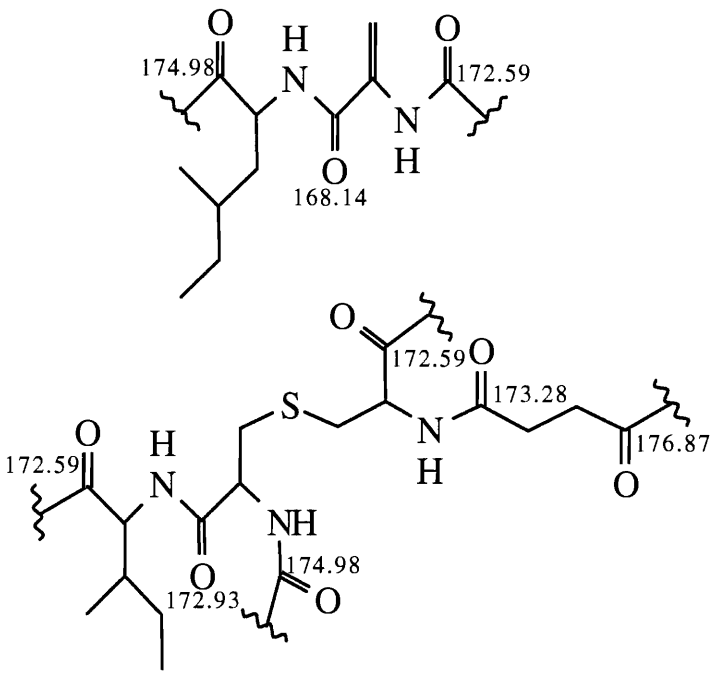

Figure 2.38. Partial sequential assignment of vitilevuamide

on vitilevuamide in order to provide additional sequential information. This experiment is a carbon detected experiment and it was hoped that it would provide the necessary resolution needed for resolving the ambiguity posed by the overlapping carbonyls. However, this experiment is not very sensitive. As a result it only served to corroborate data derived from the HMBC experiments, and did not show any new correlations. After attempting several NMR experiments with marginal success, a new method for the determination of sequential information was employed.

Mass Spectrometry Analysis

MS was used in conjunction with NMR to elucidate the structure of vitilevuamide. Electrospray mass spectrometry (ESMS) performed on the hydrolysate of **49** showed peaks at *m/z* of 90, 106, 116, 118, 120, 132, 146 and 166. These correspond to the protonated masses of Ala, Ser, Pro, Val, Thr, Ile, Hil and Phe respectively. While the detection of amino acids in the hydrolysate is supportive of their presence in the peptide, the absence of any could be related to their instability to the hydrolytic procedure. As a result, the presence of Dha in the hydrolysate was not detected or expected. Figure 2.39 illustrates the ES spectrum of the hydrolysate of vitilevuamide.

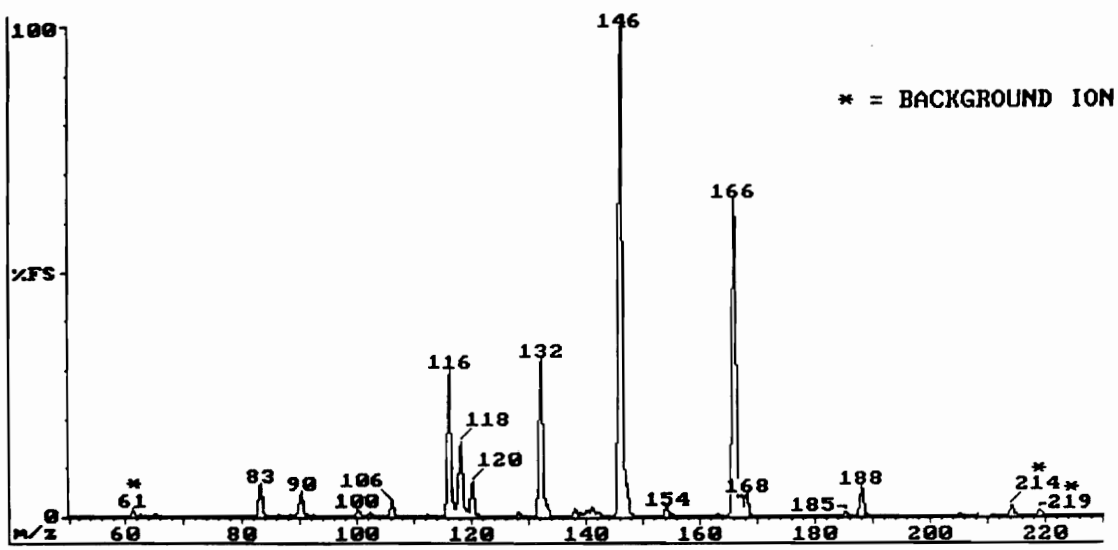

Figure 2.39. ESMS of the hydrolysate of vitilevuamide

ESMS was instrumental in the sequential assignment of the fragments isolated and identified via NMR. However, the peptide has to be linear in order to be amenable to MS/MS. This was done by using NH_3 in MeOH at O^oC for 18 hours. Figure 2.40 depicts the partial linearization scheme used. The ES spectrum of the resulting partially linear peptide showed an *m/z* at 1620 which was consistent with the expected product.

A tandem MS/MS experiment was performed on the linearized peptide. The MS/MS was dominated by fragment ions as depicted in Figure 2.41. The major fragmentation pattern showed sequential losses from the amidated C-terminal to produce *m/z* 1603.9, 1517, 1372.1, 1272.8, 1145.6, 1076.5, 963.5 ions. These correlate to the loss of ammonia (*m/z* = 17), Ser (*m/z* = 87), Nmm (*m/z* = 145), Val (*m/z* = 99), Hil (*m/z* = 127), Dha (*m/z* = 69) and Ile (*m/z* = 113). Figure 2.42 illustrates the analysis of the fragmentation pattern.

Subsequent fragmentation occurs after a rearrangement, resulting in the loss of 166 mass units formed by Pro and part of the Lan residue. The Lan is eliminated in the form of dehydroalanine to give *m/z* 797.4.[80] The cleavage of the Lan bridge as proposed in figure 2.39 occurs with a transfer of a pair of electrons from the electron rich sulfur atom to the α-proton of Lan 7. This results in breaking of the sulfur bridge between Lan and the formation of a Dha residue instead of Lan 7. This sulfur is retained by Lan 14 as a thiol yielding cysteine in subsequent cleavages.

The fragmentation continued with loss of amino acids resulting in *m/z* 650.2, 549.2, 422.2, and 351.3 corresponding to Phe (*m/z* = 147), Thr (*m/z* = 101), Hil (*m/z* = 127) and Ala (*m/z* = 71). The next loss of 250 mass units was a coupled loss of Phe and Cys, leaving the terminal succinate fragment of 101 massunits. A loss of 18 mass units was observed throughout the spectrum which can be attributed to the loss of a moleucle of H_2O.

MS in conjunction with NMR spectroscopy was instrumental in determination of the structure of vitilevuamide, a bicyclic depsipeptide. Vitilevuamide is also the first lanthionine containing peptide isolated from marine sources.

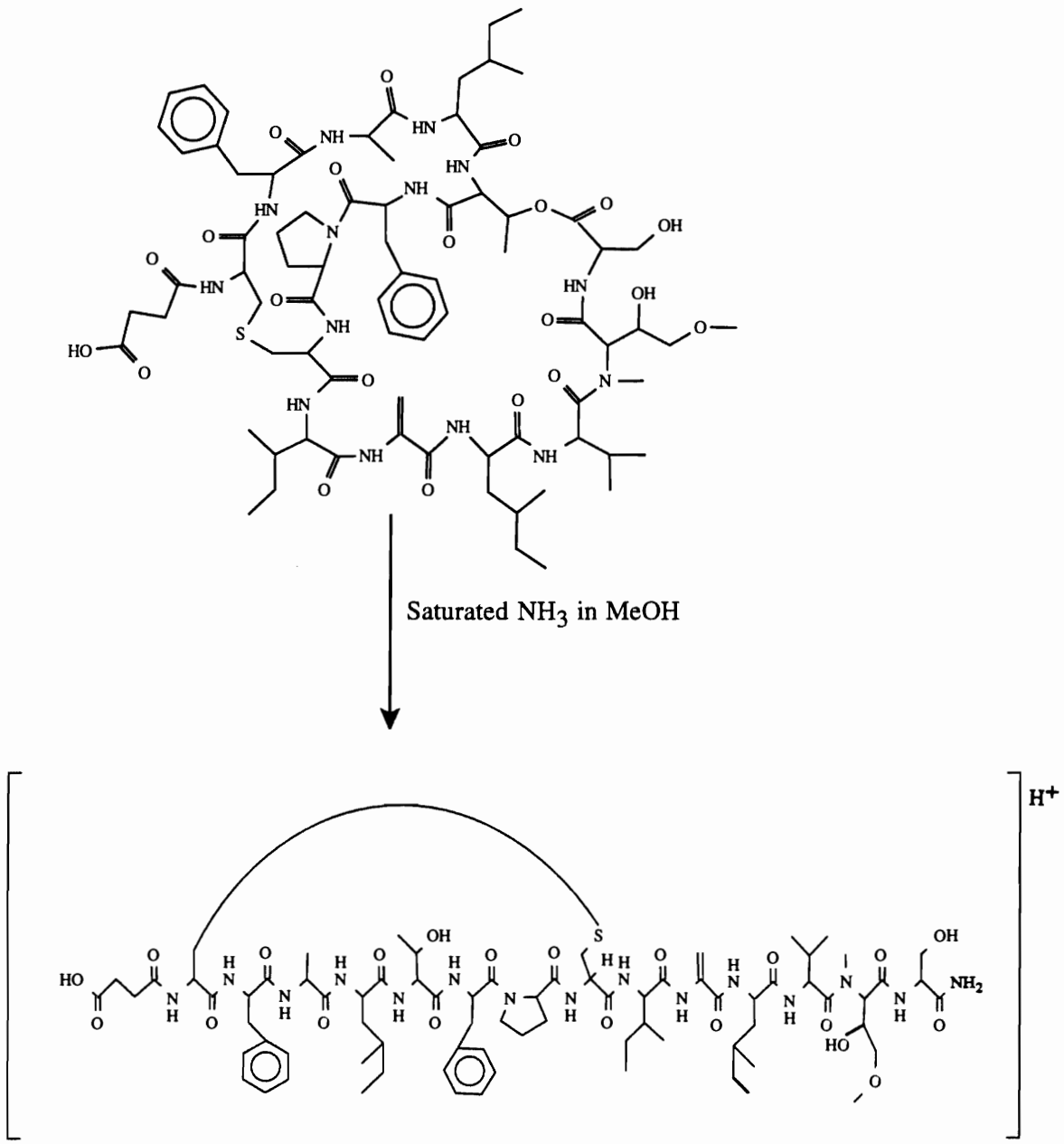

Figure 2.40. Partial linearization scheme for vitilevuamide

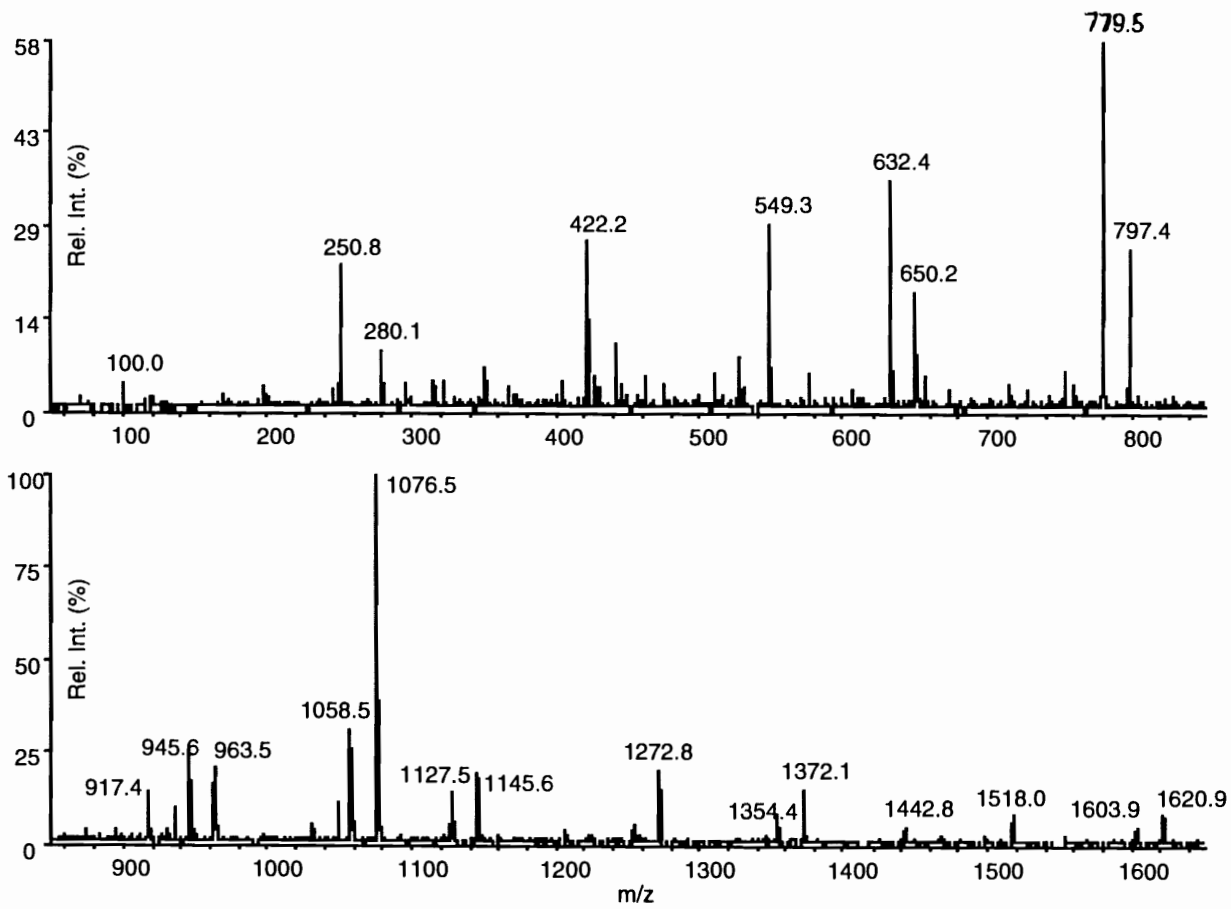

Figure 2.41. Tandem MS of partially linearized vitilevuamide

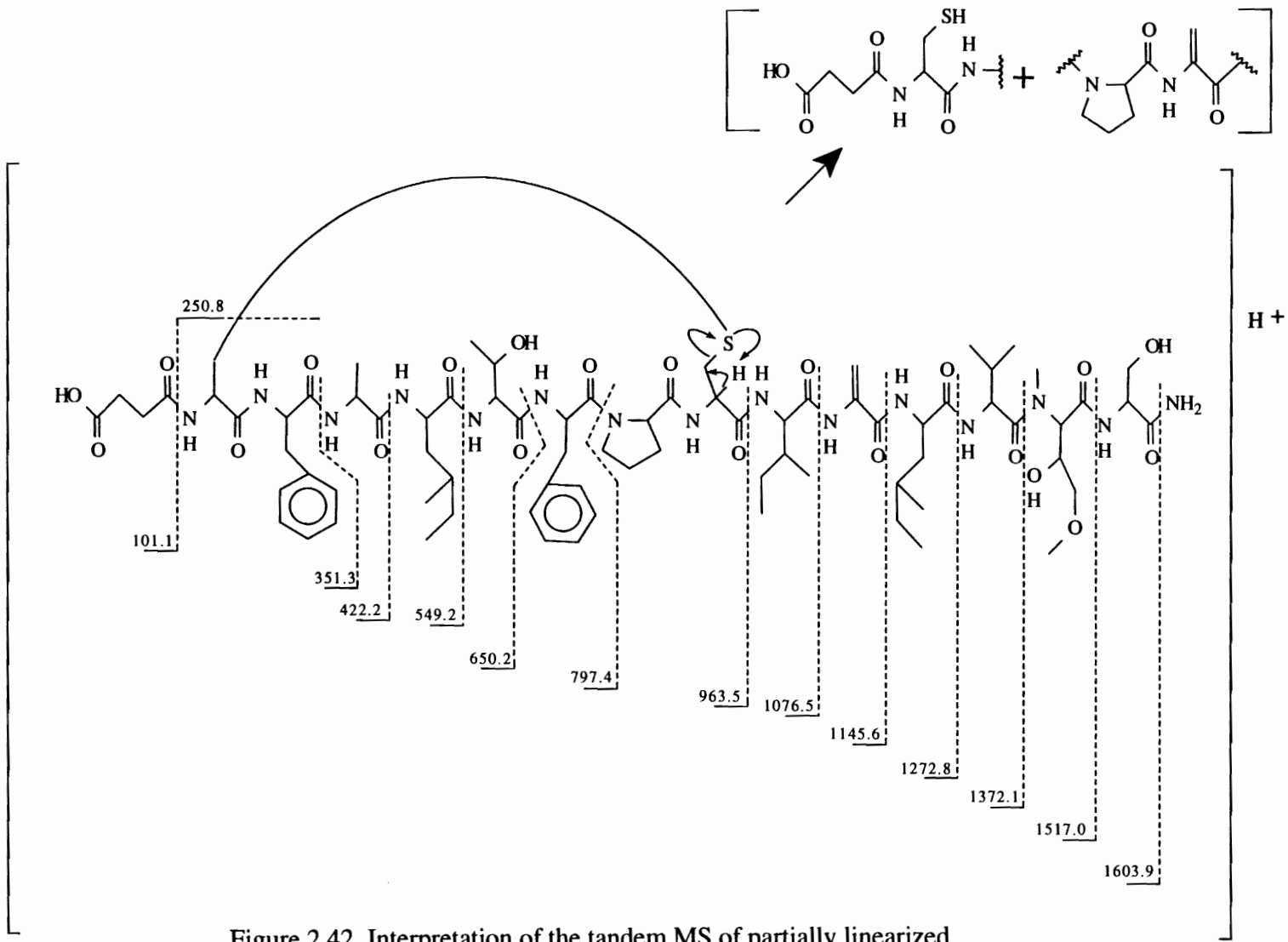

Figure 2.42. Interpretation of the tandem MS of partially linearized vitilevuamide

CHAPTER 3

THE SYNTHESIS OF NOVEL AMINO ACIDS

Synthesis of Hil

In order to verify the stereochemistry of amino acids present in vitilevuamide, it was necessary to synthesize the amino acids not commercially available. These included the amino acids Hil and Nmm. The method of Han and Pascal was followed for the synthesis of all four isomers of Hil.[81] (S)-(+)-1-bromo-2-methylbutane (**51**) was added to an alkaline solution of diethyl acetamidomalonate (**52**). The resulting brown oil was purified by silica gel column chromatography to yield ethyl (S)-2-acetamido-2-(ethoxycarbonyl)-4-methylhexanoate (**53**) in 78% yield.

Compound **53** was refluxed in 6N HCl overnight and the resulting mixture was concentrated *in vacuo* to yield (2RS, 4S)-2-amino-4-methylhexanoic acid hydrochloride (**54**) in 75% yield. In order to isolate one of the isomers in an optically pure form degradative enzyme chemistry was performed with L amino acid oxidase and catalase. This results in the selective degradation of the L isomer with the formation of its α-keto acid. The keto acid being nonpolar compared to the amino acid can be easily separated chromatographically. The recommended amount of the D and L oxidases (5 mg and 3 mg respectively) and catalase (2 mg) under specified conditions did not yield the molecule of interest. The final conditions adopted that resulted in a yield of 48% of (2R,4S) Hil (**55**) involved bubbling oxygen through the reaction mixture and addition of three times the recommended equivalents of enzymes as described in the experimental. The synthetic scheme is illustrated in Figure 3.1.

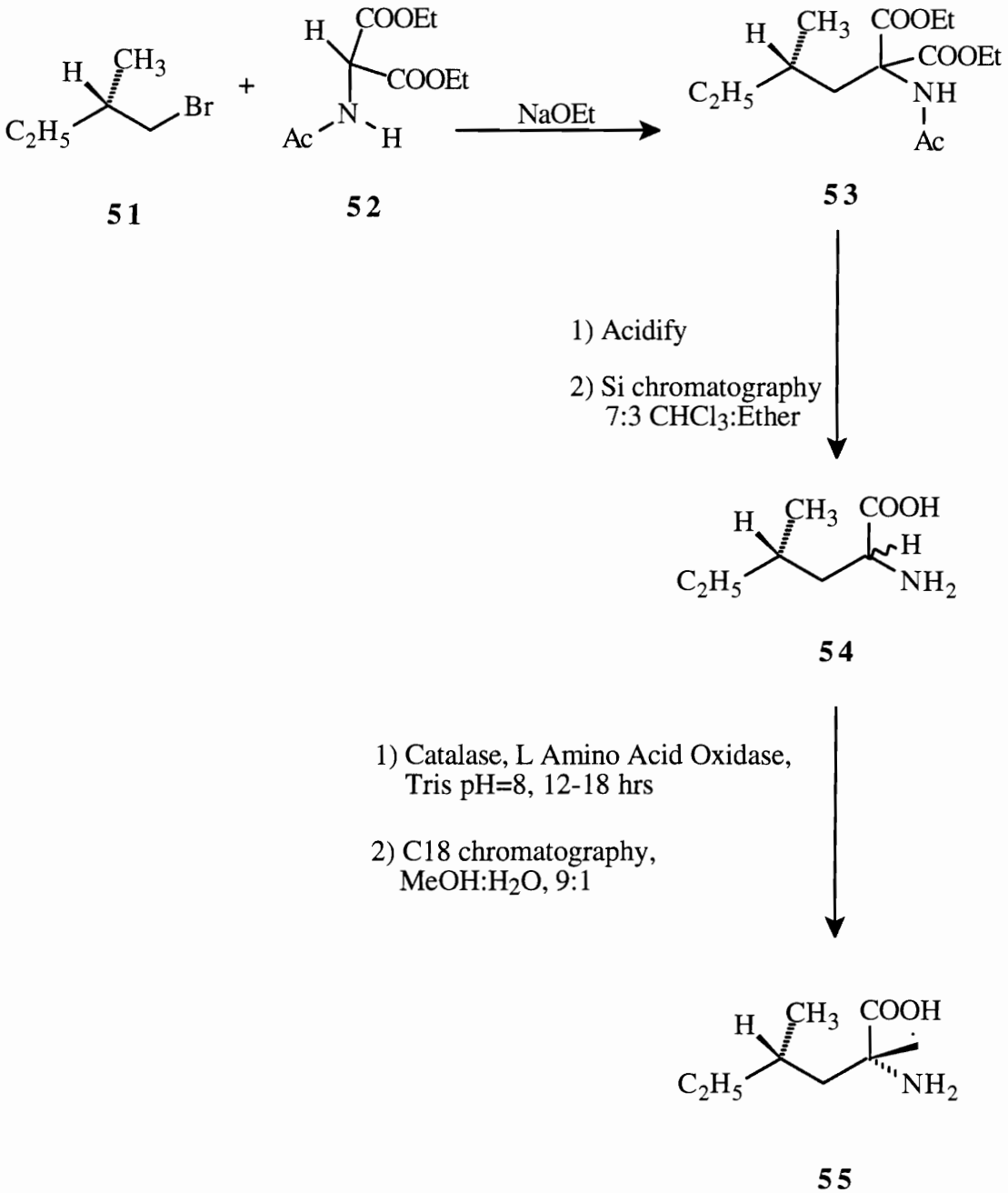

Figure 3.1. Synthetic route for (2R, 4S) Hil (**54**)

This procedure was repeated with the racemic mixture of the starting material (RS)-(+)-bromo-2-methylbutane (**56**). This yielded all the four possible stereoisomers of Hil. The derivatization of this mixture with 1-fluoro-2,4-dinitrophenyl-5-L-alanineamide (FDAA) yielded four peaks at different retention times, confirming the presence of all four isomers. Figure 3.2 illustrates the synthetic scheme adopted.

Synthesis of N-methyl Methoxinine

In order to synthesize Nmm several schemes were attempted. A brief summary of the different synthetic routes adopted is provided along with the problems associated with each scheme.

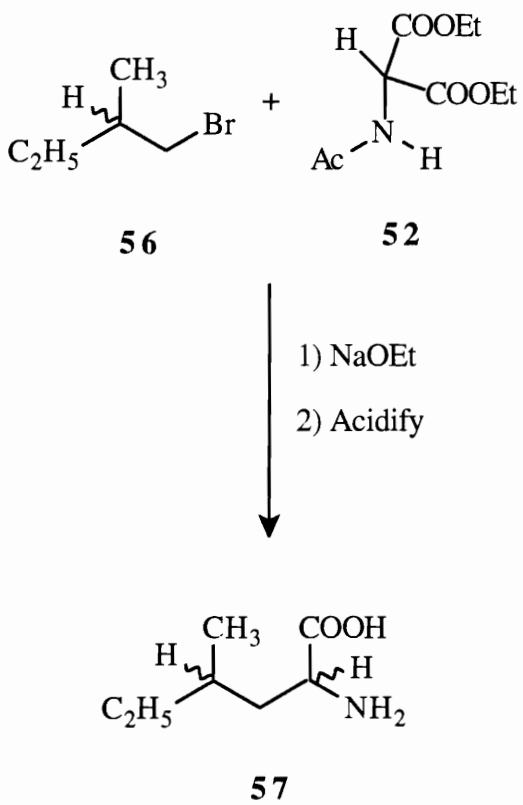

Figure 3.2. Synthetic route for all four Hil isomers

Synthetic Route 1

The first route attempted was an extension of a literature method for the synthesis of the non-N-methylated derivative of Nmm.[82] This method involved an aldol condensation of the copper glycinate intermediate (**60**) with methoxyacetaldehyde (**61**).

The synthetic protocol was followed using both glycine as well as N-methylglycine (sarcosine), in order to reproduce literature results and at the same time to synthesize the desired amino acid. Figure 3.3 illustrates the synthetic scheme adopted.

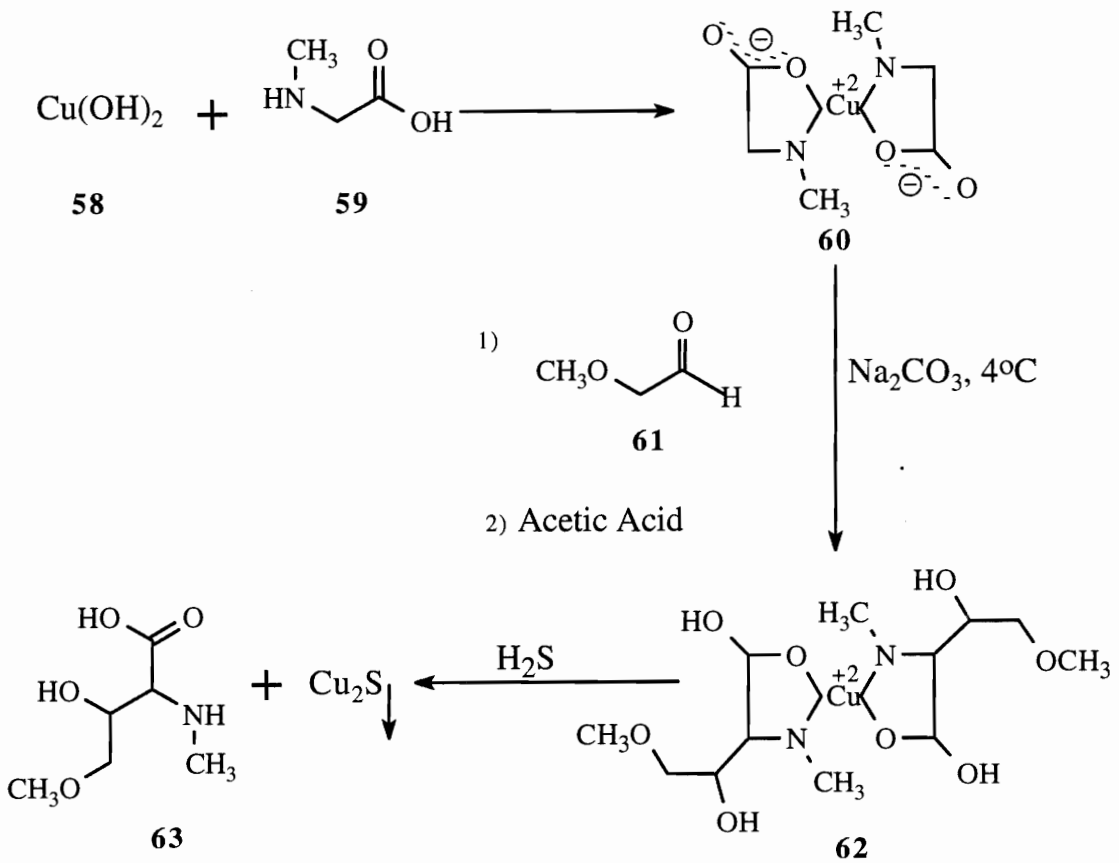

Figure 3.3. Synthetic route 1

Since Cu^{2+} is paramagnetic in nature it was not possible to characterize the copper sarcosinate (**60**) using NMR. Different MS techniques and matrices were tried in order to characterize **60**. Matrices for (+) FABMS included glycerol and water, glycerol and methanol, dithiothreitol, magic bullet and sulfolane. Electron impact (EI) and chemical ionization (CI) did not yield any of the expected ions. However desorbtive chemical ionization (DCI) yielded an m/z of 242 with an $(M + 2)^+$ at 244 (33% of base peak) which fits the copper isotope pattern.

End product formation was suggested by IR data. The presence of the carbonyl stretch at 1680 was consistent in both glycine, sarcosine and the copper conjugate **60**. However there was no such success in the characterization of **62**. All the MS techniques mentioned above did not yield expected ions. Hence the next step of copper displacement by precipitation with hydrogen sulfide was carried out without purification and characterization of **62**. Repeated trials of this step failed to yield Nmm (**63**). Due to the distinct irreproducibility of the synthetic scheme a new route was employed.

Synthetic Route 2

Mild oxidation conditions were used to oxidize glycidol (**64**) to the aldehyde (**65**) using tetra propyl ammonium perruthenate (TPAP) and N-morpholino oxide (NMO).[83, 84] This reaction has a very poor yield of 12%. Ring opening of the epoxide was attempted using dry sodium methoxide in anhydrous methanol. This should result in the formation of the aldehyde (**66**). However, after repeated attempts of the same chemistry, no aldehyde could be isolated. Figure 3.4 illustrates the synthetic route.

Synthetic Route 3

Under the assumption that use of protection-deprotection chemistry might solve the problem, a modification of the above scheme was attempted. This involved protection of glycidol (**64**) using a β-methoxyethoxymethyl (MEM) group (90% yield). Ring opening of **68** resulted in the formation of MEM mono protected diol (**69**) at a yield of 60% .

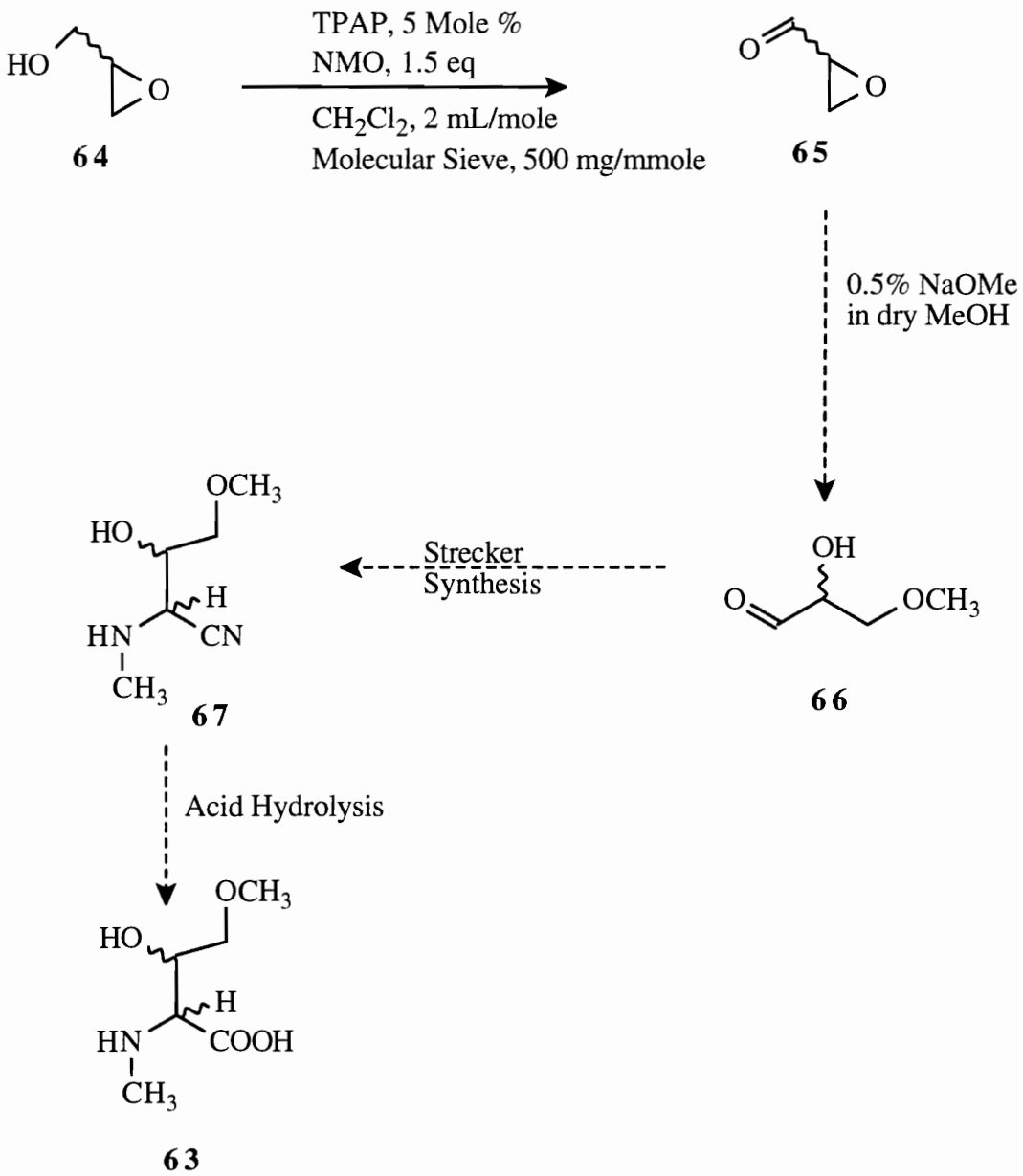

Figure 3.4. Synthetic route 2

When further protection of the newly formed secondary alcohol was attempted with tert-butyldimethylsilyltriflate (TBDMSOTf),[85] it resulted in a complex mixture of compounds that were difficult to analyze. As a result further progression of this scheme was halted. Figure 3.5 shows the synthetic route.

Synthetic Route 4

The procedure of Wong *et al.* [86] was adopted for the synthesis of 3-methoxy-2-hydroxypropionaldehye (3-O-methylglyceraldehye) (**66**) at a yield of 47%. Figure 3.6 illustrates the synthetic route. NMR results were consistent with the published data. The absence of an aldehydic proton and carbonyl carbon in the NMR data suggested that the aldehyde was isolated as a dimer. The presence of a resonance at 89.7 ppm suggested that the aldehyde may exist in the form shown in Figure 3.7.

The Strecker synthesis[87] was performed on **66** using methylamine. This resulted in a complex mixture of nitrogenous compounds. Repeated trials of the Strecker synthesis did not yield **66**, as suggested by the lack of a nitrile stretch in the IR data. Hence an alternative method for the synthesis of the nitrile was used. This involved an addition of methylamine to the aldehyde (**66**) in an alkaline medium followed by potassium cyanide. This results in the formation of 2-aminomethyl-3-hydroxy-4-methoxybutane nitrile (**67**) at a yield of 80%. This is depicted in Figure 3.8.

A series of NMR experiments, ^{1}H, ^{13}C, multiple quantum COSY, HMBC and HMQC were performed on the amino nitrile (**67**). Positive HR FABMS showed a protonated molecular ion at m/z 145.09631 in agreement with the molecular formula of $C_7H_{16}NO_2$. The NH proton was not seen in the proton spectrum. At the same time it was difficult to assign the OH proton because of extensive signal overlap around 4.04 - 4.08 ppm. Table 3.1 gives the NMR assignments for **67**. Figure 3.9 shows the HMBC corelations for the nitrile (**67**). Two sets of carbons are seen because of the presence of isomers of the nitrile.

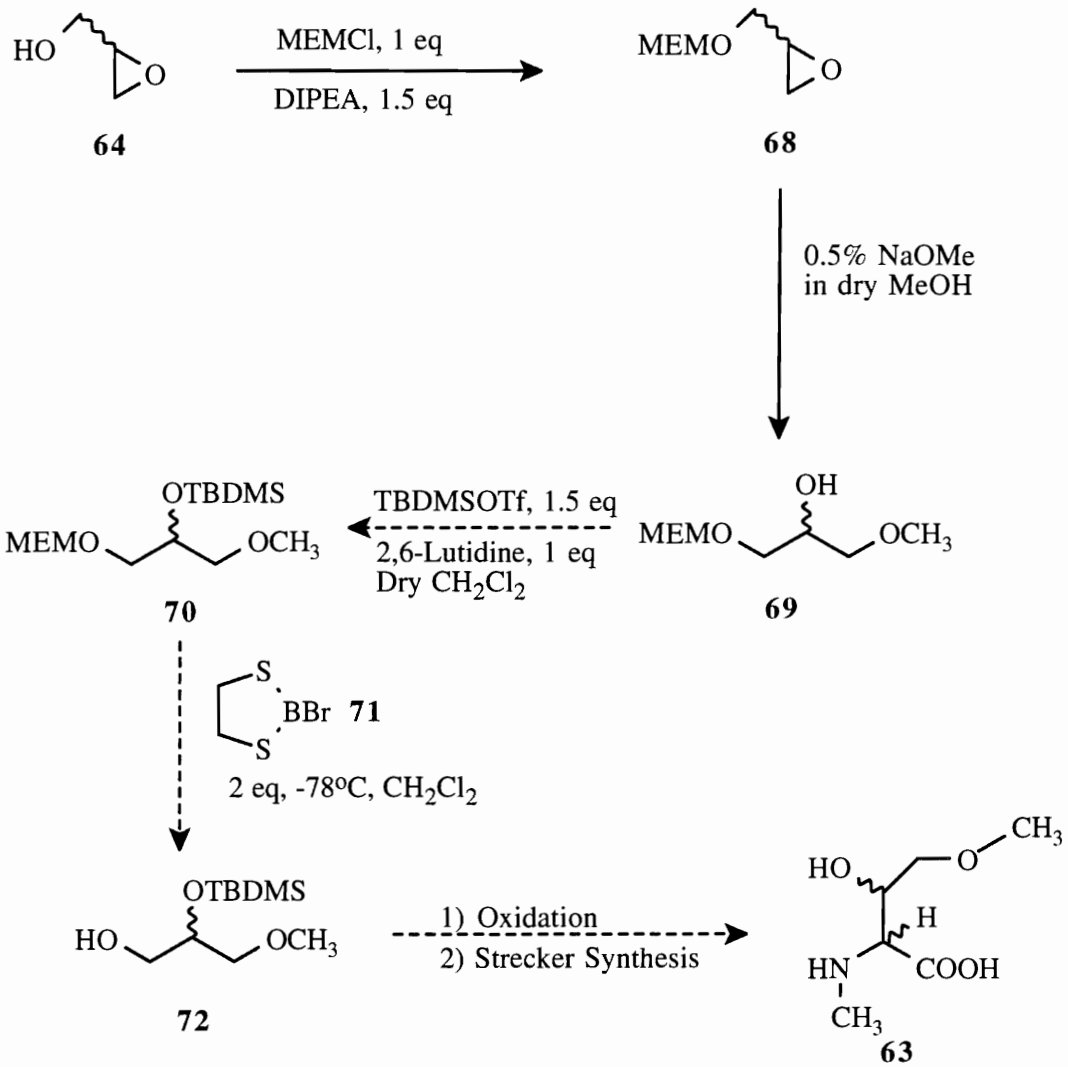

Figure 3.5. Synthetic route 3

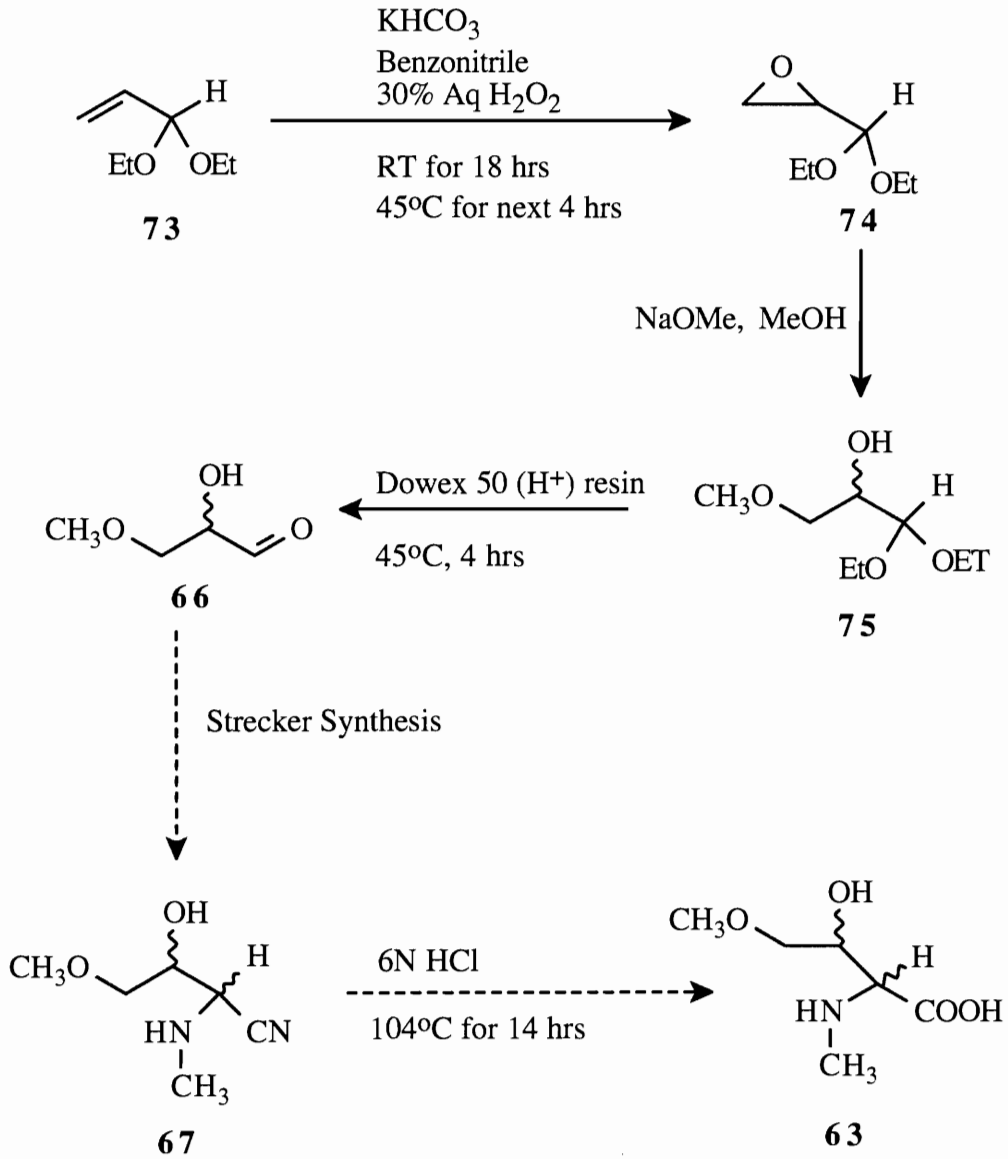

Figure 3.6. Synthetic route 4

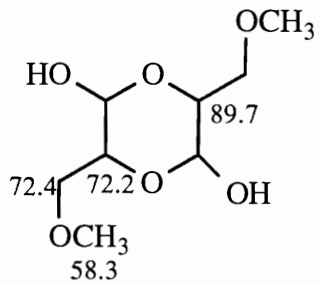

Figure 3.7. Dimeric form of hydroxy propionaldehyde (**75**)

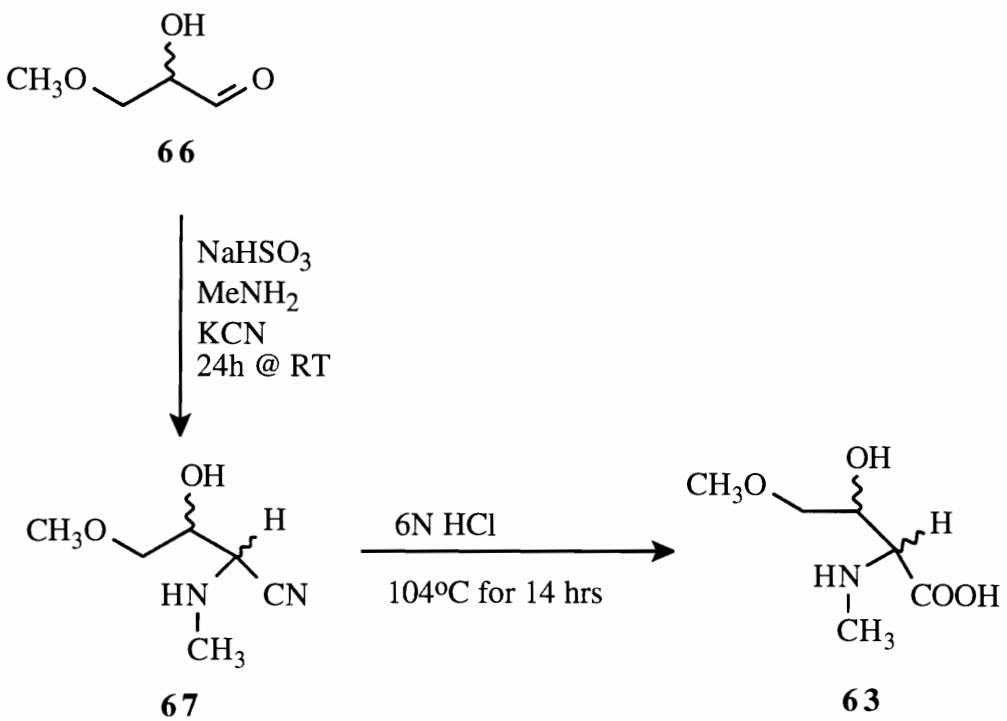

Figure 3.8. Synthetic scheme for the formation of Nmm (**63**) from the aldehyde (**66**)

The nitrile (**67**) was subjected to acid hydrolysis resulting in Nmm (58% yield). The amino acid was synthesized as a mixture of all isomers. Proton and carbon data are included in Appendix B.

Table 3.1. NMR assignments for the nitrile (**67**)

atom no	δ ^{13}C	(mult.)	δ ^{1}H	(mult.)	HMBC corelations
1	117.19, 118.10	s			
2	54.15, 55.38	d	4.08	m	C1, N-CH3
3	69.61, 69.64	d	4.40	m	C1, C2
4	72.80, 73.46	t	4.05	m	C3, O-CH3
$N\text{-}CH_3$	33.71, 34.05	q	2.80	s	C2
$O\text{-}CH_3$	59.02	q	3.80	s	C4
OH			4.05	m	

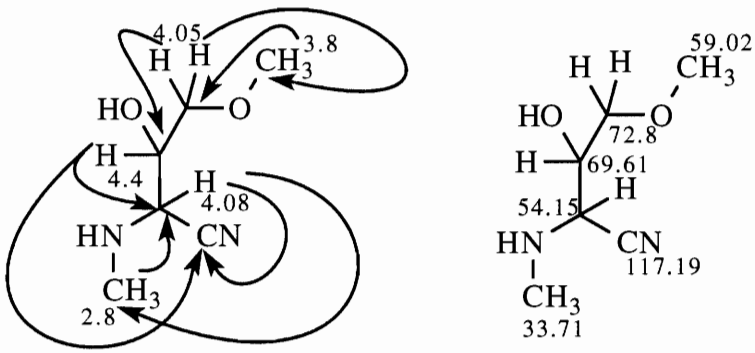

Figure 3.9. NMR assignments for the nitrile (**67**)

CHAPTER 4

THE STEREOCHEMISTRY OF AMINO ACIDS IN VITILEVUAMIDE

Introduction

Peptides usually contain distinct enantiomers of amino acids. Hence identification of the amino acid composition as well as enantiomeric purity is of great importance.[88] HPLC resolution of amino acid enantiomers can be accomplished by using chiral stationary phases,[89-91] chiral eluents,[92-94] or derivatization with chiral reagents prior to chromatography.[95-97] The diastereomers formed by the latter method can often be separated by conventional reverse phase chromatography, and special chiral columns are not necessary. However, optically pure derivatization agents are required, as are reaction conditions where no epimization occurs.

In 1984, Marfey reported that a mixture of D- and L-amino acids could be separated into each enantiomer by reverse phase HPLC after derivatization with FDAA (1-fluoro-2,4-dinitrophenyl-5-L-alanine-amide).[98] This method has been referred to as "Marfey's method". It determines the stereochemistry of an amino acid based on the retention time (rt) of the FDAA diastereomers.

Marfey applied his method to only five amino acids Ala, Aspartic acid (Asp), Glutamic acid (Glu), Methionine (Met) and Phe. Since then this method has been examined extensively for its applicability and limitation. Throughout these experiments, Marfey's method proved to have a wide applicability to normal α-amino acids except for a few basic amino acids.[99] Figure 4.1 shows the synthetic scheme for synthesis of the FDAA derivative.

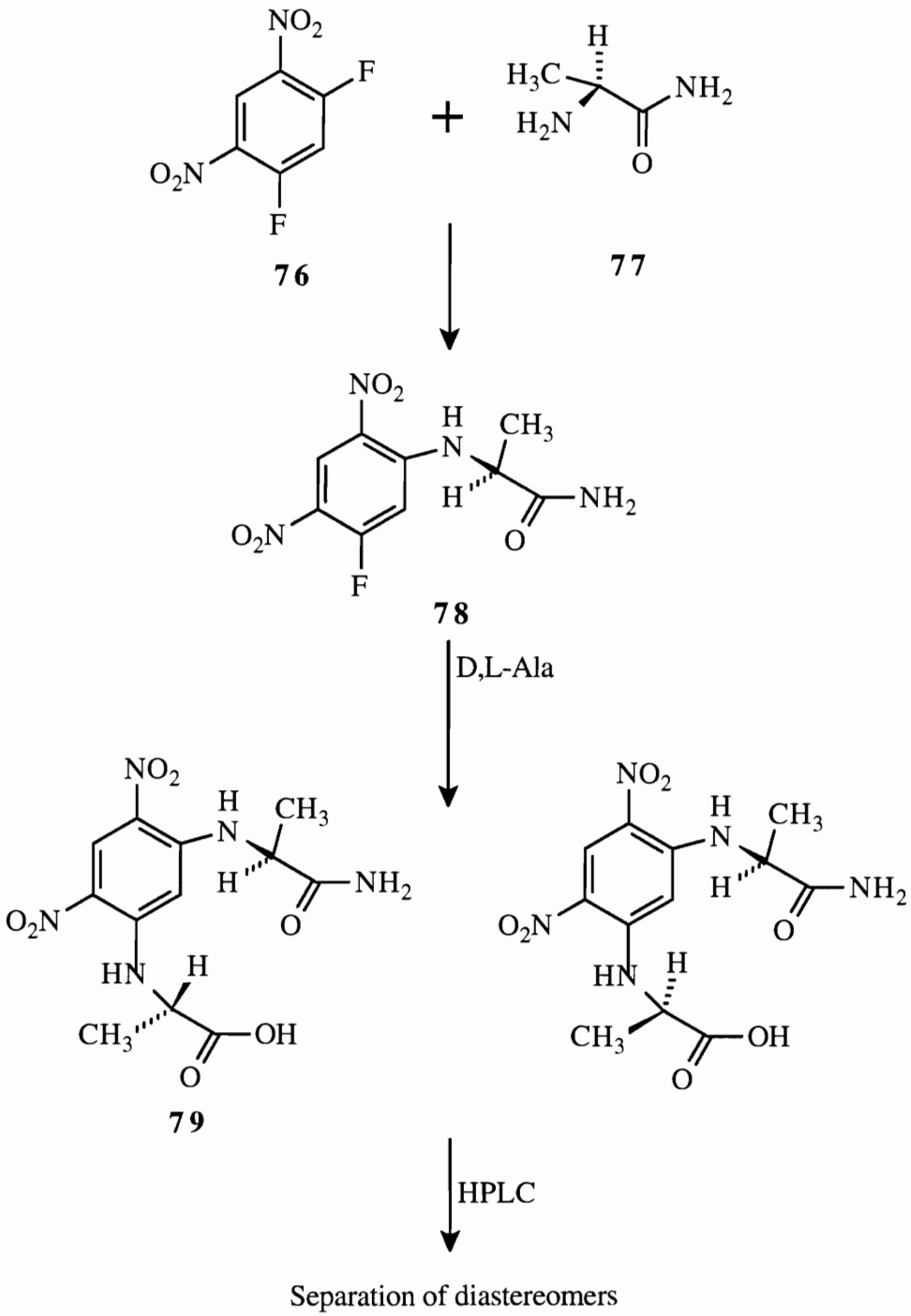

Fig. 4.1. Synthetic scheme for the preparation of FDAA derivatives

The derivatization of an amino acid with FDAA involves a nucleophilic attack by the amino nitrogen on the fluorine atom. This results in the displacement of the fluorine and attachment of the amino acid. The nucleophilic attack is carried out under basic conditions maintained by the addition of 1 M sodium bicarbonate solution. The excess base is neutralized by addition of 2 M HCl.

The standard analytical conditions used are RP HPLC with acetonitrile and 0.05 M triethylamine (TEA) phosphate buffer at pH 3.0 as the eluent. A linear gradient of 10% CH_3CN to 40% CH_3CN in 45 min. is recommended at a flow rate of 2.0 mL/min. at 25°C.[411] The chromophoric nitro groups on FDAA gives the compound a deep yellow color that has a strong absorbance at 340 nm. Under the above mentioned conditions, excess unreacted FDAA is also detected.

Marfey reported that the diastereomeric derivative prepared from the L-amino acid had the lower retention in a reverse phase system. This was ascribed to greater intramolecular hydrogen bonding of the D rather than the L diastereomer. The former would therefore be more hydrophobic and interact more strongly with the nonpolar stationary phase. For those pairs of diastereomers that are separated on silica gel in the normal phase mode, it is the D diastereomer that has the higher R_f. This is consistent with the above observation on the reverse phase system. The diastereomer with the greater degree of intramolecular hydrogen bonding would be expected to have a weaker interaction with the silica surface and thus would have the higher R_f.

HPLC Analysis of Vitilevuamide Hydrolysate

Acid hydrolyzed vitilevuamide was derivatized with FDAA according to Marfey's method. Similarly, commercially available as well as synthesized amino acids corresponding to those present in the peptide were also derivatized. Under Marfey's HPLC conditions severe back pressure precluded the use of a flow rate of 2 mL/min. As a

peaks after 45 min. suggested that the elution time could be shortened to 45 min.. These were the final conditions adopted for most of the amino acids. Figure 4.2 illustrates the HPLC trace of FDAA under the new conditions adopted. This served as a positive control for the identification of excess unreacted **78** in standard amino acids as well as test mixture.

The protocol adopted for the identification of the enantiomers in vitilevuamide involved a series of injections of the standard amino acids, i.e.; D or L isomer and in some cases the D-allo and L-allo isomer, where there are more than one stereocenter. This was followed by an injection of the test mixture and a coinjection of the test with the appropriate amino acid based on retention times. An increase in the peak height and area under the curve of the right isomer upon coinjection is suggestive of its presence in the hydrolysate.

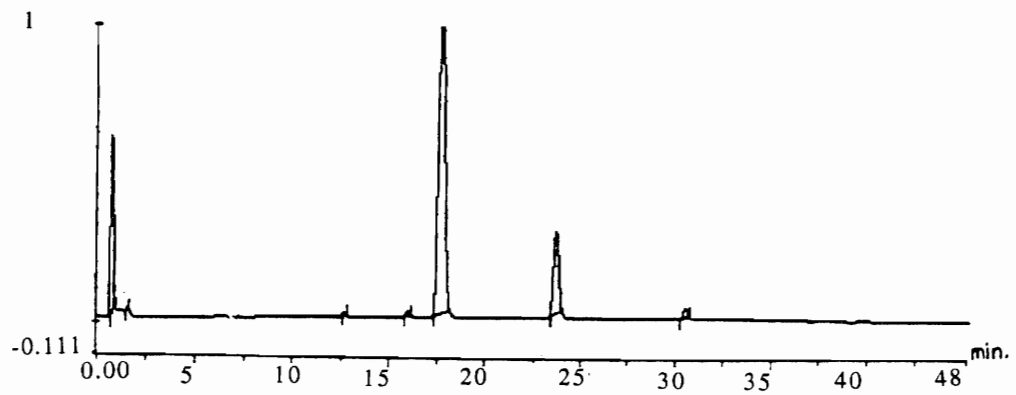

Figure 4.2. HPLC trace of FDAA (**78**)

An example is demonstrated in the following figures. Figure 4.3 illustrates the HPLC trace of D,L-Ala while Figure 4.4 shows the HPLC trace of the derivatized hydrolysate of vitilevuamide. The rt of the standards is indicative of the appropriate amino acid present in the peptide. This was confirmed by a coinjection of the test with the standard. This is shown in Figure 4.5.

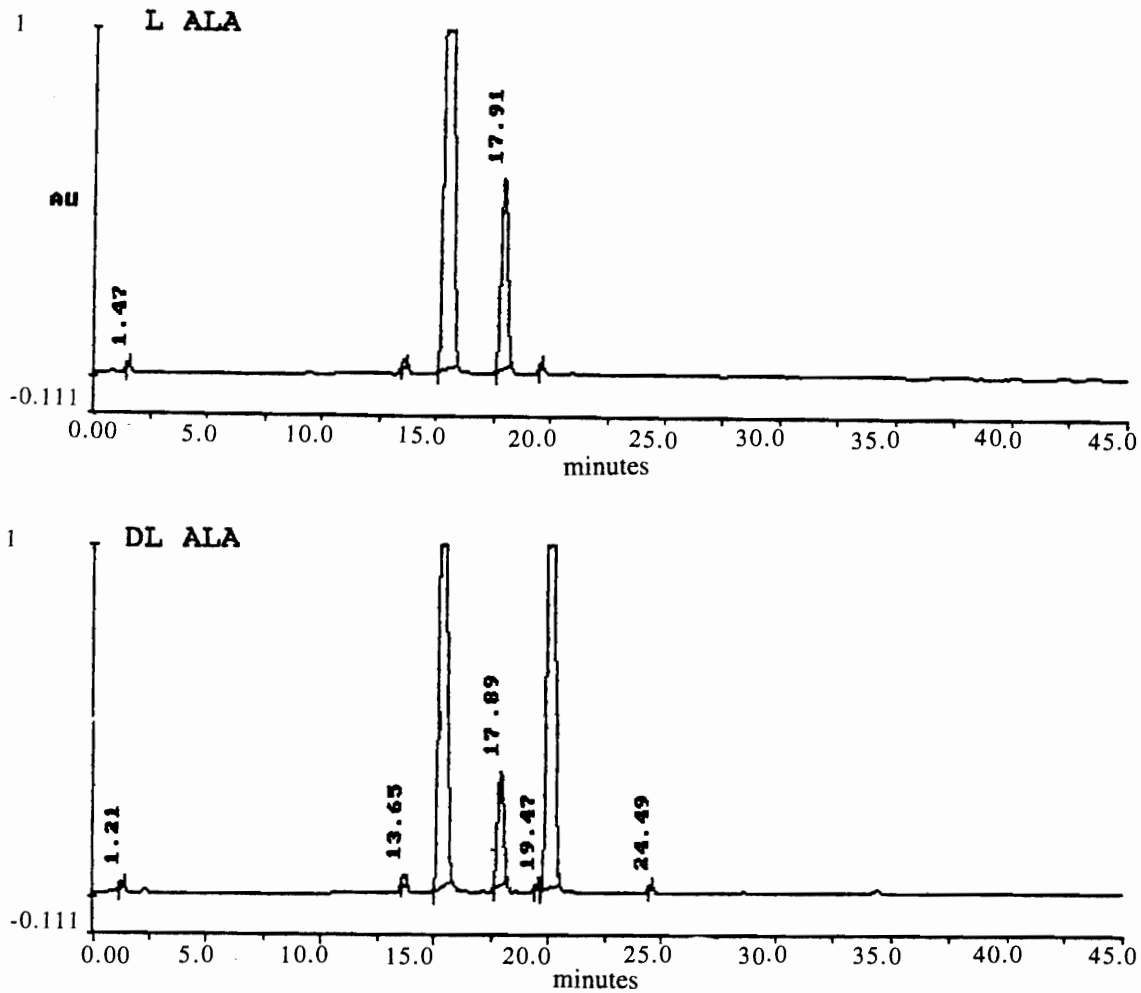

Figure 4.3. HPLC analysis of D,L-Ala

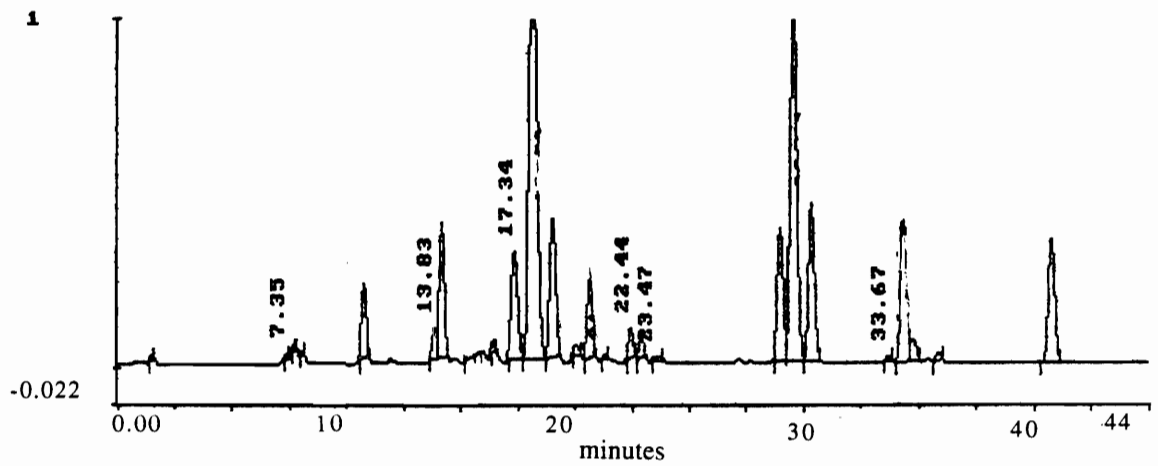

Figure 4.4. HPLC analysis of vitilevuamide hydrolysate

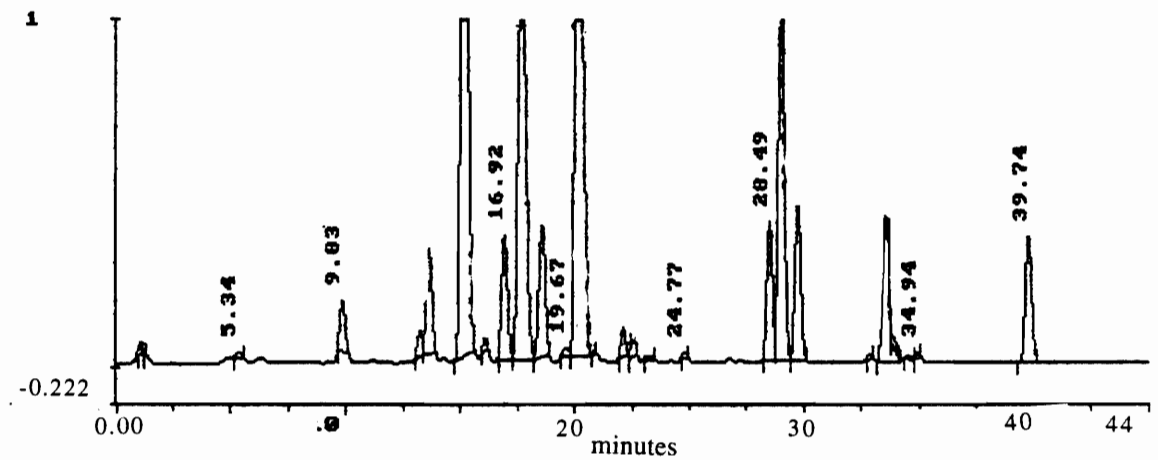

Figure 4.5. HPLC analysis of a coinjection of D,L-Ala and vitilevuamide hydrolysate

The above experiment was suggestive of the presence of D-Ala in the peptide. The same protocol was adopted for Val, Pro, Phe, Thr and Ser. The HPLC traces for each of the amino acids are illustrated in Appendix C. These experiments revealed the presence of D-alloThr, D-Val, D-Phe, L-Ser and L-Pro.

HPLC Analysis of Ile

When the above conditions were utilized for the analysis of Ile, there was no base line separation of the L and L-allo isomers. As a result unambiguous chirality could not be assigned. After several trials and errors using different solvent systems and solid supports, cyano-HPLC with MeOH and 1% acetic acid proved most appropriate. A linear gradient of 35% MeOH to 42% MeOH for 30 min. at a flow rate of 1 mL/min. was adopted. This revealed the presence of L-Ile in the peptide. Relevant HPLC traces are included in Appendix C.

HPLC Analysis of Hil

New HPLC conditions had to be identified for the base line separation of the four Hil isomers. As in the case of Ile, after several trials and errors using different solvent systems and solid supports, cyano HPLC with MeOH and 1% acetic acid proved most appropriate. A linear gradient of 25% MeOH to 90% MeOH for 50 min. at a flow rate of 1 mL/min. was adopted.

It was imperative to assign the chirality of the four Hil isomers prior to analysis of the test mixture. This was done by analysis of two spectra simultaneously. From the HPLC traces of (2R, 4S)- and (2RS, 4S)-Hil it was possible to identify the D-allo (2R, 4S) isomer from the L (2S, 4S) isomer. Comparison of the HPLC traces of (2RS, 4S) and (2RS, 4RS) allowed for identification of the remaining two isomers. Coinjection of all standards with the test mixture revealed the presence of D-allo and L-Hil in the peptide. Relevant HPLC traces are included in Appendix C.

HPLC Analysis of Nmm

The synthetic scheme adopted for the synthesis of Nmm did not allow for the individual isolation of each isomer. However in order to verify the presence of Nmm in the peptide, it was imperative that one of the four isomers elute at the same retention time as the peak assigned as Nmm. RP HPLC was used with a linear gradient of 10% CH_3CN to 60% CH_3CN for 45 min. at a flow rate of 1 mL/min. at 25°C. The other solvent used was 25mM acetic acid. The peak of FDAA derivatized Nmm that coeluted with one of the unassigned peaks in the FDAA derivatized hydolysate of vitilevuamide was collected. ESMS verified the mass to be the same as that of FDAA derivatized Nmm. Negative HR FABMS (glycerol): *m/z* 414.12585; $C_{15}H_{20}O_9N_5$ requires 414.12610 (Δ = 0.25 mmu).

HPLC Analysis of Lan

FDAA derivatization of commercially available Lan did not yield a clean trace like the other amino acid standards. In order to unambiguously confirm the presence of Lan in the peptide hydrolysate, LCMS was the method adopted.

Two reference samples of Lan were prepared. One of the reference samples was treated under the same hydrolytic conditions as the peptide **49**, but the other was not. LCMS of the nonhydrolyzed reference sample of dextro, levo, meso (DLM)-Lan showed an *m/z* ion at 460 (MH^+ = 461), confirming the presence of the FDAA derivative of Lan. When the hydrolyzed reference sample of DLM-Lan was subjected to similar conditions, no *m/z* of 460 was observed. This implied that if Lan was present in the peptide it would not survive the hydrolytic procedure. As a result no further effort was made to determine its chirality. The LCMS traces of Lan are included in Appendix C.

CHAPTER 5

THE BIOLOGY OF VITILEVUAMIDE

Screening in Human Tumor Cell Lines

A mechanism directed screening approach is adopted in the Ireland laboratory to identify molecules of potential interest to the group. One approach involves initial cytotoxicity studies using the human colon cancer cell line, HCT 116, available from American Type Culture Collection (ATCC), Rockville, Maryland. HCT 116 is one of three strains of malignant cells isolated by M. Brattain, *et al.*, in 1979 from a male patient with colonic carcinoma .[100] The cells form colonies in semisolid agarose medium and were cultured according to the specifications of ATCC.[101] They had a doubling time of 20-22 hours with a saturation density of approximately 4 X 10^5 cells/cm^2.

Based on initial results, a thorough examination of the cytotoxicity profile of a new molecule is instigated. This involves screening the molecule through a panel of human tumor cell lines maintained in-house by one of our collaborators, Dr. Barrows. The cell lines include the A549 human adenocarcinoma line, which was initiated in 1972 by D. J. Giard *et al.* through the explant culture of lung carcinomatous tissue from a 58-year-old Caucasian male.[102]

SK-MEL-5, human malignant melanoma cell line, was developed using cells obtained from the thoracic duct of a patient with widespread and rapidly progressing malignant melanoma.[103] A 498 is a human kidney carcinoma cell line.[104] It was developed from the carcinoma of a 52 year old male.

Screening is performed in a 96 well microtitre plate using the standard 3-[4,5-dimethylthiazol-2-yl]-2,5-phenyltetrazolium bromide; thiazolyl blue (MTT) cell inhibition

assay adopted for anticancer drug screening at NIH.[105] Positive controls are run simultaneously to allow determination of potencies of the new isolates relative to the specific tumor type and the standard drug. These standards are normally cytotoxic and clinically relevant drugs.

Purified drugs are also screened for *in vivo* activity in a P388 protocol at Wyeth-Ayerst Research. This screen involved injecting CDF1 mice intraperitonially on day 0 with $1x10^6$ P388 tumor cells. Five animals are randomly placed in a group. On day 1, 5 and 9 of posttumor implantation these mice are treated with either placebo or drug intraperitonially. Animals are checked twice daily and the day of the death of every mice posttumor implantation is recorded. A positive drug response is defined as a greater than 25% increase in the mean life span (% ILS) relative to placebo control.

Tubulin Inhibition Assay

A major specific target of a substantial number of cytotoxic agents is the cellular microtubule system, which forms the framework of the mitotic spindle. Drugs that bind to microtubule components, particularly tubulin, cause cells to accumulate in metaphase arrest .[106] The most important mitotic inhibitors, particularly from a clinical point of view, are the Vinca alkaloids vincristine and vinblastine.[107]

The tubulin inhibition assay exploits a tubulin dependent change of rodent astrocytoma and glioma cell lines. This change is manifested when the cells are treated with cyclic AMP (cAMP) analogs such as dibuteryl-cAMP (db-cAMP).[108-109] The C6 rat glioma cells (ATCC CCL 107) assume a spherical morphology within 60 minutes in response to db-cAMP. In doing so the cells release somewhat from the substrate. This "rounding" is due to polymerization of tubulin. Cells that are exposed to tubulin-active compounds display a different morphological change.[110] These cells flatten and adhere to the substrate. This forms the basis of the assay.[111]

The assay is adapted to a 96 well microtitre plate that renders the results quantifiable by an objective measure. The rat glioma cells are seeded in the microtitre plate and allowed

to incubate for a day. The cells are then treated with a range of drug concentrations (normally covering five orders of magnitude) and incubated for a further 4 hours. The cells are then treated with 1mM db-cAMP and incubated for another hour.

All the wells are then jet aspirated with a customized tool that delivers an even flow of phosphate buffered saline (PBS) to the bottom of each well. For optimal results the dynamic effect of the buffer flow combined with the aspirating vacuum must be relatively even. In the case of anticancer drugs like vincristine, visual inspection under a microscope of the plates upon aspiration confirms morphological changes in keeping with their tubulin disruption mechanism.

Following aspiration all culture wells are resupplied with fresh medium to which MTT has been added. The glioma cells metabolize MTT to a dark formazan dye.[112-113] Four hours are allowed for the metabolite to accumulate. The comparison between treated and untreated cultures, and between tubulin active and inactive compounds can then be quantified. This is done via semiautomated analysis of the metabolite using light absorbance at 450 nM by cells surviving the aspiration. The software then computes the response to that of colchicine (25 μg/mL) which acts as a positive control.

Biological Activity of Vitilevuamide

Vitilevuamide was strongly cytotoxic against the HCT 116 cell line with an IC_{50} of 10 ng/mL. Figure 5.1 shows the fractional survival graph of vitilevuamide for a dose range of 1 mg to 100 μg. Figure 5.2 provides the cytotoxicity profiles of vitilevuamide in the A5249 lung cancer cell lines where it exhibited an IC_{50} of 0.2 μg/mL. In the SK MEL-5 melanoma tumor cell lines vitilevuamide had an IC_{50} of 0.5 μg/mL. This is depicted in Figure 5.3. Figure 5.4 provides the cytotoxicity profile of vitilevuamide in the A498 kidney cancer cells where it exhibited an IC_{50} of 5 μg/mL.

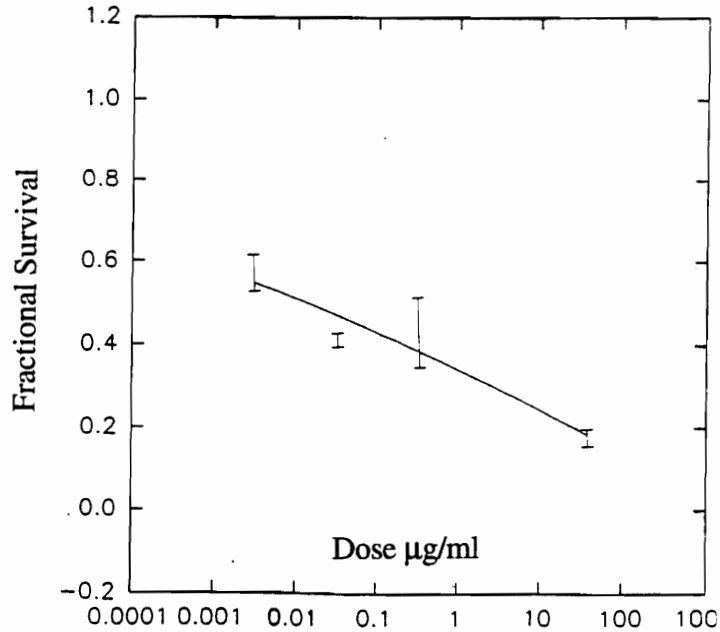

Figure 5.1 Fractional Survival of HCT 116 colon cancer cells upon treatment with Vitilevuamide

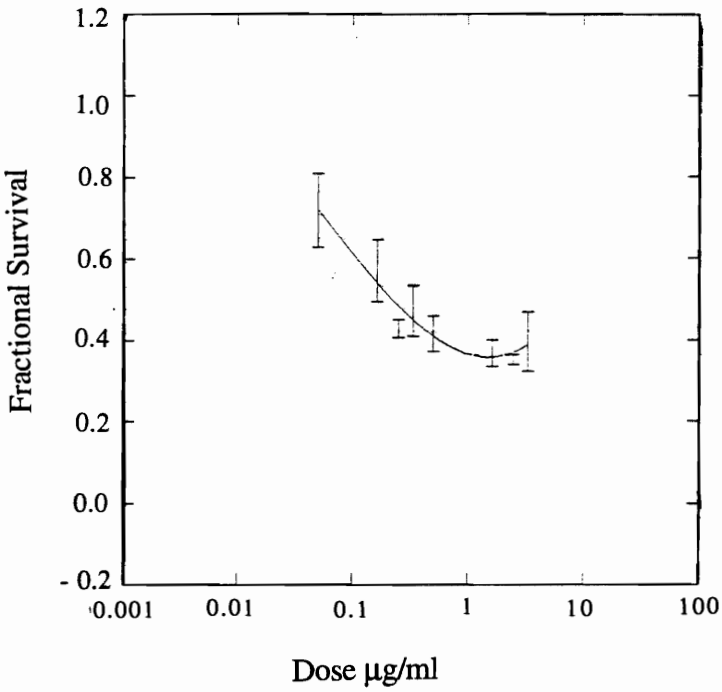

Figure 5.2. Fractional Survival of A549 lung cancer cells upon treatment with vitilevuamide

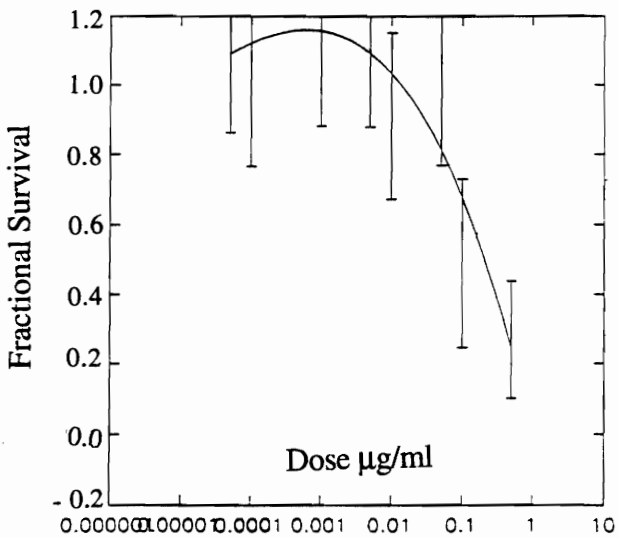

Figure 5.3. Fractional survival of SK MEL-1 melanoma cells upon treatment with vitilevuamide

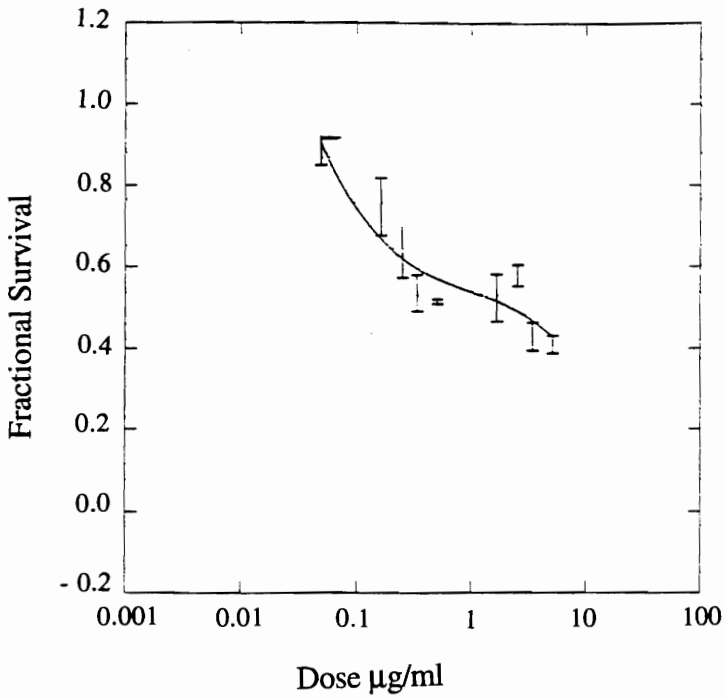

Figure 5.4. Fractional Survival of A498 kidney cancer cells upon treatment with vitilevuamide

In the tubulin inhibition assay, vitilevuamide showed the same effect as colchicine at a concentration of 4 μg/mL. Figure 5.5 depicts the absorbance of wells treated with vitilevuamide expressed as a function of the absorbance of wells treated with 25 μg/mL colchicine. In the P388 *in vivo* experiment vitilevuamide exhibited a %ILS of 70 at a concentration of 30 μg/mL. The results are presented in Table 5.1.

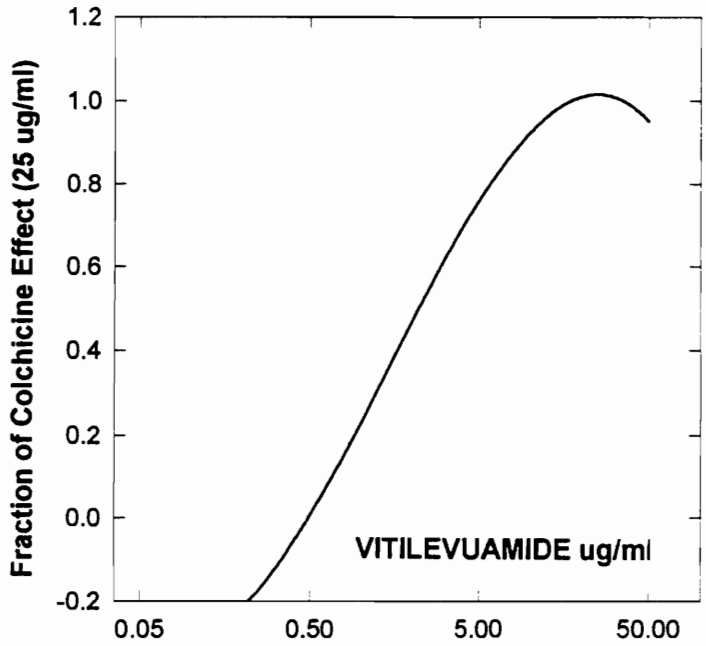

Fig. 5.5. Absorbance of wells treated with vitilevuamide expressed as a fraction of the absorbance of wells treated with 25 µg/mL colchicine.

Table 5.1. %ILS of vitilevuamide at different doses

Dose (mg/kg/dose)	%ILS
0.13	-45 (toxic)
0.06	-13 (toxic)
0.03	70
0.012	20
0.006	8

CHAPTER 6

SUMMARY

The objective of my thesis was isolation, structure elucidation and characterization of a novel bicyclic peptide from marine sources. This project was initially pursued because of interesting cytotoxicity exhibited by vitilevuamide. After working with different isolation procedures, it was possible to narrow down the isolation scheme to a definite protocol that gave reasonable recovery. Structure elucidation was effected using one- and two-dimensional NMR spectroscopy along with MS.

Commercially nonavailable amino acids were synthesized using both literature precedence as well as novel strategies. Marfey's methodology allowed assignment of the chirality of some amino acids in the peptide. During this process new methods for separation of Ile and Thr isomers nondistinguishable by Marfey's protocol were developed. The HPLC regimen was modified for identification of Hil and Nmm in the peptide hydrolysate. LCMS was used to study the stability of Lan.

In order to find out the mechanism of action various assays were carried out both in house as well as at Wyeth-Ayerst Research. Vitilevuamide exhibits a profile of a tubulin inhibitor. In house tubulin inhibition assays and *in vivo* assays were run in order to get a mechanistic profile of this molecule.

The structure elucidation of vitilevuamide however is not complete at this point of time. There are a few aspects that need to be addressed and resolved. One of these issues is the chirality of Nmm. We were able to confirm its presence in the peptide, but we were unable to assign its chirality. Stereospecific synthesis of Nmm or synthesis geared towards the identification of all four isomers of Nmm would help resolve this issue.

The same issue exists with assigning the chirality of Lan. The problem here however is the hydrolytic procedure adopted results in the degradation of the amino acid. A milder hydrolytic approach or a hydrolysis protocol aimed at retaining the Lan amino acid in vitilevuamide would allow for the detection of Lan. Marfey's procedure could then be followed for derivatization and detection as in the case with the standard amino acids.

An interesting observation in the case of vitilevuamide is the presence of two Hil residues of different chirality. This has been observed in peptides like salinamide[114] which has two different Ile residues and in the case of kahalalide F[115] which has L-Thr and D-alloThr residues. At this juncture it is difficult to place one of the two isomers at a definite site. However, one could possibly synthesize this peptide by stationary solid phase synthesis and come up with different structures to generate a structure activity relationship profile for vitilevuamide which might help solve this issue.

CHAPTER 7

EXPERIMENTAL

Chemicals, Reagents, and Organisms

The isolation and chemical characterization of vitilevuamide along with the synthesis of novel amino acids are described in this chapter. The purity of these compounds was assessed by chromatography and NMR analysis. Reagent grade solvents were distilled prior to use. Solvents for HPLC use were either purchased as such from Baxter (McGaw Park, IL) or distilled solvents were filtered and degassed before usage. NMR solvents were purchased from Aldrich (Milwaukee, WI), Cambridge Isotope (Woburn, MA), or Isotec Inc. (Miamisburg, OH).

FDAA reagent and amino acid standards were purchased from Sigma Chemical Company (St. Louis, MO.). Inorganic compounds were purchased from Aldrich Chemical Company, Inc. (Milwaukee, WI.). Organic chemicals like S-(+)-1-bromo-2 methylbutane, diethyl acetamidomalonate, (±)-1-bromo-2-methylbutane, hydroquinone, MEMCl, DIPEA, acrolein diethylacetal, benzonitrile, methylamine, TBDMSOTf, glycidol, TPAP and NMO were obtained from Aldrich Chemical Company, Inc. (Milwaukee, WI.) or from Sigma Chemical Company. Methoxyacetaldehyde was ordered from TCI America (Portland, OR).

Enzymes like catalase and L amino acid oxidase as well as dowex resins were obtained from Aldrich. Solid support for chromatography (silica gel, C-18, amino silica gel and LH20) was ordered from EM Science (Gibbstown, NJ) or Baxter. Thin layer chromatography was done with Whatman K6F Gel 60 Å TLC plates, HPTLC-Fertigplatteen RP-18 plates and HPTLC-Fertigplatteen NH_2 plates.

General Experimental Procedures

Nuclear Magnetic Resonance (NMR) Spectroscopy

^1H and ^{13}C experiments were obtained at 500 and 125 MHz respectively, on a Varian Unity spectrometer or an IBM AF 200 spectrometer at 200 and 50 MHz, respectively. Variable temperature studies were performed at -20, -15, -10, -5, 0, 5, 10, 15, 20, 25, 30 and 35°C and variable solvent studies were performed using CD_2Cl_2, $CDCl_3$ and C_6D_6. Based on these results, all NMR experiments were carried out in benzene at 22°C. ^1H chemical shifts were reported in ppm relative to undeuterated benzene resonance at 7.15 ppm while ^{13}C chemical shifts were reported in ppm relative to solvent resonance at 128 ppm. For synthetic molecules, the proton chemical shifts were reported in ppm relative to the residual solvent resonance (7.24 ppm for $CDCl_3$ and 3.30 ppm for MeOH-d_4 relative to TMS used as an internal standard). ^{13}C chemical shifts were similarly reported in ppm relative to the solvent resonance (77.0 ppm for $CDCl_3$ and 49.0 ppm for MeOH-d_4).

IR and UV Spectroscopy

IR spectra were recorded on a Perkin-Elmer 1600 FT spectrophotometer using a thin film of compound on sodium chloride plates. UV spectra were recorded on a Hewlett-Packard HP8452A spectrophotometer.

Mass Spectrometry

High and low resolution mass measurements (FAB, EI, CI) were made on a ZAB-SE or on a Varian MAT-731 (Dr. Elliot M. Rachlin) mass spectrometer. Electrospray mass measurements were made on a VG Fisons Trio (Dr. John Peltier) quadrupole mass spectrometer. Tandem MS (Mr. Steve Pomerantz) was performed on the SIAX API III spectrometer. LCMS (Dr. Andy Whitehill) was performed on a VG Quattro II triple quadrupole mass spectrometer. Positive HRFAB on vitilevuamide was performed by Dr. K. L. Rinehart's laboratory.

The Chemistry of *Didemnum cuculliferum* and *Polysyncraton lithostrotum*

Collection, Extraction, and Isolation

The ascidians, *Didemnum cuculliferum* and *Polysyncraton lithostrotum*, were collected by SCUBA in the Fiji islands and were kept frozen until extracted. The MeOH extract of the frozen tunicate *Didemnum cuculliferum* (350 grams) was repeatedly extracted with 2.5L of MeOH. The crude homogenate (reduced to 50 mL) was separated into fractions of increasing polarity by extracting first with hexanes (3 x 500 mL) followed by chloroform (5 x 500 mL) using a modified Kupchan solvent partitioning scheme.

The resulting 325.1 mg of chloroform extract was subjected to silica gel flash chromatography using a 28 mm I.D. x 46 mm long column with 60Å, 35-70 μm silica support. Using stepped gradient elution, $CHCl_3$; 99:1 $CHCl_3$ / MeOH; 98:2 $CHCl_3$ / MeOH; 97.5:2.5 $CHCl_3$ / MeOH, the active component was identified in the 98:2 $CHCl_3$ / MeOH fraction. A second silica flash chromatography step was performed with identical column specifications using 3:7 CH_3COCH_3 / C_6H_{14}; 7:3 CH_3COCH_3 / C_6H_{14} and 100% CH_3COCH_3 in a gradient fashion.

The 7:3 CH_3COCH_3 / C_6H_{14} fraction was subjected to RP HPLC using a 4.6 mm I.D. x 250 mm long C-18 Rainin Microsorb column with 100Å, 5μ silica gel. A mobile phase of 9:1 CH_3CN / H_2O with UV detection at 220 nm was used to yield **49** as a clear glass (10.2 mg, 0.0029% yield).

In the case of *Polysyncraton lithostrotum*, an identical procedure was followed until the silica gel flash chromatography step. Reverse phase flash chromatography was performed (28 mm I.D. x 46 mm long column) with LiChroprep RP-18, 40-63 μm, using stepped gradient elution with vitilevuamide (**49**) eluting in the 90% MeOH H_2O fraction. This fraction was then subject to Bakerbond amino, 40 μm, solid support (gradient flash chromatography, 28 mm I.D. x 46 mm long column) with vitilevuamide eluting in the 5% MeOH / $CHCl_3$ fraction (12.5 mg, 0.00025% yield).

Physical and Spectral Properties of Vitilevuamide

White amorphous solid; IR (neat film) V_{max} 3280, absorbtions centered at 2928, 1734, 1652, 1558,1538 cm^{-1}; UV (MeOH) λmax = 230 nm (ε = 2032.38); LRFABMS (glycerol) and ESMS: *m/z* 1603.8 $(M+H)^+$; HRFAB (glycerol): 1603.811768; (Δ 3.574 mmu), $C_{77}H_{114}N_{14}O_{21}S$ requires 1603.808195; NMR data contained in Table 2.2.

Tandem Mass Spectrometry

Tandem mass spectra were obtained on a SIAX API III spectrometer. Five μL of sample were dissolved in 190 μL of 50:50:1 H_2O:CH_3OH:CH_3COOH and injected into the probe at a flow rate of 2 μL/min.

LCMS on Lan and Vitilevuamide hydrolysate

LCMS was performed on the VG Quattro II triple quadrupole mass spectrometer. Two types of FDAA derivatized Lan standards were used. The first standard consisted of DLM-Lan (a mixture of all the three isomers of Lan; dextro, levo and meso) derivatized using standard Marfey's procedure. The second standard consisted of DLM-Lan which was subjected to the same hydrolytic procedure as **49** (DLM-Lan (1 mg) heated in HCl (5 mL, 6N) at 104°C for 18 h) and derivatized using Marfey's procedure .

For the LC analysis 5 μL of the sample was injected into the RP Rainin Microsorb column of 4.6 mm I.D. x 250 mm length with 100Å, 5μ silica gel. A mobile phase of 1% CH_3COOH acid / CH_3CN (90:10) was used. The gradient went from 10% CH_3CN to 60% CH_3CN over a period of 45 min. at a flow rate of 1 mL/min. at 25°C. UV detection at 340 nm was used.

Assays

Assay for tubulin inhibition and cytotoxicity assays were performed in the laboratory of Prof. Louis R. Barrows and are described elsewhere. The *in vivo* experiment was performed at Wyeth-Ayerst Research and is described elsewhere.

Partial Linearization of Vitilevuamide using Ammonia

Saturated NH_3 in HPLC grade MeOH (1.5 mL) was added to vitilevuamide **49** (1.2 mg) in MeOH (5 mL). The solution was placed in a capped vial in a freezer at 0°C for 18 h. The resulting mixture was then chromatographed by RP HPLC (Waters NOVAPAK C_{18}; 4.6 I.D. x 100 mm long column), isocratic elution using 90% MeOH / H_2O to afford the partially linear peptide **50** (1.1 mg, 91.67 % yield).

Physical and Spectral Properties of Partially Linearized Vitilevuamide (50)

Colorless solid: UV (MeOH) λmax = 230 nm (ε = 2032.38); ESMS: *m/z* 1620.8 $(M+H)^+$.

General Hydrolysis and Derivatization

Hydrolysis of vitilevuamide (1 mg) was carried out in HCl (6N, 5 mL) under a nitrogen atmosphere in a sealed bomb at 104°C for 18 h. After removing traces of HCl by repeated evaporation *in vacuo*, the residual hydrolysate was suspended in acetone (300 µL) and derivatized with FDAA using Marfey's procedure. According to this procedure, hydrolyzed vitilevuamide **50** (0.69 mg, 5 µmol) was dissolved in acetone (100 µL). FDAA (200 µL, 1% (w/v) solution in acetone) was added followed by the addition of sodium bicarbonate (40 µL, 1.0 M). The solution was heated in a sealed vial at 40°C for 1 h. After cooling to room temperature HCl (20 µL, 2M) was added and the sample was degassed by placing it in a sonicator for 25 min. All standards were derivatized in a similar manner.

HPLC analysis (Waters NOVAPAK C_{18}; 4.6 x 100 mm column; linear gradient elution, triethylammonium phosphate (50 mM, pH 3.0) / acetonitrile, 90:10 to 60:40 in 45 min. at a flow rate of 1.5 mL/min.; UV detection at 340 nm) of the FDAA derivatized hydrolysate in conjunction with similarly derivatized amino acid standards established the stereochemistry of the constituent amino acids.

Preparation of Hil (**55**)

Diethyl acetamidomalonate **52** (2.5 g, 11.5 mmol) was added to a solution of sodium metal (0.270 g, 11.7 mmol) in ethanol (100 mL) at room temperature. After 5 min. (*S*)-(+)-1-bromo-2-methylbutane **51** (2.00 g, 13.2 mmol) was added. The solution was heated at reflux for 24 h. After cooling, the reaction mixture was acidified with 1N HCl (pH = 5), poured into water, and extracted with chloroform (3 x 50 mL). The organic extract was dried by passing it through anhydrous sodium sulfate. The resulting brown oil was purified by silica gel column chromatography (7:3 $CHCl_3$ / $C_2H_5OC_2H_5$). Concentration of the appropriate fractions gave ethyl (S)-2-acetamido-2-(ethoxycarbonyl)-4-methyl-hexanoate **53**. The compound is a pale yellow solid: 2.5 g, 9.0 mmol, 78% yield. ^1H NMR (200 MHz, $CDCl_3$) δ 0.81 (d, *J* = 6 Hz, 3 H, 4-methyl), 0.81 (t, *J* = 7 Hz, 3 H, terminal methyl), 1.24 (overlapping t (*J* = 7 Hz) and m, 9 H total; ethoxy methyls, 4-H and 5-H_2), 2.02 (s, 3 H, acetyl methyl), 2.16 (dd, *J* = 15, 7 Hz, 1 H, 3-H), 2.44 (dd, *J* = 15, 4 Hz, 1H, 3-H), 4.23 (m, 4H, ethoxy methylenes), 6.83 (br s, 1 H, NH); FABMS: *m/z* 288 $(M+H)^+$.

Ethyl-S-2-acetamido-2-(ethoxy carbonyl)-4-methylhexanoate **53** (1 g, 3.48 mmol) obtained was heated at reflux in HCl (6N, 5 mL) overnight. The resulting mixture was concentrated *in vacuo* to yield (2*RS*, 4*S*)-2-amino-4-methylhexanoic acid hydrochloride (**54**). The compound is a colorless solid: 0.45 g, 2.6 mmol, 75% yield. ^1H NMR (200 MHz, D_2O) δ 0.87 (t, *J* = 7 Hz, 3 H, terminal methyl), 0.94 (d, *J* = 6 Hz, 3 H, 4-methyl), 1.2-2.0 (m, 5 H), 4.04 (m, 1H, α-H); HRFABMS (glycerol): *m/z* 146.11915 $(M+H)^+$ calc for $C_7H_{16}NO_2$ 146.11810 (Δ = 1.05 mmu).

54 (0.48 g , 2.64 mmol) was dissolved in tris buffer (0.2 M, pH 8.0, 50 mL) which contained L-amino acid oxidase (15 mg, 15 units) and catalase (10 mg, 46000 units) buffered at pH = 8 for 18 h at room temperature. The reaction mixture was acidified (pH = 5) and extracted with ether (3 x 50 mL). Upon C18 column chromatography (46 mm I.D.

x 250 mm long, 60Å, 40-63 μm silica, 9:1 MeOH/H_2O) pure (2*R*, 4*S*)-Hil (**55**) was obtained as a colorless solid: 0.24 g, 1.4 mmol, 52% yield. ^1H NMR (200 Mz, D_2O) δ 0.8 (t, *J* = 7 Hz, 3 H, terminal methyl), 0.94 (d, *J* = 6 Hz, 3 H, 4-methyl), 1.2-2.0 (overlapping m's, 5 H), 4.04 (m, 1H, α-H); LRFABMS (glycerol): *m/z* 146 $(M+H)^+$; HRFABMS (glycerol): 146.11821 $(M+H)^+$ calc for $C_7H_{16}NO_2$ requires 146.11810 (Δ = 1.1 mmu).

Preparation of Hil (**57**)

The above procedure was repeated with racemic bromo-2-methylbutane **56** (2.00 g, 13.2 mmol) to yield (2*RS*,4*RS*) Hil (**57**) as a colorless solid: 1.88 g, 10.34 mmol, 75% yield. ^1H NMR (200 Mz, D_2O) δ 0.87 (t, *J* = 7 Hz, 3 H, terminal methyl), 0.94 (d, *J* = 6 Hz, 3 H, 4-methyl), 1.2-2.0 (m, 5 H), 4.04 (m, 1H, α-H); HRFABMS: *m/z* 146.11898 $(M+H)^+$ calc for $C_7H_{16}NO_2$ 146.11810 (δ = 0.88 mmu).

Preparation of Nmm (**62**), Route 1

$Cu(OH)_2$ **58** (5 g, 51 mmol) was added to a solution of sarcosine **59** (6 g, 67 mmol) in H2O (300 mL). The solution was stirred for 15 min. and filtered to remove undissolved **58**. The filtrate was lyophilized to give copper sarcosinate **60** (10 g, 41 mmol, 91% yield); DCI: *m/z* 242, $(M + 2)^+$ 244 (33% of base peak). **60** (10g, 41 mmol) was dissolved in sodium carbonate solution (0.2M, 300 mL). The reaction mixture was cooled to 4°C and methoxy acetaldehyde **61** (20 mL, 186 mmol) was added to it in four equal portions over a period of 8 h. The alkalinity of the solution was tested after each addition and maintained by the addition of sodium carbonate (0.2 M). The reaction mixture was maintained at 4°C overnight with constant stirring. The reaction was quenched by acidification with acetic acid. Through this mixture was passed H_2S gas until there was no more precipitation. The reaction mixture was filtered and analyzed.

Preparation of Nmm (**62**), Route 2

In a three-necked round bottomed flask equipped with a magnetic stirbar were placed powdered, preactivated molecular sieves (2 g), TPAP (141 mg, 0.4 mmol) and NMO (1.41g, 12 mmol) in anhydrous CH_2Cl_2 (10 mL). The greenish mixture was cooled in an acetone / dry ice bath. Glycidol **64** (593 mg, 8 mmol) in CH_2Cl_2 (7 mL) was added via a syringe under anhydrous conditions, followed by removal of the acetone / dry ice bath. The temperature of the reaction was allowed to raise to 0°C as the color turned dark green. After 2 h of stirring at 0°C, the mixture was passed through a silica gel plug (6 cm x 1 cm i.d.) with CH_2Cl_2. The solution was concentrated *in vacuo* at 0°C. Chromatography using a 28 mm i.d. x 460 mm long column with 60 Å, 35 - 70 μm silica gel and CH_2Cl_2 yielded glycidal (**65**) as a colorless liquid: 1.06 g with residual CH_2Cl_2, 12% yield. ^1H NMR (200 Mz, CD_2Cl_2) δ 3.04 (dd, J = 3 Hz, 1 H, ^1H at epoxy methylene), δ 3.15 (dd, J = 5 Hz, 1 H, ^1H at epoxy methylene), 3.30 (m, ^1H at epoxy methine), δ 8.90 (d, J = 7, H at carbonyl). Further reactions did not yield desired products and were not characterized.

Preparation of Nmm (**62**), Route 3

In a three-necked round bottomed flask equipped with a magnetic stirbar were placed powdered, preactivated molecular sieves (2 g). The flask was stoppered in an argon environment. Glycidol **64** (0.6 g, 8 mmol) in anhydrous CH_2Cl_2 (7 mL) was added via a syringe under argon to the reaction vessel. MEMCl (1.25 g, 10 mmol) in anhydrous CH_2Cl_2 (5 mL) was added via a syringe followed by the addition of DIPEA (1.15 g , 9 mmol) in CH_2Cl_2 (5 mL). The reaction mixture was stirred at room temperature under argon for 24 h. It was filtered through a buchner funnel to yield MEM glycidol, **67**, a colorless liquid: 1.2 g , 4 mmol, 90% yield. ^1H NMR (200 Mz, CD_2Cl_2) δ 2.3-2.5 (m, side chain methylene) δ 3.04 (dd, J = 3 Hz, 1 H, ^1H at epoxy methylene), 3.30 (s, MEM methyl), 3.5 (m, MEM methylene), 3.7 (m, MEM methylene), 3.8-4.0 (m, glycidol methylene), 4.5 (s, H at acetal carbon).

67 (0.5 g, 3 mmol) was added to a three-necked flask equipped with a Leibegs condenser and containing powdered, preactivated molecular sieves (2 g). The entire system was kept in an inert state by passage of agron. Sodium methoxide (0.5 g, 9 mmol) in anhydrous MeOH (5 mL) was added via a syringe. The reaction was gently refluxed for 4 h. The reaction mixture was filtered through a buchner funnel. H2O (25 mL) was added to the filtrate. The filtrate was extracted with CH_2Cl_2 (25 mL x 3) and dried *in vacuo* to yield 3-methoxy-1-O-MEM-propane-1, 2 diol, (**68**), a colorless liquid: 0.3 g , 2 mmol, 60% yield. ^1H NMR (200 Mz, CD_2Cl_2) δ 3.04 (dd, J = 3 Hz, 1 H, ^1H at epoxy methylene), δ 3.15 (dd, J = 5 Hz, 1 H, ^1H at epoxy methylene), 3.30 (m, ^1H at epoxy methine), δ 8.90 (d, J = 7, H at carbonyl). ^{13}C NMR (50 Mz, CD_2Cl_2) δ 58.7 (q, MEM methyl), 66.7 (t, bridge methylene), 69.1 (t, MEM methylene), 69.7 (t, MEM methylene), 75.6 (d, epoxide methine), 77.6 (t, epoxide methylene), 95.7 (t, acetal methylene).

68 (0.6 g , 3 mmol) was added to a three-necked flask containing powdered, preactivated molecular sieves (2 g) and a magnetic stirbar. The entire system was kept in an inert environment by passage of agron. Lutidine (0.87 mL, 3 mmol) in anhydrous CH_2Cl_2 (5 mL) was added via a syringe. Ten min. later TBDMSOTf (1.05 mL, 3 mmol) in anhydrous CH_2Cl_2 (5 mL) was added via a syringe. After 1 h the reaction mixture was filtered. H_2O (25 mL) was added to the filtrate. The mixture was extracted with CH_2Cl_2 (25 mL x 3). The aqueous and organic phases were dried *in vacuo* and examined for the presence of 2-O-TBDMS-3-methoxypropane-1, 2-diol (**70**).

Preparation of Nmm (**62**), Route 4

To a suspension of $KHCO_3$ (1.5 g) in MeOH (50 mL) in a 500 mL round bottomed flask was added acrolein diethyl acetal **72** (12.84 g, 88 mmol). The reaction mixture was allowed to stir for 15 min. at room temperature. Benzonitrile (9.2 mL, 90 mmol) and 30% aqueous H_2O_2 (10.56 g, 93 mmol) were added. The flask was stoppered and the solution stirred at room temperature for 18 h. The reaction mixture was further stirred at 45°C for 4

h. H_2O (50 mL) was added to the mixture. MeOH (50 ml) was removed *in vacuo* from the reaction mixture. This resulted in the precipitation of benzamide.

Benzamide was filtered and the solution was extracted repeatedly with $CHCl_3$ (3 x 50 mL). The organic layers were combined, dried over $MgSO_4$, and evaporated to dryness. Hexane was added to precipitate the traces of benzamide present. This benzamide was again removed by filtration and the hexane was removed *in vacuo* to yield glycidaldehyde diethyl acetal (**73**) as a pale yellow oil: 7.5 g, 52 mmol, 58% yield. ^1H NMR (200 MHz, $CDCl_3$) δ 1.0-1.2 (2t, 6H, CH_3), 2.6 (m, 2H, H_3), 2.9-3.0 (m, 1H, H2), 3.3-3.9 (m, 4H, OCH_2), 4.2 (d, 1H, H1).

Anhydrous methanol (15 mL) was added to a dry three-necked stoppered round bottomed flask containing 7.3 g (50 mmol) of **73** and dry, activated, powdered molecular sieves (2 g). The reaction mixture was stirred under argon for 15 min. Sodium methoxide (2% solution) in anhydrous methanol (5 mL) was added via a syringe to the stirring reaction mixture. This was then stirred for 4 h under argon. The reaction mixture was filtered to remove the molecular sieves. The filtrate was then fractionally distilled under reduced pressure using a short path distillation unit to give glycidaldehyde diethyl acetal (**74**) as a pale yellow colored liquid (bp 86°C, 50 mm Hg). ^1H and ^{13}C NMR spectra showed traces of impurity. Hence the molecule was further purified by silica flash chromatography using a 28 mm I.D. x 46 mm long column with 60Å, 35-70 μm silica support. The desired compound eluted at a solvent composition of 45% acetone and 55% hexane as a colorless oil: 6.7 g, 38 mmol, 58% yield. ^1H NMR (500 MHz, $CDCl_3$) δ 1.2-1.5 (m, 6H, CH_3), 3.0 (d, 1H, OH), 3.4 (s, 3H, OCH_3), 3.1-3.8 (m, m, 7H, H1, CH_2, CH), 4.5 (d, 1H, H2). ^{13}C NMR (125 MHz, $CDCl_3$) δ 17.3 (CH_3), δ 60.9 (CH), δ 64.8 (CH_2), δ 65.4 (CH_3), δ 73.1 (CH), δ 75.3 (CH), δ 104.7 (CH).

A solution of **74** (5.3 g, 30 mmol) in water (50 mL) was stirred with dowex 50 (H^+) resin (2 g, pH 2.8) for 4 h. The reaction was monitored by TLC until the disappearance of the starting material. The resin was filtered and the filtrate concentrated under reduced

pressure to give 3-O-methyl glyceraldehyde **75** as a clear viscous liquid: 2.5 g, 2 mmol, 47% yield. ^{1}H NMR (500 MHz, CD_2Cl_2) δ 3.2 (s, 3H, OCH_3), 3.3 (m, 2H, CH_2), 3.4 – 3.5 (m, 1H, CH). ^{13}C and DEPT (125 MHz) δ 58.3 (CH3), 72.2 (CH), 72.4 (CH2), 89.7 (CH); was in keeping with the published data.

75 (1.25 g, 1 mmol) was added to a dry three-necked flask maintained in an inert argon environment containing anhydrous ZnI_2 (0.3 g, 10 mmol) in anhydrous CH_2Cl_2 (5 mL) and equipped with a Leibeigs condenser. TMSCN (2 mL, 2 mmol) was added via a syringe to the flask. The reaction mixture was allowed to stir for 15 min. Anhydrous MeOH (10 mL) was added via a syringe. After stirring for 5 min. anhydrous $MeNH_2$ was passed through the reaction mixture for 5 min. The reaction mixture was refluxed for 3 h. The resulting mixture was ether partitioned and examined for the presence of Nmm after drying *in vacuo*.

Preparation of Nmm (**62**), Route 5

$NaHSO_3$ (0.52 g, 1 eq) was added to a solution of **74** (0.5 g, 0.5 eq) in H_2O (10 mL). The reaction was allowed to stir for 15 min. in a non stoppered round bottomed flask. $MeNH_2$ (0.15 g, 1 eq) was added to the basic solution. After another 15 min. KCN (0.3 g, 1 eq) was added with constant stirring. The stirring was continued for 15 h at room temperature. Organic extraction of the resultant solution with CH_2Cl_2 (3 x 25 mL) yielded the nitrile (**75**) as a pale yellow colored solid: 0.4 g, 0.003 mmol, 80% yield. NMR data are depicted in Table 3.1; HRFABMS (glycerol): $(M + H)^+$ 145.09631 in agreement with the molecular formula of $C_7H_{16}NO_2$; theoretical mass 145.09769 (Δ = 1.38 mmu).

The nitrile (0.1 g, 0.7 mmol) was subjected to hydrolysis using HCl (5 mL, 6N) at a temperature of 104°C for 18 h. A RP VLC (70 mm long x 30 mm i.d.) was performed to remove all the salts. An LH-20 column, (900 mm long x 30 mm i.d.) with 0.5% TFA in MeOH / $CHCl_3$ 90:10 as the mobile phase was used for further purification. Drying down of the appropriate fractions *in vacuo* yielded Nmm **63** as a colorless solid: 58 mg, 0.0004

mmol, 58% yield. UV (MeOH) λmax = 230 nm (ε = 2032.38); LRFABMS (glycerol): *m/z* 164 $(M+H)^+$; HRFABMS (glycerol): *m/z* 164.09817 $(M+H)^+$; $C_6H_{12}O_4N$ requires 164.09228 (Δ = 0.041mmu). ^1H NMR (500 MHz, CD_3OD) δ 2.6 (s, 3H, NCH_3), 3.2 (s, 3H, OCH_3), 3.4 (m, 2H, CH_3), 3.5-3.7 (m, 2H, CH_3), 4.3 (m, 1H, αH). ^{13}C and DEPT (125 MHz, CD_3OD) δ 32.2 (q, NCH_3), 58.1 (d, α CH), 63.5 (q, CH_3), 67.6 (d, OH-CH), 73.8 (t, CH_2), 169.7 (s, COOH).

HPLC of FDAA Derivatized Vitilevuamide Hydrolysate

Gradient RP HPLC was performed using a Waters Novapak C18, 4.6 x 100 mm column with TEA phosphate buffer (50 mM, pH = 3) / CH_3CN, 90:10 - 60:40, in 45 min. at a flow rate of 1.0 mL/min. at 25 °C. UV detection at 340 nm was used.

HPLC of FDAA Derivatized Hil Isomers

Gradient cyano HPLC was performed using a 4.6 mm I.D. x 250 mm long Rainin Microsorb column with MeOH / 1 % CH_3COOH, 25:75-90:10, at a flow rate of 1 mL/min. UV detection at 340 nm was used.

HPLC of FDAA Derivatized Ile Isomers

Gradient cyano HPLC was performed using a 4.6 mm I.D. x 250 mm long Rainin Microsorb column with MeOH / 1% Acetic acid, 35:65-42:58, for 45 min. at a flow rate of 1 mL/min. UV detection at 340 nm was used.

HPLC of FDAA derivatized Nmm Isomers

Gradient RP HPLC was performed using a 4.6 mm I.D. x 250 mm long Rainin Microsorb column with MeOH / 1% Acetic acid, 10:90-60:40, for 45 min. at a flow rate of 1 mL/min. UV detection at 340 nm was used.

Stereochemistry of Vitilevuamide

Coinjection of standard amino acid derivatives established the presence of D-alloThr, D-Val, D-Phe, D-Ala, L-Ser, L-Pro, L-Ile, D-allo Hil and L-Hil.

APPENDIX A

NMR SPECTRAL DATA OF VITILEVUAMIDE

```
exp4  dept

      SAMPLE              DEC. & VT
date      Sep 20 94  dn               H1
solvent       c6d6  dof           234.5
file      /usr4/fer~ dm              nny
nand/Bertha_Benzen~  dmm             ccw
             e/dept  dmf           15136
   ACQUISITION       dpwr            56
sfrq       125.706  temp          22.0
tn             C13      PROCESSING
at           0.723  lb             4.00
np           32768  wtfile
sw         22650.1  proc             ft
fb           12400  fn            32768
bs              16  math              f
ss               2
pw             7.1  werr
tpwr            62  wexp          deptp
pp            40.0  wbs
pplvl           62  wnt
dl           2.000 ..     DISPLAY
satdly           0  sp           -14.6
j           140.00  wp         22650.1
mult           1.5  vs            3697
tof         -646.9  sc               0
nt           1e+06  wc             250
ct           15520  hzmm          5.80
alock            n  is          500.00
gain            52  rfl        16103.8
      FLAGS         rfp        16089.2
il               n  th              15
in               n  ins          1.000
dp               y  ai    ph
hs              nn
```

Figure A1. Parameter set for DEPT spectrum of vitilevuamide

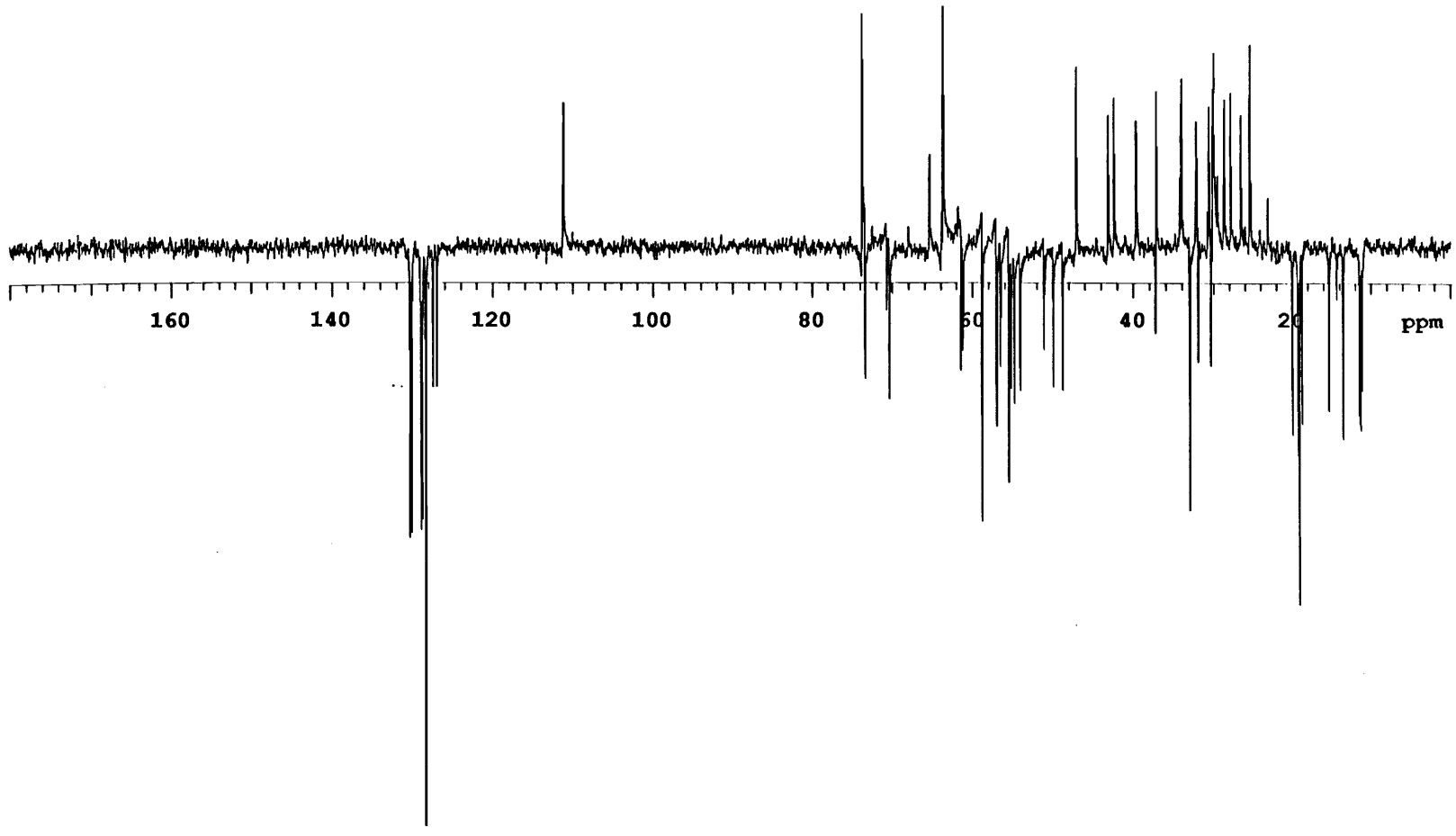

Figure A2. 125 MHz DEPT spectrum of vitilevuamide

```
exp4  dqcosy

      SAMPLE              DEC. & VT          ACQUISITION ARRAYS
date      Oct 16 93  dn              H1    array          phase
solvent       c6d6   dof            74.7   arraydim         640
file      /usr4/fer~ dm              nnn
nand/Bertha_Benzen~  dmm             c     i              phase
             e/cosy  dmf           200     1                1
   ACQUISITION       temp         22.0     2                2
sfrq        499.843      PROCESSING
tn               H1   gf           0.198
at            0.808   gfs       not used
np             8896   wtfile
sw           5502.1   proc           ft
fb             3100   fn           4096
bs                8   math            i
ss                8
tpwr             62   werr
pw             11.0   wexp
dl            1.000   wbs
presat            0   wnt
tof           486.0     2D PROCESSING
nt               72   gf1          0.027
ct               66   gfs1      not used
alock             n   wtfile1
gain             10   proc1          ft
      FLAGS           fn1          1024
il                y        DISPLAY
in                n   sp          245.6
dp                y   wp         5502.1
hs               yn   vs           5000
sspul             y   sc              6
  2D ACQUISITION      wc            225
sw1          5502.1   hzmm         0.63
ni              320   is           7.28
phase      arrayed   rf1          2961.4
    2D DISPLAY       rfp          3207.0
sp1           252.2   th              4
wp1          5502.1   ins          2.400
sc2               0   ai    ph
wc2             130
rf11         2954.8
rfp1         3207.0
```

Figure A3. Parameter set for 500 MHz DQF-COSY spectrum of vitilevuamide

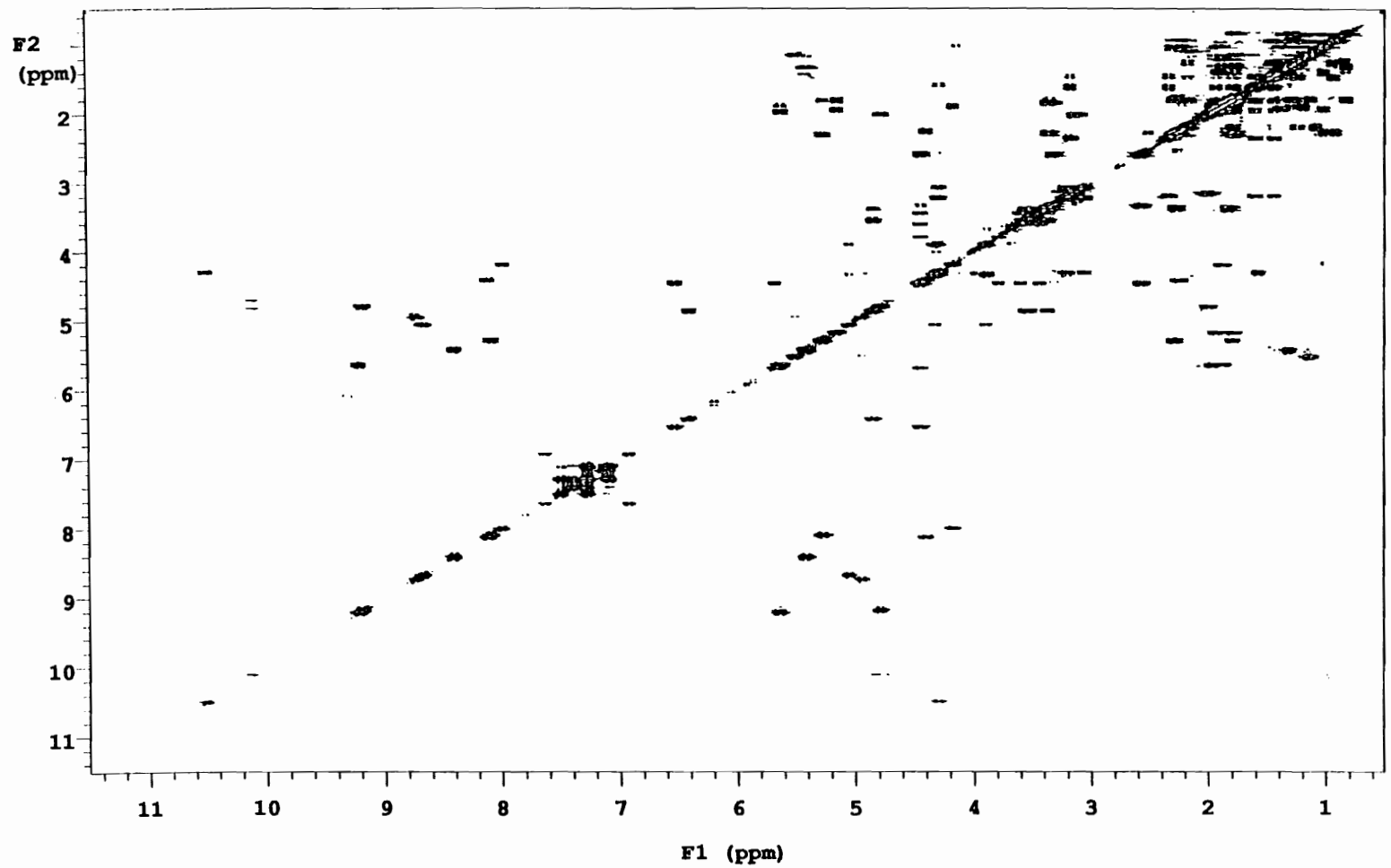

Figure A4. 500 MHz DQF COSY spectrum of vitilevuamide

exp4 tocsy

SAMPLE		DEC. & VT		ACQUISITION ARRAYS	
date	Nov 1 93	dn	H1	array	phase
solvent	c6d6	dof	0	arraydim	1024
file	/usr4/fer~	dm	nnn		
nand/Bertha_Benzen~		dmm	c	i	phase
	e/TOCSY	dmf	200	1	1
ACQUISITION		dpwr	30	2	2
sfrq	499.843	homo	n		
tn	H1	temp	22.0		
at	0.366	PROCESSING			
np	4032	gf	0.050		
sw	5502.1	gfs	not used		
fb	3100	wtfile			
bs	16	proc	ft		
ss	8	fn	1024		
tpwr	52	math	f		
pw	32.0				
pllvl	62	werr			
pl	10.5	wexp			
p2	undefined	wbs			
dl	1.500	wnt	..		
presat	0	2D PROCESSING			
mix	0.030	gf1	0.042		
trim	0.0020	gfs1	not used		
tof	234.5	wtfile1			
nt	28	proc1	ft		
ct	28	fn1	1024		
alock	n	DISPLAY			
gain	23	sp	-4.8		
FLAGS		wp	5502.1		
il	n	vs	100		
in	n	sc	6		
dp	y	wc	225		
hs	n	hzmm	0.84		
sspul	n	is	33.57		
2D ACQUISITION		rf1	3578.7		
sw1	5502.1	rfp	3573.9		
ni	512	th	4		
phase	arrayed	ins	1.000		
2D DISPLAY		ai cdc ph			
sp1	-4.8				
wp1	5502.1				
sc2	0				
wc2	130				

Figure A5. Parameter set for 500 MHz TOCSY spectrum of vitilevuamide

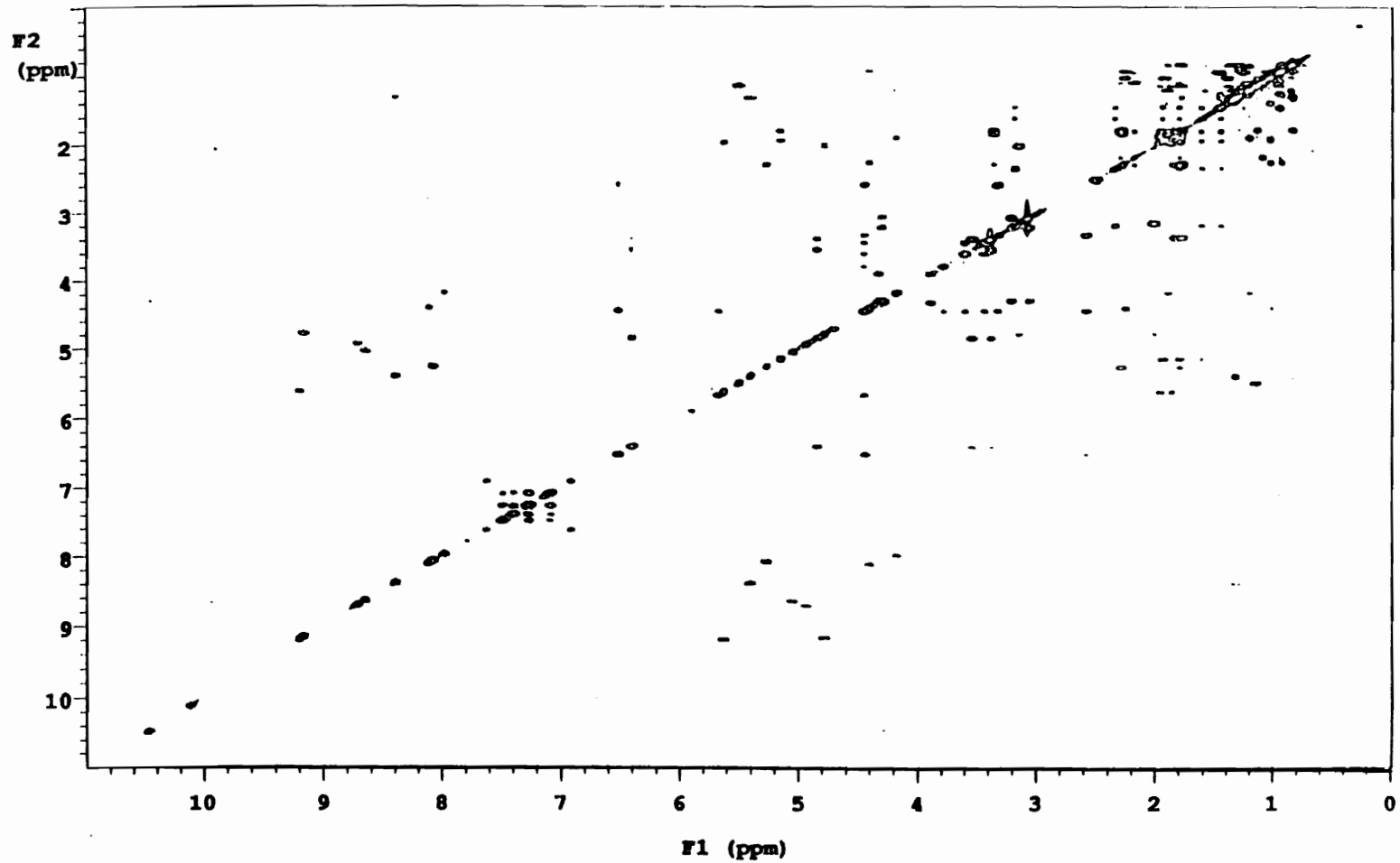

Figure A6. 500 MHz TOCSY spectrum of vitilevuamide

exp4 hmqc

SAMPLE		DEC. & VT	
date	Oct 30 93	dn	C13
solvent	c6d6	dof	-1246.0
file	/usr4/fer~	dm	nny
nand/Bertha_Benzen~		dmm	ccs
	e/HMQC2	dmf	16259
ACQUISITION		dpwr	46
sfrq	499.843	pwxlvl	54
tn	H1	pwx	21.0
at	0.372	homo	n
np	4096	temp	22.0
sw	5502.1	satflg	nn
fb	3100	satdly	0
bs	8	satfrq	0
ss	8	satpwr	0
tpwr	62	PROCESSING	
pw	10.9	gf	0.204
d1	1.500	gfs	not used
tof	234.5	wtfile	
nt	40	proc	ft
ct	40	fn	4096
null	0.4	math	f
j	140.0		
mbond	n	werr	
taumb	0	wexp	
alock	n	wbs	
gain	23	wnt	
FLAGS		2D PROCESSING	
il	y	gf1	0.014
in	n	gfs1	not used
dp	y	wtfile1	
hs	n	proc1	ft
2D ACQUISITION		fn1	1024
sw1	17644.5	DISPLAY	
ni	512	sp	15.3
2D DISPLAY		wp	3986.1
sp1	1937.0	vs	1000
wp1	16746.7	sc	6
sc2	0	wc	225
wc2	130	hzmm	42.32
rfl1	12057.8	is	33.57
rfp1	13960.3	rfl	2415.7

Figure A7. Parameter set for 500 MHz HMQC spectrum of vitilevuamide

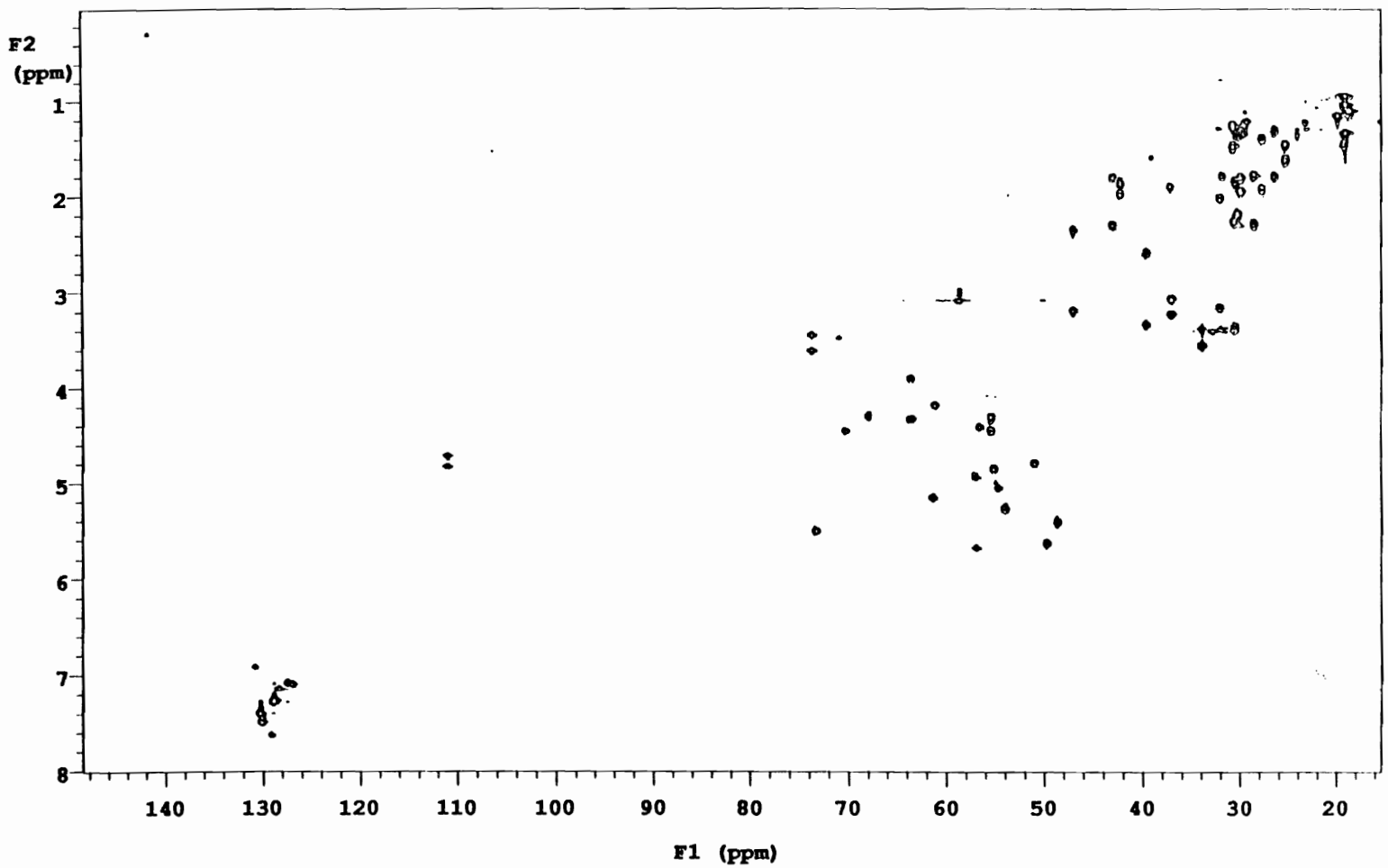

Figure A8. 500 MHz HMQC spectrum of vitilevuamide

exp4 hmqctocsy

SAMPLE		DEC. & VT	
date	Oct 10 92	dn	C13
solvent	cdcl3	dof	-3143.0
file	/usr4/fer~	dm	nny
nand/Bertha_Benzen~		dmm	ccs
	e/hmqctocsy	dmf	16226
ACQUISITION		dpwr	45
sfrq	499.843	pwxlvl	56
tn	H1	pwx	15.0
at	0.192	homo	n
np	1344	temp	22.0
sw	3507.2	satflg	nn
fb	2000	satdly	0
bs	8	satfrq	0
ss	8	satpwr	0
tpwr	63	PROCESSING	
pw	20.2	gf	0.069
pl	10.1	gfs	not used
dl	0.900	wtfile	
tof	-440.1	proc	ft
nt	64	fn	1024
ct	64	math	f
null	0.4		
j	140.0	werr	
mbond	n	wexp	
taumb	0	wbs	
alock	n	wnt	
gain	20	2D PROCESSING	
FLAGS		gf1	0.010
il	y	gfs1	not used
in	n	wtfile1	
dp	y	proc1	ft
hs	n	fn1	1024
2D ACQUISITION		DISPLAY	
sw1	16207.5	sp	-482.1
ni	300	wp	3507.2
2D DISPLAY		vs	7500
sp1	387.1	sc	6
wp1	16207.5	wc	225
sc2	0	hzmm	11.49
wc2	130	is	80.92
rfl1	15702.1	rfl	4060.1
rfp1	16089.2	rfp	3578.0
		th	2

Figure A9. Parameter set for 500 MHz HMQC-TOCSY spectrum of vitilevuamide

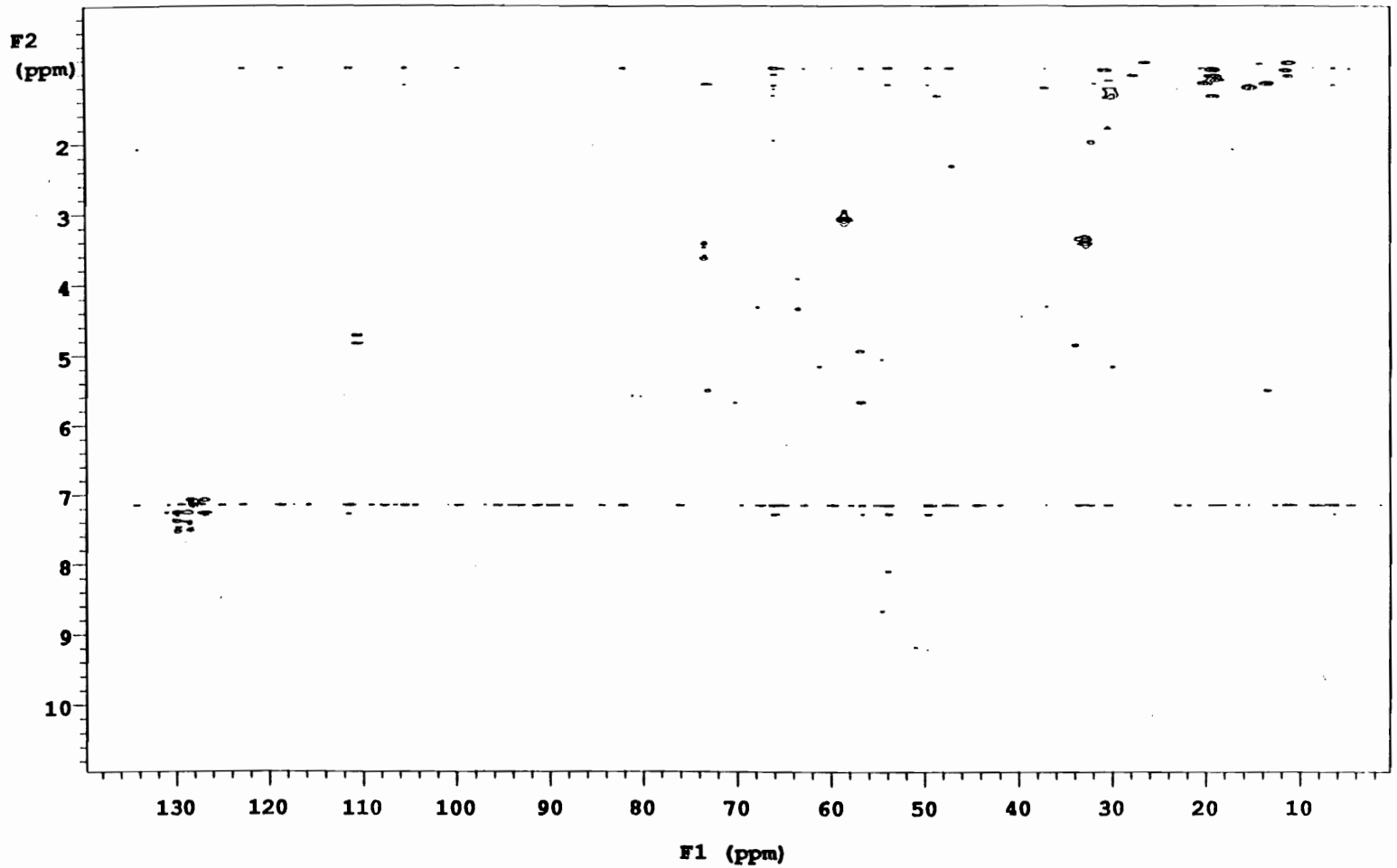

Figure A10. 500 MHz HMQC-TOCSY spectrum of vitilevuamide

exp4 roesy

SAMPLE		DEC. & VT		ACQUISITION ARRAYS	
date	Apr 19 94	dfrq	499.881	array	phase
solvent	c6d6	dn	H1	arraydim	1024
file	/usr4/fer~	dpwr	30		
nand/Bertha_Benzen~		dof	0	i	phase
	e/roesy	dm	nnn	1	1
ACQUISITION		dmm	c	2	2
sfrq	499.882	dmf	200		
tn	H1	dseq			
at	0.186	dres	1.0		
np	2048	homo	n		
sw	5502.1	temp	22.0		
fb	3100	DEC2			
bs	16	dfrq2	0		
ss	8	dn2			
tpwr	62	dpwr2	1		
pw	3.8	dof2	0		
pl	11.2	dm2	n		
dl	1.700	dmm2	c		
presat	0	dmf2	200		
tof	234.5	dseq2			
ratio	0	dres2	1.0		
mix	0.200	homo2	n		
nt	32	PROCESSING			
ct	32	gf	0.086		
alock	n	gfs	not used		
gain	27	wtfile			
FLAGS		proc	ft		
il	n	fn	2048		
in	n	math	f		
dp	y				
hs	yn	werr			
sspul	y	wexp			
rocomp	n	wbs			
2D ACQUISITION		wnt			
sw1	5502.1	2D PROCESSING			
ni	512	gf1	0.046		
phase	arrayed	gfs1	not used		
DISPLAY		wtfile1			
sp	-3.5	proc1	ft		
wp	5502.1	fn1	1024		
vs	1000				
sc	6				

Figure A11. Parameter set for 500 MHz ROESY spectrum of vitilevuamide

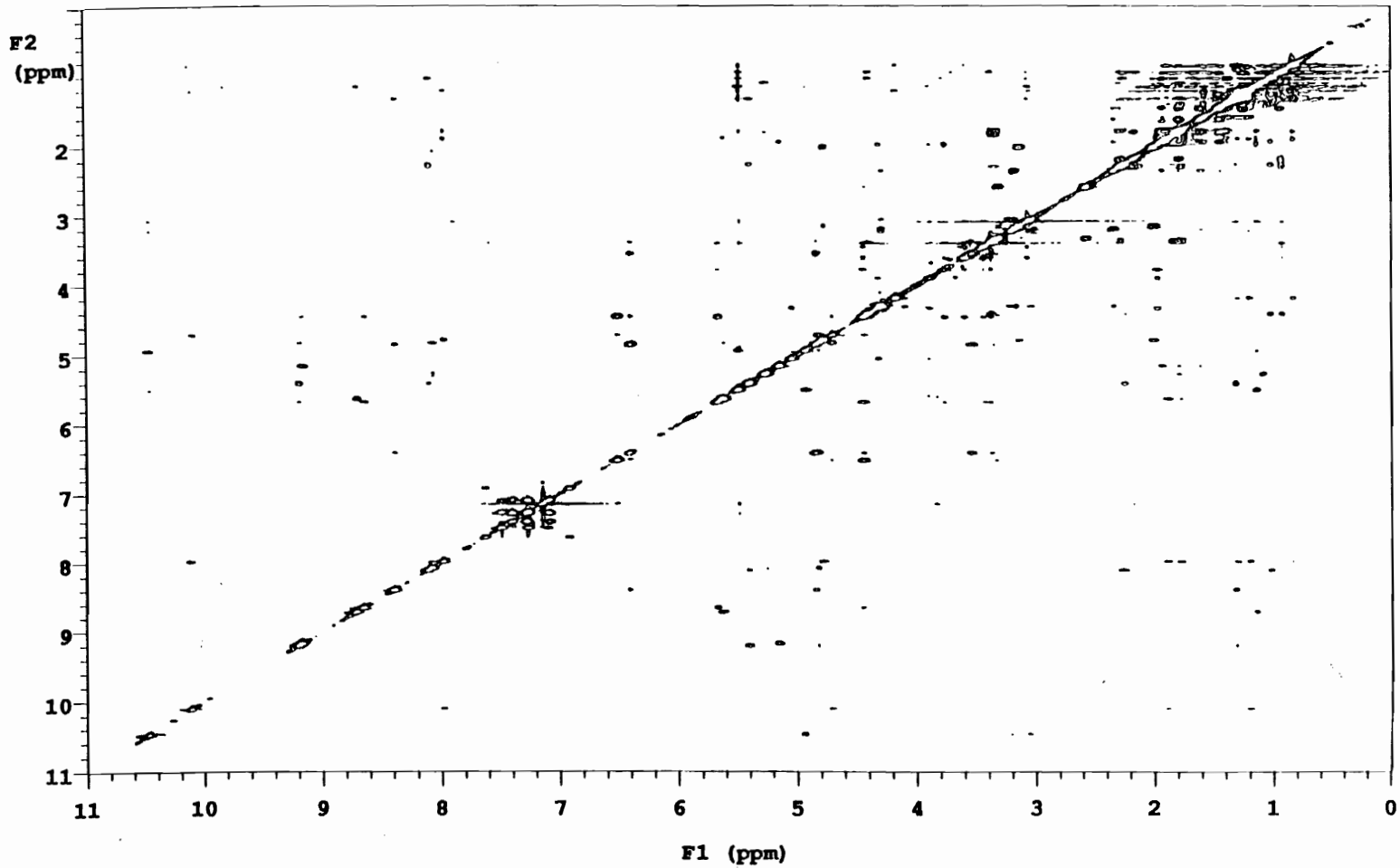

Figure A12. 500 MHz ROESY spectrum of vitilevuamide

exp3 hmqc

SAMPLE		DEC. & VT	
date	Nov 5 93	dn	C13
solvent	c6d6	dof	-228.2
file	/usr4/fer~	dm	n
nand/Bertha_Benzen~		dmm	ccs
	e/HMBC2	dmf	16259
ACQUISITION		dpwr	46
sfrq	499.843	pwxlvl	54
tn	H1	pwx	21.0
at	0.372	homo	n
np	4096	temp	22.0
sw	5502.1	satflg	nn
fb	3100	satdly	0
bs	8	satfrq	0
ss	8	satpwr	0
tpwr	62	PROCESSING	
pw	10.9	sb	0.185
dl	1.500	sbs	not used
tof	234.5	wtfile	
nt	40	proc	ft
ct	40	fn	4096
null	0	math	f
j	140.0		
mbond	y	werr	
taumb	0.063	wexp	
alock	n	wbs	
gain	23	wnt	
FLAGS		2D PROCESSING	
il	y	gf1	0.011
in	n	gfs1	not used
dp	y	wtfile1	
hs	n	proc1	ft
2D ACQUISITION		fn1	1024
sw1	22002.2	DISPLAY	
ni	512	sp	-4.4
2D DISPLAY		wp	5502.1
sp1	725.4	vs	10000
wp1	22002.2	sc	6
sc2	0	wc	225
wc2	130	hzmm	97.7[illegible]
rfl1	15363.8	is	33.5'
rfp1	16089.2	rf1	3578.

Figure A13. Parameter set for 500 MHz HMBC spectrum of vitilevuamide

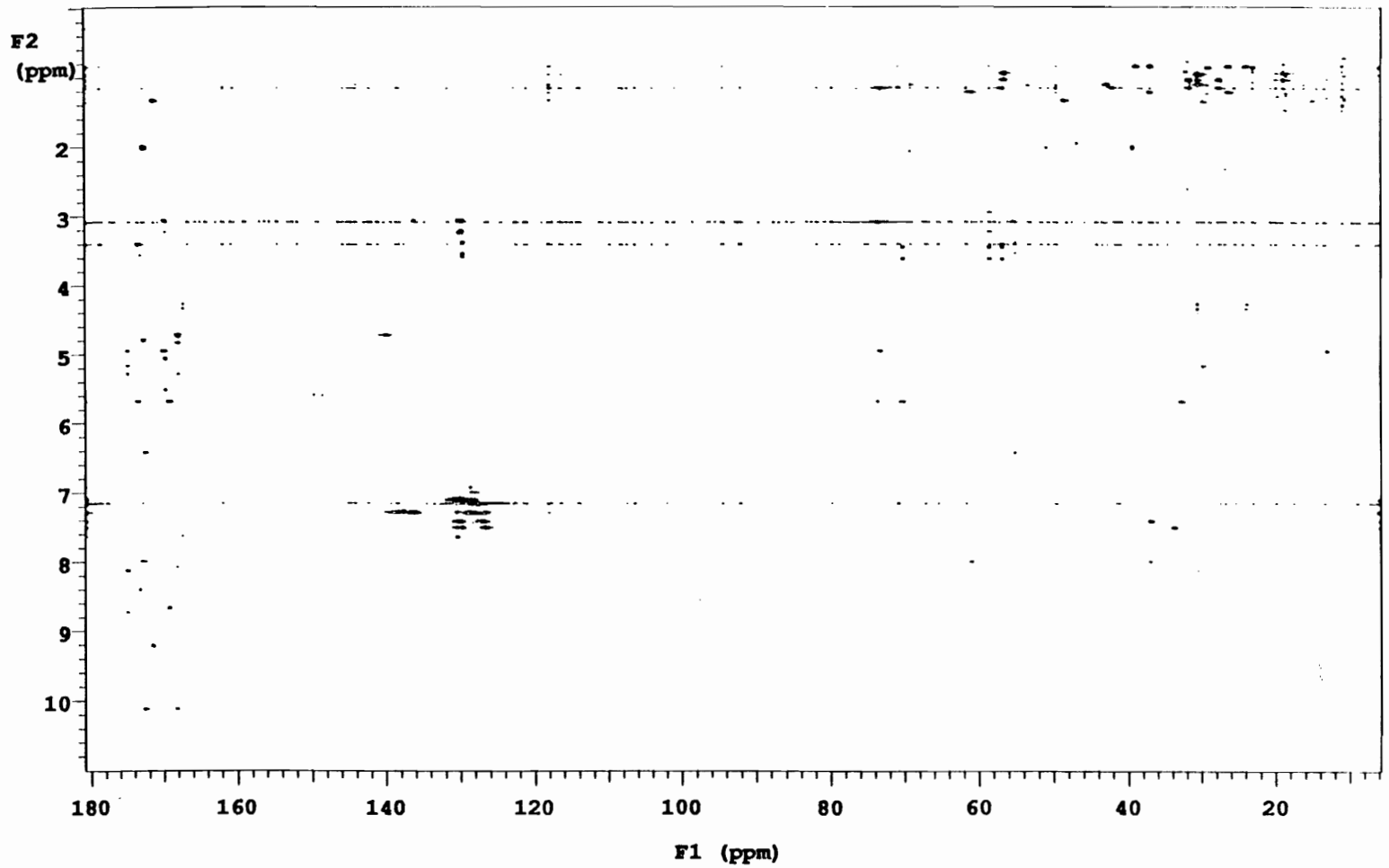

Figure A14. 500 MHz HMBC spectrum of vitilevuamide

```
exp4  lrhetcor

      SAMPLE              DEC. & VT
date      May  8 94  dfrq       not usec
solvent        c6d6  dn                 H:
file      /usr4/fer~ dpwr               56
nand/Bertha_Benzen~ dof            234.5
    e/lrhetcorBB_1   dm                 nny
   ACQUISITION       dmm               · ccw
sfrq        125.707  dmf            14912
tn              C13  dseq
at            0.181  dres             1.0
np             8192  homo               n
sw          22624.4  temp            22.0
fb            12400          DEC2
bs               16  dfrq2              0
ss                1  dn2
tpwr             63  dpwr2              1
pw              7.1  dof2               0
d1            1.000  dm2                n
tof           -16.1  dmm2               c
nt             1024  dmf2           15136
ct             1024  dseq2
alock             n  dres2            1.0
gain             55  homo2              n
j1xh          140.0       PROCESSING
jnxh            8.0  sb             0.045
hmult             n  sbs         not used
pp             33.0  wtfile
pplvl            63  proc               ft
presat            n  fn               4096
      FLAGS         math                 f
i1                n
in                n  werr
dp                y  wexp
hs               nn  wbs
  2D ACQUISITION     wnt
sw1          5502.1    2D PROCESSING
ni              256  sb1            0.002
phase     undefined  sbs1       not used
     DISPLAY         wtfile1
sp            629.0  proc1              ft
wp          22624.4  fn1              1024
vs             5000
```

Figure A15. Parameter set for 500 MHz LRHETCOR spectrum of vitilevuamide

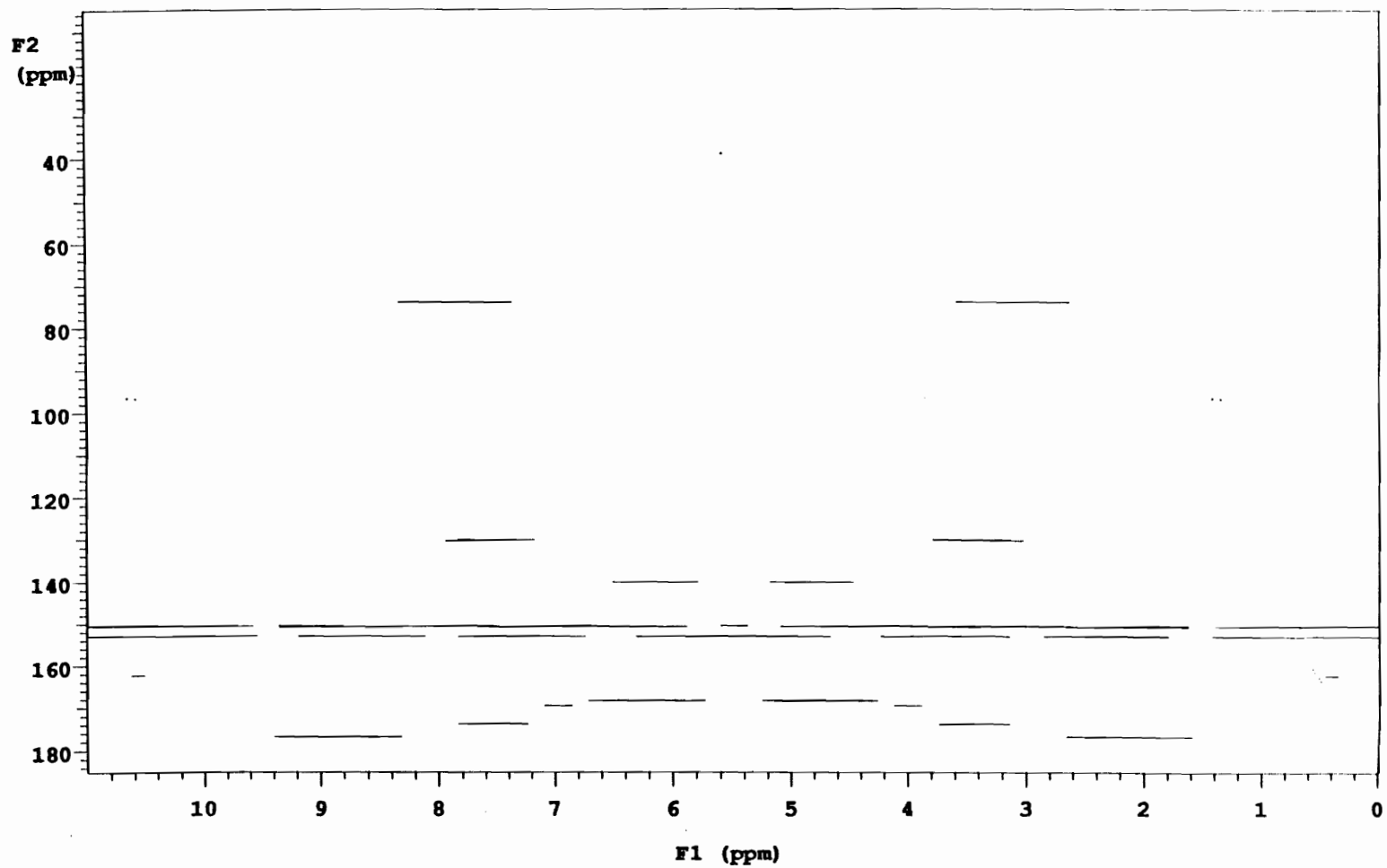

Figure A16. 500 MHz LRHETCOR spectrum of vitilevuamide

APPENDIX B

NMR SPECTRA OF SYNTHETIC COMPOUNDS

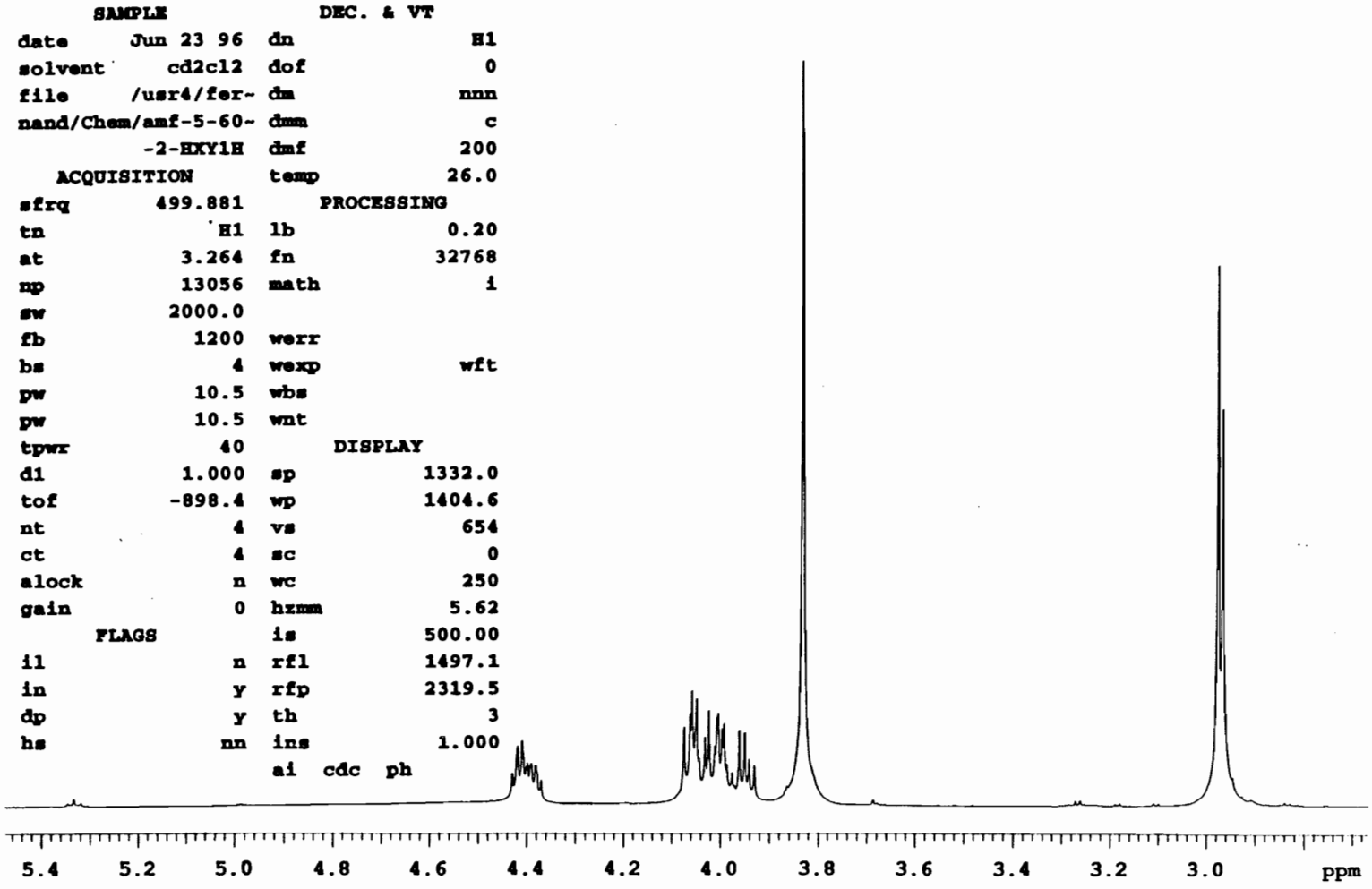

Figure B1. 500 MHz proton spectrum of nitrile (**67**)

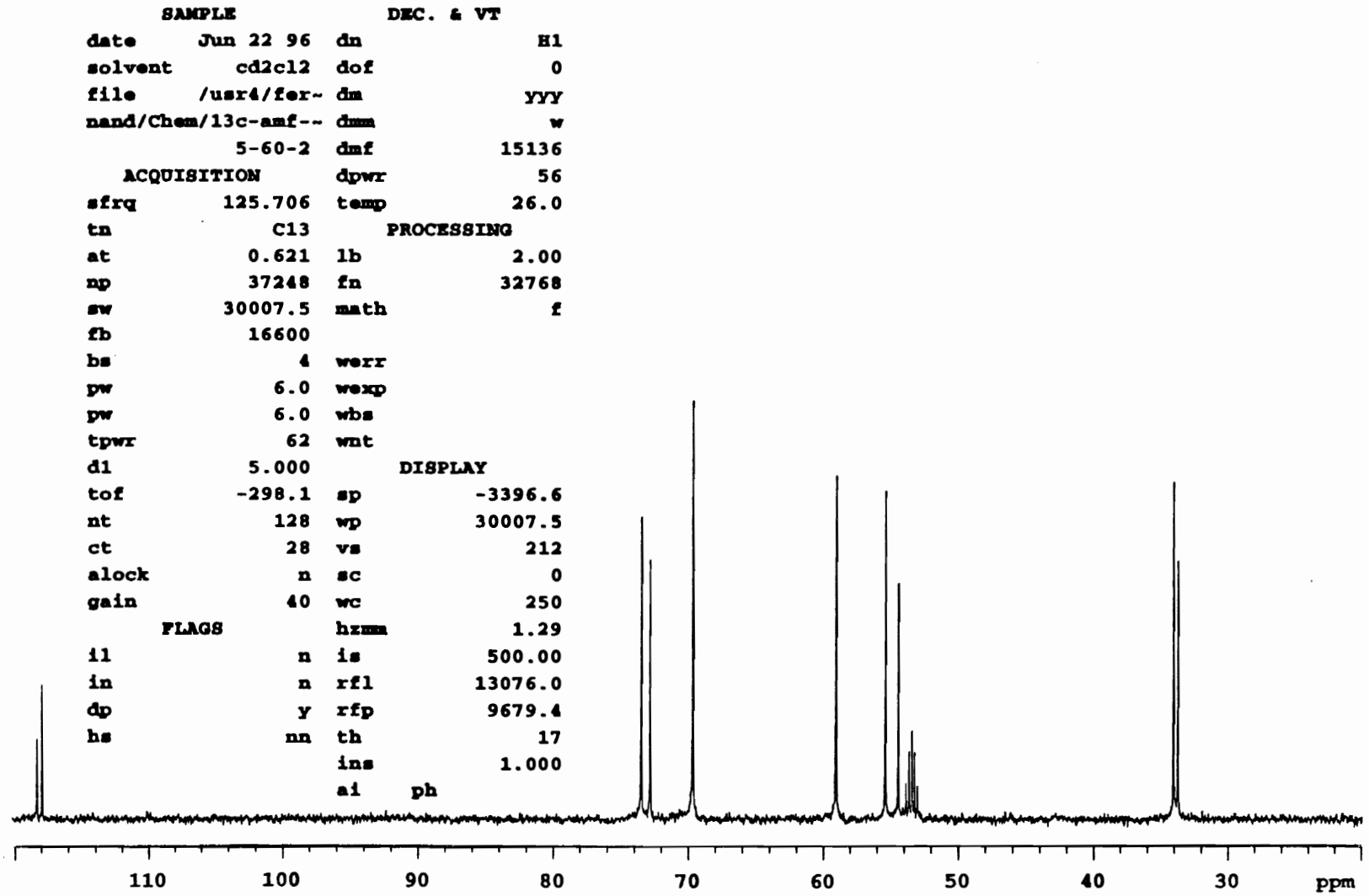

Figure B2. 125 MHz carbon spectrum of nitrile (**67**)

```
exp1  dept

      SAMPLE            DEC. & VT
date      Jun 22 96  dfrq       499.883
solvent         d2o  dn                H1
file      /usr4/fer-  dpwr              56
nand/Chem/dept-amf-  dof                0
            -5-60-2  dm               nny
   ACQUISITION       dmm              ccw
sfrq        125.707  dmf            15136
tn              C13  dseq
at            0.621  dres             1.0
np            32768  homo               n
sw          26402.6  temp            24.0
fb            14600      PROCESSING
bs                4  lb               1.50
ss                8  wtfile
tpwr             62  proc               ft
pw              6.0  fn              32768
d1            5.000  math               f
tof          -298.1
nt              128  werr
ct               44  wexp       procplot
alock             n  wbs
gain             40  wnt
pp             33.0
pplvl            63
j             125.0
mult            1.5
satdly             0
      FLAGS
il                 n
in                 n
dp                 y
hs                nn
     DISPLAY
sp          -1591.0
wp          26402.6
vs              308
sc                0
wc              250
hzmm           2.71
is           500.00
rfl          8931.4
rfp          7340.4
th                9
```

Figure B3. Parameter set for the 125 MHz DEPT spectrum of nitrile (**67**)

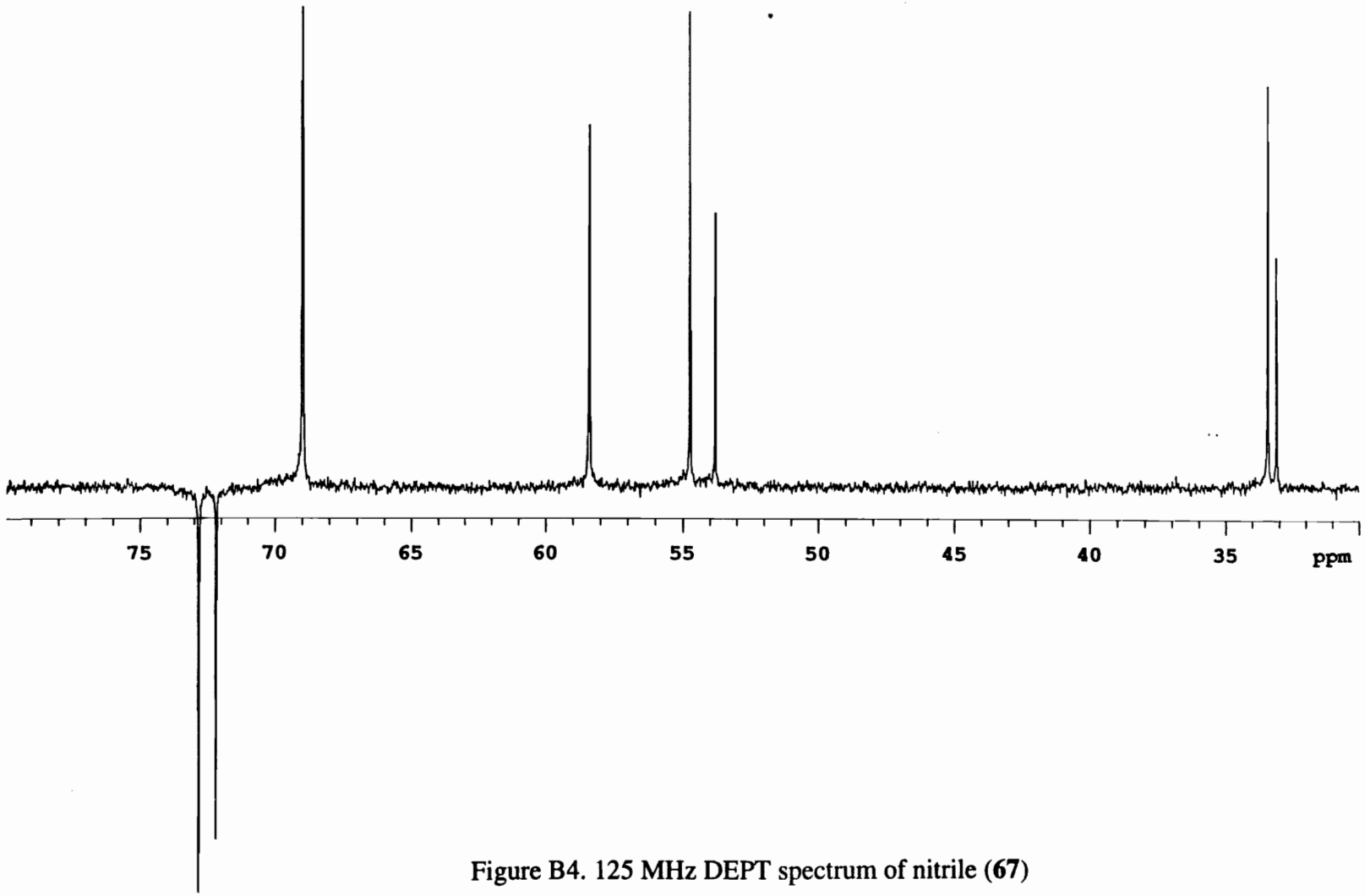

Figure B4. 125 MHz DEPT spectrum of nitrile (**67**)

```
exp1  gmqcosyps

      SAMPLE            DEC. & VT         ACQUISITION ARRAYS
date      Jun 23 96  dfrq      not used    array         phase
solvent      cd2cl2  dn               H1   arraydim        512
file      /usr4/fer- dpwr             1
nand/Chem/GCOSY-am-  dof              0    i             phase
           f-5-60-2  dm               n    1                 1
   ACQUISITION      dmm              c    2                 2
sfrq        499.881  homo             n
tn               H1  temp          26.0
at            0.512      GRADIENTS
np             2048  gzlvl              2
sw           2000.0  gzlvl1         10000
fb             1200  gt1         0.002500
bs                1  grise       0.000010
ss                2  gstab              0
tpwr             61  taud2              0
pw              9.0  tau1               0
d1            2.000    PRESATURATION
d2                0  satpwr             0
tof          -898.4  satdly             0
nt                2      PROCESSING
ct                2  gf             0.204
gain             20  gfs        not used
      FLAGS          proc              ft
dp                y  fn              4096
hs               nn
  2D ACQUISITION     werr
sw1          2000.0  wexp
ni              256  wbs
phase      arrayed  wnt
     DISPLAY            2D PROCESSING
sp           2178.5  gf1            0.060
wp             42.0  gfs1       not used
vs               29  proc1             ft
sc                6  fn1            2048
wc              225
rf1          1497.1
rfp          2319.5
th                5
ins          26.684
ai  cdc  ph
    2D DISPLAY
sp1          1938.7
wp1           131.0
```

Figure B5. Parameter set for 500 MHz GCOSY spectrum of nitrile (**67**)

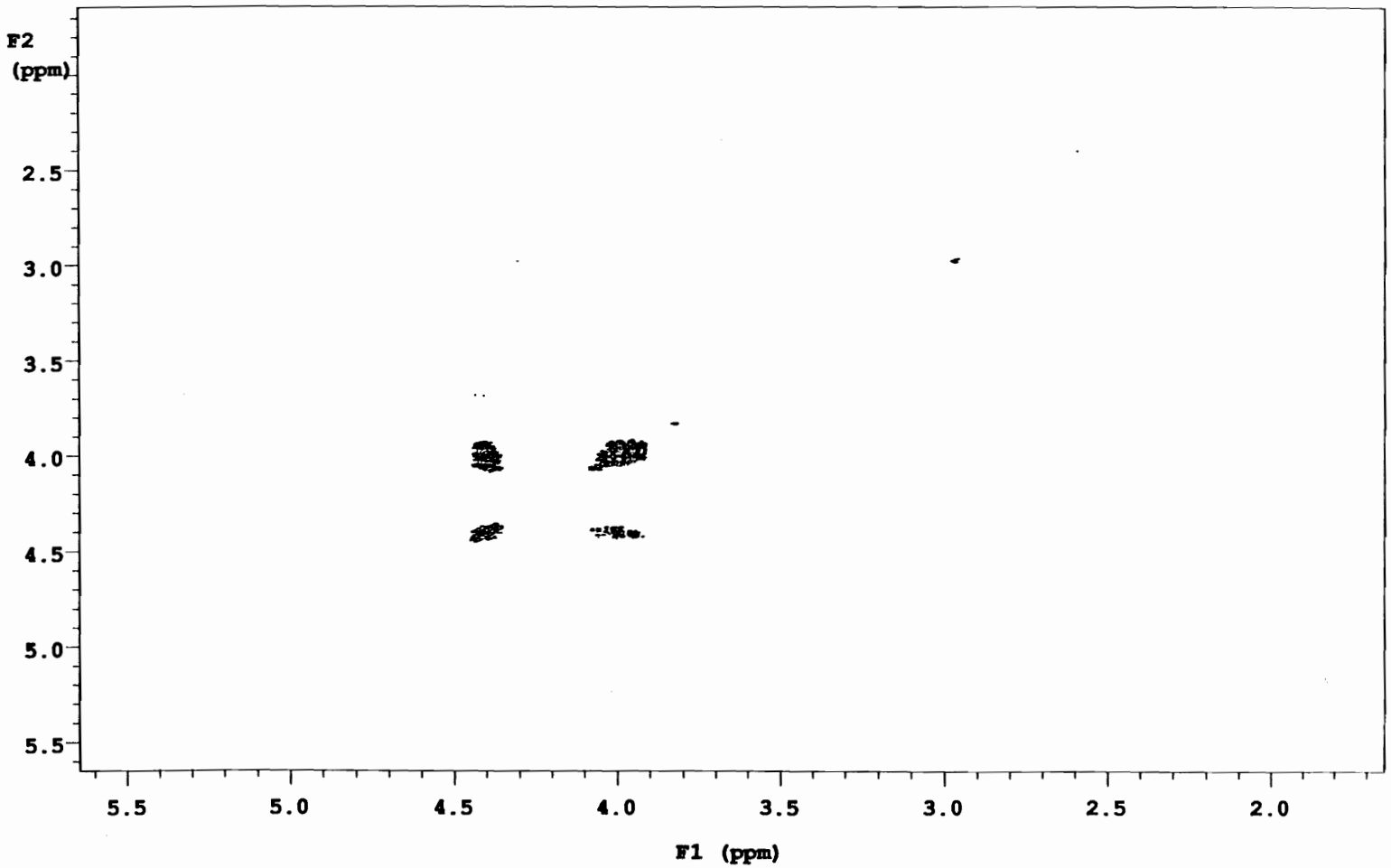

Figure B6. 500 MHz GCOSY spectrum of nitrile (**67**)

```
exp1  ghmqcps

   ACQUISITION            SAMPLE          ACQUISITION ARRAYS
sw          2000.0  date      Jun 23 96    array         phase
at           0.256  solvent         d2o    arraydim        512
np            1024  file      /usr4/fer-
fb            1200  nand/Chem/GHMQC-am-    i             phase
bs              32            f-5-60-2    1                 1
ss               2       SPECIAL           2                 2
d1           2.000  temp       not used
nt               1  gain              40
ct               1  spin               0
  2D ACQUISITION    hst            0.008
sw1        14886.5  pw90          11.400
ni             256        FLAGS
phase      arrayed  sspul              y
   TRANSMITTER          PROCESSING
tn              H1  gf             0.102
sfrq       499.882  gfs        not used
tof         -898.4  fn              4096
tpwr            62
pw          11.400    2D PROCESSING
    DECOUPLER        gf1            0.007
dn              C13  gfs1       not used
dof        -1611.7  fn1             1024
pwxlvl          63       DISPLAY
pwx         12.000  sp           1287.9
dm              nny  wp           1129.5
dmm             ccp  sp1          2927.5
dmf           29851  wp1          7690.9
dpwr               rf1           337.2
       HMQC         rfp          1499.0
nullflg          n  rf11         3864.5
j1xh        150.0  rfp1         6762.9
    GRADIENTS             PLOT
gzlvl1         10000  wc            225.0
gt1         0.001000  sc                0
gzlvl3          5000  wc2           130.0
gt3         0.001000  sc2               0
gstab       0.000200  vs               10
hsgpwr         10000  th                3
hsgt        0.005000  ai    ph
```

Figure B7. Parameter set for 500 MHz GHMQC spectrum of nitrile (**67**)

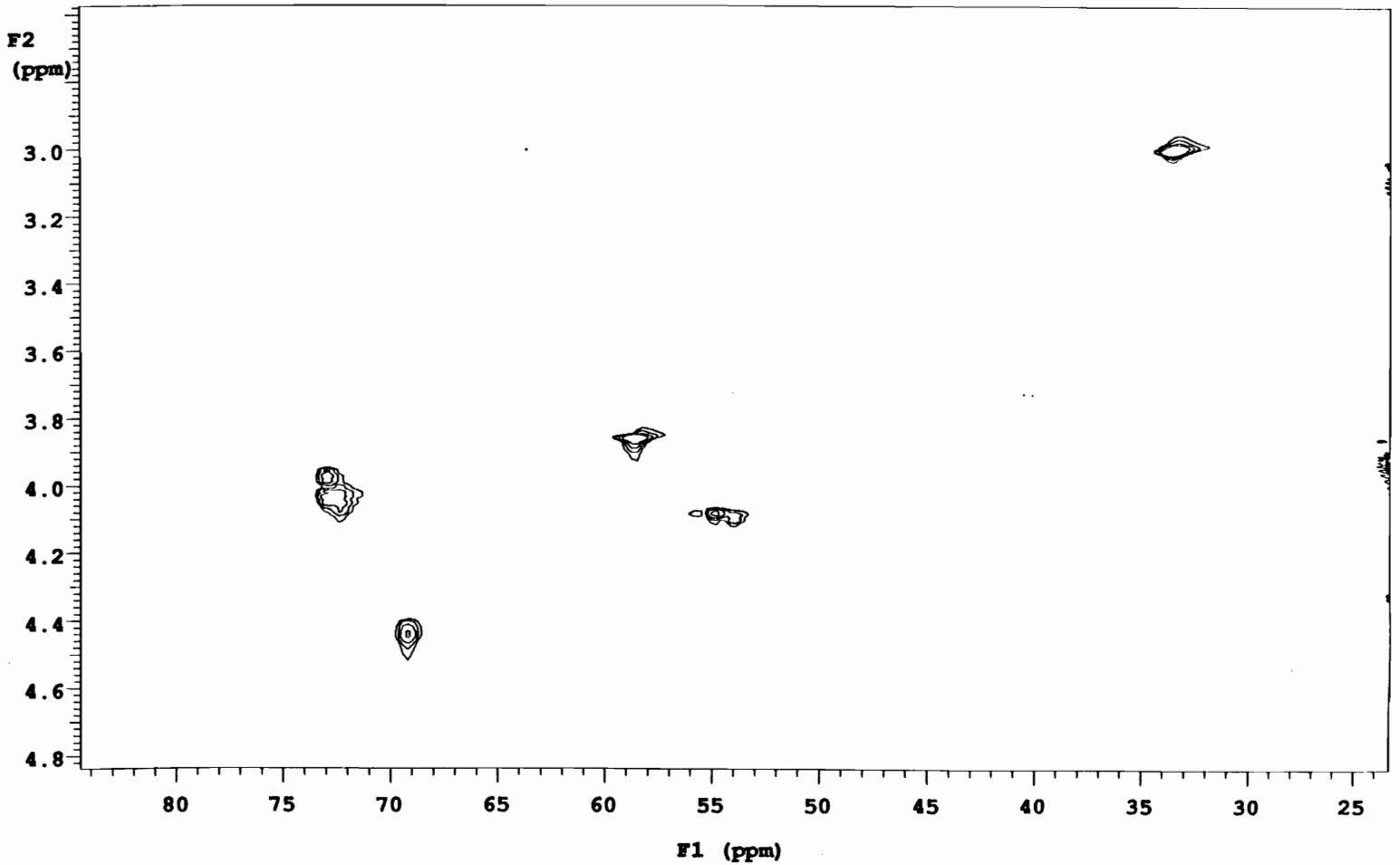

Figure B8. 500 MHz GHMQC spectrum of nitrile (**67**)

```
exp1  ghmqc

      SAMPLE              DEC. & VT          ACQUISITION ARRAYS
date      Jun 23 96  dfrq       not used    array          phase
solvent      cd2cl2  dn               C13   arraydim         512
file      /usr4/fer- dpwr              44
nand/Chem/GHMBC-am-  dof         -1611.7     i              phase
          f-5-60-2   dm               nnn    1                  1
   ACQUISITION       dmm              ccp    2                  2
sfrq        499.881  dmf            29851
tn               H1  dseq         wurst1
at            0.416  dres             9.0
np             1664  homo               n
sw           2000.0  temp            26.0
fb             1200      PROCESSING
ss                2  sb             0.210
tpwr             62  sbs        not used
pw             11.4  wtfile
d1            2.000  proc              ft
tof          -898.4  fn              2048
nt                1  math               f
ct                1
gain             46  werr
      FLAGS          wexp
il                y  wbs
dp                y  wnt
hs               nn    2D PROCESSING
  2D ACQUISITION     sb1            0.009
sw1         14886.5  sbs1       not used
ni              256  wtfile1
phase       arrayed  proc1             ft
     DISPLAY         fn1             1024
sp           1334.6      GRADIENTS
wp           1040.1  gzlvl1         10000
vs              100  gt1         0.002000
sc                6  gzlvl2         10000
wc              225  gt2         0.002000
hzmm          45.30  gzlvl3          5000
is            75.32  gt3         0.002000
rf1         1497.1   grise       0.000010
rfp         2319.5   gstab       0.000010
th                9
ins           1.240
ai    av
    2D DISPLAY
sp1          2985.8
```

Figure B9. Parameter set for 500 MHz GHMBC spectrum of nitrile (**67**)

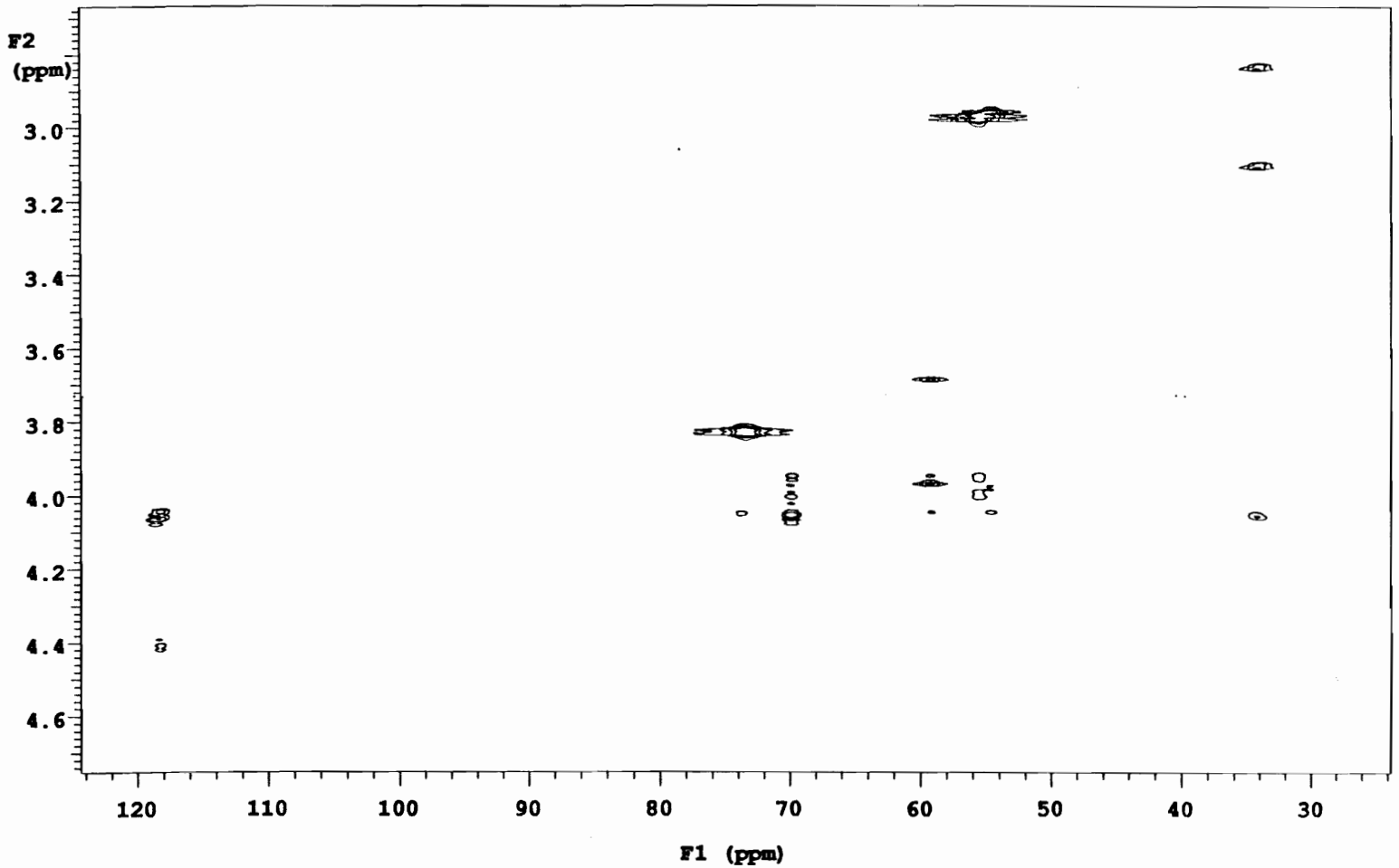

Figure B10. 500 MHz GHMBC spectrum of nitrile (**67**)

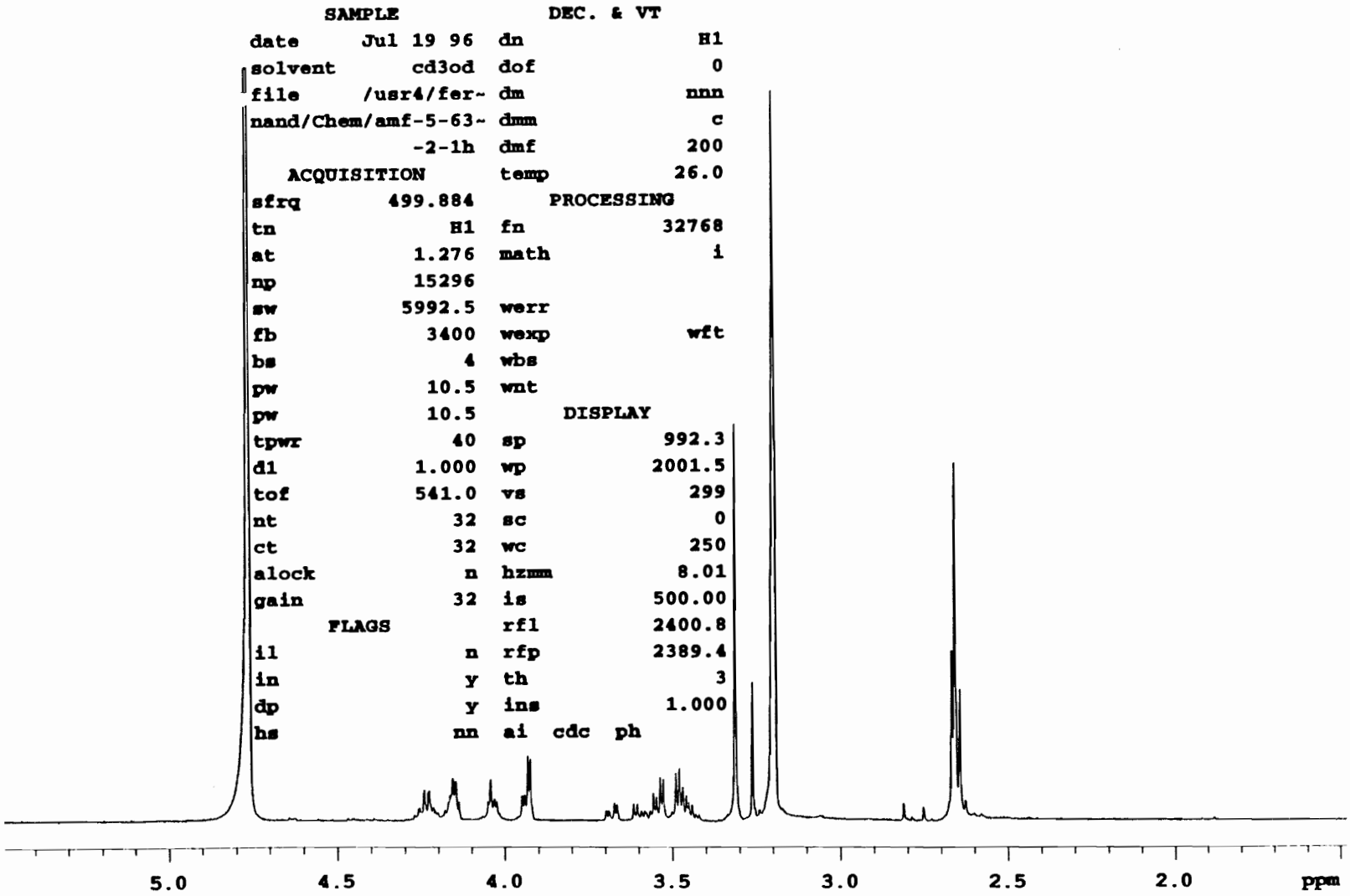

Figure B11. 500 MHz proton spectrum of Nmm (**63**)

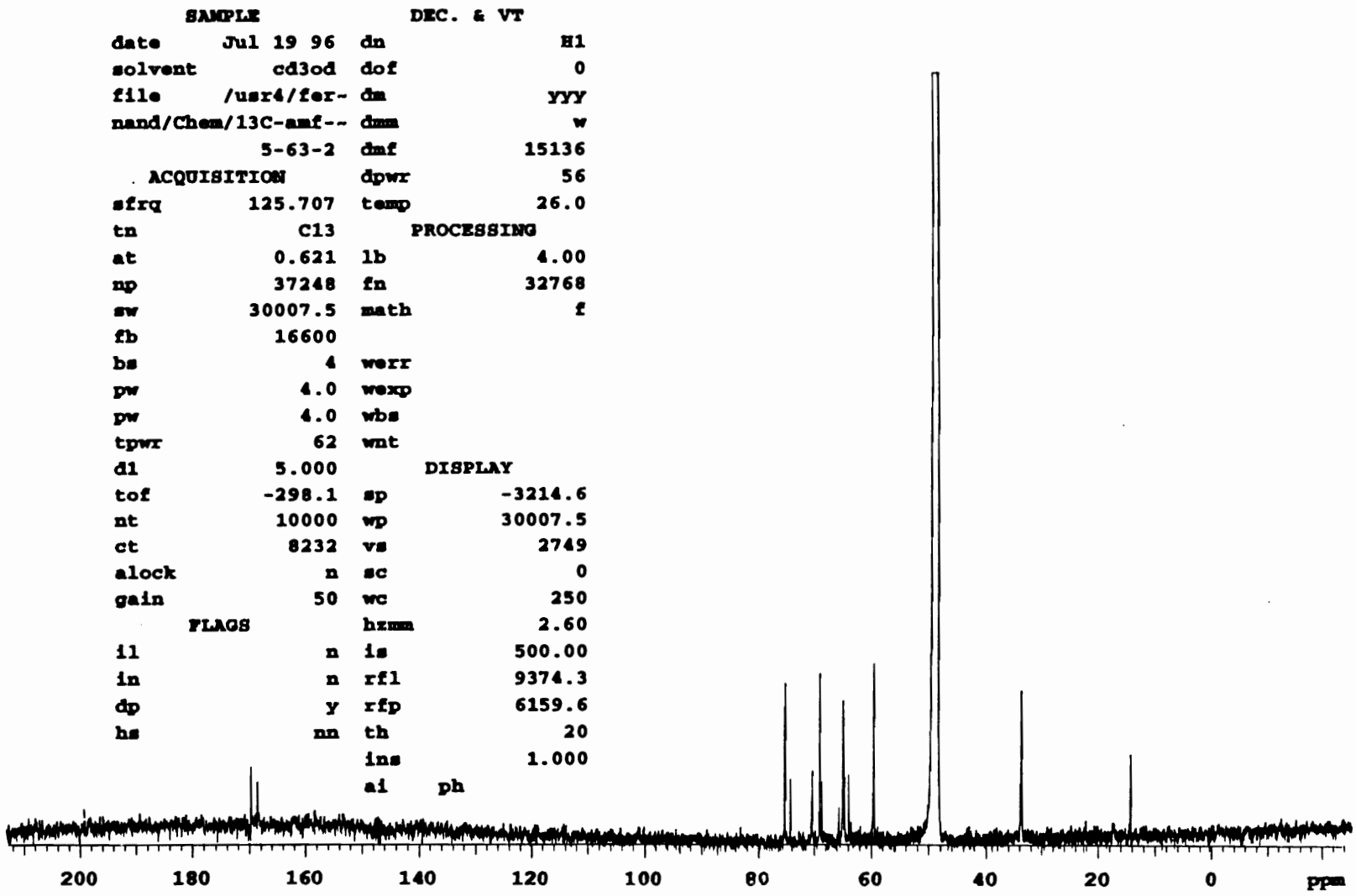

Figure B12. 125 MHz carbon spectrum of Nmm (**63**)

```
exp1  dept

      SAMPLE                DEC. & VT
date      Jul 20 96  dfrq        499.883
solvent       cd3od  dn                H1
file      /usr4/fer- dpwr              56
nand/Chem/DEPT-5-6-  dof               0
                3-2  dm                nny
   ACQUISITION       dmm               ccw
sfrq        125.706  dmf            15136
tn              C13  dseq
at            0.620  dres             1.0
np            29824  homo               n
sw          24038.5  temp            26.0
fb            13200      PROCESSING
bs                4  lb               3.00
ss                8  wtfile
tpwr             62  proc              ft
pw              6.0  fn             32768
d1            5.000  math               f
tof         -1378.7
nt           100000  werr
ct             7216  wexp       procplot
alock             n  wbs
gain             56  wnt
pp             33.0
pplvl            63
j             125.0
mult            1.5
satdly .          0
      FLAGS
il                n
in                n
dp                y
hs               nn
     DISPLAY
sp          2532.3
wp          7528.6
vs            1036
sc               0
wc             250
hzmm         30.11
is          500.00
rfl         8829.9
rfp         7340.4
th              16
```

Figure B13. Parameter set for 125 MHz DEPT spectrum of Nmm (**63**)

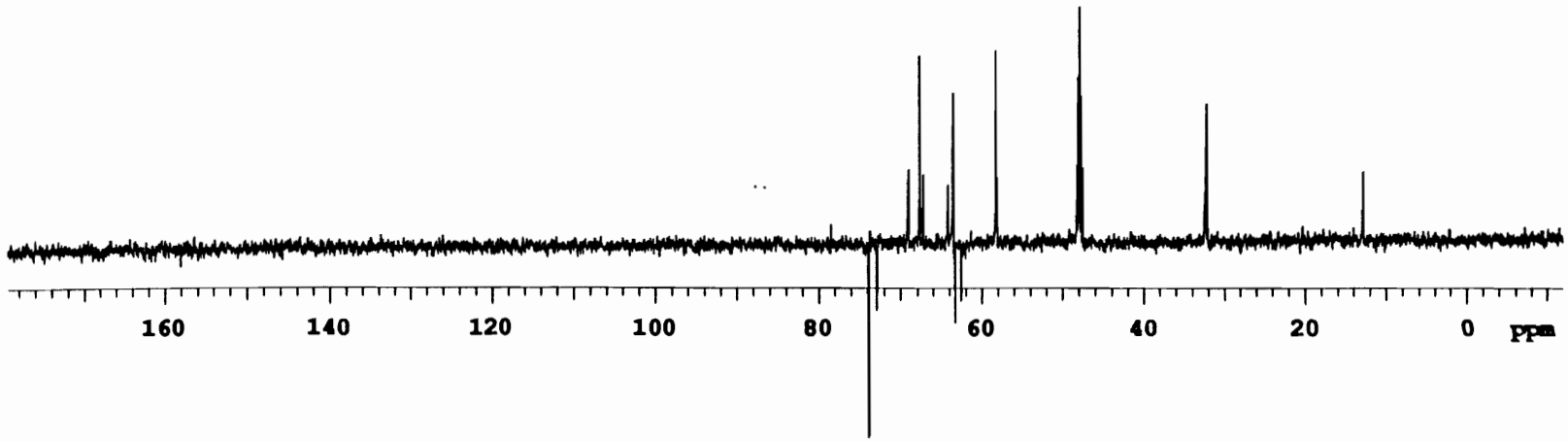

Figure B14. 125 MHz DEPT spectrum of Nmm (**63**)

APPENDIX C

HPLC AND LCMS SPECTRA

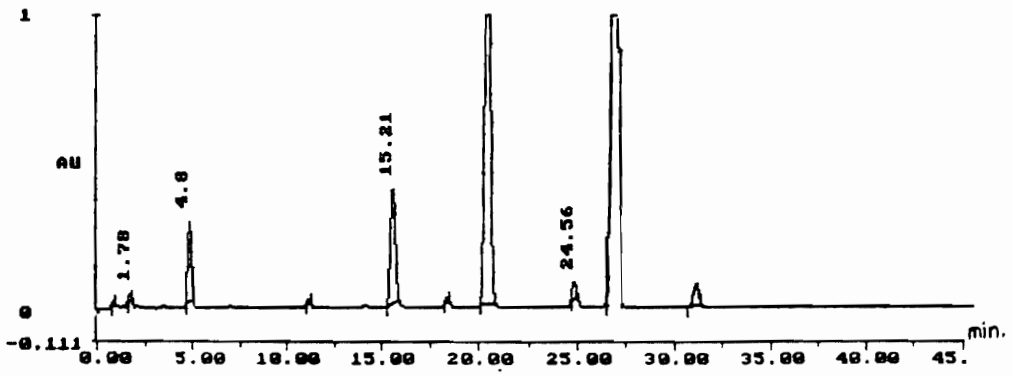

Figure C1. HPLC trace of FDAA derivatized D,L-Val

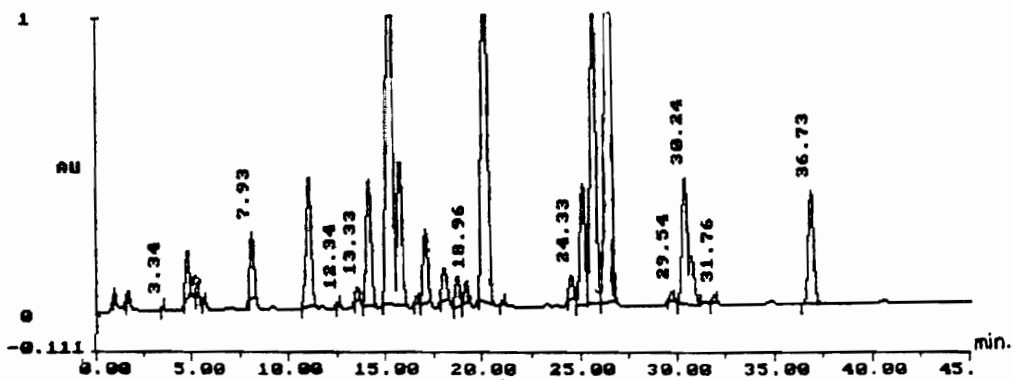

Figure C2. HPLC trace of a coinjection of FDAA derivatized D,L-Val and vitilevuamide

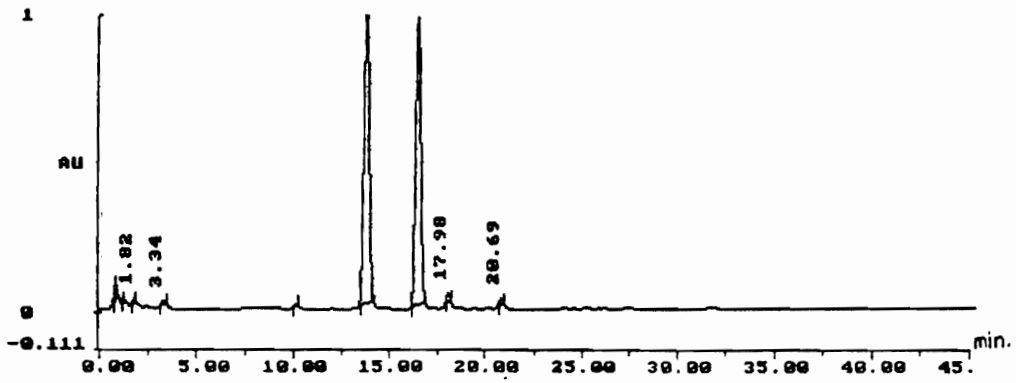

Figure C3. HPLC trace of FDAA derivatized D,L-Pro

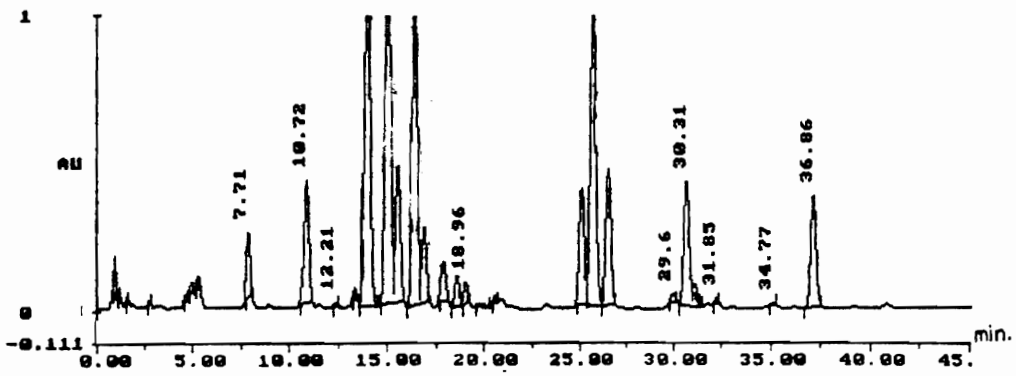

Figure C4. HPLC trace of a coinjection of FDAA derivatized D,L-Pro and vitilevuamide

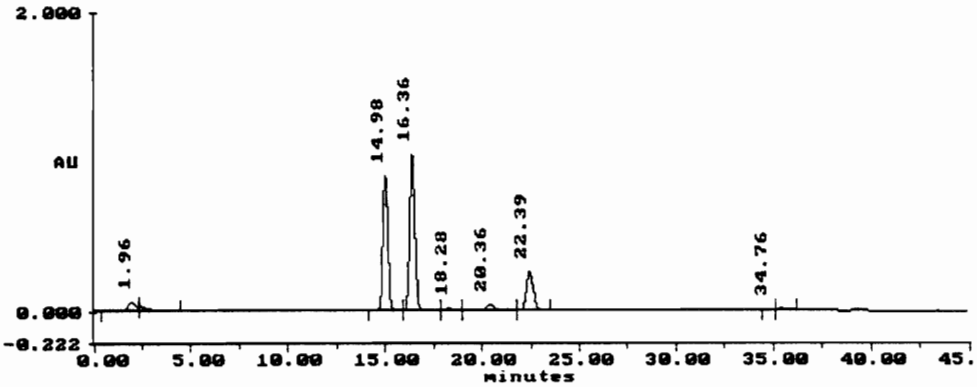

Figure C5. HPLC trace of FDAA derivatized D,L-Ser

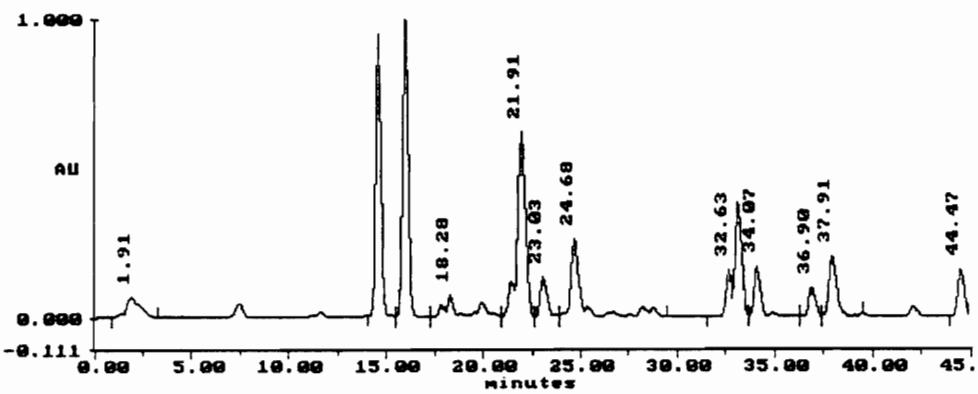

Figure C6. HPLC trace of a coinjection of FDAA derivatized D,L-Ser and vitilevuamide

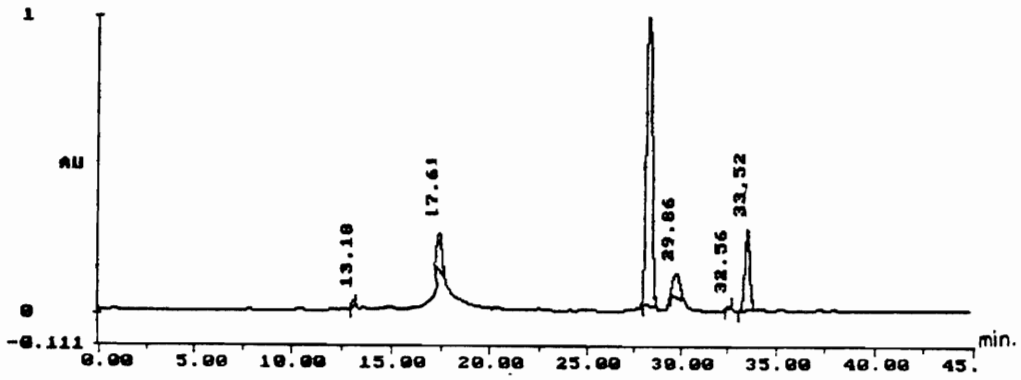

Figure C7. HPLC trace of FDAA derivatized D,L-Phe

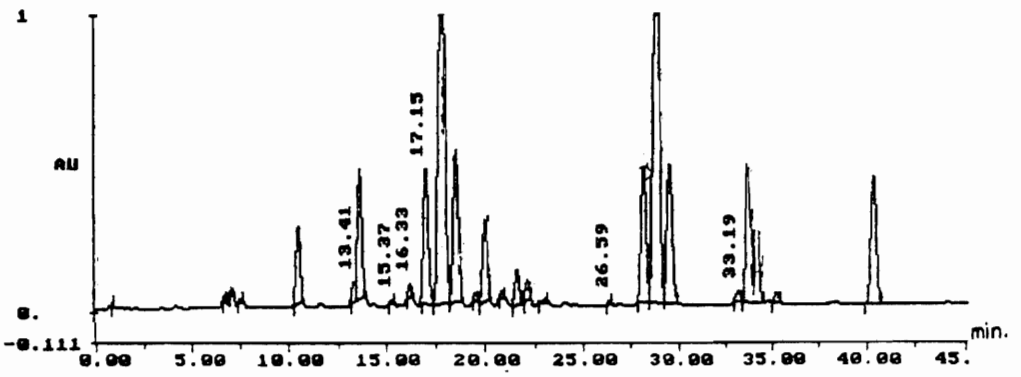

Figure C8. HPLC trace of a coinjection of FDAA derivatized D,L-Phe and vitilevuamide

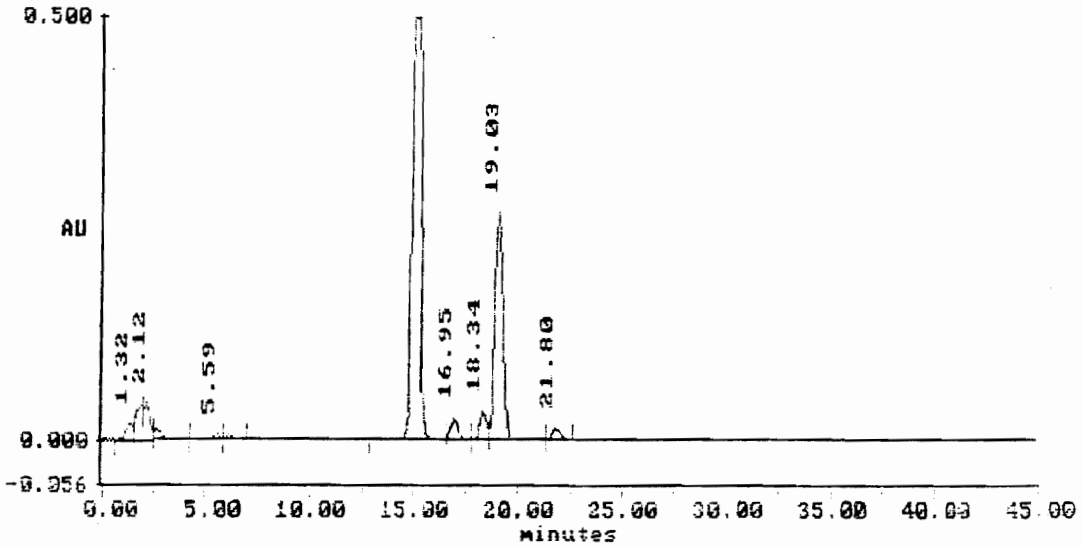

Figure C9. HPLC trace of FDAA derivatized D,L-Thr

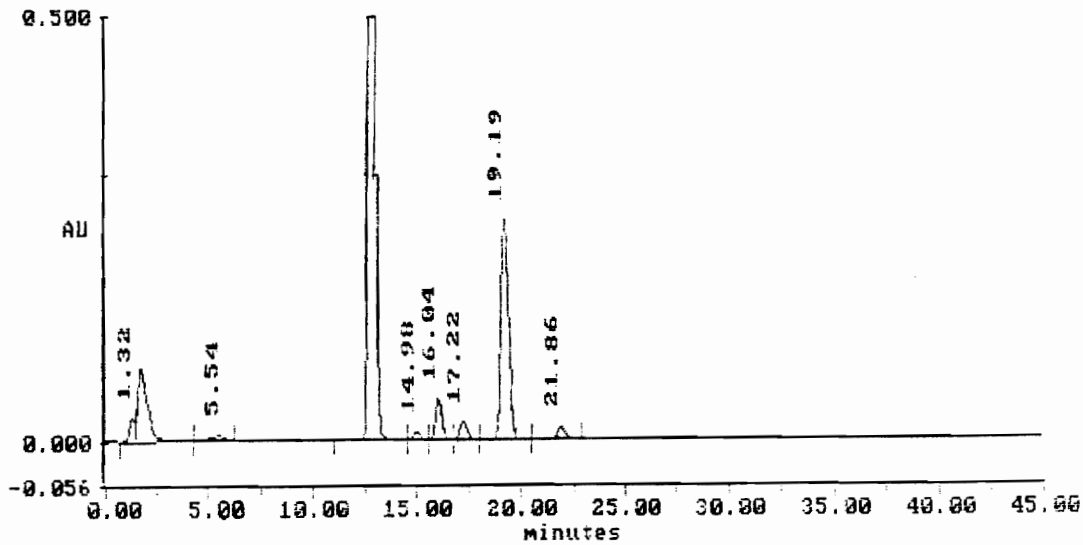

Figure C10. HPLC trace of FDAA derivatized L-alloThr

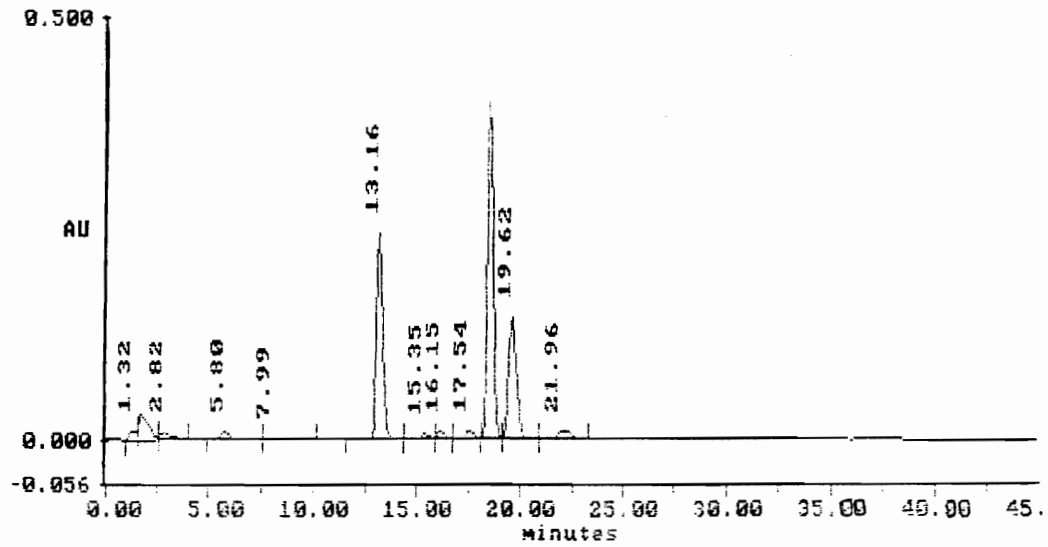

Figure C11.HPLC trace of FDAA derivatized D-alloThr

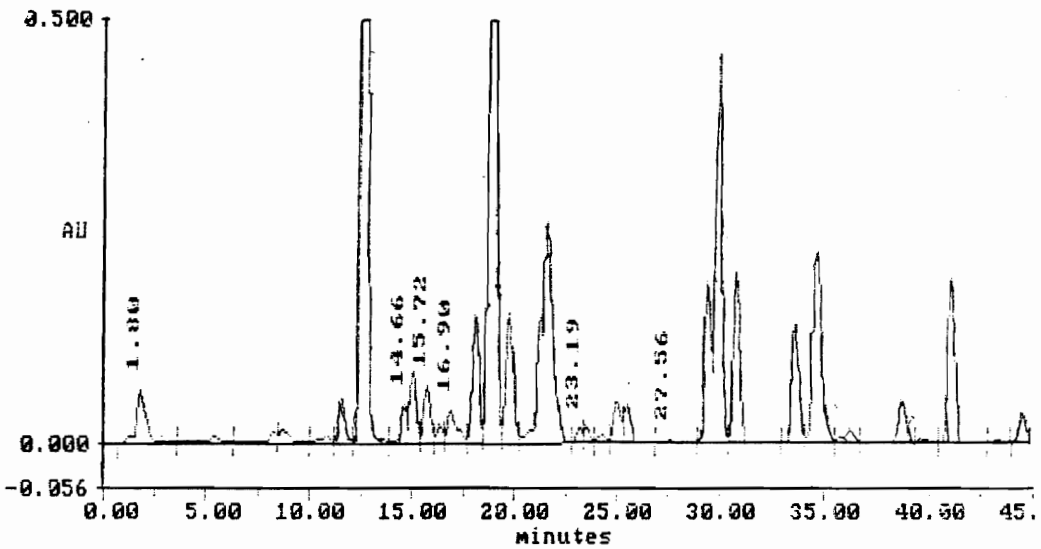

Figure C12. HPLC trace of coinjection of FDAA derivatized D, L-Thr and vitilevuamide

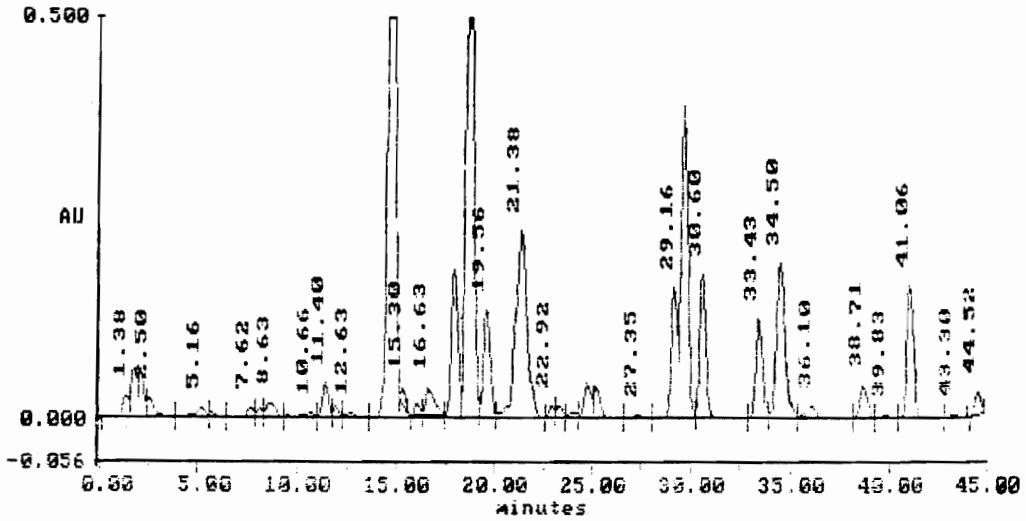

Figure C13. HPLC trace of coinjection of FDAA derivatized D-alloThr and vitilevuamide

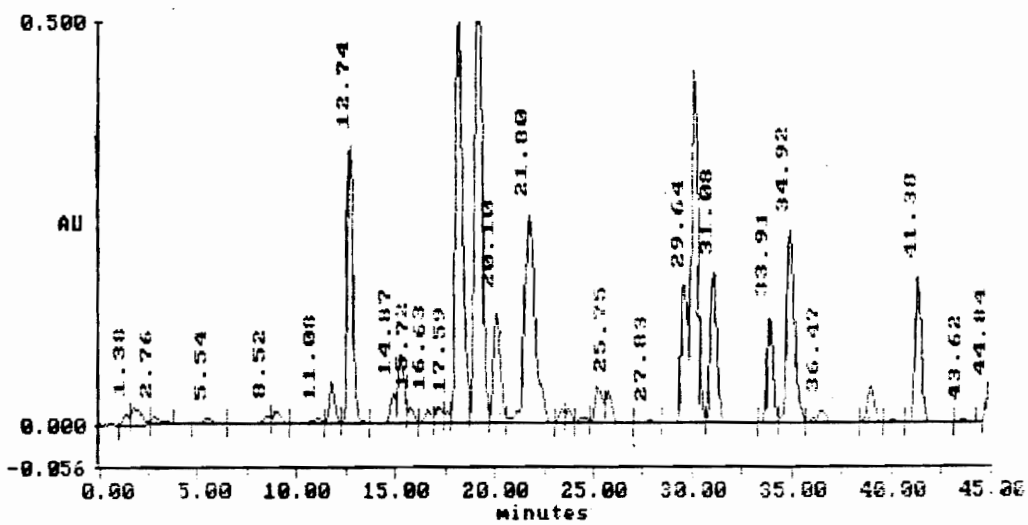

Figure C14. HPLC trace of coinjection of FDAA derivatized L-alloThr and vitilevuamide

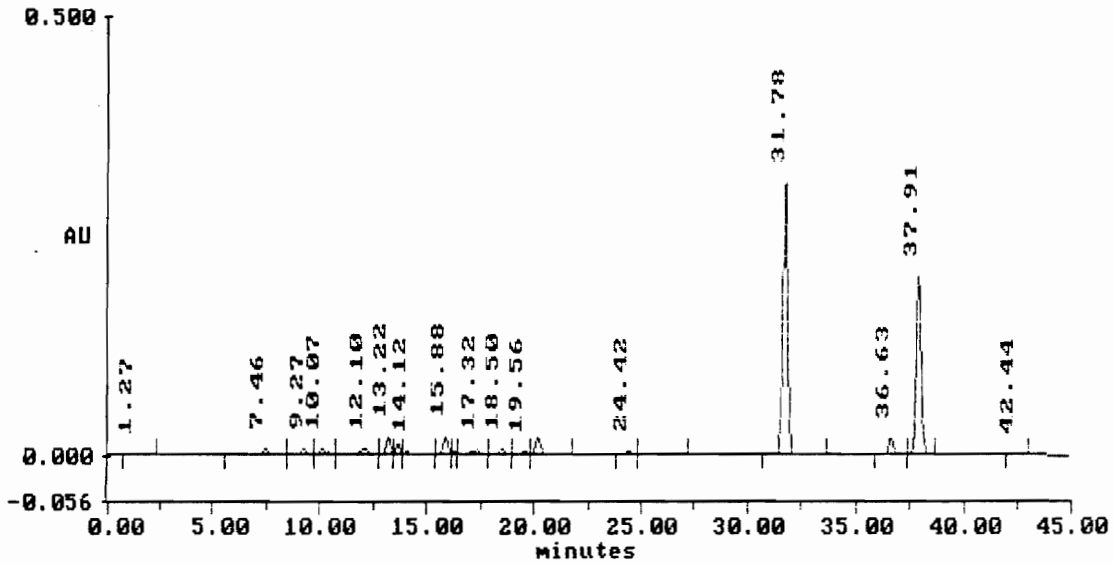

Figure C15.HPLC trace of FDAA derivatized D,L-Ile

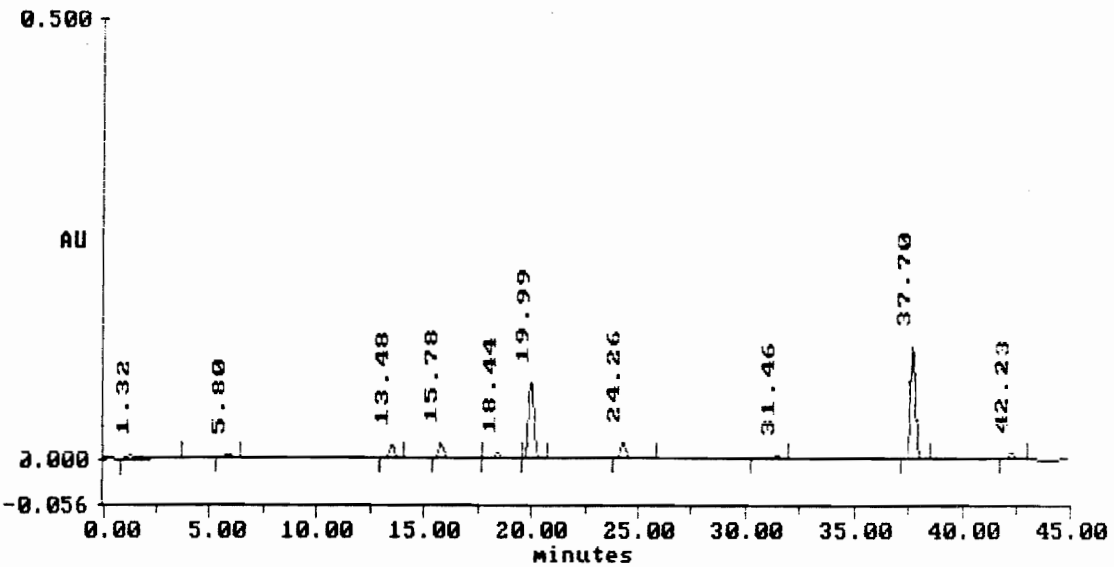

Figure C16.HPLC trace of FDAA derivatized D-alloIle

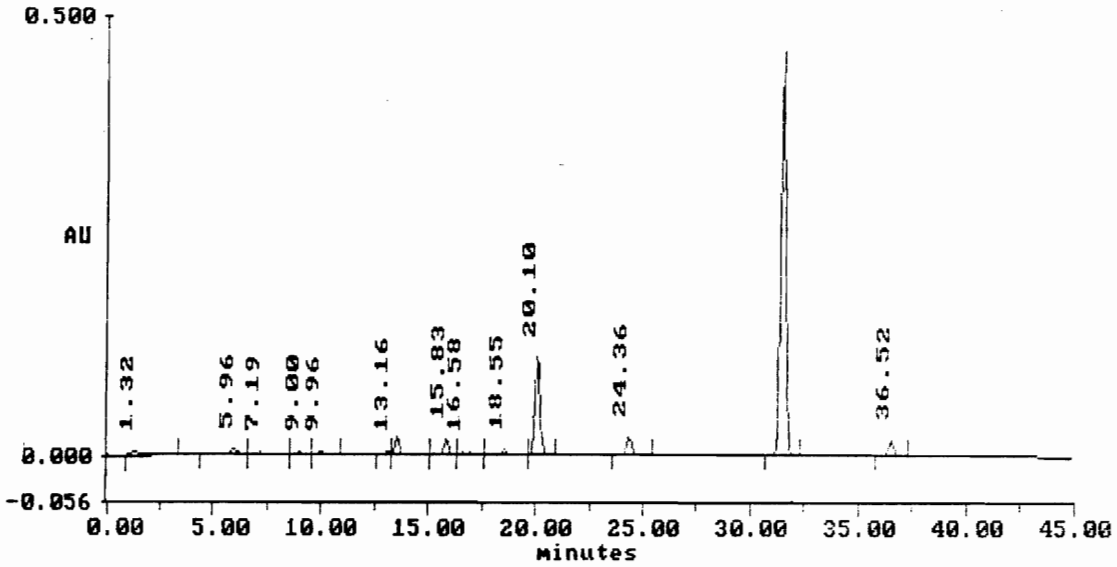

Figure C17.HPLC trace of FDAA derivatized L-alloIle

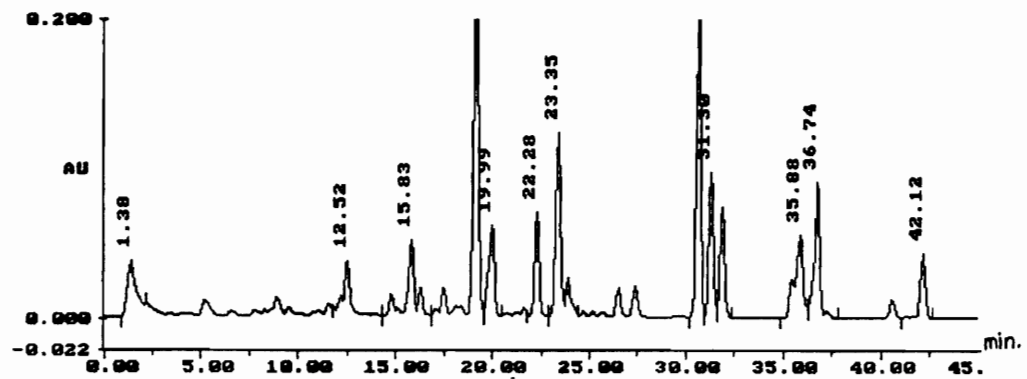

Figure C18. HPLC trace of coinjection of FDAA derivatized D,L-Ile and vitilevuamide

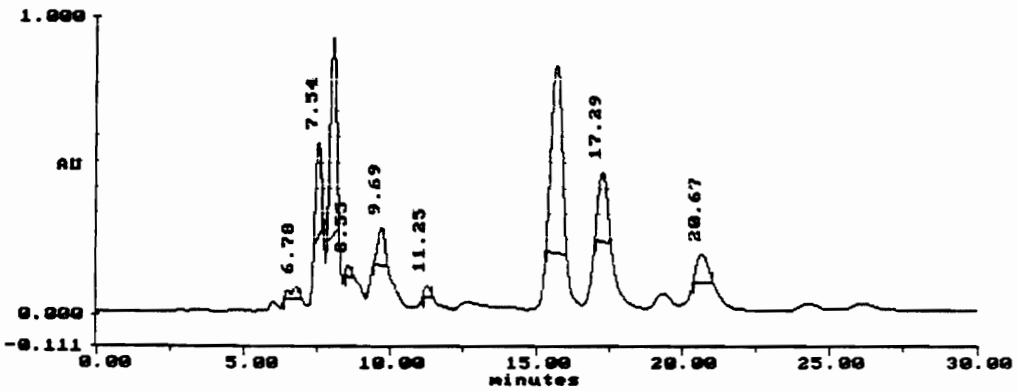

Figure C19. HPLC trace of coinjection of FDAA derivatized L-Ile and vitilevuamide

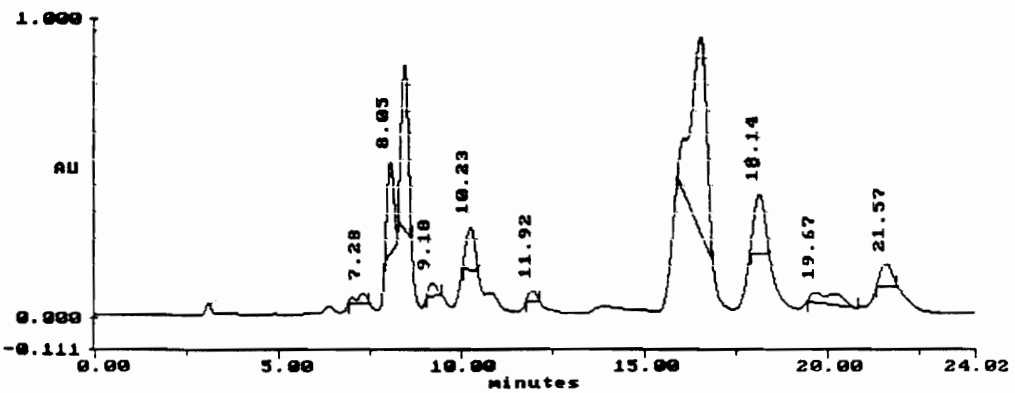

Figure C20. HPLC trace of coinjection of FDAA derivatized L-alloIle and vitilevuamide

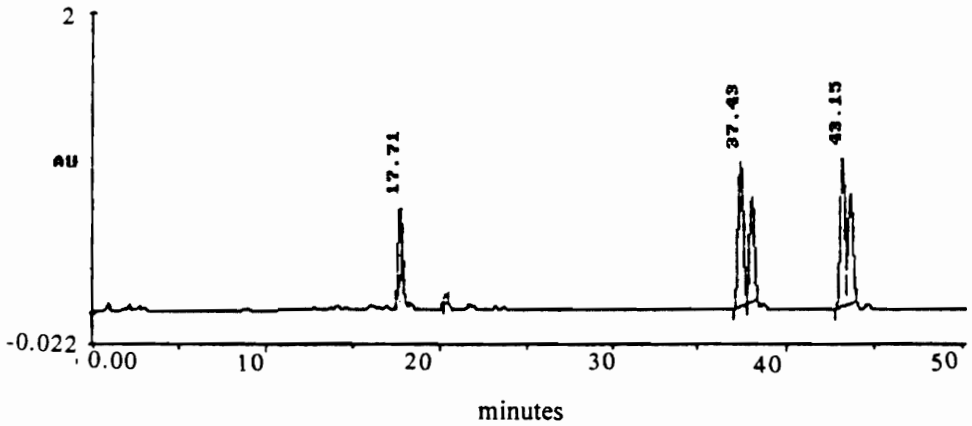

Figure C21. HPLC trace of FDAA derivatized (2*RS*, 4*RS*) Hil

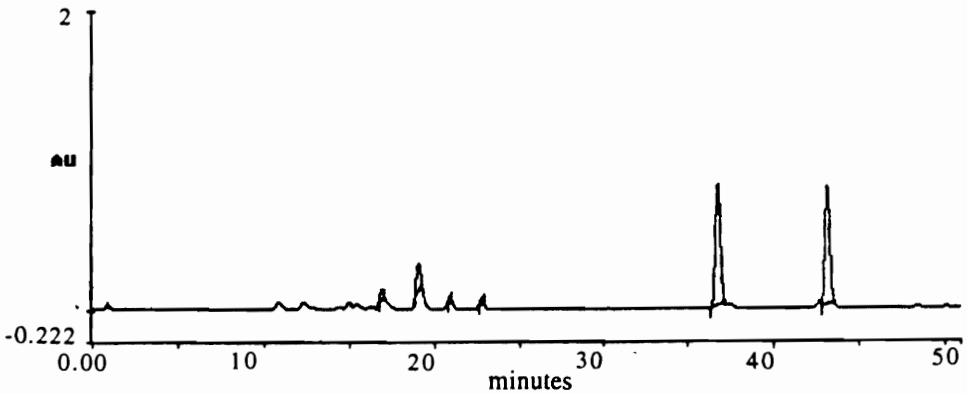

Figure C22. HPLC trace of FDAA derivatized (2*RS*, 4*S*) Hil

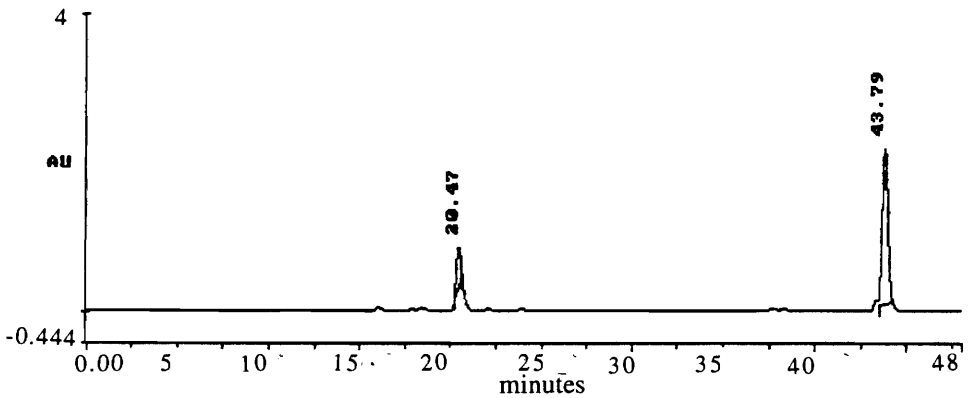

Figure C23. HPLC trace of FDAA derivatized (2*R*, 4*S*) Hil

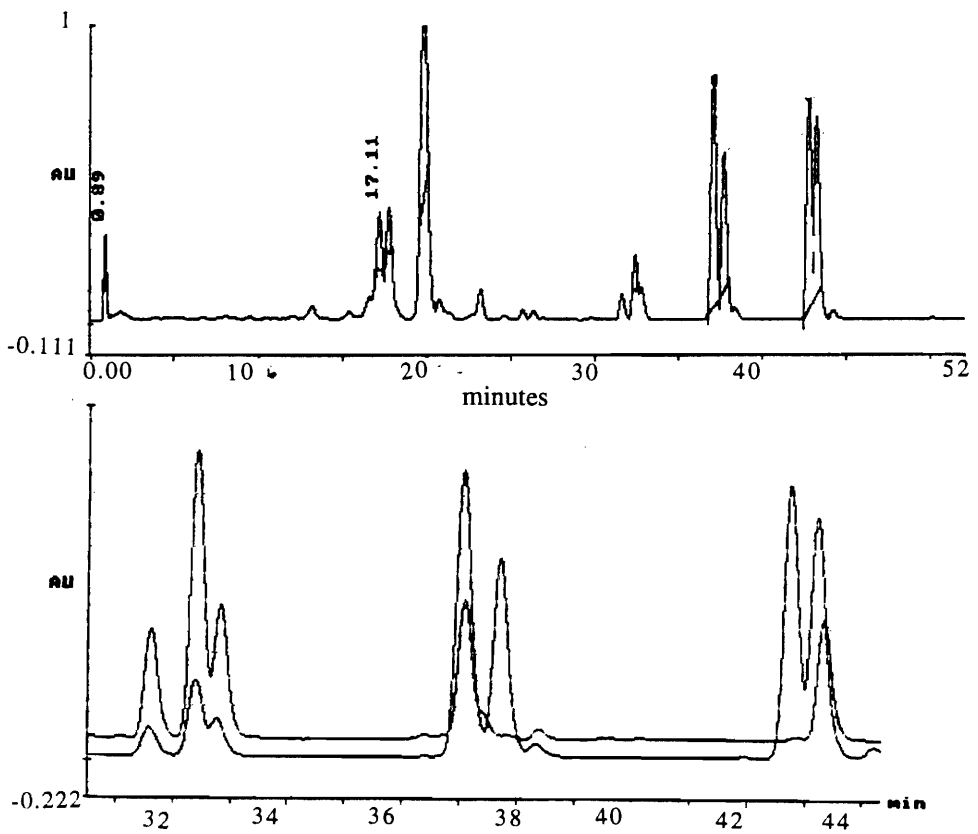

Figure C24. HPLC trace of coinjection of FDAA derivatized (2*RS*, 4*RS*) Hil and vitilevuamide

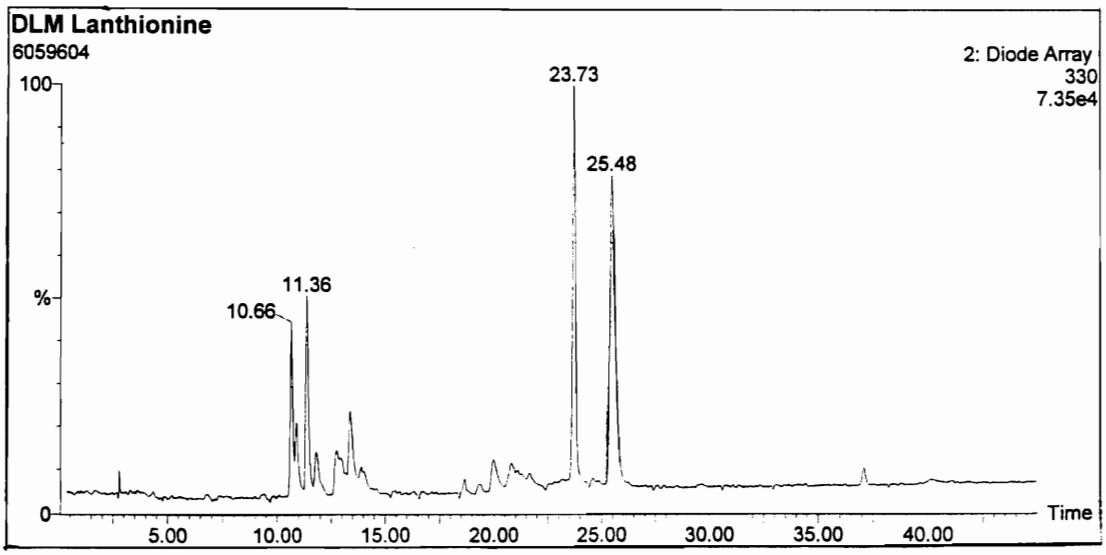

Figure C25. LC trace of FDAA derivatized non-hydrolyzed DLM-Lan

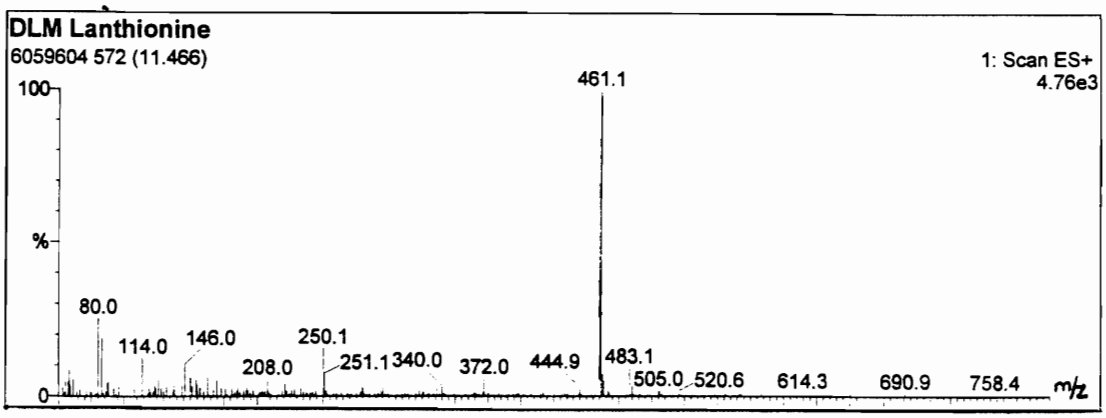

Figure C26. ES of rt = 10.66 min.

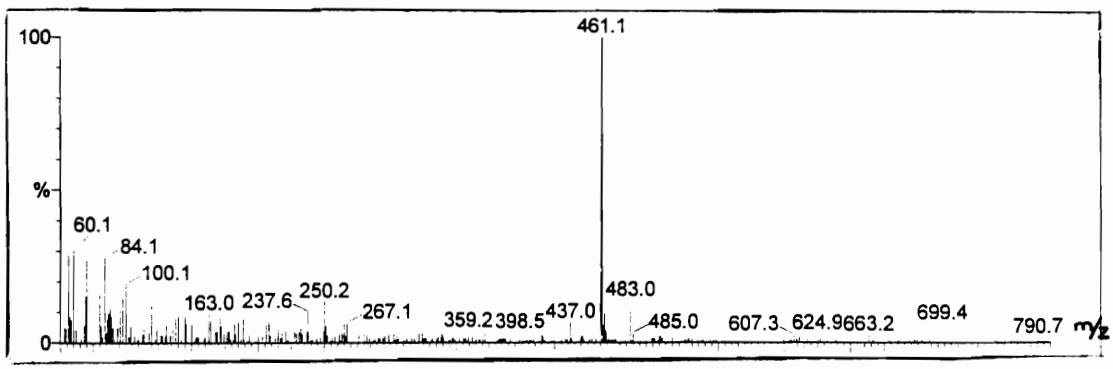

Figure C27. ES of rt = 11.36 min.

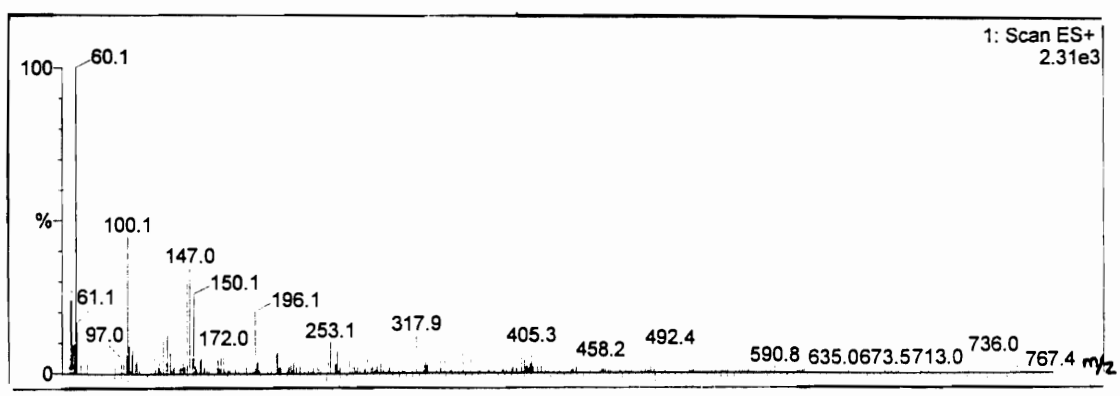

Figure C28. ES of rt = 23.73 min.

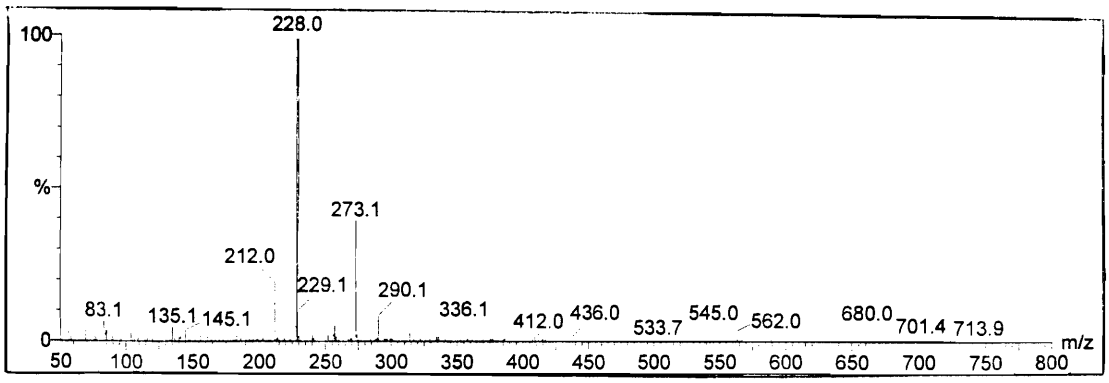

Figure C29. ES of rt = 25.48 min.

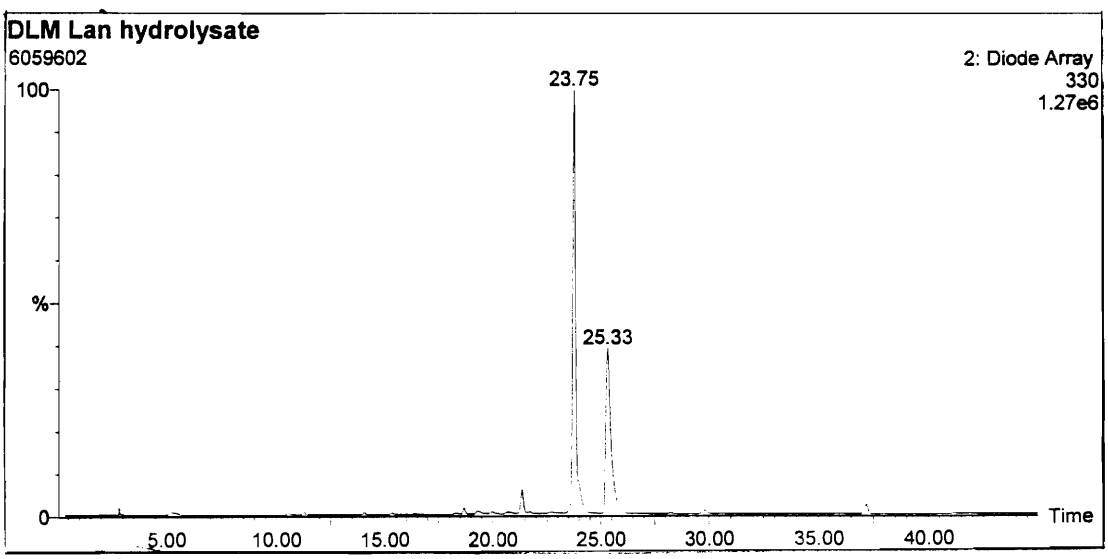

Figure C30. LC trace of FDAA derivatized hydrolyzed DLM-Lan

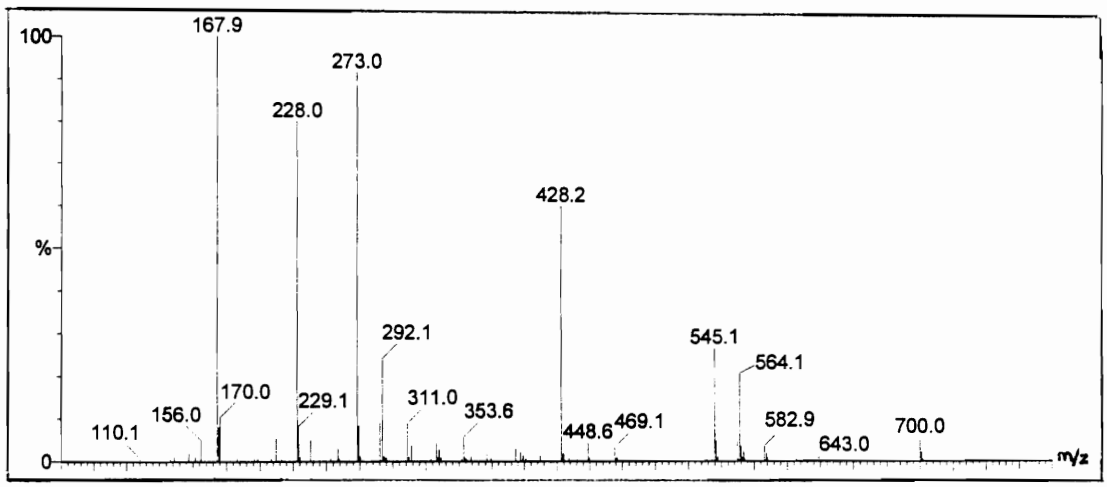

Figure C31. ES of rt = 23.75 min.

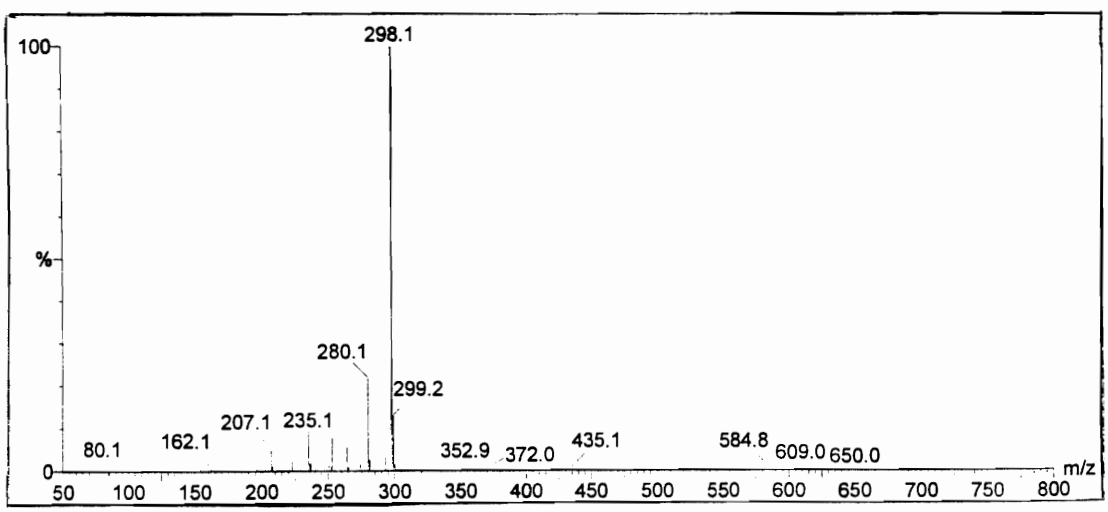

Figure C32. ES of rt = 25.33 min.

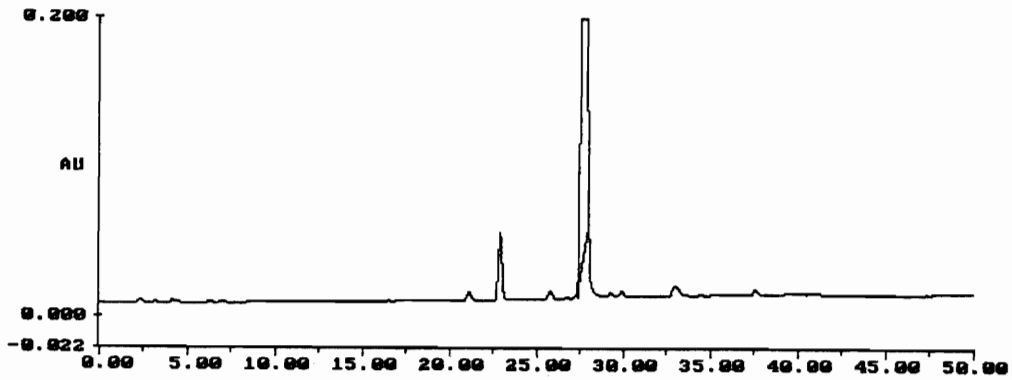

Figure C33. HPLC trace of FDAA derivatized NMM **63**

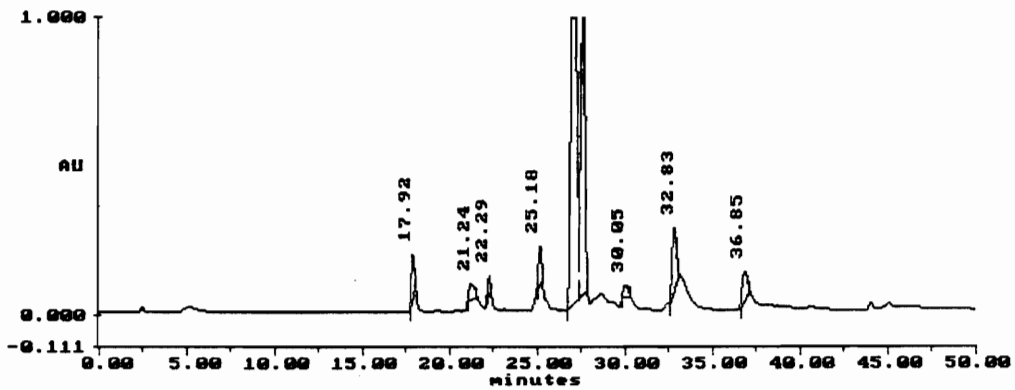

Figure C34. HPLC trace of coinjection of FDAA derivatized NMM **63** and vitilevuamide

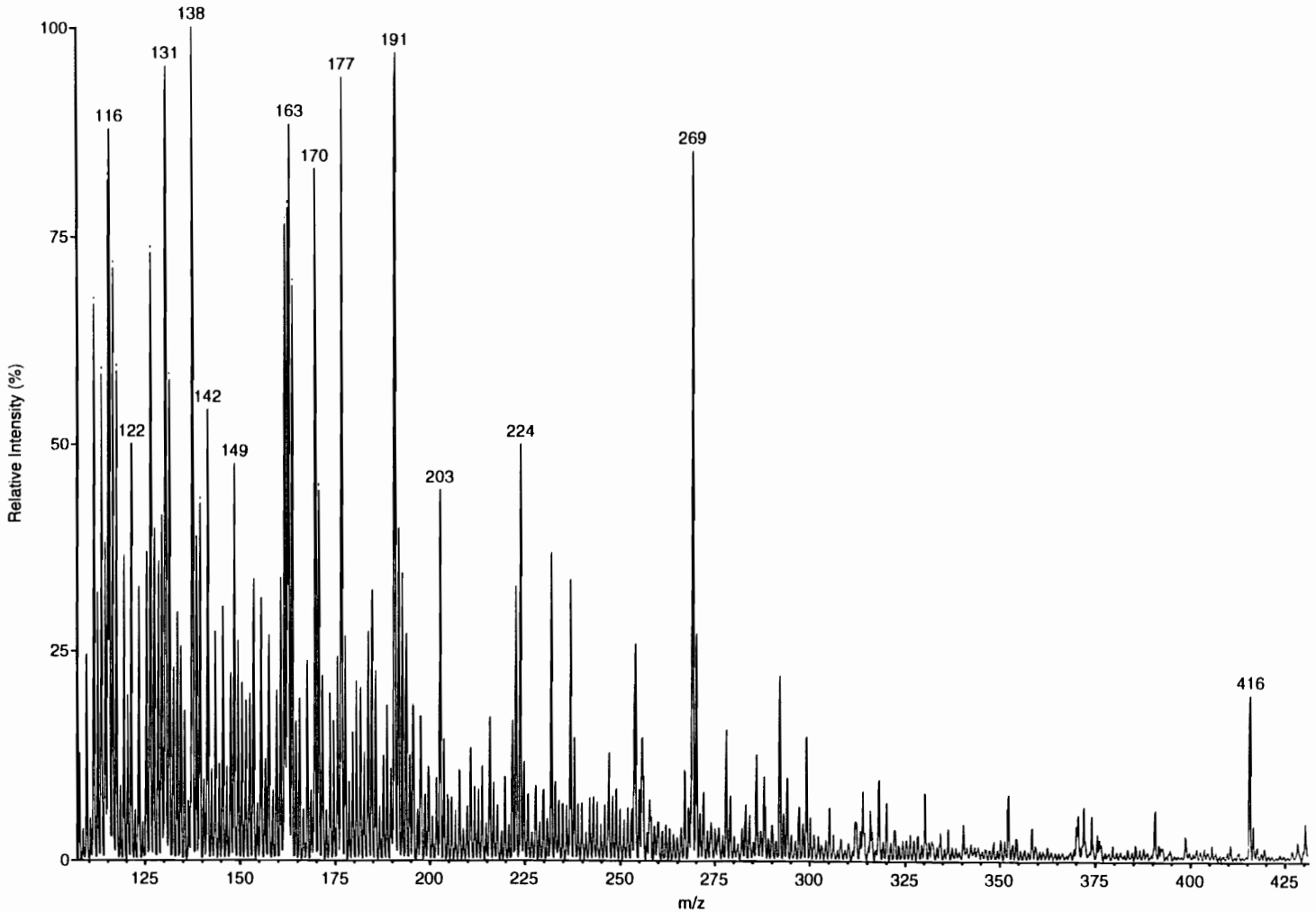

Figure C35. ESMS of rt = 22.29 min.

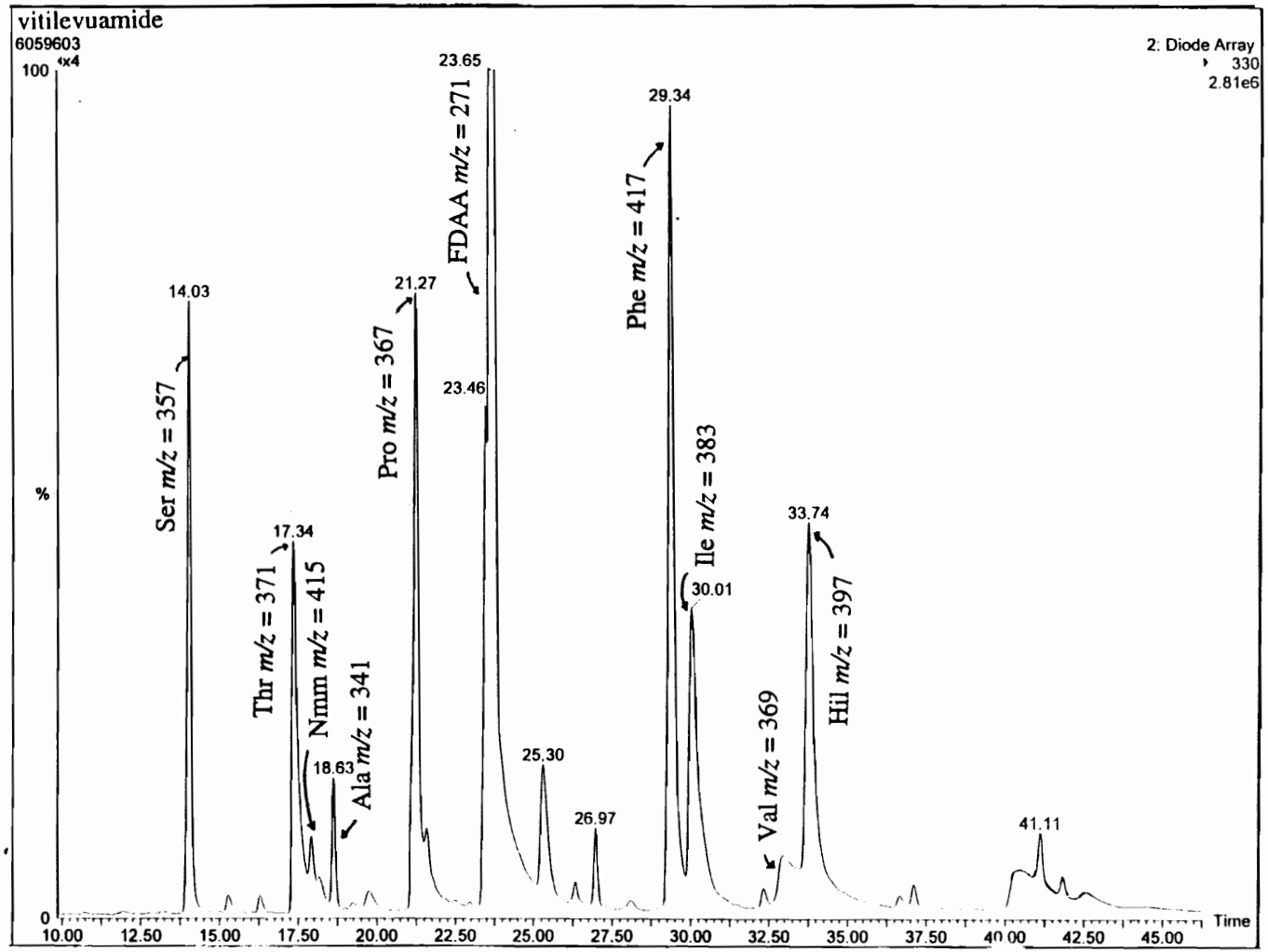

Figure C36. LC of FDAA derivatized vitilevuamide hydrolysate.
Assignments based on ESMS.

REFERENCES

1. Barth, R. H.; Broshears, R. E. *The Invertebrate World*; CBS College Publishing: New York, NY, **1982**; pp 646.

2. George, J. D.; George, J. J. *Marine Life*; Wiley-Interscience: New York, NY, **1979**, pp 8.

3. Pomponi, S. A. In *Biomedical Importance of Marine Organisms*; D. G. Fautin, Ed.; California Academy of Sciences: San Francisco, **1988**, Vol 13; pp 7.

4. Ireland, C. M.; Copp, B. R.; Foster, M. P.; McDonald, L. A.; Radisky, D. C.; Swersey, J. C. In *Marine Biotechnology*; D. H. Attaway and O. R. Zaborsky, Ed.; Plenum Press: New York, **1993**; Vol 1, Pharmaceutical and Bioactive Natural Products; pp 1.

5. Ireland, C. M.; Roll, D. M.; Molinski, T. F.; McKee, T. C.; Zabriskie, T. M.; Swersey, J. C. *Proc. Calif. Acad. Sci* **1987**, *13*, 41.

6. Bergann, W.; Feeney, R. J. *J. Am. Chem. Soc.* **1950**, *72,* 2809.

7. Ireland, C. M.; Molinski, T. F.; Roll, D. M.; Zabriskie, T. M.; McKee, T. C.; Swersey, J. C.; Foster M. P. In *Bioorganic Marine Chemistry*; P. J. Scheuer, Ed.; Springer-Verlag: Berlin, **1987**; Vol 3; pp 3

8. Paul, V. J.; Fenical, W. In *Bioorganic Marine Chemistry*; P. J. Scheuer, Ed.; Springer-Verlag: Berlin, **1987**; Vol 1; pp 1.

9. Scheuer, P. J. *Science* **1990**, *248*, 173.

10. Fenical, W. Proc. *Food-Drugs Sea* **1976**, 1974, 388.

11. Ireland, C. M.; Roll, D. M.; Molinski, T. F.; McKee, T. C.; Zabriskie, T. M.; Swersey,J. C. In *Biomedical Importance of Marine Organisms*; D. G. Fautin, Ed.; California Academy of Sciences: San Francisco **1988**; Vol 13; pp 41.

12. Faulkner, D. J. *Natural Product Reports* **1984**, *1*, 585.

13. Monniot, C.; Monniot, F.; Laboute, P. In *Coral Reef Ascidians of New Caledonia*, Orstom Editions: Paris **1991**, pp 11.

14. Lewis, R. A.; Cheng, L. *Phycologia* **1975**, *14*, 149.

15. Newcomb, E. H.; Pugh, T. D. *Nature* **1975**, *253*, 533.

16. Parry, D. L. *Symbiosis* **1988**, *5*, 1.

17. Parry, D. L. *Symbiosis* **1988**, *5*, 23.

18. Taylor, D. C.; *Proc. R. Soc. (Ser. B)* **1978**, *201*, 401.

19. Begnan, B. M.; Hawkins, C. J.; Lavin, M. F.; McCaffrey, E. J.; Parry, D. L.; Watters, D. J.; *J. Med. Chem.* **1989**, *32*, 1354.

20. Ireland, C. M.; Scheuer, P. J. *J. Am. Chem. Soc.* **1980**, *102*, 5688.

21. Shioiri, T.; Hamada, Y.; Kato, S.; Shibata, M.; Kondo, Y.; Nakagawa, H.; Kohda, K. *Biochem. Pharmacol.* **1987**, *36*, 4181.

22. Wasylyk, J. M.; Biskupiak, J. E.; Costello, C. E.; Ireland, C. M. *J. Org. Chem.* **1983**, *48*, 4445.

23. Williams, D. E.; Moore, R. E.; Paul, V. J. *J. Nat. Proc.* **1989**, *52*, 732.

24. Ireland, C. M.; Durso, A. R.; Newman, R. A.; Hacker, M. P. *J. Org. Chem.* **1982**, *47*, 1807.

25. Biskupiak, J. E.; Ireland, C. M. *J. Org. Chem.* **1983**, *48*, 2302.

26. Sessin, D. F.; Gaskell, S. J.; Ireland, C. M. *Bull. Soc. Chim. Belg.* **1986**, *95*, 853.

27. Degnan, B. M.; Hawkins, C.J.; Lavin, M. F.; McCaffrey, C. J.; Parry, D. L.; van den Brenk, A. L.; Watters, D. J. *J. Med. Chem.* **1989**, *32*, 1349.

28. McDonald, L.A.; Ireland, C. M. *J. Nat. Proc.* **1992**, *55*, 376.

29. Hamamoto, Y.; Endo, M.; Nakagawa, M.; Nakanishi, T.; Mizukawa, K. *J. Chem. Soc., Chem. Commun.* **1983**, 323.

30. McDonald, L. A.; Foster, M. P.; Phillips, D. R.; Ireland, C. M. *J. Org. Chem.* **1992**, *57*, 4616.

31. Schmitz, F. J.; Ksebati, M. B.; Chang, J. S.; Wang, J. L.; Hossain, M. B.; van der Helm, D.; Engel, M. H.; Serban, A.; Silfer, J. A. *J. Org. Chem.* **1989**, *54*, 3463.

32. Hawkins, C.J.; Lavin, M. F.; Marshall, K. A.; van den Brenk, A. L.; Watters, D. J. *J. Med. Chem.* **1990**, *33*, 1634.

33. Zabriskie, T. M. Doctoral Dissertation, University of Utah **1989**.

34. Zabriskie, T. M.; Foster, M. P.; Stout, T. J.; Clardy, J.; Ireland, C. M. *J. Am. Chem. Soc.* **1990**, *112*, 8080.

35. Romanowska K.; Kopple, K. D. *Int. J. Pep. Protein Res.* **1987**, *30*, 289 and references therein.

36. Hambley, T. W.; Hawkins, C. J.; Lavin, M. F.; van den Brenk, A.; Watters, D. J. *Tetrahedron* **1992**, *48*, 341.

37. Prinsep, M. R.; Moore, R. E.; Levine, I. A.; Patterson, G. M. L. *J. Nat. Prod.* **1992**, *55*, 140.

38. Gerwick, W. H.; Fenical, W. *J. Org. Chem.* **1981**, *46*, 22.

39. Foster, M. P.; Concepcion, G. P.; Caraan, G. B.; Ireland, C. M. *J. Org. Chem.* **1992**, *57*, 6671.

40. Foster, M. P.; Ireland, C. M. *Tetrahedron Lett.* **1993**, *34*, 2871.

41. Petit, G. R.; Herald, C. L.; Boyd, M. R.; Leet, J. E.; Dufresne, C.; Doubek, D.; Schmidt, J. M.; Cerny, R. L.; Hooper, J. A.; Rutzler, K. C. *J. Med. Chem.* **1991**, *34*, 3340.

42. Kong, F.; Burgoyne, D. L.; Andersen, R. J.; Allen, T. *Tetrahedron Lett.* **1992**, *33*, 3269.

43. Rinehart, K. L.; Gloer, J. B.; Cook, J. C.; Mizak, S.A.; Scahill, T. A. *J. Am. Chem. Soc.* **1981**, *212*, 933.

44. Rinehart, K. L.; Gloer, J. B.; Hughes, R. G.; Renis, H. E.; McGovern, F. A.; Swynenberg, E. B.; Stringfellow, D. A.; Kuentzel, S. L.; Li, L. H. *Science* **1981**, *212*, 933.

45. Rinehart, K. L.; Kishore, V.; Nagarjan, S.; Lake, R. J.; Gloer, J. B.; Bozich, F. A.; Li, K. M.; Maleczka, R. E.; Todsen, W. L.; Munro, M. H. G.; Sullins, D. W.; Sakai, R. *J. Am. Chem. Soc.* **1987**, *109*, 6846.

46. Jiang, T. L.; Liu, R. H.; Salmon, S. E. *Cancer Chemother. Pharmacol.* **1983**, *11*, 1.

47. Gloer, J. B. Doctoral Dissertation, University of Illinois, Urbana-Champaign **1988**.

48. Jouin, P.; Poncet, J.; Dufor, M. N.; Pantaloni, A.; Castro, B. J. *J. Org. Chem.* **1989**, *54*, 617.

49. McKee, T. C.; Ireland, C. M.; Linquist, N.; Fenical, W. *Tetrahedron Lett.* **1989**, *30*, 3053.

50. Rinehart, K. L.; Sakai, R.; Stroh, J. G. US Patent Appl. ser. No. 335, 903, Apr. 10, **1989**.

51. Rinehart, K. L.; Holt, T. G.; Fregau, N. L.; Keifer, P. A. *J. Nat. Prod.* **1990**, *53*, 771.

52. Boulanger, A.; Abou-Mansor, E.: Badre, A.; Banaigs, B.; Combaut, G.; Francisco, C. *TetrahedronLett.* **1994**, *35*, 4345.

53. Pezzuto, J. M.; Che, C. T.; McPherson, D. D.; Zhu, J. P.; Topcu, G.; Erdelmeir, C. A.; Cordell, G. A. *J. Nat. Prod.* **1991**, *54,* 1522.

54. Aracil, J. M.; Badre, A.; Fadli, M.; Jeanty, G.; Banaigns, B.; Francisco, C.; Lafargue, F.; Heitz, A.; Aumelas, A. *Tetrahedron Lett.* **1991**, *32*, 2609.

55. Linquist, N.; Fenical, W.; Van Duyne, G. D.; Clardy, J. *J. Am. Chem. Soc.* **1991**, *113*, 2303.

56. Kupchan, S. M.; Britton, R. W.; Ziegler, M. F.; Siegel, C. W. *J. Org. Chem.* **1973**, *38*, 178.

57. Levitt, M. H.; Sorenson, O. W.; Ernst, R. R. *Chem. Phys. Lett.* **1983**, *94*, 540.

58. Nahkashima, T. T.; John, B. K.; McClung, R. E. D. *J. Mag. Reson.* **1984**, *57*, 149.

59. Nahkashima, T. T.; John, B. K.; McClung, R. E. D. *J. Mag. Reson.* **1984**, *59*, 124.

60. Bax, A.; Subramanian, S. *J. Mag. Reson.* **1986**, *69*, 565.

61. Muller, L. *J. Am. Chem. Soc.* **1979**, *101*, 4481.

62. Piantini, U.; Sorenson, O. W.; Ernst, R. R. *J. Am. Chem. Soc.* **1982**, *104*, 6800.

63. Rance, M.; Sorenson, O. W.; Bodenhausen, G.; Ernst, R. R.; Wuthrich, K. *Biochem. Biophys. Res. Commun.* **1983**, *117*, 458.

64. Braunschweiler, L.; Ernst, R. R. *J. Mag. Reson.* **1983**, *53*, 521.

65. Bax, A.; Davis, D. G. *J. Mag. Reson.* **1985**, *53*, 521.

66. Lerner, L.; Bax, A. *J. Mag. Reson.* **1986**, *69*, 375.

67. Davis, D. G. *J. Mag. Reson.* **1989**, *84*, 417.

68. Crouch, R. C.; McFayden, R. B.; Daluge, S. D.; Martin, G. E. *Mag. Reson. Chem.* **1990**, *78*, 792.

69. Neuhaus, D.; Williamson, M. The Nuclear Overhauser Effect in Structural and Conformational Analysis, VCH pubishers, New York, **1989**.

70. Jeener, J.; Meier, B. H.; Bachmann, P.; Ernst, R. R. *J. Chem. Phys.* **1979**, *71*, 4546.

71. Kumar, A.; Wagner, G.; Wuthrich, K; Ernst, R. R. *J. Am. Chem. Soc.* **1981**, *103*, 3654.

72. Macura, S.; Ernst, R. R. *Mol. Phys.* **1980**, *41*, 95.

73. Bothner-By, A. A.; Stevens, R. L.; Lee, J,; Warren, C. D.; Jeanloz, R. W. *J. Am. Chem. Soc.* **1984**, *106*, 811.

74. Bax, A.; Davis, D. G. *J. Mag. Reson.* **1985**, *63*, 207.

75. Kessler, H.; Griesinger, C.; Kerssebaum, R.; Wagner, K.; Ernst, R. R. *J. Am. Chem. Soc.* **1987**, *109*, 607.

76. Bull, E. E. *J. Mag. Reson.* **1987**, *72*, 397.

77. Summers, M. F.; Marzilli, L. G.; Bax, A. *J. Am. Chem. Soc.* **1986**, *108*, 4285.

78. Zhu, G.; Bax, A. *J. Mag. Reson.* **1992**, *98*, 192.

79. Krishnamurthy, V. V.; Casida, J. E. *Mag. Reson. in Chem.* **1988**, *26*, 367.

80. Craig, A.G. *Biological Mass Spec.* **1991**, 20, 195.

81. Han, H.; Pascal, R. A. *J. Org. Chem.* **1990**, *55*, 5173.

82. Otani, T. T.; Briley, M. R. *J. Pharm. Sci.* **1974**, *63*, 1253

83. Lu X, Doctoral Dissertation, University of Utah, Salt Lake City, Utah **1990**.

84. Grillith, W. P.; Ley, S. V. *Aldrichimica Acta* **1990**, *23*, 13.

85. Corey, E. J.; Cho, H.; Rucker, C.; Hua, D. H. *Tetrahedron Lett.s*, **1981**, *22*, 3455.

86. Durrwachter, J. R.; Druckhammer, D. G.; Nozaki, K.; Sweers, M.; Wong, C. H. *J. Am. Chem. Soc.* **1986**, *108*, 7812.

87. Harada, K. *Nature* **1963,** *200*, 1201.

88. Lindner, W. *Chimia* **1981**, *35*, 294.

89. Guebitz, F.; Juffman, F.; Jellenz, W. *Chromatographia* **1982**, *16*, 103.

90. Roumeliotis, P.; Unger, K. K.; Kurganov, A. A.; Davankov, V. A. *J. Chromatogr.* **1983**, *255*, 51.

91. Roumeliotis, P.; Kurganov, A. A.; Davankov, V. A. *J. Chromatogr.* **1983**, *266*, 439.

92. Nimura, N.; Susuki, T.; Kasahara, Y.; Kinoshita, T. *Anal. Chem.* **1981**, *53*, 1380.

93. Nimura, N.; Toyama, A.; Kasahara, Y.; Kinoshita, T. *J. Chromatogr.* **1982**, *239*, 671.

94. Weinstein, S.; Engel, H. M.; Hare, P. E. *Anal. Biochem.* **1982**, *121*, 370.

95. Natchmann, F. *Int. J. Pharm.* **1980**, *4*, 337.

96. Aswad, D. W., *Anal. Biochem.* **1984**, *137*, 405.

97. Nimura, N.; Ogura, H.; Kinoshita, T. *J. Chromatogr.* **1980**, *202*, 375.

98. Marfey, P. *Carlsberg Res. Commun.* **1984**, *49*, 591

99. Adamson, J. G.; Hoang, T.; Crivici, A.; Lajoie, G. A. *Anal. Biochem.* **1992**, *202*, 210.

100. Brattain, M. *Cancer Res.* **1986**, *41*, 1751.

101. Alley, M. C.; Scudiero, D. A.; Monks, A.; Hursey, M. L.; Czerwinski, M.J.; Fine, D. L.; Abbott, B. J.; Mayo, J. G.; Shoemaker, R. H.; Boyd, M. R. *Cancer Res.* **1988,** *48*, 589.

102. Giard, D. J.; *J. Nat. Cancer Inst.* **1973**, *51*, 1417.

103. Oteggen, H. F. *J. Nat. Cancer Inst.* **1968**, *41*, 827.

104. Aaronson S. *J. Nat. Cancer Inst.* **1973**, *51*, 1417.

105. Carmichael, J. ; De Graff, W. G.; Gazdar, A. F.; Minna, J. D.; Mitchell, J. B. *Cancer Res.* **1987**, *47*, 936.

106. Bai, R.; Petit, G. R; Hamel, E. *Biochem. Pharm.* **1990**, *39*, 1941.

107. Creasy, W. A. *Cancer, A Comphrensive Treatise*, Plenum Press, New York, **1977**, *5*, 379.

108. Furmanski, P.; Silverman, D. J.; Lobin, M. *Nature* **1971**, *233*, 413.

109. Prasad, K. N.; Hsie, A. W. *Nat. New. Biol.* **515**, *233*, 141.

110. Igarshi, K.; Ikeyama, S.; Takeuchi, M.; Sugino, Y. *Cell Struct. Funct.* **1978**, *3*, 103.

111. Kokoshka, J. M.; Ireland, C. M.; Barrows, L.R. Mauscript in press.

112. Twentyman, P. R.; Luscombe, M. *Br. J. Cancer* **1987**, *56*,279.

113. Denizot, F.; Lang, R. *J. Immunol. Methods* **1986**, *89*, 271.

114. Trischman, J. A.; Tapiolas, D. M.; Jensen, P. R.; Dwight, R.; Fenical, W.; McKee, T. C.; Ireland, C. M.; Stout, T. J.; Clardy, J. *J. IAm. Chem. Soc.* **1994**, *116*, 757.

115. Hamman, M. T.; Scheuer, P. J.. *J. Am. Chem. Soc.***1993**, *115*, 5825.